DYNAMICS OF ARRESTIN – RHODOPSIN INTERACTIONS

by

Martha E. Sommer

A DISSERTATION

Presented to the Department of Biochemistry and Molecular Biology

and the Oregon Health & Science University

in partial fulfillment of the requirements for the degree of

Doctor of Philosophy

April 2006

School of Medicine
Oregon Health & Science University

CERTIFICATE OF APPROVAL

This is certify that the Ph.D. Dissertation of

Martha E. Sommer

has been approved by the following:

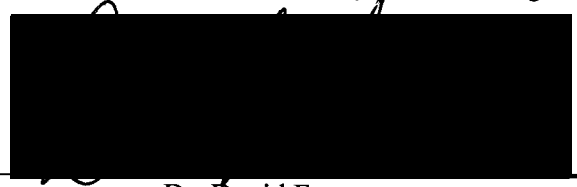

Dr. David Farrens, mentor

Dr. Svetlana Lutsenko, committee chair

Dr. David Dawson, committee member

Dr. Richard Brennan, committee member

Dr. Ujwal Shinde, committee member

Table of Contents

List of Tables

List of Figures

List of Abbreviations

7PP	phosphopeptide analogous to the fully phosphorylated C-terminal tail of rhodopsin ($_{NH2}$DDEApSpTpTVpSKpTEpTpSQVAPA$_{COOH}$)
α	alpha
α_{GTP}	GTP-bound alpha subunit of the heterotrimeric G-protein
A	Arrhenius pre-exponential factor
A (amino acid)	alanine
Å	angstrom
A2E	di-retinal conjugate with phosphatidylethanolamine
ABCR	ATP-driven photoreceptor specific ABC cassette transporter
ABS	absorption
Ala	alanine
AP-1	oxidative sensitive transcription factor
AP-2	adaptor protein 2 of the cellular endocytosis machinery
Arg	arginine
Arr	arrestin
Asn	asparagine
aso	asolectin
Asp	aspartic acid
ATP	adenosine triphosphate
atR	all-*trans* retinal
A.U.	arbitrary units
β	beta

B	bimane label
χ^2	chi-squared, which describes the deviance of the residuals to a fit
C (atom)	carbon
C (amino acid)	cysteine
C-	carboxyl-
°C	degrees Celsius
Ca	calcium
cal	calorie
cDNA	complementary DNA synthesized from a mature mRNA
cGMP	cyclic guanosine monophosphate
Cl	chlorine
cm	centimeter
CNB	Congenital Night Blindness
CRALBP	cellular retinal binding protein
CRBP	cellular retinol binding protein
Cys	cysteine
Δ	delta, or the difference between two values
D (amino acid)	aspartic acid
Da	Dalton, unit of atomic mass
DM	*n*-dodecyl-β-D-maltopyranoside
DNA	deoxyribonucleic acid
DSP	lysine-specific, DTT-cleavable cross-liker (Dithiobis(succinimidylpropionate)

DTT	dithiothreitol
ε	extinction coefficient
E (amino acid)	glutamic acid
E-2	second extracellular loop of rhodopsin
E_a	energy of activation
EDTA	ethylenediamine-tetraacetic acid
EPR	electron paramagnetic resonance
et al.	*et alii* (Latin), "and others"
F (amino acid)	phenylalanine
F	fluorescence intensity
F_0	fluorescence intensity in the absence of quencher, or the fluorescence intensity before light-activation of the sample
F1	V8 proteolytic fragment of rhodopsin (~27 kDa)
F2	V8 proteolytic fragment of rhodopsin (~15 kDa)
FRET	fluorescence resonance energy trasfer
γ	gamma
g	acceleration due to gravity
G	G-factor that corrects for monochromater bias in transmitting parallel *versus* perpendicularly polarized light
G (amino acid)	glycine
G_α	alpha subunit of the heterotrimeric G-protein
$G_{\beta\gamma}$	beta and gamma subunits of the heterotrimeric G-protein
GC	guanylate cyclases

GCAP	guanylate cyclases activating protein
GDP	guanosine diphosphate
Gln	glutamine
Glu	glutamic acid
Gly	glycine
GMP	guanosine monophosphate
GPCR	G-protein coupled receptor
G-protein	guanine nucleotide-binding regulatory protein
G_t	transducin (photoreceptor G-protien)
$G_t\alpha$	alpha subunit of transducin
GTP	guanosine triphosphate
h	hour
H (atom)	hydrogen
H (amino acid)	histidine
HEPES	*N*-2-hydroxyehtylpiperazine-*N'*-2-ethanesulfonic acid
His	histidine
hν	light
I (atom)	iodine
I (amino acid)	isoleucine
I^-	free iodide
$I_{\parallel}$	intensity of fluorescence emission parallel to the plane of excitation light

$I_{\perp}$	intensity of fluorescence emission perpendicular to the plane of excitation light
I72B	bimane-labeled arrestin mutant I72C
Ile	isoleucine
IRBP	inter-photoreceptor retinoid binding protein
k	rate constant
K (atom)	potassium
K (amino acid)	lysine
K (temperature)	degrees Kelvin
kcal	kiloclalories
K_D	equilibrium dissociation constant
kDa	kilodalton
k_q	bimolecular quenching constant
K_{SV}	Stern-Volmer constant
L (amino acid)	leucine
Leu	leucine
LRAT	lecithin retinol acyl transferase
Lys	lysine
λ_{em}	wavelength of emission
λ_{ex}	wavelength of excitation
λ_{max}	wavelength of maximum absorption or emission
M	molar
M (amino acid)	methionine

MES	4-morpholineethanesulfonic acid
Me_2SO	DMSO, dimethylsulfoxide
Met	methionine
Meta I (MI)	Metarhodopsin I
Meta II (MII)	Metarhodopsin II
Meta III (MIII)	Metarhodopsin III
max	maximum or maximal
µg	microgram
mg	milligram
min	minute
µl	microliter
ml	milliliter
µM	micromolar
mM	millimolar
mol	mole
µs	microsecond
mRNA	messenger RNA
MW	molecular weight
N	normal
N (atom)	nitrogen
N (amino acid)	asparagine
N-	amino-
Na	sodium

$NaBH_4$	sodium borohydride
NADPH	nicotinamide adenine dinucleotide, reduced form
ng	nanogram
NH_2OH	hydroxylamine
nm	nanometer
nM	nanomolar
ns	nanosecond
O (atom)	oxygen
O.D.	optical density
P (atom)	phosphate
P (amino acid)	proline
p44	44 kDa splice variant of arrestin
P470	blue-light photoproduct of Meta II that is identical to Meta III
P500	blue-light photoproduct of Meta II
PA	1,2-dioleoyl-*sn*-glycero-3-phosphate
PC	1,2-dioleoyl-*sn*-glycero-3-phosphocholine
PCR	polymerase chain reaction
PDE	phosphodiesterase
PE	1,2-dioleoyl-*sn*-glycero-3-phosphoethanolamine
pH	potential of hydrogen
Phe	phenylalanine
ϕ	quantum yield
PI	L-α-phosphatidylinositol

PIPES	1,4-piperazinediethanesulfonic acid
PL	phospholipid
PMSF	phenylmethylsulfonyl fluoride
Pro	proline
PS	1,2-dioleoyl-*sn*-glycero-3-phosphoserine
PyMPO	1-(2-maleimidylethyl)-4-(5-(4-methoxyphenyl)oxazol-2-yl)-pyridinium
Q (amino acid)	glutamine
Q	anion exchange matrix
[Q]	quencher concentration
r	anisotropy
R	universal gas constant, 1.9872 cal mol^{-1} K^{-1}
R (amino acid)	arginine
RDH	retinal dehydrogenase
11-*cis* RDH	11-*cis* retinol dehydrogenase
Rho	rhodopsin
Rho*	light-activated rhodopsin
Rho-P	phosphorylated rhodopsin
RIS	rod inner segment
RK	rhodopsin kinase
RNA	ribonucleic acid
ROS	rod outer segment, or wild-type rhodopsin in native membranes
ROS*	light-activated rhodopsin in native membranes

ROS-P	phosphorylated rhodopsin in native membranes
RP	*Retinitis Pigmentosa*
RPE	retinal pigment epithelium
RPE65	all-*trans* retinylester binding protein and isomerohydrolase
s	second
S (amino acid)	serine
S251B	bimane-labeled arrestin mutant S251C
SDS	sodium dodecyl sulfate
SDS PAGE	SDS polyacrylamide gel electrophoresis
sec	second
Ser	serine
SL	nitroxide spin-label, [1-oxyl-2,2,5,5-tetramethyl-D-pyrroline-3-methyl]methanethiosulfonate
T	temperature
T (amino acid)	threonine
τ	fluorescence decay lifetime
$\langle\tau\rangle$	amplitude-weighted average fluorescence lifetime
$\bar{\tau}$	intensity-weighted average fluorescence lifetime
$t_{1/2}$	half-life
TCA	trichloroacetic acid
TCEP	tris(2-carboxyethyl)phosphine
Thr	threonine
Tricine	*N*-[2-hydroxy-1,1-bis(hydroxymethyl)ethyl]glycine

Tris	2-amino-2-hydroxymethyl-1-3-proanediol
Trp	tryptophan
Tyr	tyrosine
UV	ultraviolet
V (amino acid)	valine
V8	protease from *Staphylococcus aureus* strain V8 that cleaves to the carboxyl side of Asp and Glu residues
vs.	*versus*
Val	valine
W (amino acid)	tryptophan
WT	wild-type
Y (amino acid)	tyrosine

Acknowledgements

The road to a dissertation is certainly not traveled alone, and I am sincerely grateful to many people for their support, both scientifically and personally. Firstly, I thank my advisor and mentor Dr. David Farrens, for teaching me how to think about biology at the molecular level, for challenging me to think critically about my own work, and for his enthusiasm, which has been a constant inspiration. I also thank all the past and present members of the Farrens lab – Dr. Brian Nauert, Tom Dunham, Jonathan Fay, Dr. Jay Janz, Steven Mansoor, and Abhinav Sinha – for making the lab a fun and enjoyable environment. I especially wish to acknowledge Dr. Nauert for his assistance when I first joined the lab, Dr. Janz for teaching me so much about rhodopsin, and Steven Mansoor for his assistance and expertise on fluorescence. I also want to thank our collaborator, Dr. Clay Smith at the University of Florida, for making much of this work possible. I thank the members of my research advisory committee – Dr. Richard Brennan, Dr. David Dawson, Dr. Svetlana Lutsenko, and Dr. Ujwal Shinde – for their helpful guidance. My experience at OHSU has been blessed with so many friendships, and I especially want to thank all my classmates for making graduate life fun.

Finally, I wish to thank my family. I thank my mother, Margaret, for her constant love and always encouraging me to chase after my aspirations (and my education). I thank my sister, Dolores, for her love and friendship. I also want to thank my godparents Calvin and Susie for supporting me in difficult times, and celebrating with me in happier ones. I want to acknowledge my Uncle Walt for inspiring me to be a scientist. And last, but certainly not least, I thank my newlywed husband, Paul, for his love, support, and encouragement over these past years.

Abstract

The visual transduction system serves as a paradigm for the study of G-protein coupled receptor (GPCR) signaling and attenuation. Visual signaling begins with absorption of light by the retinal chromophore of the photoreceptor rhodopsin, which converts rhodopsin to the active Meta II species that can interact with the G-protein transducin (G_t). The ability of Meta II to activate G_t is terminated in several ways: 1) Meta II decays to opsin and free retinal, 2) Meta II decays to the long-lived retinal storage photoproduct Meta III, and 3) Meta II is phosphorylated by a kinase and bound by the protein arrestin, which blocks further G_t activation. This dissertation explains how these inactivation mechanisms are related. Specifically, it explores how arrestin affects release of the retinal chromophore and rhodopsin photoproduct formation.

Several significant findings are described. First, direct observation of arrestin binding and release from rhodopsin can be monitored using fluorescently labeled arrestin mutants. These studies show that arrestin and retinal release are directly linked in native membranes. Secondly, it was found that acidic phospholipids restore arrestin binding to detergent-purified rhodopsin. Besides implying that phospholipids play an important role in arrestin-rhodopsin interactions, this finding also enables arrestin studies in a soluble system. Thirdly, this advantage was used to gain new insights into arrestin's regulation of rhodopsin photochemistry. Arrestin stabilizes Meta II by trapping retinal in the binding pocket, and arrestin interacts with Meta III and converts it to a Meta II-like species. Finally, the short arrestin splice variant p44, which plays a different physiological role in the rod cell than arrestin, was investigated using the same methodology.

In summary, these results suggest that arrestin's role in the rod cell might be more complex than simply quenching Meta II activity. This dissertation provides biochemical evidence that p44 likely regulates rhodopsin signaling in the dim-light operational range of the rod cell, while arrestin may serve to regulate rhodopsin photochemistry and protect the rod cell from the toxic levels of retinal generated by bright light.

Chapter 1

Introduction

Vision is one of the longest studied natural phenomena. Wilhelm Kühne first isolated "visual purple" from retina over 125 years ago, and George Wald identified this pigment as a protein conjugated to a derivative of vitamin A (retinal) about 60 years ago (Kühne, 1879; Wald, 1951). The crystal structure of this protein, rhodopsin, was published just six years ago (Palczewski *et al.*, 2000), and the last few decades have yielded a wealth of information on the structure and function of most the components of visual signal transduction (Ridge *et al.*, 2003). Importantly, the visual system has served as a paradigm for the larger family of G-protein coupled receptors to which rhodopsin belongs. The following chapter will provide background information and a brief review of the literature pertinent to the experimental results presented in this dissertation. A dissertation overview is presented at the end of this chapter.

1. 1 G-PROTEIN COUPLED RECEPTORS

1. 1. 1 Diversity with a Conserved Structure

The human genome contains >800 genes that code for a class of membrane receptors termed G-protein coupled receptors (GPCR) (Fredriksson *et al.*, 2003). These receptors mediate the essential task of communicating extracellular information across the cell membrane into the cytoplasm. As expected for such a large gene family, there is enormous diversity in the types of GPCR ligands: photons, ions, odorants, hormones, peptides, and proteins, just to name a few. Because GPCRs control such a wide variety of sensory and physiological responses, they are currently the most common pharmaceutical target (Lu *et al.*, 2002; Bartfai *et al.*, 2004; Wise *et al.*, 2004; Hill, 2006).

GPCRs can be grouped into five families based on sequence similarity (Karnik *et al.*, 2003). Remarkably, the lack of sequence similarity between families suggests convergent evolution, where a conserved molecular structure was derived independently along different evolutionary paths (Bockaert and Pin, 1999). GPCRs share a common structural core of seven transmembrane α-helices and a common mechanism of signal transduction involving a heterotrimeric G-protein (guanine nucleotide-binding regulatory protein) (Figure 1. 1).

Diversity of GPCR signaling is also present at the G-protein level: multiple genes for each of the three subunits, α, β and γ, are present (Hamm, 1998; Pierce *et al.*, 2002). Different GPCRs interact with different types of G-proteins, and these G-proteins regulate the activity of different effector proteins, including adenylyl cyclases, phospholipases, phosphodiesterases, and ion channels (Karnik *et al.*, 2003; Wettschureck and Offermanns, 2005). This variety explains why such a diversity of sensory (sight, smell, taste) and physiological (cardiovascular, endocrine, immune, neurological, *et al.*) systems can be controlled by this one class of receptors (Wettschureck and Offermanns, 2005).

1. 1. 2 GPCR Signaling Activation

GPCR signal transduction begins when the receptor binds a ligand (or "agonist") in the hydrophobic core of its α-helices or within its extended N-domain. Ligand binding disrupts the stabilizing interactions in the "inactive" receptor and induces conformational changes which open cytoplasmic binding sites for the heterotrimeric G-protein (Wess, 1997; Gether and Kobilka, 1998; Hamm, 2001). Upon binding the "active" receptor, the G_α subunit releases its bound GDP, binds GTP, and then dissociates from $G_{\beta\gamma}$ (Figure 1.

1). G-protein subunits α_{GTP} and $\beta\gamma$ can then modulate several cellular signaling pathways through interactions with various second messengers. A hallmark of GPCR signaling is amplification. A single activated receptor can interact with many G-proteins, and activated G-proteins can then interact with multiple second messengers. This mechanism increases the both the sensitivity and the speed of the signal transduction cascade.

1. 1. 3 GPCR Signaling Attenuation

In order to respond to changing environmental stimuli, GPCRs must be subject to an efficient mode of signal termination. G_{α}-signaling is ultimately terminated by the hydrolysis of its bound GTP, which is enhanced by members of the RGS (regulator of G-protein signaling) family (Pierce *et al.*, 2002). Receptor deactivation begins with phosphorylation of its C-terminus by a G-protein coupled receptor kinase (GRK) (Figure 1. 2) (Claing *et al.*, 2002; Perry and Lefkowitz, 2002). Subsequent binding by β-arrestin blocks further interaction with G-proteins. In addition, β-arrestins can catalyze the removal of some GPCRs from the cell surface by interacting with the cellular internalization machinery, such as clathrin and AP-2 (Laporte *et al.*, 2000; Pierce and Lefkowitz, 2001). Once internalized in vesicles, receptors can be recycled back to the cell surface or degraded (Tsao *et al.*, 2001; Luttrell and Lefkowitz, 2002).

Being a member of the largest GPCR family ("Type A" or R-like"), which contains ~90% of all known GPCRs, the dim-light photoreceptor rhodopsin is one of the best-studied and serves as a model system (Filipek *et al.*, 2003b; Karnik *et al.*, 2003). This dissertation focuses on the interaction of rhodopsin and its deactivator, visual

arrestin, and how this interaction affects rhodopsin photochemistry and the release of its ligand, retinal. The details of visual signal transduction are described below.

1. 2 VISUAL SIGNAL TRANSDUCTION

1. 2. 1 The Structure and Function of the Retina

Visual signal transduction converts photons of light into electrical signals that can be interpreted by the brain (Arshavsky *et al.*, 2002; Burns and Arshavsky, 2005). This process occurs in the retina, a specialized neural tissue located at the back of the eye (Figure 1. 3A). Remarkably, the human eye is sensitive to light intensities that span 10 orders of magnitude (Lamb and Pugh, 2004), and this feat is accomplished in part by having two types of photoreceptors. 95% of the retina is composed of the rods, which mediate dim-light (scotopic) vision, and are capable of single-photon detection. However, these become unresponsive at brighter light intensities. In contrast, the mediators of bright-light (photopic) trichromatic (red, green and blue) vision, the cones, are insensitive at low light intensities but can function at the upper limits of vision (Nathans, 1992; Rattner *et al.*, 1999). Rod and cone cells have a highly extended morphology composed of inner and outer segments (Figure 1. 3B). The rod outer segment contains ~1000 specialized membranous organelles called disks (Figure 1. 3C) (Lamb and Pugh, 2004). Half the volume of these disks is composed of the photoreceptor rhodopsin (Figure 1. 3D) (Molday, 1998), yielding an effective concentration of 3 mM (Lamb and Pugh, 2004). Disks are generated by the inner segment, travel up the outer segment, and are eventually phagocytosed by the retinal pigment epithelium (RPE) (Anderson and Fisher, 1975).

In the dark-adapted rod cell, the ion channels within the plasma membrane are open, generating a "dark current" (Figure 1. 4A) (Stryer, 1988). The following sections will describe how the membrane polarization of the rod cell is modulated during the steps of phototransduction: activation, signal propagation, inactivation and adaptation.

1. 2. 2 Phototransduction Cascade: Activation

The photoreceptor rhodopsin consists of the protein opsin and covalently attached chromophore 11-*cis* retinal (Figure 1. 3E). Dark-state rhodopsin is extremely stable, and spontaneous activation event are extremely rare (about once every 2000 years) (Burns and Baylor, 2001). This stability is necessary to maintain a low amount of "background noise" and contributes to rod cell sensitivity. In contrast, cone opsins display a significant rate of dark-state chromophore hydrolysis (Kefalov *et al.*, 2005), and thus cones are ~100 to 1,000 times less sensitive than rods (Kefalov *et al.*, 2003). Upon the absorption of light, rhodopsin's chromophore isomerizes to the all-*trans* conformation (Palczewski and Saari, 1997; Pepe, 2001), which ultimately results in the "active" form Metarhodopsin II (Meta II). Binding of transducin (G_t) to Meta II results in guanine nucleotide exchange in the α subunit of G_t and dissociation of the subunits (Figure 1. 4B) (Stryer, 1988; Arshavsky *et al.*, 2002).

1. 2. 3 Phototransduction Cascade: Signal Propagation

Free $G_t\alpha$ activates cGMP phosphodiesterase (PDE), which quickly depletes the cell of cGMP (see Figure 1. 4B for more details). The drop in cGMP results in closure of cGMP-gated channels in the plasma membrane, leading to hyperpolarization of the rod cell and inhibition of neurotransmitter release at the synaptic terminal (Figure 1. 3B) that is sensed by secondary retinal neurons (Leskov *et al.*, 2000; Burns and Arshavsky, 2005).

1. 2. 4 Phototransduction Cascade: Inactivation

Termination of the visual signaling cascade results from inactivation of Meta II and the GTP-bound $G_t\alpha$ (Figure 1. 4C). Meta II signaling is shut down by the phosphorylation of its C-terminal tail by rhodopsin kinase (RK), followed by binding of visual arrestin, which blocks further G-protein activation (Kühn *et al.*, 1984; Wilden *et al.*, 1986). The interaction of GTP-$G_t\alpha$ with PDE is terminated by the stimulation of $G_t\alpha$'a intrinsic GTPase activity by a membrane-anchored complex including the regulator of G-protein signaling, RGS9-1 (Ridge *et al.*, 2003; Burns and Arshavsky, 2005).

1. 2. 5 Phototransduction Cascade: Adaptation

Both rods and cones are able to adapt over a range of light-intensities and remain sensitive to changes in the light flux. This feat is accomplished in large part by Ca^{2+}-regulated adaptation mechanisms (Figure 1. 4) (Polans *et al.*, 1996; Burns and Baylor, 2001). First, decreasing Ca^{2+} levels cause calmodulin to dissociate from cGMP-gated channels, which increases the channel's sensitivity for cGMP (Hsu and Molday, 1994). Second, low Ca^{2+} allows the guanylate cyclase activating protein (GCAP) to bind guanylate cyclase (GC), resulting in the recovery of cGMP levels in the cell (Dizhoor, 2000). Finally, the drop in Ca^{2+} allows RK to be released from recoverin so that it can phosphorylate and inactivate Meta II, leading to a downstream decrease in cGMP hydrolysis (Sallese *et al.*, 2000). Together, these mechanisms maintain cell sensitivity over ever increasing light fluxes by ensuring that a population of cGMP-channels remains open.

Another mechanism of adaptation in the rod cell is the formation Metarhodopsin III (Meta III), which may compose up to half the rhodopsin in the retina in bright-light

conditions (Lewis *et al.*, 1997). Meta III may serve as retinal storage in the photobleached rod, and its persistence may contribute to the slow rate of dark adaptation [1] (Lamb and Pugh, 2004). The role of arrestin in regulating Meta III is one of the topics of this dissertation.

1. 2. 6 Protein Translocation

Transducin and arrestin undergo a dramatic light-dependent translocation in the rod cell (Whelan and McGinnis, 1988; Peterson *et al.*, 2003; Elias *et al.*, 2004). In the dark, transducin is mostly present in the outer segment, and arrestin is mostly sequestered in the inner segment. Upon exposure to light, transducin migrates to the inner segment, and arrestin migrates to the outer segment, where it remains until the cell is returned to darkness. Recently, it has been suggested that arrestin's translocation occurs by mass action. In the dark, arrestin's affinity for microtubules sequesters it in the inner segment (Nair *et al.*, 2004; Hanson *et al.*, 2006a). Upon light-activation, arrestin's higher affinity for light-activated rhodopsin results in its net movement into the outer segment (Nair *et al.*, 2005). Moreover, the intensity of light required to stimulate arrestin translocation is at the upper limit of rod-cell sensitivity, suggesting that arrestin is not involved in attenuating visual signal transduction in the operational range of the rod cell (Strissel *et al.*, 2006). Interestingly, a splice variant of arrestin called p44, which is expressed at only ~10% the levels of arrestin, is present in the outer segments even in the dark (Palczewski *et al.*, 1994a; Smith *et al.*, 1994). p44 might in fact be the quencher of G_t-activity in the

[1] After exposure to bright light, the rod cell requires up to 40 minutes to regain full sensitivity. Desensitization may be caused by a long-lived photoproduct (so-called "equivalent-light"), which continues to stimulate PDE activity, even after the removal of light (Granit *et al.*, 1938). During dark adaptation, this photoproduct must be removed and regenerated to rhodopsin (Lamb and Pugh, 2004).

dim-light operational range of the rod cell (Langlois *et al.*, 1996). What role might arrestin be playing in the light-saturated rod cell? This question is addressed in this dissertation.

1. 2. 7 Regenerating Rhodopsin: the Retinoid Cycle

The final step in Meta II deactivation is the release of its ligand, all-*trans* retinal and the dephosphorylation of its C-terminal tail by protein phosphatase 2A (PP2A) (Palczewski *et al.*, 1989a; Palczewski *et al.*, 1989b). Although it is assumed that arrestin must dissociate for dephosphorylation to occur, the details of how this occurs, and how it is related to retinal release, remain unclear. As described in this dissertation, arrestin and retinal release are directly linked in native membranes (Sommer *et al.*, 2005). This observation is supported by the fact that retinal dehydrogenase (RDH) activity, which converts all-*trans* retinal to retinol, speeds arrestin release (Hofmann *et al.*, 1992). This implies that the hydrolysis of the bond linking retinal to the protein is sufficient to allow dissociation of both arrestin and retinal. However, we find that this coupling of retinal and arrestin release can be disrupted by detergent (Sommer *et al.*, 2006). One possible explanation for this is that channeling of retinal through opsin during its release (Schädel *et al.*, 2003) plays an important role in arrestin release (see section **1. 3. 4** below).

The details of what happens to the freed all-*trans* retinal are described in Figure 1. 5. In rods, all-*trans* retinal is reduced to retinol, conveyed out of the cell and across the inter-photoreceptor matrix to the RPE, where it is enzymatically converted to the 11-*cis* isomer in a multi-step process. 11-*cis* retinal is then shuttled back to the photoreceptors, where dark-state rhodopsin can be regenerated (McBee *et al.*, 2001; Lamb and Pugh, 2004).

Why is the vertebrate retinoid cycle so complex? In the more simplistic invertebrate visual cycle, a second photon absorption event is used to regenerate the photo-pigment. The vertebrate system may be advantageous because it regenerates photo-pigment independently of photon flux and enables rapid restoration of visual sensitivity, even in the dark (Saari, 2000).

Interestingly, cones have a modified retinoid cycle that employs Müller cells to convert all-*trans* retinal to 11-*cis* retinol, followed by oxidation of 11-*cis* retinol to 11-*cis* retinal in the cone cell (Mata *et al.*, 2002). This system is much faster than the RPE-based retinoid cycle and can thus support the high levels of regeneration required by cones in bright-light conditions (Golobokova and Govardovskii, 2006). Also, since rods lack 11-*cis* retinol dehydrogenase, they are precluded from "stealing" retinoid from the Müller cells (Mata *et al.*, 2002).

1. 2. 8 Retinal Diseases

Mutations in retinal proteins have been implicated in many human disease states. *Retinitis Pigmentosa* (RP) is a genetically heterogeneous disease characterized by progressive photoreceptor death, causing blindness (Molday, 1998; Rattner *et al.*, 1999; Kisselev, 2005). Some mutations can affect rhodopsin synthesis or trafficking, implying that rhodopsin is an important structural determinate for healthy ROS. In addition, some RP mutations perturb the photo-activation or photo-deactivation of rhodopsin, leading to inappropriate signaling. When the low background noise of the retina is compromised by the expression of constitutively active rhodopsin, *Congenital Night Blindness* (CNB) results (Jin *et al.*, 2003). Interestingly, constitutively active rhodopsin mutants may also

cause cell death by forming large aggregates of endocytosed rhodopsin-arrestin complexes (Li *et al.*, 1995; Rim and Oprian, 1995; Chuang *et al.*, 2004).

Mutations that knock out the activity of either rhodopsin kinase or arrestin have been shown to cause *Oguchi disease*, a form of stationary night blindness (Fuchs *et al.*, 1995; Chen *et al.*, 1999; Dryja, 2000). Recently, it has been suggested that Oguchi disease results from a block in the ability to regenerate rhodopsin during dark adaptation (Lamb and Pugh, 2004). Findings presented in this dissertation may help explain the link between arrestin function and dark adaptation.

Finally, *Stargardt's Macular Degeneration* is caused by mutation of the ABCR transporter (Figure 1. 5), which may lead to a build up of all-*trans* retinal in the ROS (Radu *et al.*, 2004). All-*trans* retinal can react with phosphatidylethanolamine to form A2E, a damaging oxidative photoproduct (Fishkin *et al.*, 2003; Dillon *et al.*, 2004). In fact, A2E is believed to be the major constituent of lipofuscin (Sparrow *et al.*, 2003), which is found in the retina of the elderly and is a possible cause of *Age Related Macular Degeneration* (AMD) (Wenzel *et al.*, 2005). This dissertation presents evidence that arrestin may limit retinal release in bright-light conditions, and could thus help protect the rod cell from a build-up of toxic retinal conjugates.

A significant advantage in the study of arrestin-rhodopsin interactions is that high-resolution structures are available for the inactive forms of both proteins, and there is a wealth of biochemical and biophysical data on their possible mechanisms of activation. The following two sections will briefly review the structure and hypothesized

mechanisms of activation of rhodopsin and arrestin, as well as other relevant topics such as rhodopsin phosphorylation, retinal release, rhodopsin and arrestin oligomerization, and the role of membrane phospholipids in rhodopsin function.

1. 3 RHODOPSIN STRUCTURE AND FUNCTION

1. 3. 1 Dark-state Rhodopsin

Currently, rhodopsin is the only GPCR for which a high-resolution crystal structure is available (Palczewski *et al.*, 2000; Teller *et al.*, 2001; Li *et al.*, 2004; Okada *et al.*, 2004). The structure is characterized by seven transmembrane α-helices and one cytoplasmic helix (VIII), connected by three extracellular (intradiskal) loops and three cytoplasmic loops (Figure 1. 6). The extracellular N-domain is glycosylated (Fukuda *et al.*, 1979), and extracellular loop II (E-II) forms a twisted β-hairpin that is stabilized by a conserved ion pair (Arg^{177} – Asp^{190}) and is linked to Helix III by a disulfide bridge. Loop E-II, the so-called "retinal plug", may serve to stabilize retinal in the binding pocket and limit the access of water (Yan *et al.*, 2002; Janz *et al.*, 2003). The cytoplasmic face of rhodopsin consists of the three cytoplasmic loops and amphipathic Helix VIII, which lies along the plane of the membrane and is anchored by two palmitoyl groups. The C-terminal tail of rhodopsin folds back over the loop connecting Helices I and II, although it is most likely very mobile (Langen *et al.*, 1999; Palczewski *et al.*, 2000). Furthermore, phosphorylation may increase disorder within the C-terminal tail (Getmanova *et al.*, 2004), and subsequent arrestin binding may then induce a helical structure (Kisselev *et al.*, 2004a; Kisselev *et al.*, 2004b).

The chromophore of rhodopsin, 11-*cis* retinal, is linked to Lys^{296} on Helix VII *via* a protonated Schiff-base. The Schiff-base linkage is stabilized by a salt-bridge to Glu^{113} on Helix III. Protonated Schiff-bases absorb at ~440 nm, and rhodopsin's absorption is red-shifted to ~500 nm due to additional interactions between the chromophore and the amino acids of the protein (Rando, 1996; Kochendoerfer *et al.*, 1999). Although cone opsins also contain Schiff-base linked 11-*cis* retinal, they are spectrally-tuned to their respective wavelengths by virtue of the different residues that line their chromophore binding pockets (Stenkamp *et al.*, 2002; Teller *et al.*, 2003).

The ability of the apoprotein opsin to activate transducin (G_t) is only 10^{-6} that of Meta II (Melia *et al.*, 1997). However, 11-*cis* retinal bound opsin (rhodopsin) has an even lower activity, suggesting that 11-*cis* retinal acts is an inverse agonist and locks the protein in an inactive conformation (Okada *et al.*, 2001; Filipek *et al.*, 2003a). Inactivating structural constraints include the salt bridge between the protonated retinal Schiff-base and the counter-ion Glu^{113}, as well as various H-bond and hydrophobic interactions between the α-helices. For example, at the cytoplasmic distal end of Helix III the highly conserved E(D)RY sequence (Figure 1. 6, *right*) is located in an extremely hydrophobic pocket and involved in ionic interactions with Helix VI. Another highly conserved sequence NPXXY on Helix VII is involved in stabilizing interactions with Helices VI and VIII (Menon *et al.*, 2001; Okada *et al.*, 2001; Filipek *et al.*, 2003a).

1. 3. 2 Rhodopsin Activation and Spectral Photo-intermediates

The ultra-fast response time (femtoseconds) of rhodopsin is achieved by the fact that the agonist all-*trans* retinal is formed by the photon-induced isomerization of the pre-bound inverse agonist 11-*cis* retinal (Figure 1. 7) (Menon *et al.*, 2001). Within the first

few milliseconds after the absorption of light, the protein relaxes through a series of short-lived intermediates to the first long-lived intermediate Metarhodopsin I (Meta I). Meta I is characterized by a protonated Schiff base that absorbs at ~480 nm and is in a pH- and temperature sensitive equilibrium with Meta II. Meta I formation also involves a switch of the Schiff-base counter-ion from Glu^{113} on Helix III to Glu^{181} on loop E-II (Yan *et al.*, 2003). The conformation of Meta I appears to differ significantly from dark-state rhodopsin only in the vicinity of Trp^{265} on helix VI (Ruprecht *et al.*, 2004; Schertler, 2005), which may enable the conformational changes involved in the formation of Meta II (Lin and Sakmar, 1996; Hubbell *et al.*, 2003). These conformational changes are catalyzed by the deprotonation of the Schiff-base and the breaking of the salt-bridge with Glu^{113}, resulting in a large absorption shift to ~380 nm (Filipek *et al.*, 2003a). Formation of Meta II is characterized by an outward movement and rotation of Helix VI (Altenbach *et al.*, 1996; Farrens *et al.*, 1996; Dunham and Farrens, 1999), which may expose the E(D)RY sequence and open a hydrophobic cytoplasmic cleft for binding G_t (Altenbach *et al.*, 1996; Janz and Farrens, 2004a). Specifically, the salt bridge between Glu^{134} and Arg^{135} of the E(D)RY sequence breaks, due to the uptake of a proton from the cytoplasm by Glu^{134} (Arnis *et al.*, 1994), which is necessary for interaction with G_t (Resek *et al.*, 1993; Hamm, 2001).

Alternatively, Meta I can decay to the long-lived photoproduct Meta III, which results from an isomerization around the Schiff-base (15-*anti* to 15-*syn*) (Figure 1. 7) (Vogel *et al.*, 2003; Vogel *et al.*, 2004b). Meta III can also be formed when Meta II absorbs blue light (<420 nm) (Ritter *et al.*, 2004). Meta III binds all-*trans* retinal *via* a protonated Schiff-base (λ_{max} = 470 nm) (Kolesnikov *et al.*, 2003) and displays some

ability to bind and activate transducin (Zimmermann *et al.*, 2004). As shown in this dissertation, it can also bind arrestin. Interaction with G_t or arrestin converts Meta III to a Meta II-like species, and absorption of light by Meta III can also convert it to Meta II (Vogel *et al.*, 2004a). Although the physiological role of Meta III is still unclear, it appears to be a major bright-light retinal photoproduct (Lewis *et al.*, 1997).

Blue-light irradiation of Meta II also results in another photoproduct, P500 (Arnis and Hofmann, 1995; Ritter *et al.*, 2004). Although P500 appears to resemble dark-state rhodopsin by its absorbance (λ_{max} = 500 nm), it binds an all-*trans* retinal (Bartl *et al.*, 2001). The role of arrestin in the formation of these photoproducts is one topic of this dissertation.

1. 3. 3 Rhodopsin Phosphorylation

Meta II-deactivation begins with its phosphorylation (Kühn and Dreyer, 1972; Frank *et al.*, 1973) by rhodopsin kinase (RK) (Shichi and Somers, 1978; Pulvermüller *et al.*, 1993). Seven potential serine and threonine sites are present on the C-terminal tail (Hurley *et al.*, 1998). Although these multiple phosphorylation sites are speculated to be important in allowing the rods to generate reproducible electrical responses and to adapt to different light-fluxes (Wilden, 1995; Rieke and Baylor, 1998), there is conflicting evidence as to the sequence and extent of rhodopsin phosphorylation. *In vitro* analysis suggested that under continuous illumination, Ser^{343} and Ser^{338} (and to a lesser extent Ser^{334}) are the preferred RK targets (McDowell *et al.*, 1993; Ohguro *et al.*, 1993; Papac *et al.*, 1993; Ohguro *et al.*, 1994a). However, the first *in vivo* experiments showed that rhodopsin is primarily monophosphorylated, at Ser^{338} after a single bright flash and at Ser^{334} in continuous illumination (Ohguro *et al.*, 1995). The most recent studies using

transgenic mouse models indicate that multiple phosphorylations are required for efficient and reproducible deactivation of rod-cell signaling (Mendez *et al.*, 2000). Specifically, when mouse rods are exposed to a flash that photo-activates 20% of the rhodopsin, phosphates are added to Ser^{343} and Ser^{338} within the first few seconds. Within minutes, phosphorylation at Ser^{338} and at nearby threonine residues can also be detected (Kennedy *et al.*, 2001). In addition, rod cells demonstrate high-gain phosphorylation, where RK is stimulated by its interaction with Meta II to phosphorylate neighboring inactive rhodopsin proteins (Aton, 1986; Binder *et al.*, 1996; Shi *et al.*, 2005).

In the absence of arrestin, phosphorylation alone can decrease the catalytic activity of Meta II by ~50% (Xu *et al.*, 1997). Subsequent arrestin binding is necessary to completely quench Meta II activity (Wilden *et al.*, 1986), and arrestin's affinity appears to increase with the extent of phosphorylation (Wilden, 1995; Gibson *et al.*, 2000). What is the minimal phosphorylation requirement for arrestin binding? Although there are some discrepancies as to which specific residues must be phosphorylated, most studies agree that two to three phosphates are required for efficient arrestin binding (Zhang *et al.*, 1997; Brannock *et al.*, 1999; Vishnivetskiy *et al.*, 2000; Ling *et al.*, 2004). In addition, arrestin and its splice variant p44 might have different phosphorylation requirements (Ascano and Robinson, 2006). Although still not completely understood, rhodopsin phosphorylation represents a complex system that is undoubtedly useful for timely deactivation and adaptation within the rod cell (Arshavsky, 2002; Maeda *et al.*, 2003).

1. 3. 4 Retinal Schiff-base Hydrolysis and Ligand Channeling

The retinal Schiff-base of Meta II is susceptible to cleavage (Matthews *et al.*, 1963; Blazynski and Ostroy, 1984), and this reaction occurs in a temperature-dependent way that follows first-order kinetics (Farrens and Khorana, 1995). The mechanism of hydrolysis is still somewhat unclear, but recent work suggests it involves a carbinolamine intermediate that results from the attack of the Schiff-base by a water molecule in the binding pocket (Cooper *et al.*, 1987; Janz and Farrens, 2004b).

Once cleaved, all-*trans* retinal dissociates from opsin. How retinal release occurs is still largely unknown. The hydrophobic retinal may leave the protein and enter the lipid phase of the membrane (Matthews *et al.*, 1963; Wald, 1968). Alternatively, cleaved retinal may bind in possible secondary pockets within the transmembrane helices (Palczewski *et al.*, 2000; Teller *et al.*, 2001), and experimental evidence suggests that retinal may use these pockets to move unidirectionally through opsin during regeneration, Meta II decay, and release. For example, free all-*trans* retinal can form a noncovalent complex with the apoprotein opsin capable of stimulating G_t (Cohen *et al.*, 1992; Jäger *et al.*, 1996; Sachs *et al.*, 2000b), binding arrestin (Hofmann *et al.*, 1992; Sachs *et al.*, 2000a), and being phosphorylated by RK (Buczylko *et al.*, 1996). However, when 11-*cis* retinal is added to these complexes, regeneration occurs uninhibited, suggesting that the all-*trans* and 11-*cis* may occupy different sites (Heck *et al.*, 2003b). Furthermore, removal of the palmitoyl anchors from Helix VIII, or addition of detergent to the membrane, disrupts the formation of noncovalent all-*trans* retinal/opsin complexes (Sachs *et al.*, 2000b). Together, these results may suggest that all-*trans*/11-*cis* retinal enters opsin *via* an "entrance" site, which may be a cavity formed by Helices I, VII, VIII

and the palmitoyl groups (Figure 1. 5C) [2]. Once cleaved, all-*trans* retinal may leave *via* an "exit" site, which may be located on the cytoplasmic surface of opsin between Helix VIII and the C-terminal tail (Schädel *et al.*, 2003). Reduction of all-*trans* retinal by RDH may occur while retinal is bound in this exit site (Figure 1. 5C). Finally, the fact that all-*trans* retinal release during Meta II decay occurs at the same rate as regeneration with 11-*cis* retinal suggests that opsin may undergo a single concerted movement to simultaneously release and take-up retinal (Heck *et al.*, 2003b).

Once retinal is free from the protein, it can react with free amine groups to form "pseudo-photoproducts". For example, *N*-retinylidine-opsin (NRO) arises from the attachment of retinal to peripheral lysine groups in opsin other than Lys^{296} (Blazynski and Ostroy, 1984; DeGrip and Rothschild, 2000). In addition, absorbing Schiff-base species result from the condensation of retinal with phosphatidylethanolamine (Sparrow *et al.*, 2003). Although these species have little ability to activate G_t, rhodopsin kinase or arrestin, they are probably formed *in vivo* (Fishkin *et al.*, 2003).

1. 3. 5 Rhodopsin Dimerization

Many GPCRs undergo functional homo- and hetero-dimerization (Angers *et al.*, 2002; Park *et al.*, 2004). For rhodopsin, the issue of dimerization is still contentious (Chabre and le Maire, 2005). Early measurements of the diffusion rate of rhodopsin in the membrane indicated it to be near the upper limit of membrane protein mobility (10^{-9} cm^2/s) (Cone, 1972; Liebman and Entine, 1974; Poo and Cone, 1974; Wey *et al.*, 1981). For this reason, rhodopsin was long considered to operate as a monomer. However, recent atomic force microscopy (AFM) visualization of the mouse disk membrane reveals

[2] However, molecular dynamics simulations suggest that retinal may be able to enter opsin from the membrane by slipping through Helices V and VI (Huber *et al.*, 2006).

an ordered paracrystalline array of rhodopsin (see Figure 1. 3D) (Fotiadis *et al.*, 2003; Liang *et al.*, 2003). Furthermore, the addition of molecular cross-linkers to rhodopsin in native membranes results in dimers and higher oligomers that can be resolved by gel electrophoresis (Jastrzebska *et al.*, 2004; Medina *et al.*, 2004). Finally, recent fluorescence resonance energy transfer (FRET) experiments have also suggested that rhodopsin self-associates in a process that could be interpreted as dimers or higher order oligomers (Kota *et al.*, 2006; Mansoor *et al.*, 2006).

Although the issue of whether rhodopsin forms functional oligomers is still unresolved, the fact that rhodopsin exists at such high concentrations in the disk membrane means that individual rhodopsin proteins are probably closely associated with each other, whether it be by specific dimer interfaces or nonspecific aggregation. The implications of these associations on rhodopsin's interaction with G_t, RK and arrestin are a topic of current active investigation.

1. 3. 6 The Phospholipid Environment of Rhodopsin

As an integral membrane protein, rhodopsin is intimately associated with its surrounding lipids. Each rhodopsin immobilizes ~25 phospholipids and induces a reorganization of these lipids upon activation (Hessel *et al.*, 2001; Marsh and Pali, 2004). The major ROS disk phospholipids, phosphatidylcholine (PC), phosphatidylethanolamine (PE), and phosphatidylserine (PS), are enriched in the highly unsaturated long fatty acid docosahexaenoic acid (22:6*n*3) (DHA) (Anderson and Maude, 1970; Aveldano and Bazan, 1983; Aveldano, 1988). Dietary deficiency of DHA results in several visual defects (Salem *et al.*, 2001), which can probably be attributed to the fact that DHA favors proper rhodopsin function (Litman *et al.*, 2001). Rhodopsin photoactivation involves a

change in the shape and volume of the protein. The highly unsaturated chains are extremely mobile and create a very elastic membrane that lowers the free energy of photoactivation (Mitchell *et al.*, 1992; Botelho *et al.*, 2002; Feller and Gawrisch, 2005). Thus, DHA-containing membranes favor the fast photoactivation and G_t-coupling of rhodopsin needed for visual signal transduction (Mitchell *et al.*, 2001; Niu *et al.*, 2001; Mitchell *et al.*, 2003).

Recent molecular dynamics simulations also suggest that DHA may specifically intercalate between the transmembrane helices (Feller *et al.*, 2003; Grossfield *et al.*, 2006). Moreover, rhodopsin may recruit DHA-containing lipids in a solvation shell that excludes cholesterol (Polozova and Litman, 2000; Pitman *et al.*, 2005), which may help to arrange rhodopsin in lateral arrays (Fotiadis *et al.*, 2003). If rhodopsin forms oligomers in the disk membrane, lipids are probably a key determinate (Feller and Gawrisch, 2005). This possibility may explain why high detergent concentrations inhibit cross-linking of rhodopsin in membranes (Jastrzebska *et al.*, 2004).

It has long been known that purification and solubilization in detergent diminishes rhodopsin's ability to activate G_t , but this loss can be rescued to some extent by the addition of exogenous phospholipids (Bubis, 1998). G_t may interact directly with membrane lipids, since GDP-bound G_t specifically inhibits the extraction of PS from the membrane (Hessel *et al.*, 2003). In addition, Helix VIII, which is involved in G_t binding (Hamm, 2001), is anchored by palmitoyl groups and its helical structure may be dependent on the presence of PS (Krishna *et al.*, 2002). Together, these results emphasize the importance of phospholipids for rhodopsin and G_t function. This dissertation presents evidence that arrestin has similar phospholipid requirements.

1. 4 ARRESTIN STRUCTURE AND FUNCTION

1. 4. 1 Arrestin Structure

Four crystal structures of arrestin have been published (two for visual, one for β and one for cone arrestin) (Granzin *et al.*, 1998; Hirsch *et al.*, 1999; Han *et al.*, 2001; Sutton *et al.*, 2005). All arrestin structures share the same basic elongated bi-lobed structure comprised primarily of β-sheet (Figure 1. 8B). Other notable features are the small amphipathic α-helix 1 in the N-domain and the C-terminal tail (C-tail). In the crystal structure, the hydrophobic side of α-helix 1 is buried and in contact with hydrophobic residues from the N-domain and C-tail (Figure 1. 8C), and the solvent-exposed side contains primarily basic residues. The C-tail of arrestin originates within the C-domain and contacts the N-domain at the N-terminal β-sheet and α-helix 1. The C-tail also makes contact with the region between the two lobes of the protein, termed the polar core (Figure 1. 8D). This region is unusual in that it contains buried charged residues that are neutralized by their interaction with each other. As described in the next section, the C-tail and the polar core may be key players in arrestin activation.

The receptor binding interface on arrestin has been explored using a variety of methods (Kieselbach *et al.*, 1994; Ohguro *et al.*, 1994b; Smith *et al.*, 1999; Pulvermüller *et al.*, 2000; Dinculescu *et al.*, 2002; Smith *et al.*, 2004; Vishnivetskiy *et al.*, 2004; Hanson *et al.*, 2006b; Hanson and Gurevich, 2006). All studies agree that the concave surfaces of both domains are involved in receptor binding and specificity.

The visual arrestin crystal structures contain two conformers of arrestin, termed α and β, that differ mostly in three loop regions in the rhodopsin-binding surface (see Figure 1. 8B). For example, in the α-conformer, residues 155-165 form a short helix,

whereas in the β-conformer they form a strand-turn-strand. The loop containing residues 68-79 is extended in the α-conformer but is folded down into the N-domain in the β-conformer. Although small, these conformational differences may represent activating conformational changes within arrestin, and this possibility is explored in Appendix 2 of this dissertation. In fact, various biophysical methods have failed to detect any large-scale conformational changes within arrestin upon activation (Palczewski *et al.*, 1992; Wilson and Copeland, 1997; Shilton *et al.*, 2002; Carter *et al.*, 2005). However, these studies used polyanions or mutations to activate arrestin. As described below, other experimental evidence may suggest large scale conformational changes occur when arrestin interacts with the phosphorylated, active receptor.

1. 4. 2 Possible Arrestin Activation Mechanism

Arrestin shows strict selectivity for light-activated, phosphorylated rhodopsin (Rho*-P) (Kühn *et al.*, 1984; Gurevich and Benovic, 1992). How is this selectivity achieved? Over the past fifteen years, extensive mutagenesis has contributed to a theory of arrestin activation (Gurevich and Gurevich, 2004; Gurevich and Gurevich, 2006). However, until the crystal structure of the arrestin-rhodopsin complex is determined, these theories remain speculative. The high activation energy associated with arrestin binding to Rho*-P (~140 kJ/mol) suggests that considerable conformational changes are involved (Schleicher *et al.*, 1989; Pulvermüller *et al.*, 1997). The C-tail of arrestin was the first element to be implicated: removal of the C-tail by proteolysis creates an arrestin that binds phosphorylated rhodopsin independent of its exposure to light (Palczewski *et al.*, 1991a; Gurevich and Benovic, 1992). Early studies also implicated the need for negative charges to activate arrestin, since polyanions such as heparin could inhibit

arrestin binding to Rho*-P (Palczewski *et al.*, 1991b; Gurevich *et al.*, 1994). Subsequently, the mutation of certain basic residues, especially Arg^{175}, Lys^{14} and Lys^{15}, led to the idea that arrestin has a "phosphate sensor" (Gurevich and Benovic, 1993; Gurevich and Benovic, 1995; Gray-Keller *et al.*, 1997; Gurevich and Benovic, 1997; Gurevich, 1998; Vishnivetskiy *et al.*, 1999; Vishnivetskiy *et al.*, 2000; Celver *et al.*, 2002).

Once the crystal structure of arrestin was available (Hirsch *et al.*, 1999), the mutagenesis data could be put into context. The activation of arrestin might involve a sequential, two-step mechanism (summarized in Figure 1. 9). The C-terminal phosphates of Rho-P would first destabilize arrestin's basal structure, which would then expose or properly align arrestin's high affinity binding sites for Rho*. In addition, arrestin activation might involve its recruitment to the membrane by amphipathic α-helix 1 (Han *et al.*, 2001) and a significant movement of the N- and C–domains (Figure 1. 9). Because arrestin activation requires an extended and flexible hinge between the two domains (Vishnivetskiy *et al.*, 2002), a movement reminiscent of a closing clam-shell has been proposed (Gurevich and Gurevich, 2004).

Which receptor elements are required for arrestin binding? Besides the C-terminal phosphates, all three cytoplasmic loops have generally been implicated in binding, and in particular, residues Asn^{73}, Pro^{142} and Met^{143} in the first and second loops of rhodopsin (Krupnick *et al.*, 1994; Shi *et al.*, 1998; Raman *et al.*, 1999; Raman *et al.*, 2003). Rhodopsin's conserved E(D)RY sequence may also be important for arrestin binding (Shi *et al.*, 1998), and a recent study indicates that the Pro and Ala residues close to this sequence in the second cytoplasmic loop regulate β-arrestin binding to GPCRs

(Marion *et al.*, 2006). It is reasonable to hypothesize that similar structural requirements for G_t binding, including the movement of Helix VI that opens a cytoplasmic cleft and exposes the E(D)RY sequence (Farrens *et al.*, 1996; Hamm, 2001; Janz and Farrens, 2004a), might also be required for arrestin binding (Gurevich and Gurevich, 2006). However, detailed information on which residues of arrestin interact with these structural features in rhodopsin is lacking.

1. 4. 3 The Splice Variant p44

A short arrestin variant called p44 results when an intron is retained in the Ser^{369} codon of the arrestin mRNA. The protein that is translated from this mRNA is identical to full-length arrestin, except that its last 35 amino acids are replaced by a single alanine (Palczewski *et al.*, 1994a; Smith *et al.*, 1994). As most of the "inhibitory" C-tail is missing in p44 (Figure 1. 8B), this splice variant displays increased binding affinity for nonphosphorylated Rho* as well as dark Rho-P (Schröder *et al.*, 2002). Furthermore, p44 binds to Rho*-P much faster and with a lower energy of activation (~70 kJ/mol) than full-length arrestin (Pulvermüller *et al.*, 1997). Since p44 is ten times more efficient at shutting down rhodopsin signaling (Langlois *et al.*, 1996), is present in the rod outer segment even in the dark (Smith *et al.*, 1994; Schröder *et al.*, 2002), and is expressed at only ~1% of the rhodopsin concentration (Palczewski *et al.*, 1994a), it may actually be the "shut-off" protein in the dim-light operation range of the rod. The dynamics of p44's interaction with rhodopsin are described in Appendix 1 of this dissertation.

1. 4. 4 Arrestin Oligomerization

The asymmetric unit of the visual arrestin crystal structure contains a tetramer composed of a dimer of dimers (Figure 1. 8A). Each dimer is composed of an α and β

conformer, dimerized in a "head-to-tail" fashion (Hirsch *et al.*, 1999). Do these crystallographic oligomers represent a physiological association? Analytical ultracentrifugation indicates that arrestin forms dimers with a K_D of ~30 μM, and tetramers were detected at higher concentrations (~240 μM) (Schubert *et al.*, 1999). Another study reports that arrestin primarily forms tetramers (K_D ~ 110 μM) and that tetramerization is highly cooperative (Imamoto *et al.*, 2003). Arrestin concentration in the rod cell might be near that of rhodopsin (in the millimolar range) (Strissel *et al.*, 2006), so arrestin may exist primarily as dimers and tetramers in the cell. Does arrestin self-associate in the same manner as observed in the crystal structure? This dimer orientation buries a favorable ~2000 $Å^2$ (Schubert *et al.*, 1999) and some data might support it (Imamoto *et al.*, 2003), but other studies have found evidence that the C-domains of two arrestins associate (Shilton *et al.*, 2002; Francis *et al.*, 2006).

If arrestin does self-associate in a way that occludes its N- and C-domain surfaces, it is unclear how this might affect its association with microtubules. Arrestin binds microtubules within the same two concave surfaces that bind Rho*-P (Hanson *et al.*, 2006a), and this interaction may be how arrestin is sequestered in the inner segment of the dark-adapted rod cell (Nair *et al.*, 2004; Nair *et al.*, 2005). It is currently unknown whether arrestin can self-associate in the presence of microtubules and what this may mean physiologically.

Questions regarding arrestin self-association inevitably lead to questions regarding the stoichiometry of the arrestin-rhodopsin complex. Being that arrestin is bi-lobed structure that spans ~75 Å, and that the cytoplasmic face of rhodopsin is only ~35 to 40 Å across, it is tempting to speculate that a single arrestin may be able to bind a

dimer of rhodopsin (Liang *et al.*, 2003). Although the "extra-Meta II assay" [3] implies that arrestin binds rhodopsin 1:1 (Schleicher *et al.*, 1989; Pulvermüller *et al.*, 1997; Gibson *et al.*, 2000), this data would not rule out a 2:2 stoichiometry. The fact that arrestin has such a large binding surface area compared to rhodopsin has contributed to the theory that arrestin must undergo a dramatic change in its conformation in order to bind (Gurevich and Gurevich, 2004; Gurevich and Gurevich, 2006). Unfortunately, the arrestin-rhodopsin complex stoichiometry has never been directly addressed and remains unresolved.

1. 4. 5 β-Arrestin

Although β-arrestin is not the focus of this dissertation, our findings regarding visual arrestin's regulation of retinal release may be applicable to understanding β-arrestin mediated GPCR desensitization. The non-visual arrestins, β-arrestin 1 and β-arrestin 2, are expressed ubiquitously and bind to a wide variety of GPCRs in a phosphorylation-dependent way (Ferguson and Caron, 1998; Pierce and Lefkowitz, 2001). A hallmark of β-arrestin mediated attenuation is the removal of the receptor from the cell surface by virtue of β-arrestin's interaction with the internalization machinery of the cell (Laporte *et al.*, 2000; Tsao *et al.*, 2001; Claing *et al.*, 2002; Marchese *et al.*, 2003) (Figure 1. 2). The clathrin and AP2 binding domains have been localized to the loop between the C-domain and the C-tail of β-arrestin (Krupnick *et al.*, 1997; Kim and Benovic, 2002), which unfortunately, are not visible in the crystal structure (Han *et al.*, 2001) (Figure 1. 8). Interestingly, the displacement of the C-tail of β-arrestin, which is

[3] The extra-Meta II assay is an indirect measure of arrestin (or G_t) binding to Rho*-P based on the fact that Meta II is favored at the expense of Meta I (see Figure 1. 7), which can be observed using absorbance spectroscopy (Emeis and Hofmann, 1981).

reminiscent of visual arrestin's activation mechanism, may be necessary to expose the clathrin/AP2 binding domains (Xiao *et al.*, 2004). Both the N- and C-domains of β-arrestin also contain inositol hexakisphosphate binding sites (IP6) (Milano *et al.*, 2006), which may be important for β-arrestin oligomerization and recruitment to clathrin-coated pits (Gaidarov *et al.*, 1999; Balla, 2005).

Besides being a signal terminator, β-arrestin can serve as a parallel means of signal transduction (Luttrell and Lefkowitz, 2002; Perry and Lefkowitz, 2002; Lefkowitz and Shenoy, 2005). β-arrestin interacts with a long list of different proteins, including small G-proteins and guanine nucleotide exchange factors, various protein kinases, ubiquitin ligase, and others. By acting as a scaffold for these various components, β-arrestin can assist in alternative GPCR receptor signaling pathways.

Recent studies have indicated that the stability of the β-arrestin-receptor complex dictates the fate of the internalized receptor (Oakley *et al.*, 2000; Gurevich and Gurevich, 2006). If β-arrestin dissociates quickly after internalization, the receptor is likely to be quickly dephosphorylated and returned to the cell surface (Figure 1. 2). However, a very stable arrestin-rhodopsin complex often leads to degradation of the receptor. In addition, β-arrestin binding modulates the affinity of the receptor for its ligand (Gurevich *et al.*, 1997), and different ligands may impart different receptor affinities for β-arrestin. This complexity may explain why certain ligands induce receptor internalization and others do not (Keith *et al.*, 1998; Hsieh *et al.*, 1999; Kieffer and Evans, 2002).

1. 4. 6 Cone Arrestin

Cone arrestin binding of light-activated cone opsin is enhanced by phosphorylation (Zhu *et al.*, 2003), but in contrast to rod arrestin, which shows strict

selectivity for rhodopsin, cone arrestins will bind other GPCRs besides cone opsin (Sutton *et al.*, 2005). Also, the complex between cone arrestin and cone opsin is much less stable (Sutton *et al.*, 2005), perhaps because cone opsins are less stable (Kefalov *et al.*, 2005). This might be why light-dependent cone arrestin migration within the cone cell is not as complete as seen for rod arrestin (Zhu *et al.*, 2002; Elias *et al.*, 2004). The fast dissociation of the complex would also allow the fast rates regeneration needed for cone cell function in bright light (Mata *et al.*, 2002).

1. 5 DISSERTATION OVERVIEW

The focus of this dissertation is to understand how the interaction between rhodopsin and arrestin affects the release of the retinal chromophore and rhodopsin photoproduct formation. These investigations were made possible by the development of novel methods for observing arrestin binding and release, which employ a fluorescently labeled arrestin mutant and mixed micelles of detergent and phospholipid that preserve arrestin function.

Chapter 2 describes the characterization of two fluorescently labeled arrestin mutants, I72C and S251C. The probes on these labeled mutants are located in the arrestin-rhodopsin interface, and upon binding light-activated, phosphorylated rhodopsin, their spectral characteristics change. Importantly, these spectral changes can be used to track arrestin's interaction with the receptor over time. For example, by simultaneously monitoring arrestin and retinal, we found that arrestin and retinal release appear to be directly linked in native membranes. Intriguingly, the fluorescently labeled arrestin mutants also showed that arrestin binds a post-Meta II decay product. However, the

identification of this photoproduct was not possible due to the experimental challenges of using membranes.

Earlier spectroscopic and structural studies of arrestin-rhodopsin interactions have been hampered by the inability of arrestin to bind purified rhodopsin in detergent. As described in Chapter 3, we discovered that acidic phospholipids are required for arrestin to bind rhodopsin in detergent. Besides being interesting from a functional point of view, this discovery allowed us to spectroscopically observe arrestin's interaction with rhodopsin, free of scattering artifacts. As described in both Chapters 3 and 4, we found that arrestin inhibits retinal release and Meta III formation from rhodopsin in mixed micelles. Arrestin stabilizes and "traps" retinal in the binding pocket with an intact Schiff-base and a Meta II-like absorbance. Furthermore, arrestin can interact with Meta III, formed either by thermal decay or blue-light irradiation, and convert it to a Meta II-like species. Altogether, these findings suggest that arrestin may play a protective role in the rod cell by limiting retinal release in bright-light conditions. The physiological evidence for this possibility and the implications on the visual cycle are discussed.

Another intriguing finding described in Chapter 3 is that retinal and arrestin release are no longer linked in mixed micelles as they are in native membranes. In the presence of acidic phospholipids, ~50% of retinal is released even though arrestin remains bound to the receptor in a long-lived complex. Although the cause of this phenomenon is still unresolved, its implications on the arrestin-rhodopsin complex are discussed in Chapters 3 and 5.

Finally, the appendices of this dissertation present on-going investigations related to this dissertation project. Appendix 1 explores p44 - rhodopsin interactions and how

p44 is suited to be the dim-light regulator of rhodopsin signaling. Appendix 2 presents data that indicate that the loop that contains Ile^{72} (Figure 1. 8B) may undergo a folded to extended conformational change upon arrestin activation.

Figure 1. 1 **G-protein coupled receptor signaling.** GPCRs share a common structure of seven transmembrane α-helices with an extracellular N-terminus and a cytoplasmic C-terminus. Although different GPCRs bind different ligands and interact with different cognate G-proteins, they share a common mechanism of signal transduction. Coupling of the heterotrimeric G-protein to the ligand-bound, "active" receptor induces guanine nucleotide exchange in the α subunit, which causes the subunits to dissociate. The subunits then interact with effectors, which eventually culminates in a cellular response. Different G-proteins interact with different effectors, and a few examples for G_α are listed (Hamm, 1998). Signal amplification, a hallmark of GPCR signaling, results because a single activated GPCR can interact with many G-proteins, and the dissociated subunits can then interact with many downstream effectors. Figure is derived from (Bockaert and Pin, 1999). *AC*, adenylyl cyclase; *PLC*, phospholipase C; *PDE*, cGMP phosphodiesterase.

Figure 1. 1

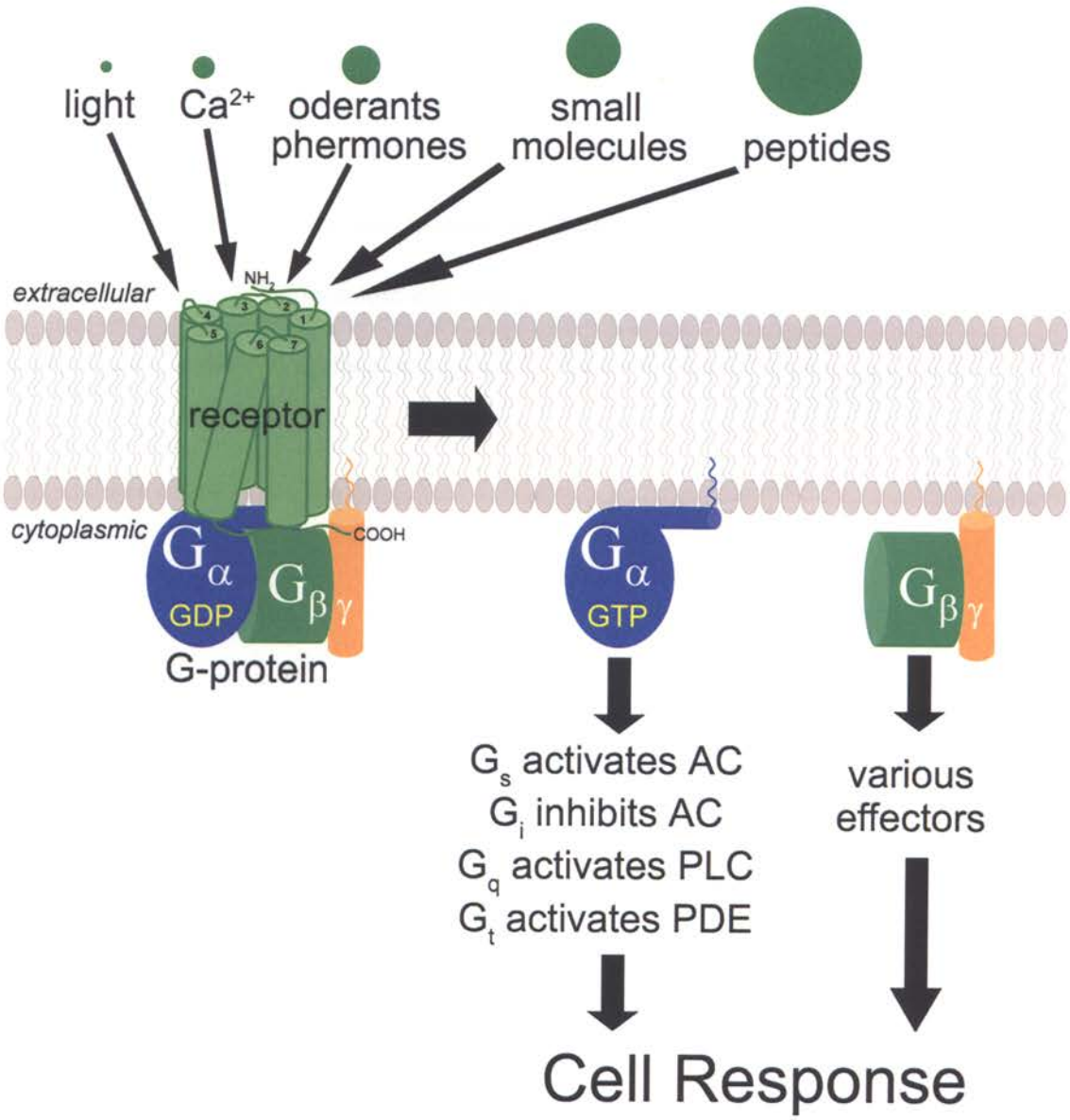
light
Ca2+
oderants
phermones
small
molecules
peptides
extracellular
NH2
receptor
cytoplasmic
COOH
Gα
GDP
Gβγ
G-protein
Gα
GTP
Gβγ
Gs activates AC
Gi inhibits AC
Gq activates PLC
Gt activates PDE
various
effectors
Cell Response

Figure 1. 2 **GPCR signaling attenuation by β-arrestin.** Ligand-bound receptors bind heterotrimeric G-proteins and catalyze their dissociation. Free $G_{\beta\gamma}$ subunits recruit G-protein coupled receptor kinases (GRKs) to the membrane, where they phosphorylate the C-terminal tail of the receptor (Ferguson and Caron, 1998; Lodowski *et al.*, 2003). Activated, phosphorylated receptor is bound by β-arrestin, which blocks further G-protein activation. β-arrestin also targets the receptor to clathrin-coated pits, where the receptor is internalized into acidic endosomes. Internalized receptor can either be recycled back to the cell surface or degraded. Figure is from (Pierce *et al.*, 2002).

Figure 1. 2

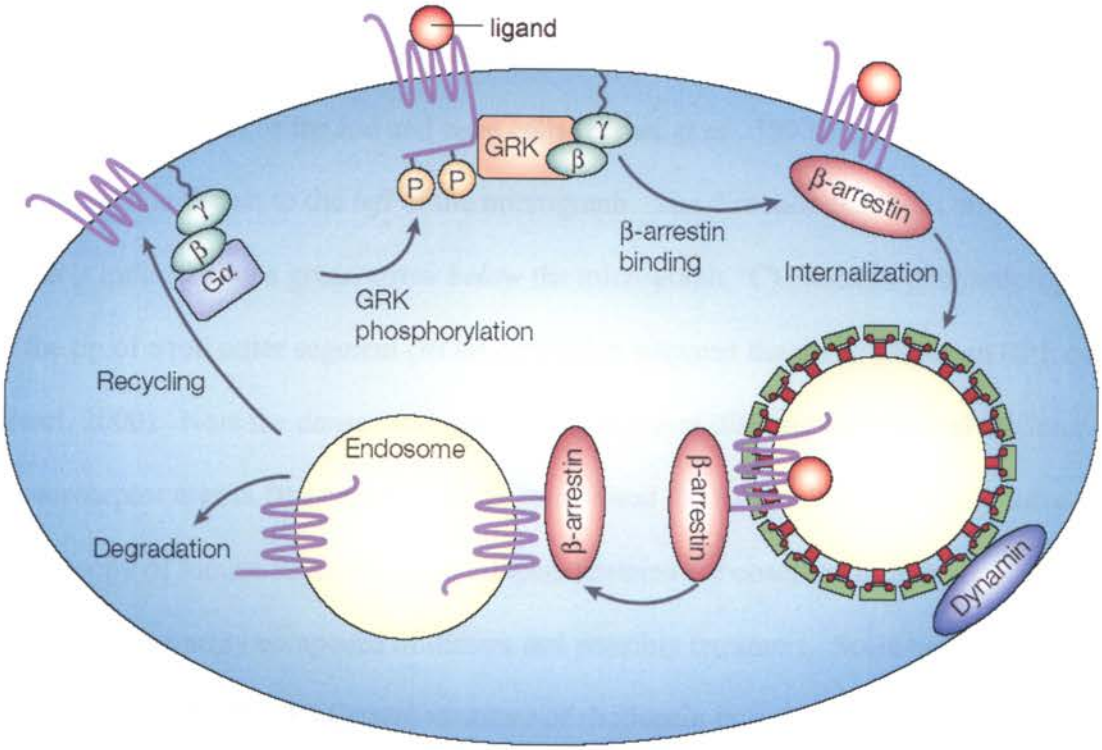
ligand
GRK
γ
β
P
P
β-arrestin
β-arrestin binding
Internalization
γ
β
Gα
GRK phosphorylation
Recycling
Endosome
β-arrestin
β-arrestin
Degradation
Dynamin

Figure 1. 3 **Structure of the retina, rod cells and rhodopsin at different levels of magnification.** **A)** Cartoon illustration of the human eye. The retina is shown as a red rim at the back of the eye-cup (Kolb *et al.*, 2006). **B)** Light micrograph of a cross section of the primate retina showing the choroid (*CH*), Bruch's membrane (*BM*), the retinal pigment epithelium (*RPE*) and the outer segments (*OS*), inner segments (*IS*) and the outer nuclear layer (*ONL*) of the rod and cone cells (Fisher *et al.*, 1993). A cartoon schematic of a rod cell is shown to the *left* of the micrograph. The direction that light enters the retina is indicated by a green arrow *below* the micrograph. **C)** Electron photomicrograph of the tip of a rod outer segment (*ROS*) embedded between the microvilli of an RPE cell (Saari, 2000). Note the dense stacking of outer segment disk membranes and the inter-photoreceptor matrix (the space between the rod and the RPE cell). **D)** Atomic force microscopy of mouse ROS disks. Rhodopsin proteins are observed to form a paracrystalline array composed of dimers and possibly tetramers. Scale bar = 50 nm (Fotiadis *et al.*, 2003). **E)** Crystal structure of rhodopsin in a phospholipid bilayer. The peptide backbone is modeled as a *red ribbon*, the chromophore 11-*cis* retinal is modeled in *yellow*, N-linked oligosaccharides in the N-terminus are *black*, and the two palmitoyl groups that anchor Helix 8 are modeled in *blue*. Model was generated using the program DS Viewer Pro 5.0 (Accelrys, Inc.) using the coordinates derived from the crystal structure (1U19) (Okada *et al.*, 2004).

Figure 1. 3

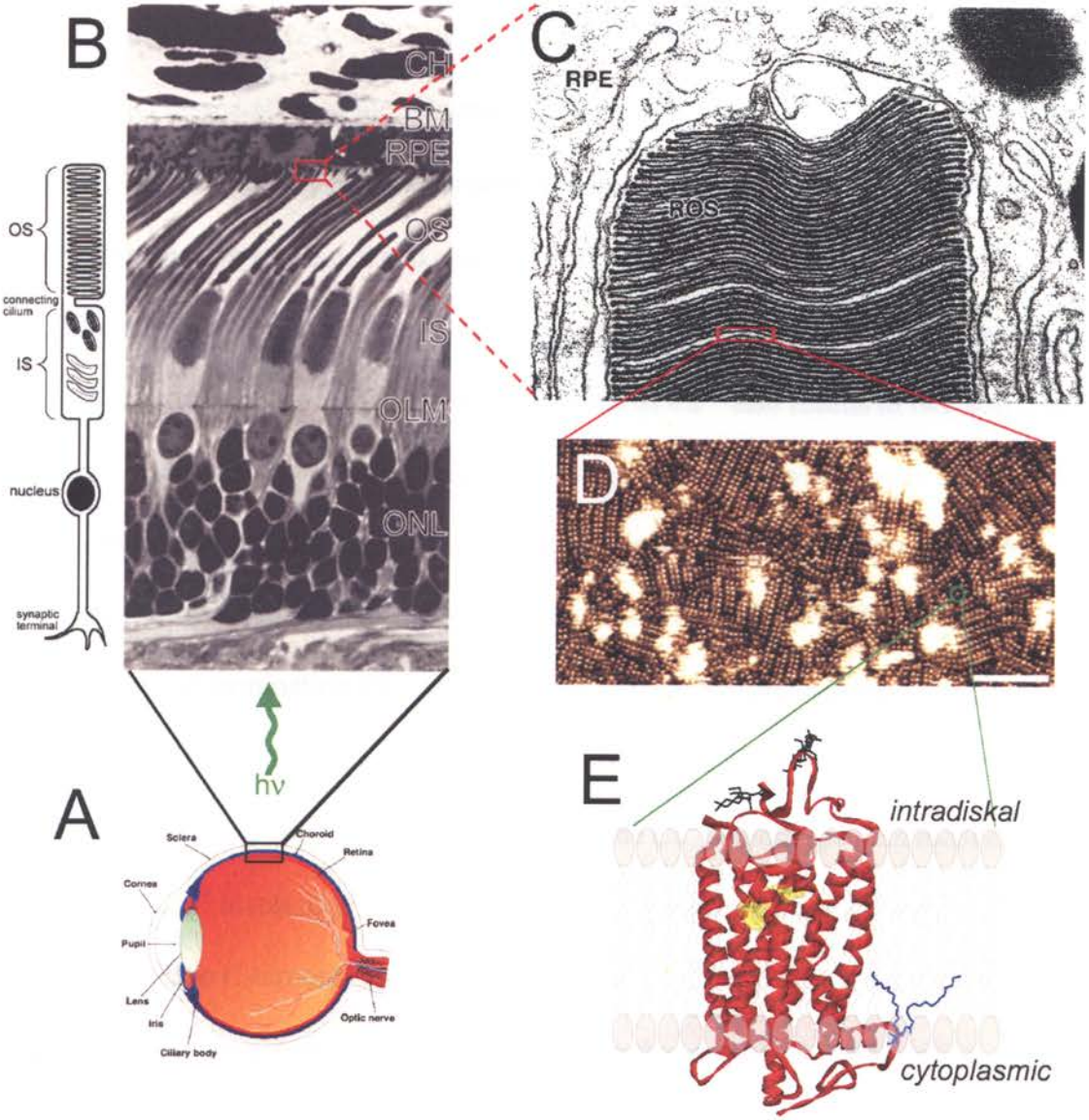
B
CH
BM
RPE
OS
IS
OLM
ONL
OS
connecting cilium
IS
nucleus
synaptic terminal
C
RPE
ROS
D
E
intradiskal
cytoplasmic
hν
A
Sclera
Choroid
Retina
Cornea
Fovea
Pupil
Lens
Iris
Optic nerve
Ciliary body

Figure 1. 4 **The phototransduction cascade.** **A)** In the dark, the rod cell is depolarized, since its cGMP-gated channels remain open. **B)** Signal propagation begins with the absorption of light by rhodopsin, yielding the active Metarhodopsin II (M II), which couples with the G-protein transducin (G_t) to catalyze guanine nucleotide exchange and dissociation of the subunits. $G_t\alpha$ activates cGMP phosphodiesterase (PDE) by removing the inhibitory constraints of its γ-subunit, resulting in a rapid decrease in cGMP concentration in the cell and closure of cGMP-gated channels. Since the Na^+ - Ca^{2+}, K^+ exchanger remains active, the cell hyperpolarizes (Stryer, 1988; Palczewski and Saari, 1997; Arshavsky *et al.*, 2002). The depletion of Ca^{2+} also results in two adaptation events: 1) the dissociation of calmodulin (CaM) from cGMP-gated channels increases the affinity of the channel for cGMP, and 2) guanylate cyclase activating protein (GCAP) to binds guanylate cyclase (GC) and stimulates the production of cGMP (Burns and Baylor, 2001). **C)** Signal termination can be divided into two parts: deactivation of the receptor (*upper scheme*) and deactivation of $G_t\alpha$ (*lower scheme*). In the dark, when Ca^{2+} levels are high, rhodopsin kinase (RK) is sequestered by the Ca^{2+}-binding protein recoverin (Rec). When Ca^{2+} levels drop due to activation, RK is released from Rec and phosphorylates the C-terminal tail of M II (Sallese *et al.*, 2000). RK also interacts the $G_t\beta\gamma$, which both sequesters $G_t\beta\gamma$ and recruits RK to the membrane (Lodowski *et al.*, 2003). Phosphorylated M II is bound by arrestin, which blocks further interactions with G_t (Kühn *et al.*, 1984; Wilden *et al.*, 1986). GTP-bound $G_t\alpha$ is inactivated by stimulating its intrinsic GTPase activity. This is accomplished by the protein RGS9-1 in complex with Gβ5L and the membrane anchor R9AP. GDP-bound $G_t\alpha$ dissociates from PDE and

returns it to the inactive state (Slep *et al.*, 2001; Ridge *et al.*, 2003; Burns and Arshavsky, 2005).

Figure 1. 4

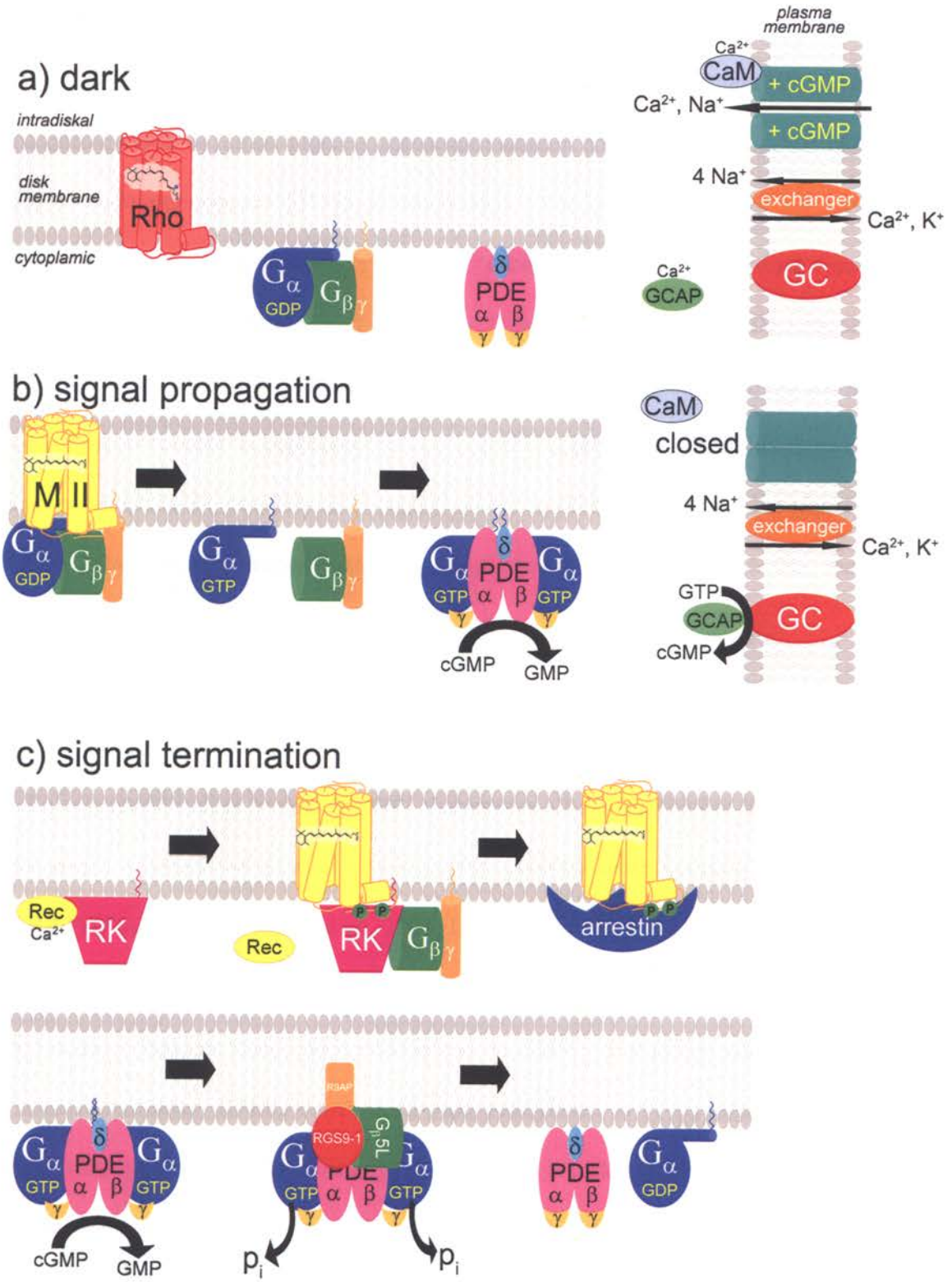
a) dark
intradiskal
disk membrane
Rho
cytoplamic
Gα GDP
Gβγ
δ PDE α β γ γ
plasma membrane
Ca2+
CaM
+ cGMP
Ca2+, Na+
+ cGMP
4 Na+
exchanger
Ca2+, K+
Ca2+
GCAP
GC
b) signal propagation
M II
Gα GDP
Gβγ
Gα GTP
Gβγ
Gα GTP
δ PDE α β γ γ
Gα GTP
cGMP
GMP
CaM
closed
4 Na+
exchanger
Ca2+, K+
GTP
GCAP
GC
cGMP
c) signal termination
Rec
Ca2+
RK
Rec
RK
Gβγ
arrestin
Gα GTP
δ PDE α β γ γ
Gα GTP
cGMP
GMP
RGAP
RGS9-1
Gβ5L
Gα GTP
δ PDE α β γ γ
Gα GTP
pi
pi
δ PDE α β γ γ
Gα GDP

Figure 1. 5 **The retinoid cycle.** The main steps of the vertebrate retinoid cycle and the sub-cellular compartmentalization of each enzyme is illustrated in this schematic diagram. Part (**A**) shows an overall view of the cycle, and Parts (**B**) and (**C**) show magnified views of retinal pigment epithelium smooth endoplasmic reticulum (RPE SER) and the rod outer segment (ROS), respectively.

Photoactivation of rhodopsin, Meta II decay, and the reduction of all-*trans* retinal to all-*trans* retinol by the NADPH-dependent retinal dehydrogenase (RDH) occur in the rod outer segment (ROS) disks (Saari, 2000). Retinal that is released on the intradiskal side of the membrane is transported to the cytosolic side by the ATP-binding cassette transporter (ABCR), possibly as an adduct with phosphatidylethanolamine (Sun *et al.*, 1999). However, it is unclear what percentage of retinal is transported by this mechanism (Weng *et al.*, 1999).

All-*trans* retinol leaves the ROS and is chaperoned across the inter-photoreceptor matrix space by the inter-photoreceptor retinoid binding protein (IRBP) to the RPE. The cellular retinol binding protein (CRBP) chaperones all-*trans* retinol to the enzymatic machinery, where it is first esterified to a retinylester by lecithin retinol acyl transferase (LRAT) (Saari, 2000; McBee *et al.*, 2001; Lamb and Pugh, 2004). Large quantities of all-*trans* retinylester (2.5 times all the retinal in the ROS) are also stored within the RPE (*not shown*) (Bridges *et al.*, 1982; Imanishi *et al.*, 2004). The retinal chaperone and "isomerohydrolase" RPE65 converts all-*trans* retinylester to 11-*cis* retinol and free fatty acid (Moiseyev *et al.*, 2005). Finally, 11-*cis* retinol is oxidized to 11-*cis* retinal by 11-*cis* retinol dehydrogenase (11-*cis* RDH) and chaperoned to the RPE plasma membrane by a cellular retinal binding protein (CRALBP). 11-*cis* retinal traverses the inter-

photoreceptor matrix to the ROS, where it can bind opsin to form rhodopsin (Saari, 2000; McBee *et al.*, 2001; Lamb and Pugh, 2004).

In Part **(C)** of the figure, the retinal is illustrated as entering and exiting opsin in different sites, as has been proposed for "ligand channeling" (Schädel *et al.*, 2003). The abbreviations attached to the end of the retinoids in the illustration denote the form of the retinoid (*AL*, aldehyde; *OL*, alcohol; *E*, ester). Figure is adapted from (Lamb and Pugh, 2004).

Figure 1. 5

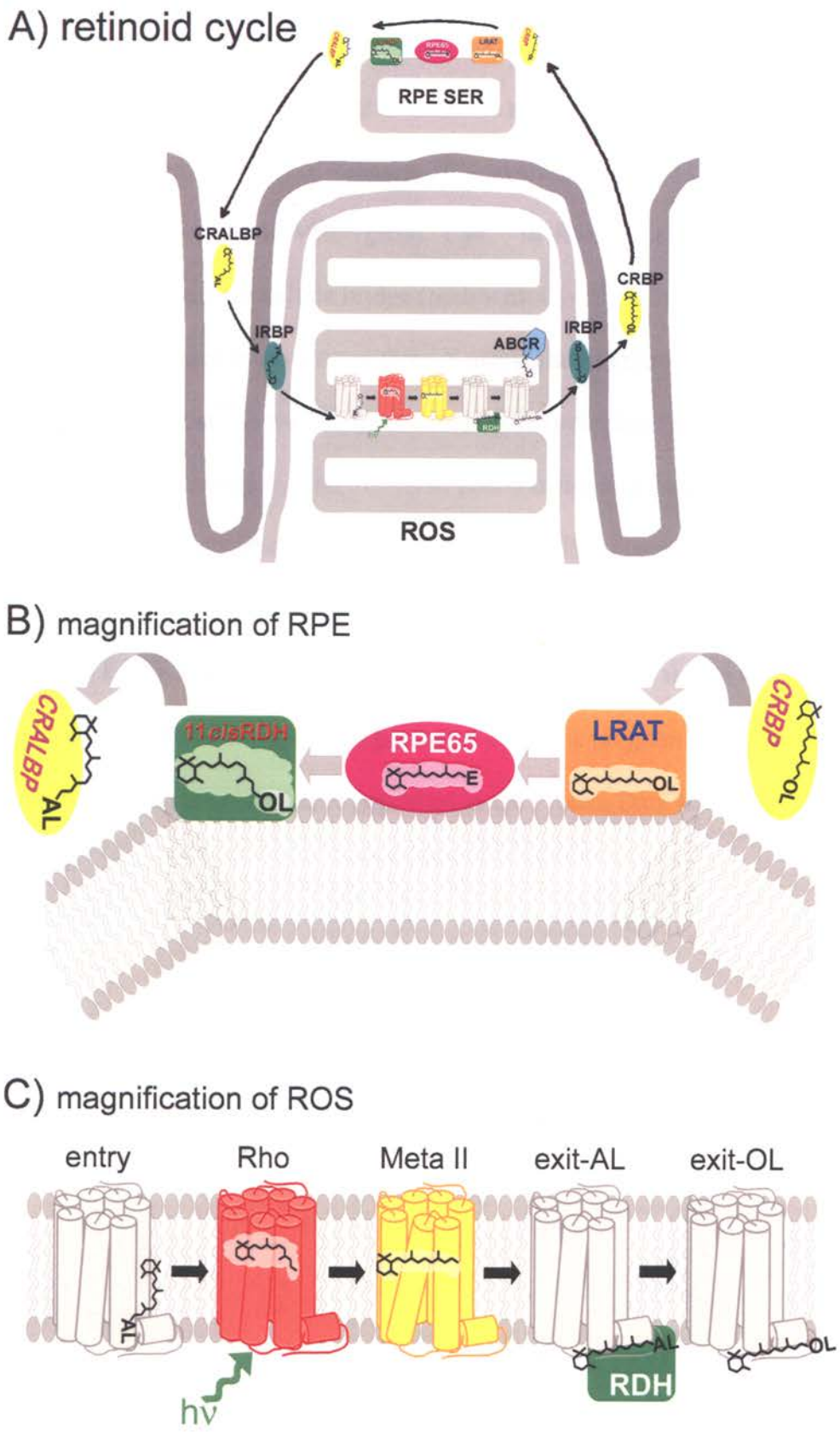
A) retinoid cycle
RPE SER
CRALBP
IRBP
ABCR
IRBP
CRBP
ROS
B) magnification of RPE
CRALBP
AL
11cisRDH
OL
RPE65
E
LRAT
OL
CRBP
OL
C) magnification of ROS
entry
Rho
Meta II
exit-AL
exit-OL
AL
hν
AL
RDH
OL

Figure 1. 6 **Crystal structure of bovine rhodopsin.** Two faces of rhodopsin are shown, related by a 180° rotation about an axis normal to the membrane plane. The intradiskal N-terminus and cytoplasmic C-terminus are labeled, and the transmembrane helices are color-coded (I – *red*; II – *orange*; III – *greenish yellow*; IV – *greenish blue*; V – *blue*; VI – *pink*; VII – *purple*; VIII – *gray*). Cys^{187} in the extracellular (or intradiskal) loop II (E-II, *blue*) forms a disulfide bridge (*teal*) with Cys^{110} Helix III. Carbohydrate groups consisting of three mannose and three *N*-acetylglucosamines ($Man_3GlcNAc_3$) are attached at Asn^2 and Asn^{15} in the N-domain, and lipids (palmitate) are attached at Cys^{322} and Cys^{323} in C-terminal region. Both of these post-translational modifications are modeled in *black*. The chromophore 11-*cis* retinal (11-RET) is covalently attached to Lys^{296} in Helix VII and is modeled in *yellow*. Two important GPCR motifs involved in activation, the E(D)RY in Helix III and NPXXY in Helix VII, are shown with spheres at their Cα positions. These models were generated using the program DS Viewer Pro 5.0 (Accelrys, Inc.) using the coordinates deposited in the Protein Data Bank (1U19) (Okada *et al.*, 2004).

Figure 1. 6

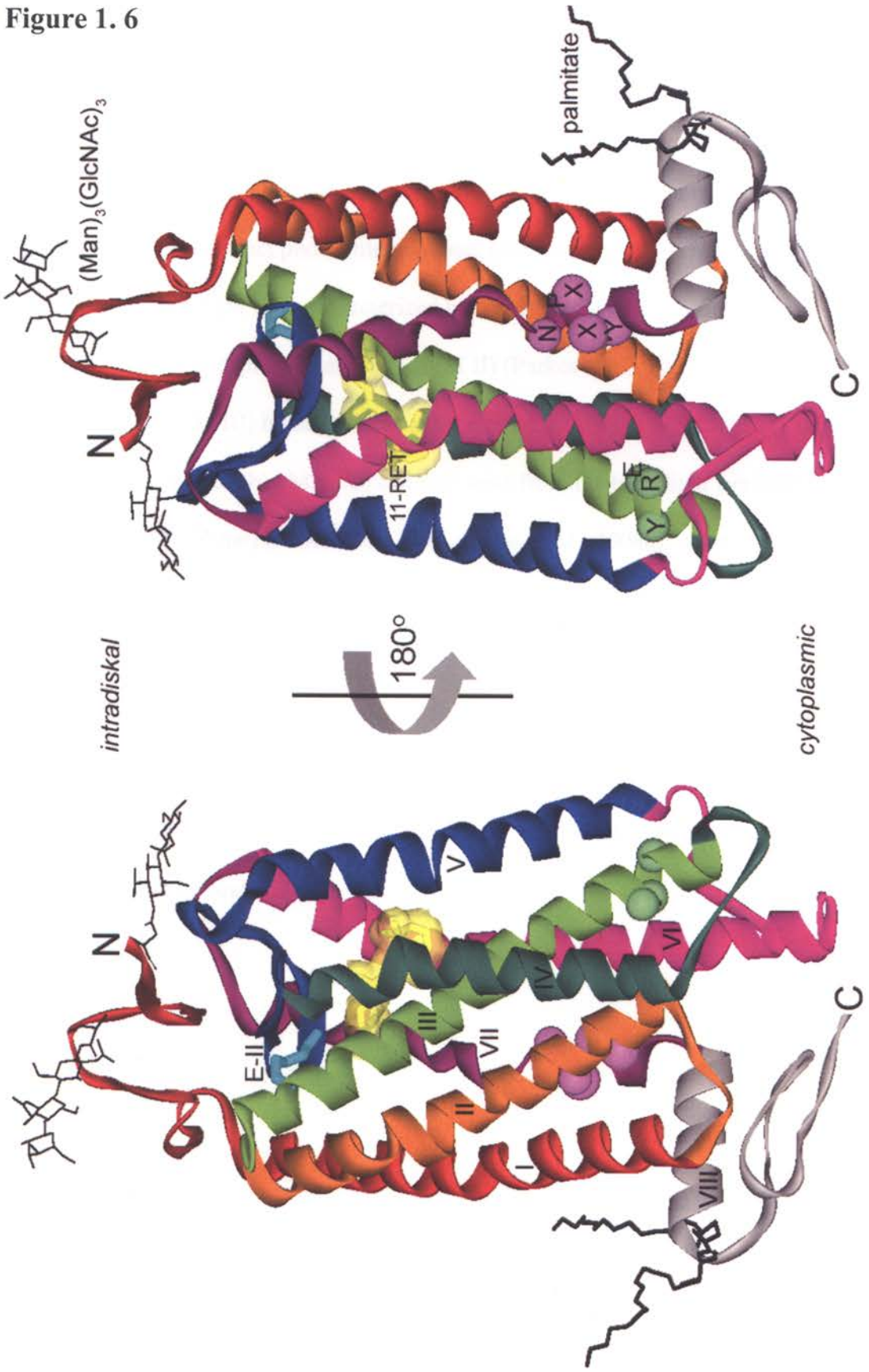
(Man)3(GlcNAc)3
palmitate
N
C
11-RET
intradiskal
180°
cytoplasmic
E-II
I
II
III
IV
V
VI
VII
VIII

Figure 1. 7 **Rhodopsin photo-intermediates.** This schematic illustrates the relative time course of rhodopsin photoproduct formation. Within femtoseconds after the absorption of light (*green arrow, >495 nm*), the 11-*cis* retinal of rhodopsin (Rho) isomerizes to all-*trans*. Over the next few milliseconds, the protein relaxes through a series of spectrally distinct photo-intermediates (Menon *et al.*, 2001). The first long-lived intermediate, Meta I (M I), is characterized by a protonated Schiff-base and is in equilibrium with the deprotonated Meta II (M II) (Parkes *et al.*, 1999). Meta I can also decay to Meta III (M III) by an isomerization around the retinal Schiff-base (Vogel *et al.*, 2003; Vogel *et al.*, 2004b). Meta III can also arise from the blue-light irradiation of Meta II (*blue arrow, <420 nm*) (Ritter *et al.*, 2004; Vogel *et al.*, 2004a). At physiological temperatures, Meta II decays to opsin and free all-*trans* retinal within a few minutes (Matthews *et al.*, 1963; Sommer *et al.*, 2005). Meta III also decays to opsin and free retinal, although this process occurs much slower (Heck *et al.*, 2003a), and it is unclear whether this occurs directly or through additional photo-intermediates. In the figure, the retinal conformation, Schiff-base protonation state, and the absorbance of each photoproduct are indicated.

Figure 1. 7

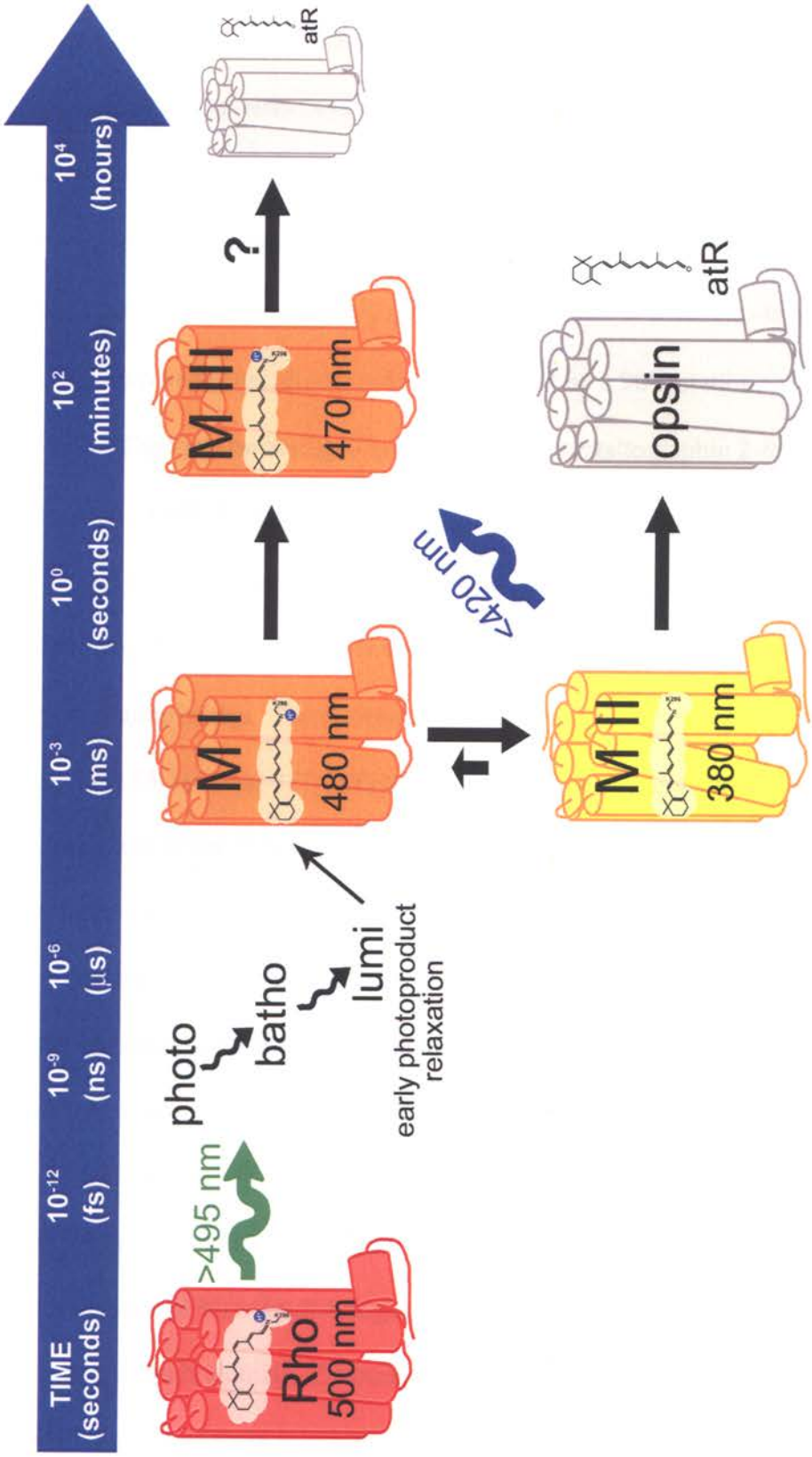
TIME
(seconds)
10-12
(fs)
10-9
(ns)
10-6
(μs)
10-3
(ms)
100
(seconds)
102
(minutes)
104
(hours)
Rho
500 nm
>495 nm
photo
batho
lumi
early photoproduct
relaxation
M I
480 nm
M II
380 nm
420 nm
M III
470 nm
?
opsin
atR
atR

Figure 1. 8 **Crystal structure of visual arrestin.** **A)** The crystallographic asymmetric unit of visual arrestin contains a tetramer, or a dimer of dimers. Each dimer pair is composed of two arrestin conformers, α and β. The domains of the α conformer are colored: N-domain, *blue*; C-domain, *orange*; C-tail, *green*. The domains of the β conformers are colored the same, but in lighter hues. In each dimer, the N-domain of the α conformer interacts with the C-domain of the β conformer in a head-to-tail configuration. Two views are shown, which are related by a 90° rotation about the horizontal axis. The view on the *right* is down the noncrystallographic 2-fold rotation axis (Hirsch *et al.*, 1999; Schubert *et al.*, 1999). **B)** The structure of the α-conformer of arrestin is shown with the same domain coloring as described in (A). The region shown in *gray*, containing residues 363-371, is not visible in the crystal structure and is modeled as a short polyalanine bridge. The regions that differ most between α and β conformers (residues 68-79, 155-165, and 337-347) are indicated. The *straight dotted line* indicates the approximate site of the C-terminal truncation (residue 370) found in the splice variant p44 (Palczewski *et al.*, 1994a). Residues believed to be important in arrestin activation are illustrated in the *dashed ellipses* (acidic, *red*; basic, *blue*; hydrophobic, *green*). These areas are elaborated in (C) and (D). **C)** The three-element interaction between hydrophobic residues in the N-terminal β-strand 1 (Ile^{12}), α-helix 1 (Leu^{103}, Leu^{107}, Leu^{111}) and the C-tail (Phe^{375}, Phe^{377}) might be destabilized when Lys^{14} and Lys^{15} interact with the phosphorylated tail of rhodopsin (Vishnivetskiy *et al.*, 2000). **D)** The polar core consists of a network of buried salt-bridges (Arg^{175} – Asp^{296} and Asp^{30} – Arg^{382} – Asp^{303}) that holds together the N-domain, C-domain and the C-tail (Gurevich and Gurevich, 2004). The disruption of these interactions by the phosphorylated tail of rhodopsin may

be a key step in the activation of arrestin (Vishnivetskiy *et al.*, 1999). The views in (C) and (D) are slightly rotated compared to that shown in (B), and parts of the protein are omitted for clarity. All models were generated with the program DS Viewer Pro 5.0 (Accelrys, Inc.) using the coordinates deposited in the Protein Data Bank (1cf1) (Hirsch *et al.*, 1999).

Figure 1. 8

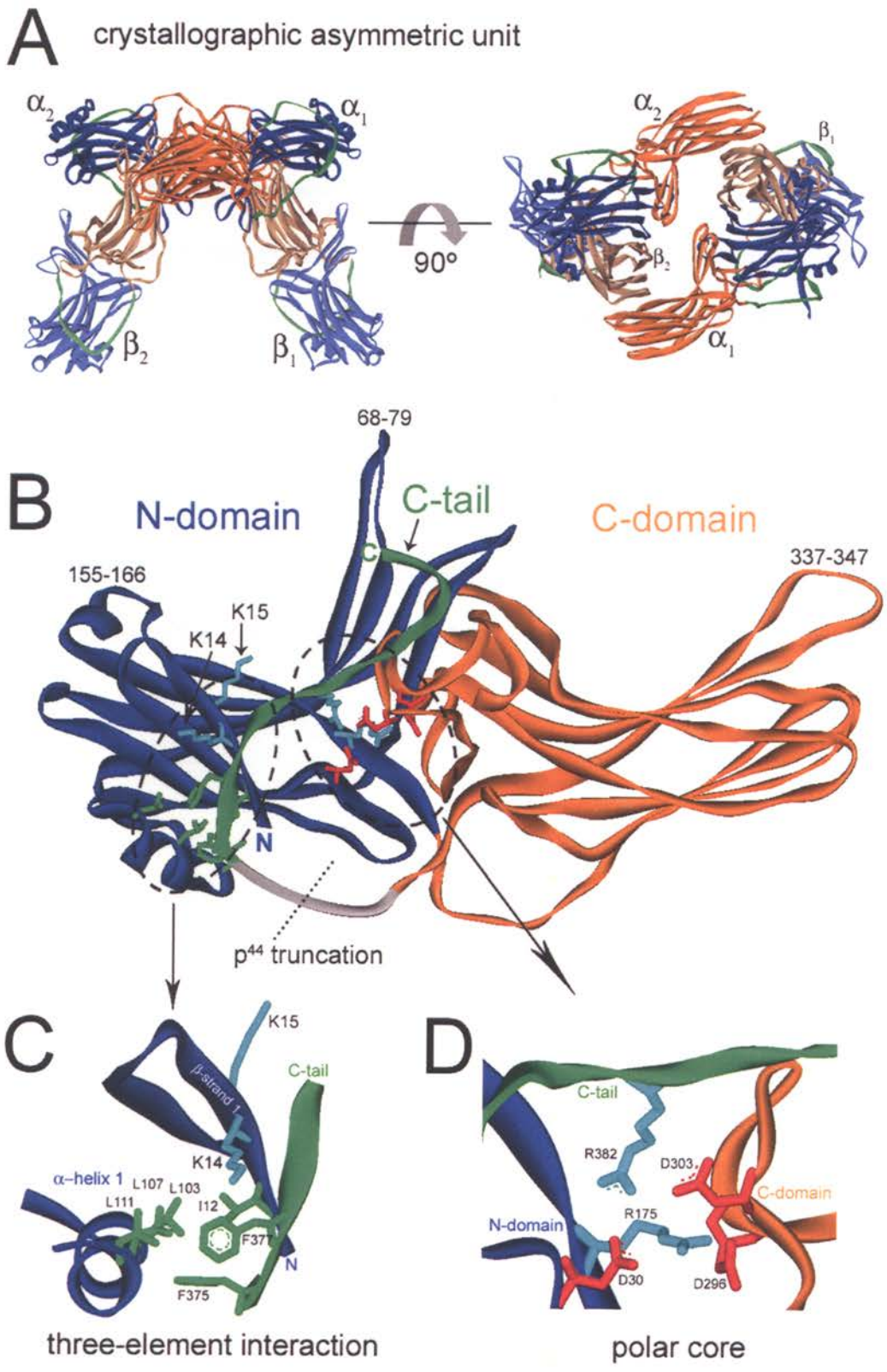
A
crystallographic asymmetric unit
α2
α1
β2
β1
90°
α2
β1
β2
α1
B
N-domain
C-tail
C-domain
68-79
155-166
337-347
K15
K14
C
N
p44 truncation
C
K15
β-strand 1
C-tail
K14
α–helix 1
L107
L103
L111
I12
F371
N
F375
three-element interaction
D
C-tail
R382
D303
C-domain
N-domain
R175
D30
D296
polar core

Figure 1. 9 **Arrestin activation mechanism.** This cartoon illustrates a possible mechanism by which arrestin recognizes and binds activated, phosphorylated receptor. The inactive basal state of arrestin (*left*) is characterized by an intact polar core (*blue-red dots*) that holds together the N- (*pink*) and C- (*blue*) domains as well as the C-tail (*yellow*). Phosphate residues (*pink*) on the C-terminal tail of the receptor (*green*) would first be recognized by basic residues (Lys^{14} and Lys^{15}, *blue semicircles*) in arrestin's N-domain. This interaction would destabilize the three-element interaction (Figure 1. 8C) between the amphipathic α-helix, the N-terminal β-strand, and the C-tail. Ultimately, this destabilization would free the C-tail, open the polar core, and allow the N-and C-domains to move relative to each other (*right*). This event might expose high affinity binding sites on arrestin for the cytoplasmic face of the activated receptor and could be further enhanced by the anchoring of α-helix 1 in the membrane. Figure is from (Han *et al.*, 2001).

Figure 1. 9

Chapter 2

Dynamics of Arrestin-Rhodopsin Interactions:

Arrestin and Retinal Release are Directly Linked Events

Martha E. Sommer [‡], W. Clay Smith [§], and David L. Farrens [‡]

[‡] Department of Biochemistry and Molecular Biology, Oregon Health & Science University, Portland, OR 97239-3098, USA

[§] Departments of Ophthalmology and Neuroscience, University of Florida, Gainesville, FL 32610-0284, USA

2. 1 SUMMARY

In this study, we address the mechanism of visual arrestin release from light-activated rhodopsin using fluorescently labeled arrestin mutants. We find that two mutants, I72C and S251C, when labeled with the small, solvent-sensitive fluorophore monobromobimane, exhibit spectral changes only upon binding light-activated, phosphorylated rhodopsin. Our analysis indicates that these changes are probably due to a burying of the probes at these sites in the rhodopsin-arrestin or phospholipid-arrestin interface. Using a fluorescence approach based on this observation, we demonstrate that arrestin and retinal release are linked and are described by similar activation energies. However, at physiological temperatures, we find that arrestin slows the rate of retinal release ~2-fold and abolishes the pH dependence of retinal release. Using fluorescence, EPR, and biochemical approaches, we also find intriguing evidence that arrestin binds to a post-Meta II photodecay product, possibly Meta III. We speculate that arrestin regulates levels of free retinal in the rod cell to help limit the formation of damaging oxidative retinal adducts. Such adducts may contribute to diseases like atrophic age-related macular degeneration (AMD). Thus, arrestin may serve to both attenuate rhodopsin signaling and protect the cell from excessive retinal levels under bright light conditions.

All experiments and data analysis reported in this chapter were performed by the author of this dissertation. Purified arrestin mutants I72C and S251C were supplied by Dr. W. Clay Smith. This work has been previously published (Sommer, M.E., Smith, W.C., and Farrens, D.L. (2005) *J. Biological Chemistry* **280**: 6861-6871) and presented (platform talk at the 49th Annual Biophysical Society Meeting, Long Beach, CA, 2005).

2. 2 INTRODUCTION

The visual photoreceptor rhodopsin is perhaps the best model system for understanding the mechanisms used in G-protein-coupled receptor (GPCR) signaling, as detailed information exists on the structures and dynamic interactions of the protein constituents (Ridge *et al.*, 2003). Visual activation begins with absorption of light by the 11-*cis*-retinal chromophore in rhodopsin. The photoactivated form of rhodopsin, Rho* or "Meta II," interacts with and activates the G-protein transducin, which exchanges nucleotide and then diffuses to interact with downstream effectors. Signaling by Rho* is terminated by slow thermal decay and the release of retinal. Alternatively, signaling can be quickly terminated by a process that begins with phosphorylation of rhodopsin's C-terminal tail through the action of rhodopsin kinase (Kühn, 1978; Maeda *et al.*, 2003). The phosphorylated Rho* is then bound by arrestin, which stops signaling by physically occluding the G-protein binding site (McBee *et al.*, 2001; Gurevich and Gurevich, 2004).

In the present study, we address how these two inactivation mechanisms are related and, specifically, what governs arrestin release from rhodopsin. Arrestin is known to bind to phosphorylated Meta II, a form in which the photolyzed chromophore all-*trans*-retinal is still attached to the receptor by a deprotonated Schiff base. Arrestin does not bind phosphorylated opsin, but all-*trans* retinal added exogenously can stimulate arrestin binding to phosphorylated opsin (Hofmann *et al.*, 1992; Sachs *et al.*, 2000a). Early studies showed indirectly that retinal release and arrestin release are probably interrelated events (Hofmann *et al.*, 1992; Palczewski *et al.*, 1994b). However, how these processes are linked or whether arrestin binds other photo-intermediates of rhodopsin (such as the storage form Meta III) is still unknown.

In this chapter, we demonstrate that arrestin binding and release can be directly observed in real time by monitoring spectral changes in fluorescently labeled arrestin mutants. Our studies employed two different cysteine mutants of arrestin, I72C and S251C, two sites that lie within the experimentally proposed rhodopsin-binding surface on arrestin (Pulvermüller *et al.*, 2000; Dinculescu *et al.*, 2002; Smith *et al.*, 2004; Vishnivetskiy *et al.*, 2004). When these mutants are labeled with the fluorescent probe monobromobimane and incubated with phosphorylated rhodopsin, they exhibit changes in fluorescence upon rhodopsin photoactivation. Importantly, these changes do not occur in the presence of nonphosphorylated rhodopsin, and subsequent analysis suggests that the spectral changes are a direct result of interaction with activated, phosphorylated rhodopsin. In the present study, we demonstrate how these spectral changes can be exploited to obtain information on the rate of arrestin release. Our results provide direct evidence that arrestin and retinal release are indeed linked events and that arrestin slows the rate of retinal release from Rho*-P by ~2-fold, possibly through a kinetic trap mechanism. In addition, we find that arrestin binding eliminates the pH dependence of retinal release. Surprisingly, we find that a subfraction of arrestin consistently remains bound to phosphorylated rhodopsin long after the decay of the active Meta II species. This latter result provides compelling evidence that arrestin binds Meta III or some other photodecay product.

2. 3 MATERIALS and METHODS

2. 3. 1 Materials

Frozen bovine retinas were obtained from Lawson and Lawson, Inc. (Lincoln, NE). GBX red light filters were purchased from Eastman Kodak Co., and [γ-^{32}P]ATP was from PerkinElmer Life Sciences. Nitrocellulose filters (0.45 μm) and Biomax centrifugal concentrators (10-kDa cut-off) were from Millipore Corp. (Bedford, MA). Monobromobimane was obtained from Molecular Probes, Inc. (Eugene, OR), and [1-oxyl-2,2,5,5-tetramethyl-D-pyrroline-3-methyl]methanethiosulfonate spin label was from Toronto Research Chemicals (North York, Canada). 11-*cis*-Retinal was a generous gift from Rosalie Crouch (Medical University of South Carolina and NEI, National Institutes of Health). Cuvettes were purchased from Uvonics (Plainview, NY), and round capillaries for EPR measurements were from VitroCom, Inc. (Mountain Lakes, NJ). Band pass filters and long pass filters were acquired from Oriel (Stratford, CT). Acrylamide/bisacrylamine solution (37.5:1) and microcolumns were purchased from Bio-Rad. Spectroscopic grade buffers were from USB Corp. All other chemicals and reagents were obtained from Sigma.

2. 3. 2 Preparation of Rod Outer Segments (ROS)

ROS were isolated from bovine retinas as described previously (Papermaster, 1982). All sucrose solutions were made in ROS buffer (70 mM potassium phosphate, 1 mM magnesium acetate, pH 6.8), and all procedures were done at 4 °C under red lights. Rhodopsin concentration was assessed by difference spectra in the presence of hydroxylamine (ε_{500} = 40,800 liters cm^{-1} mol^{-1}). Stocks were snap-frozen and stored at -80 °C.

Highly phosphorylated ROS (ROS-P) were prepared by suspending ROS (10 μM final rhodopsin concentration) in ROS buffer, with 20 μM GTP and 3 mM ATP (10-ml final volume). Phosphorylation of rhodopsin by the native rhodopsin kinase was initiated by illumination with a 15-watt bulb from a Kodak safelight (without filter) placed ~20 cm away, and sedimentation of the membranes was prevented by gently rocking the sample. After 2 hours, the reaction was stopped by a 4-fold dilution with ROS buffer (plus 50 mM hydroxylamine and 2% bovine serum albumin). Phosphorylated opsin membranes were then collected by centrifugation (40,000 x *g*, 50 min). Levels of phosphorylation were quantified with the use of [γ-^{32}P]ATP (10–100 cpm/pmol) as a tracer. Aliquots were removed from the tracer reaction, spotted onto nitrocellulose filters, washed, and subjected to scintillation counting. Our assay indicated that ROS-P with ~6.4 ± 1.5 phosphates/rhodopsin was created (Kühn and Wilden, 1982).

Phosphorylated opsin membranes were washed by resuspending the pellet using a tissue homogenizer, followed by centrifugation. Membranes were washed twice with low ionic strength buffer (5 mM PIPES, 1 mM EDTA, pH 7.0) to remove peripheral proteins (Kühn, 1982), followed by three additional washes with ROS buffer. The final washed opsin membranes were regenerated overnight by the addition of a 2-fold excess of 11-*cis*-retinal (4 °C). The regenerated samples were washed once with ROS buffer containing 2% bovine serum albumin and 50 mM hydroxylamine, twice with 2% bovine serum albumin in ROS buffer, and three times with ROS buffer alone. Nonphosphorylated ROS membranes were prepared identically, except that no ATP was added during the phosphorylation procedure. The turbidity of ROS samples was reduced by continuous sonication using a Branson 1210 bath sonicator (4 °C, 3 min). More than

95% of the rhodopsin retained function after sonication, as assessed by absorption spectroscopy.

2. 3. 3 Synthesis of Synthetic Phosphopeptide 7PP

The 19-amino acid-long peptide analogous to the fully phosphorylated C-terminal tail of rhodopsin was synthesized and purified as described previously (Puig *et al.*, 1995).

2. 3. 4 Construction, Expression, and Purification of Arrestin

Recombinant bovine visual arrestin with an N-terminal His tag was expressed and purified from *Pichia pastoris* as described previously (McDowell *et al.*, 1999). Mutant constructs I72C and S251C were created utilizing PCR, and the constructs were confirmed by DNA sequencing on both strands.

2. 3. 5 Labeling of Arrestin

Arrestin samples were buffer-exchanged and concentrated (~50 μM) in labeling buffer (10 mM MES, 150 mM NaCl, pH 6.5) by ultrafiltration (Millipore Biomax). Monobromobimane was added from a stock in Me_2SO in 10-fold molar excess to arrestin (final Me_2SO concentration below 1%). After an incubation of 3 h at room temperature with gentle agitation, samples were centrifuged briefly at 100,000 x *g* to remove aggregates. Labeled arrestin was bound by multiple passages over His-select resin (Sigma) equilibrated with buffer (10 mM HEPES, 250 mM NaCl, pH 7.4), followed by extensive washing with buffer. Arrestin was eluted with 500 mM imidazole, and the imidazole was removed by size exclusion chromatography (Sephadex G-15; Sigma; 10 mM HEPES, 150 mM NaCl, pH 7.4). The labeling efficiency was calculated using ε_{280} = 26,360 liters cm^{-1} mol^{-1} for arrestin and ε_{392} = 5,000 liters cm^{-1} mol^{-1} for bimane (Mansoor *et al.*, 1999; Schubert *et al.*, 1999). The absorbance at 392 nm was subtracted

from the 280-nm value to compensate for bimane's absorbance at 280 nm. Using this method, labeling efficiencies of ~83 and 88% were determined for arrestin mutants I72C and S251C, respectively. Since both of these mutants contain the three native cysteines of arrestin (Cys^{63}, Cys^{128}, and Cys^{143}), a sample of wild-type (WT) arrestin was labeled using the same conditions as a control. The WT cysteines labeled at less than ~2% efficiency.

To assess possible free label contamination, the fluorescence of 2 μM labeled arrestin was compared with an identical sample, which had been precipitated with trichloroacetic acid (10%). For both I72B and S251B, free label contamination was well below 1%.

2. 3. 6 Functional Pull-down Assay

A simple centrifugation assay was used to assess arrestin functionality. Briefly, sonicated ROS containing 12 μM rhodopsin or phosphorylated rhodopsin and 3 μM arrestin were mixed in 10 mM HEPES, 150 mM NaCl, pH 7.4, in the dark at room temperature (20 μl). Reactions were either kept in the dark or bleached for 5 min using a 150-watt fiber optic light source (>495 nm), followed by 10-fold dilution with ice-cold buffer and centrifugation at 100,000 x *g* for 10 min at 4 °C. The pellets were solubilized in loading buffer and subjected to SDS-PAGE (10%). Proteins were visualized by Coomassie staining, and densitometry was performed using AlphaEase FC software.

To assess arrestin affinity for post-Meta II rhodopsin, ROS-P in 10 mM HEPES, 150 mM NaCl, pH 7.0, was photobleached at room temperature for 90 s and then transferred to a 35 °C water bath. The sample was kept in the dark after the initial photobleach. After 12 min, arrestin I72B was added (1 μM) and incubated at room

temperature for an additional 3 min. The samples were diluted, centrifuged, and subjected to SDS-PAGE as described above. The fluorescently labeled arrestin was visualized with a gel-doc apparatus (Alpha-Innotech FluorChem 5500). The gel was excited from above with a short wave UV source, and the fluorescent bands were detected through a cut-off filter (535 ± 50 nm) by a CCD camera (5-min exposure). Densitometry was performed using AlphaEase FC software.

2. 3. 7 Steady-state Fluorescence Assays

All fluorescence measurements were made using a Photon Technologies QM-1 steady-state fluorescence spectrophotometer with a single excitation source and two emission detectors (T format). Temperature was controlled and monitored using a water-jacketed cuvette holder connected to a circulating water bath (VWR Scientific) and a digital thermometer, which was submerged into a water-filled well in the sample chamber. Typically, 100 µl samples containing 1 µM labeled arrestin in a 2-mm black jacketed cuvette were excited at 380 nm, and the emitted fluorescence was measured from 400 to 600 nm using 2-nm increments. Each data point was integrated for 0.25 s, and the average of two scans yielded the final spectrum. Excitation bandpass was kept at 0.25 nm to avoid bleaching of rhodopsin samples (emission bandpass at 15 nm). Spectra were smoothed and analyzed using the PTI software program Felix, and the fluorescence spectra of buffer or rhodopsin alone were subtracted where appropriate. Rhodopsin was generally present at a 4-fold excess to arrestin, which was found to be sufficient for complete arrestin binding. The samples were bleached using a 150-watt fiber optic light source (>495 nm) for 40 s.

2. 3. 8 Fluorescence Lifetime Measurements

A PTI Laserstrobe fluorescence lifetime instrument was used to measure I72B and S251B under different conditions. Typically, 500 nM arrestin in a 4-mm black jacketed cuvette (200 μl) was measured at 20 °C using 381-nm excitation pulses (full width half-maximum, ~1.5 ns) with a 298–435-nm band pass filter on the excitation beam. The emission was monitored through two >470-nm long pass filters, and neutral density filters were used to modulate the intensity. Each data point collected represented two averages of five laser shots, and typically 150 points were collected over the lifetime decay curve. The instrument response function, which must be deconvoluted from lifetime decay data, was determined from the scatter from a solution of Ludox through a 400-nm broadband interference filter. Data points were acquired randomly to minimize the impact of laser misfires on the decay curve, and data were analyzed using the commercial PTI software TimeMaster. The "goodness of fit" was evaluated by plotting the residuals and the χ^2 value ($0.7 < \chi^2 < 1.2$ was considered acceptable) (Straume and Johnson, 1992; Lakowicz, 1999).

Fluorescent lifetimes of these labeled arrestins were also measured in the presence of the phosphopeptide 7PP (100 μM) or ROS-P (2 μM in the dark state, after photoactivation, and after the addition of 50 mM hydroxylamine). The lifetime data acquisition scheme described above was found to bleach <2% of rhodopsin, and the total time elapsed from the start of photoactivation to the conclusion of the measurement was 4 min, or ~0.5 Meta II decay half-lives at 20 °C. ROS-P was found to introduce a significant amount of scatter and a fluorescent component with an extremely short lifetime (<1 ns) into the samples. To correct for these components, they were simply

subtracted from the arrestin lifetime by measuring the lifetime of ROS-P alone with matched concentration under the same conditions.

2. 3. 9 Fluorescence Quenching Analysis

To measure the quenching effects of I^- on free *versus* rhodopsin-bound arrestin, a stock of 4 μM ROS-P and 1 μM labeled arrestin was divided among five tubes (0, 10, 20, 30, or 50 mM KI). KCl was added to keep the ionic strength consistent, and 0.1 mM sodium thiosulfate was present to suppress I_3^- formation. The steady-state fluorescence of each sample was measured in the dark state and immediately after photoactivation, and the average of two independent experiments was used to calculate quenching constants. K_{SV} is derived from the Stern-Volmer equation:

$$F_0/F = 1 - K_{SV}[Q]$$

F_0 and F represent the fluorescence intensities in the absence and presence of quencher, respectively, and [Q] is the concentration of quencher.

K_{SV} values were also determined for free arrestin and arrestin in the presence of the phosphopeptide 7PP by titration with KI. The fluorescence was corrected for dilution, and an independent titration with KCl was performed to assess any potential ionic effects on the fluorescence. For time-based quenching studies of arrestin I72B, the average of a range of fluorescence values (λ_{em} = 456 nm, 35 °C) was used to derive the Stern-Volmer constants in the dark (300 s prior to activation), after photoactivation (first four points collected after activation), and at the plateau (1200–1500 s after activation).

2. 3. 10 Time-based Fluorescence Assays

To measure arrestin I72B binding, the samples were excited continuously at 380 nm, and the fluorescence emission at 456 nm was monitored (two points/s). The

excitation bandpass settings were kept below 0.2 nm, resulting in less than 1% rhodopsin bleaching over a 10-min period. Arrestin binding was measured at 8 °C (1 μM arrestin and 8 μM ROS-P, 55 μl) after irradiation from a Machine Vision Strobe light source for 5 s, which photoactivated 56% of the rhodopsin. Buffer-subtracted data were fit using the program Sigma Plot (SPSS Inc., Chicago, IL) to a monoexponential equation to define the rate of arrestin binding. Arrestin release was measured in a similar way, except that the excitation shutter was opened for 2 s and then closed for 8 s between measurements to avoid photobleaching. When used, 2 μl of a 300 mM hydroxylamine stock (pH 7.0) was added, and this was found not to have any effect on the fluorescence of labeled arrestin.

Simultaneous monitoring of retinal and arrestin release from ROS-P was accomplished by exciting the sample at 295 nm for 2 sec, followed by a 2 sec excitation at 380 nm. Fluorescence emission at 330 and 456 nm was monitored (1 point/s), and the shutter was closed for 8 s between measurements. The sample was irradiated for 8 s with a Machine Vision Strobe light source, which photobleached >90% of the rhodopsin. In this way, the change in rhodopsin tryptophan emission due to retinal release (λ_{ex} = 295 nm; λ_{em} = 330 nm) (Farrens and Khorana, 1995) and the change in bimane fluorescence due to arrestin I72B binding and release (λ_{ex} = 380 nm; λ_{em} = 456 nm) could be monitored simultaneously. The fluorescence contribution from arrestin's one native tryptophan was subtracted from retinal release data, since the fluorescence of this tryptophan does not change upon arrestin activation (Wilson and Copeland, 1997). Retinal release from ROS-P without arrestin was measured in the same way, except that no arrestin was present. Data were background-subtracted and fit to either monoexponential rise or decay equations using the program Sigma Plot to derive rates.

Goodness of fit was evaluated by plotting the residuals. Arrestin release rates and retinal release rates, with or without arrestin, were determined at 15, 20, 25, 30, 35, and 40 °C (pH 7.5), and the average of two independent experiments was used to derive the activation energy (E_a) of these events using the Arrhenius equation:

$$k = Ae^{-Ea/(RT)}$$

The pH dependence of retinal and arrestin release was determined by mixing the phosphorylated rhodopsin and arrestin into buffer (20 mM HEPES, 150 mM NaCl) at pH 6.0, 6.5, 7.0, 7.5, 8.0, or 8.5. Rates were determined as described above (35 °C).

2. 3. 11 EPR

Arrestin I72C and S251C were prepared for EPR in an identical manner as described for monobromobimane labeling, except that a 5-fold molar excess of nitroxide spin label was used during labeling. The EPR spectrum of a sample of WT arrestin, labeled using identical conditions, showed less than 10% incorporation of spin label at the native cysteines compared with I72C. For EPR measurements, a 6 μl volume of 50 μM spin-labeled arrestin and 200 μM ROS-P were measured in the dark at room temperature (19–21 °C) and at various time points following photoactivation (45 s using a 150-watt >495-nm fiber optic light source). To assess whether the observed spectral changes were due to changes in protein rotational rates, EPR spectra were also measured in the presence of 20% Ficoll 400 (Frazier *et al.*, 2002). Ficoll concentrations higher than 20% could not be used, since they caused arrestin precipitation. EPR measurements were made using a Varian E-104 instrument fitted with a loop-gap resonator and the EWWIN 5.22 data acquisition package (Scientific Software Services, Plymouth, MI). Measurements were carried out at ~9.3-GHz microwave frequency, using 2 milliwatt

incident microwave power, a modulation amplitude of ~2 gauss, and a 100-gauss sweep (29 s/scan). Multiple scans were taken and averaged where appropriate (see the legend to Figure 2. 7 for details).

2. 4 RESULTS

2. 4. 1 Rational of Experimental Approach

Numerous studies suggest the two concave surfaces of arrestin are involved in binding light-activated phosphorylated rhodopsin (Gurevich and Gurevich, 2004; Ling *et al.*, 2004; Smith *et al.*, 2004). In the present study, we introduced two cysteine residues between these surfaces and labeled them with the cysteine-specific fluorescent probe monobromobimane (Figure 2. 1). We and others have extensively characterized bimane and found that it can reliably report on protein dynamics and structure due to its small size, its sensitivity to polarity, and its ability to be quenched by nearby tryptophan and tyrosine residues (Giniger *et al.*, 1985; Kosower *et al.*, 1986; Mansoor *et al.*, 1999; Mansoor *et al.*, 2002; Mansoor and Farrens, 2004). Below, we report our studies on the bimane-labeled arrestin mutants I72C and S251C.

2. 4. 2 Fluorescently Labeled Arrestin Mutants are Functional

The relative functionality of the mutants with and without the bimane label was first assessed using a centrifugal "pull-down" assay (Figure 2. 2). Mutant I72C shows proper binding specificity to ROS*-P but binds ROS*-P with less affinity (43% of WT). Interestingly, bimane labeling of I72C (I72B) appears to restore the binding ability of this mutant to ~99% of WT levels. Both unlabeled arrestin S251C and labeled S251B bind to similar levels as WT (89 and 101%, respectively).

2. 4. 3 Spectral Properties of Labeled Arrestin Mutants

Both I72B and S251B fluoresce with a λ_{max} of ~470 nm, and their spectra do not change in the presence of an excess of dark ROS-P. However, upon photoactivation, the emission spectrum of arrestin I72B blue-shifts to a λ_{max} of 456 nm and increases in total integrated intensity by ~12% (Figure 2. 3A). The fluorescence of arrestin S251B increases ~100% upon photoactivation but displays no shift in its λ_{max} (Figure 2. 3D). Importantly, these changes are not observed using *nonphosphorylated* ROS (Figure 2. 3, B and E) and are abolished by 50 mM hydroxylamine (data not shown), presumably because hydroxylamine catalyzes the decay of activated rhodopsin by cleaving the retinal Schiff base.

2. 4. 4 Spectral Changes Require Interaction with Rhodopsin

We next assessed whether the observed spectral changes were due to conformational changes within arrestin itself rather than interactions with ROS*-P. To do this, we tested the effect of phosphopeptide 7PP, which represents the fully phosphorylated form of rhodopsin's C-terminal tail and has been shown to transactivate arrestin to bind nonphosphorylated ROS* (Puig *et al.*, 1995). The peptide 7PP causes an ~20% decrease in intensity for mutant I72B (Figure 2. 3C) and induces no change in arrestin S251B (Figure 2. 3F). We obtained similar results as for 7PP using heparin and phytic acid, two polyanionic compounds that have been reported to bind arrestin and induce activating conformational changes (data not shown) (Palczewski *et al.*, 1991b; Wilson and Copeland, 1997).

2. 4. 5 Fluorescence Lifetime Analysis

To further elucidate the cause of these spectral changes, we measured the fluorescent decay lifetimes of I72B and S251B under different conditions (Table 2. 1). The fluorescence lifetime (τ) of I72B is 11.1 ns, and this value is shortened slightly by the phosphopeptide 7PP (10.6 ns). In the presence of ROS-P, the τ shortens by ~1 ns after photoactivation but reverts to ~10.5 ns after the addition of hydroxylamine. These values are all similar to free bimane (9.1 ± 0.1 ns; data not shown), suggesting no major perturbation of the probe at this site. In contrast, the lifetime of S251B is multi-exponential, with components of ~7.4 and 1.4 ns, resulting in an amplitude-weighted average fluorescence lifetime $\langle\tau\rangle$ of 2.6 ns. Note that $\langle\tau\rangle$ is proportional to steady-state intensity (Ross *et al.*, 1992; Lakowicz, 1999), and thus the short $\langle\tau\rangle$ of S251B is consistent with its quenched fluorescence compared with I72B and indicates some sort of dynamic quenching mechanism. Binding of S251B to ROS*-P causes a significant increase in its $\langle\tau\rangle$, which correlates to an increased steady-state intensity (Figure 2. 3D).

2. 4. 6 Fluorescence Quenching Analysis

Fluorescence quenching studies were carried out using the soluble quencher I^-, to determine whether binding to ROS*-P shields the probes on I72B and S251B from the solvent. The Stern-Volmer constants (K_{SV}) and bimolecular quenching constants (k_q) determined under different conditions are reported in Table 2. 2. The data indicate that the probe at Ile^{72} is more solvent-accessible on free arrestin (higher K_{SV} and k_q) than when arrestin is bound to ROS*-P (lower K_{SV} and k_q). Consistent with this observation, we note that the fluorescence intensity increase that occurs upon I72B binding ROS*-P is directly proportional to temperature (12% increase at 20 °C *versus* 50% increase at 35

°C; data not shown). We believe this effect is due to differences in solvent accessibility for the following reasons. At warmer temperatures, the probe on unbound I72B experiences more collisions with the solvent than at cooler temperatures and is thus de-excited more. Upon binding ROS*-P, the probe is protected from collisions, resulting in a higher relative change in fluorescence at warmer temperatures. These results also complement the blue shift in the I72B emission spectra upon ROS*-P binding (Figure 2. 3A), which indicates a movement of the bimane probe to a more hydrophobic environment (Dunham and Farrens, 1999; Mansoor *et al.*, 1999).

The lower K_{SV} for S251B is probably due to its shorter lifetime compared with I72B. When the quenching data are analyzed using the lifetime values to obtain the k_q, or the true number of collisions/s of quencher and probe, the probe at Ser^{251} is seen to be as accessible as at Ile^{72}. Importantly, the k_q for S251B is also significantly reduced in the presence of ROS*-P, implying that the probe at this site is also shielded from the solvent when bound to rhodopsin.

2. 4. 7 Kinetics of Arrestin Binding and Release

The fluorescence changes described above can be used to directly monitor arrestin binding to ROS*-P. As shown in Figure 2. 4A, the fluorescence of I72B increases and then plateaus after photoactivation. A second bleach produces no further increase, indicating that all of the arrestin is bound to ROS*-P after the initial bleach. The data are well fit to a monoexponential, yielding a binding rate constant of $k = 27.6 \pm 1.6 \times 10^{-3}\ s^{-1}$ or a $t_{1/2}$ value of ~25 s at 8 °C. Because the fast rate of binding required us to use a low, nonphysiological temperature to resolve the binding event, and because decreased membrane fluidity may have some effect on the affinity and rate of arrestin binding, we

did not pursue these measurements further in the present study. Instead, we focused on understanding why the fluorescence changes that occur after photobleach slowly reverse back to near starting levels in a time course reminiscent of Meta II decay (Figure 2. 4B), as described below.

2. 4. 8 Arrestin and Retinal Release are Linked Events

Light-activated rhodopsin decays either by hydrolysis of the retinal Schiff base linkage, resulting in opsin and free retinal (Farrens and Khorana, 1995; McBee *et al.*, 2001), or by formation of Meta III (Lewis *et al.*, 1997; Heck *et al.*, 2003a). Release of retinal from opsin results in an increase of opsin's intrinsic tryptophan fluorescence (Farrens and Khorana, 1995; Heck *et al.*, 2003a). We investigated how arrestin affects this process using our fluorescently labeled arrestin mutant I72B. Note that the fluorescence of these two species is well separated, enabling the rates of retinal and arrestin release to be determined simultaneously.

As shown in Figure 2. 5A, after the initial increase upon binding ROS*-P, I72B fluorescence decreases over time with a rate that mirrors the increase in opsin tryptophan fluorescence during retinal release. As expected, we find the rate of retinal release from ROS*-P increases with temperature (Figure 2. 5B), as described previously (Farrens and Khorana, 1995; Heck *et al.*, 2003a). However, although we find that arrestin and retinal release occur at the same rate, it appears that arrestin slows retinal release ~2-fold at physiological temperatures (Figure 2. 5B). This slowing of retinal release is also observed with unlabeled arrestin (data not shown), indicating that these results are not simply due to the use of the bimane-labeled arrestin. It should be noted that, although arrestin is present in excess in these samples, not all rhodopsin proteins might be bound

by arrestin after illumination. A portion may be inaccessible to arrestin, due to inside-out vesicles or heterogeneous phosphorylation. Thus, the experiment shown in Figure 2. 5A may reflect two different rates of retinal release, from unbound rhodopsin and from arrestin-bound rhodopsin, and this may account for the slight deviance of the residuals for the calculated curve.

Analysis of Arrhenius plots using these rates reveals that retinal release from ROS*-P occurs with an E_a of 21.6 kcal/mol (Figure 2. 5C), in good agreement with previous findings (Farrens and Khorana, 1995; Heck *et al.*, 2003a). The E_a values for arrestin release and retinal release in the presence of arrestin are similar (E_a = 18.0 and 19.4 kcal/mol, respectively). However, it is important to note that these Arrhenius plots are kinetically shifted below that of retinal release without arrestin.

We also find that at 35 °C and above pH 6.5, the rate of retinal release from ROS*-P in the absence of arrestin increases with increasing pH (Figure 2. 5D). Strikingly, in the presence of arrestin, the rates of retinal and arrestin release are pH-independent. These results are intriguing, since they closely mirror those seen by Heck *et al.* (Heck *et al.*, 2003a) using a peptide analogue derived from the C terminus of the α-subunit of transducin ($G_t\alpha$-HAA) and suggest a coupling between events at the cytoplasmic face and Schiff base hydrolysis.

2. 4. 9 Dynamics of Arrestin Release from Post-Meta II Photoproducts

Rather than decay to opsin and free retinal, a significant population of rhodopsin can also decay to a photoproduct called Meta III at physiological temperature and pH (Lewis *et al.*, 1997; Heck *et al.*, 2003a). Although the exact nature of Meta III is still under active investigation, it is clear that Meta III differs from Meta II in its absorbance

(λ_{max} = 470 nm), its structure, and its ability to activate transducin. Below, we describe our surprising finding that suggests that long after Meta II decay, arrestin remains bound to Meta III or some post-Meta II photoproduct.

As shown in Figure 2. 6A, after the initial increase that occurs upon I72B binding to ROS*-P, the fluorescence decreases at a rate that matches Meta II decay and retinal release, yet consistently plateaus at some value ~20% higher than the initial dark state intensity. To make the fluorescence fully return to the starting value, we find it necessary to add hydroxylamine, which cleaves the Schiff base and converts all rhodopsin photo-intermediates to opsin. This effect is highly reproducible. To ensure that this "plateau effect" is not simply a spectral artifact, we carried out centrifugal pull-down analysis, and we find the same result (Figure 2. 6A, *inset*). A majority of arrestin I72B is pulled down 90 s after photoactivation with Meta II ROS*-P, and ~25% of this arrestin is still pulled-down with ROS*-P more than 1600 s after photoactivation (35 °C). Note that this effect cannot be due to Meta II rhodopsin, since Meta II decays with a $t_{1/2}$ of ~90 s at 35 °C, and thus after 1600 s, less than 0.4 x 10^{-4}% of the original pool of Meta II remains. Again, as noted for the fluorescence assay described above, we find that it is necessary to add hydroxylamine to abolish this binding.

We explored this phenomenon further by measuring how accessible the probe at Ile^{72} is to the quencher I^- in the presence of (*a*) dark ROS-P, (*b*) immediately after photobleach, and (*c*) at 15 half-lives after Meta II decay (35 °C) (Figure 2. 6B). The probe at Ile^{72} is relatively accessible in the dark (K_{SV} of 22.6 M^{-1}), but upon arrestin binding to ROS*-P, the probe becomes more buried (K_{SV} = 5.9 M^{-1}). Interestingly, even after 15 Meta II decay half-lives, the accessibility of the probes has not returned to that of

the original dark state (K_{SV} = 14.5 M^{-1}), indicating that some population of the probes on I72B are still buried relative to the original dark state.

2. 4. 10 Fluorescent Changes Are Not Simply Due to Spectral Artifacts

Fluorescence experiments involving rhodopsin must take into account possible complications caused by the spectral properties of rhodopsin. We are confident that the fluorescence changes described above are not simply due to trivial optical artifacts for the following reasons. (*a*) Under the conditions used, the optical density of the samples was measured to be less than 0.1; thus, the data should be free of inner filter effects. (*b*) Similar results were obtained when these mutants were labeled with the fluorophore PyMPO, whose excitation (415 nm) and emission (550 nm) wavelengths are red-shifted compared with that of bimane (data not shown). (*c*) The EPR spectrum of nitroxide spin-labeled I72C (I72-SL) also changes upon arrestin binding ROS*-P. The spectral changes indicate that the spin label at Ile^{72} becomes significantly less mobile (Figure 2. 7A), further suggesting that the probe at Ile^{72} becomes buried in the arrestin-ROS*-P interface. This immobilization of the probe at Ile^{72} could not be mimicked by 20% Ficoll 400; thus, the spectral changes are not simply due to a decreased rotational mobility of the protein upon binding to the ROS membranes (Figure 2. 7B) (Frazier *et al.*, 2002). Furthermore, even after 12 Meta II decay half-lives (90 min, 20 °C), the EPR spectrum of I72-SL differs significantly from the starting state dark spectrum (Figure 2. 7A), again suggesting that arrestin binds to some post-Meta II photodecay product [4]. Similar results were obtained with spin-labeled S251C (data not shown). EPR measures absorption of

[4] A quantitative comparison of the EPR and fluorescence spectra of labeled arrestin is not possible due to the different concentrations involved, since arrestin undergoes concentration-dependent oligomerization (Schubert *et al.*, 1999; Shilton *et al.*, 2002; Imamoto *et al.*, 2003).

microwave radiation and is thus not affected by rhodopsin's spectral properties (Farrens, 1999; Hubbell *et al.*, 2000).

2. 4. 11 Post-Meta II Decay ROS-P Binds Arrestin

To ensure that the results described above were not simply due to the slowing effect of arrestin on Meta II decay, we tested arrestin's affinity for ROS*-P that had first decayed in the absence of arrestin. As shown in Figure 2. 8, we find that a significant amount of arrestin is pulled down when added to post-Meta II ROS-P, and the amount of arrestin pulled-down is roughly proportional to the amount of post-Meta II ROS-P. Note that these samples had decayed through eight half-lives and thus contained less than 0.4% of the original Meta II. As a control, we again find that hydroxylamine abolishes arrestin binding to post-Meta II ROS*-P. These results clearly indicate that arrestin can interact specifically with some photodecay product of rhodopsin, possibly Meta III.

2. 5 DISCUSSION

Arrestin attenuates rhodopsin signaling by binding to ROS*-P and blocking the G-protein binding site. In the present work, we have employed bimane-labeled arrestin mutants to address how arrestin and rhodopsin interact and how arrestin is released from rhodopsin after binding. Our results are discussed below.

2. 5. 1 Labeled Arrestin Mutants are Functional

The two bimane-labeled arrestin mutants used in this study, I72B and S251B, have similar binding specificities as WT when assessed by a centrifugal pull-down assay (Figure 2. 2). Interestingly, the decreased binding affinity of unlabeled I72C is restored

upon attaching the probe bimane to this site, suggesting that some hydrophobic and/or steric bulk at this site may be important for affinity.

2. 5. 2 Possible Reasons for Fluorescence Changes Observed upon Binding ROS*-P

The fluorescence of the bimane-labeled arrestin mutants changes upon binding to ROS*-P, and control experiments demonstrate that these changes require phosphorylated rhodopsin and cannot be mimicked by the phosphopeptide 7PP. What causes the fluorescent changes? For I72B, the blue shift in fluorescence, the fluorescence quenching analysis, and the EPR data all suggest that the probe becomes buried in a rhodopsin-arrestin or phospholipid-arrestin interface. Similarly for S251B, the fluorescence quenching analysis and EPR data also suggest that the probe becomes buried upon binding ROS*-P. In contrast to I72B, no blue shift in fluorescence is observed for S251B, but instead a dramatic increase in fluorescence intensity is observed. What causes this large increase? We believe that the most likely explanation is a conformational change in arrestin itself. Structural analysis using coordinates provided by Hirsch *et al.* reveals that two tyrosine residues, 67 and 250, lie very close to Ser^{251} (see Figure 2. 1) (Hirsch *et al.*, 1999). Since tyrosine residues can quench bimane fluorescence, albeit much less effectively than tryptophan (Sato *et al.*, 1988), the probe at Ser^{251} is probably susceptible to quenching from at least one of these nearby tyrosine residues, which results in perturbed fluorescence. Upon binding to ROS*-P, this quenching is partially relieved, which suggests that at least one of the quenching tyrosines may move away from the probe at Ser^{251} upon binding. A possible candidate is Tyr^{67}, since it is unlikely that neighboring Tyr^{250} can move very far from Ser^{251}. However, since Tyr^{67} is located on the opposite lobe of arrestin, our results may support

the proposed interlobal movement in arrestin upon its activation and binding to ROS*-P (Vishnivetskiy *et al.*, 2002).

2. 5. 3 Fluorescence Changes can be used to Monitor Arrestin Binding and Release

The fluorescently labeled mutants provide a novel way to directly monitor arrestin binding and release. Using these mutants, we find the rate of arrestin binding to ROS*-P at 8 °C to be 27.6 ± 1.6 x 10^{-3} s^{-1} , or a $t_{1/2}$ of ~25 s. Note that this value is substantially lower than that obtained by Schleicher *et al.* (Schleicher *et al.*, 1989), using the extra-Meta II assay (~0.5 s^{-1} or a $t_{1/2}$ of 1.4 s). We are not sure of the cause of this discrepancy, although it may simply be due to differences in the measuring techniques and reagents.

We used this fluorescence approach to directly and simultaneously monitor both arrestin and retinal release. Our studies indicate that whereas these two events do occur at the same rate, arrestin slows retinal release by ~2-fold at physiological temperature and pH. Arrhenius analysis shows that when arrestin and ROS-P are present together, retinal and arrestin release have E_a of ~20 kcal/mol but are kinetically shifted (slower) compared with retinal release without arrestin. This intriguing finding suggests that arrestin acts to slow retinal release, perhaps through a "kinetic trap" mechanism (Figure 2. 9), by apparently stabilizing rhodopsin's structure so that the retinal remains in the binding pocket longer but not affecting the energetics of retinal release. Arrestin binding also abolishes the pH dependence of retinal release, perhaps by affecting certain protonation events, which normally speed the rate of retinal release with increasing pH. A similar effect is observed for the transducin peptide analogue $G_t\alpha$-HAA (Heck *et al.*, 2003a), suggesting that the two may bind at the same site or affect the rhodopsin structure in similar ways.

Previous work has also suggested a slowing effect of arrestin on retinal release, using the enzyme retinal dehydrogenase (RDH), which reduces all-*trans*-retinal to all *trans*-retinol (Hofmann *et al.*, 1992; Palczewski *et al.*, 1994b). Hofmann *et al.* found that arrestin slowed the rate of RDH activity by ~40% (30 °C) compared with control reactions in which no arrestin was present (Hofmann *et al.*, 1992). Similarly, we find that arrestin slows the rate of retinal release by ~42% at 30 °C using our direct fluorescent method.

2. 5. 4 Arrestin Binds to a Post-Meta II Decay Product

We were surprised to find that a population of arrestin remains bound to ROS-P, even after all Meta II has decayed [5]. Evidence for this post-Meta II decay binding includes the following. (*a*) Neither the steady-state fluorescence of I72B nor the EPR spectrum of I72-SL return to dark state levels even after Meta II decay (Figures 2. 6 and 7). (*b*) Arrestin is "pulled down" with post-Meta II ROS-P in centrifugal pull-down assays (Figure 2. 8). (*c*) Fluorescence quenching studies show that long after Meta II decay, accessibility of the probe at Ile^{72} does not return to dark state values (Figure 2. 6). Because these effects are all reversed by hydroxylamine, which converts all rhodopsin photo-intermediates into opsin and free retinal oxime, we hypothesize that arrestin may be binding to Meta III, the long lived storage form of rhodopsin (Figure 2. 9). Although it would seem counterintuitive for arrestin to bind a nonsignaling form of rhodopsin, Meta III has recently been shown to have some activating ability toward transducin

[5] We cannot rule out the possibility that some of the spectral discrepancy between labeled arrestin in the presence of dark state and post-Meta II decayed rhodopsin may be due to the protein adopting a different conformation upon dissociation from rhodopsin.

(Zimmermann *et al.*, 2004). Thus, arrestin may bind Meta III to attenuate its activity and prevent inappropriate signaling.

As far as we are aware, the work presented here is the first demonstration that arrestin binds a post-Meta II decay photoproduct of rhodopsin. Although it has been shown that arrestin will bind phosphorylated opsin membranes to which a large excess of all-*trans*-retinal has been added exogenously (Hofmann *et al.*, 1992), such a nonphysiological situation ignores the potentially important role of secondary retinal binding sites and ligand channeling (Heck *et al.*, 2003a; Schädel *et al.*, 2003; Zimmermann *et al.*, 2004).

One puzzling question raised by our results is how arrestin binding to Meta III (or some other post-Meta II photoproduct) would affect the measurement of "extra-Meta II." Arrestin stabilizes Meta II at the expense of Meta I, and measurement of this extra-Meta II has been the basis for many quantitative studies of arrestin binding (Schleicher *et al.*, 1989; Pulvermüller *et al.*, 1997; Gibson *et al.*, 2000). We do not that believe arrestin's interaction with post-Meta II photoproducts would impact measurement of extra-Meta II, since it is unlikely that any significant amount of late photoproducts exists under the conditions used to measure extra-Meta II (low temperatures and within the first minute after photoactivation).

Furthermore, since Meta III has recently been shown to evolve from Meta I (Vogel *et al.*, 2003; Vogel *et al.*, 2004b), it is reasonable to speculate that the arrestin-bound post-Meta II complex may convert Meta III to a Meta II-like species (Hofmann *et al.*, 1992), as has been suggested for transducin (Zimmermann *et al.*, 2004). We stress that the work presented in this chapter has not established the nature of the post Meta II

decay photoproduct to which arrestin binds, and this question will be addressed in Chapters 3 and 4 of this dissertation.

2. 5. 5 Possible Implications of these Findings on the Visual Cycle

In the visual retinoid cycle, all-*trans*-retinal released from opsin is reduced by RDH to all-*trans*-retinol and then transported to the retinal epithelium, enzymatically converted into 11-*cis*-retinal, and recycled to regenerate rhodopsin in the rod outer segment (McBee *et al.*, 2001). Our results imply that arrestin influences the first step of this cycle, by slowing the rate at which free all-*trans*-retinal is released and by affecting the release of retinal from Meta III or other photodecay products. Why might arrestin affect retinal release in these ways? One possibility is that full-length arrestin serves a protective role in the rod cell, by capping bleached rhodopsin and retarding the release of free retinal into the cell. Considering that the rate of RDH activity is slow compared with other visual processes, RDH may become limiting under high bleaching conditions, and levels of free all-*trans*-retinal may become quite high (Saari *et al.*, 1998). High levels of free retinal have been shown to be cytotoxic by forming adducts with phosphatidylethanolamine (A2E), which can become highly reactive epoxides that damage DNA and proteins, and thus may contribute to macular degeneration (Sparrow *et al.*, 2003). Thus, arrestin may allow the cell sufficient time to deal with the excess retinal and prevent wasteful regeneration of rhodopsin under high bleaching conditions. Consistent with this hypothesis, it has been proposed that full length arrestin serves to quench rhodopsin activity only under bright light conditions, whereas the short splice variant p^{44} carries out most of the rhodopsin inactivation within the low light operation range of the rod cell (Langlois *et al.*, 1996). Under dim light conditions, full-length

arrestin is sequestered in the inner segment of the rod cell and is only transported to the outer segment under high bleaching conditions (Peterson *et al.*, 2003; Elias *et al.*, 2004; Nair *et al.*, 2004).

2. 5. 6 Caveats for the Present Work

Although the above scenario suggests that arrestin plays a key protective role in the retinoid cycle, *in vivo* work by Palczewski, Saari, and others suggests that the situation may not be so simple, since they found no difference in retinoid levels in mouse eyes between WT and arrestin knock-out mice (Palczewski *et al.*, 1999). One possible explanation for this apparent discrepancy is that their experiments measured retinoid kinetics after a flash of light followed by recovery in the dark. This approach did not address the situation of constant illumination, where RDH activity would become limiting and arrestin's role might be more pronounced. Another difference is that our *in vitro* method required the use of pre-phosphorylated rhodopsin in washed native membranes and fluorescently labeled recombinant arrestin. Although we strove to carry out experiments under near physiological conditions (temperature, pH, ionic strength), we did not examine the role of other constituents of the visual cycle, which may also affect apparent rates. For example, Hofmann *et al.* (Hofmann *et al.*, 1992) have shown that RDH activity can speed arrestin release, presumably by reducing all-*trans*-retinal and removing it from the binding pocket.

2. 5. 7 Possible Implications of these Results on General Mechanisms of GPCR Desensitization

A hallmark of β-arrestin-mediated GPCR attenuation is receptor internalization, which removes the receptor from the cell surface and desensitizes the cell (Claing *et al.*,

2002). If β-arrestin slows the rate of ligand release from GPCRs (Gurevich *et al.*, 1997), as arrestin does for retinal, it might allow the cellular machinery more time to coordinate and induce internalization. Alternatively, perhaps different ligands for a single receptor affect β-arrestin binding in different ways, and this is why some ligands induce arrestin-mediated GPCR internationalization and others do not (Keith *et al.*, 1998; Hsieh *et al.*, 1999; Kieffer and Evans, 2002).

2. 5. 8 Summary

This chapter describes how fluorescently labeled arrestin mutants represent a novel and extremely useful method for directly observing arrestin-rhodopsin interactions. As described in the Chapters 3 and 4 of this dissertation, this approach has enabled us to study arrestin's interaction with membrane phospholipids and regulation of rhodopsin photochemistry. In addition, we have explored how the C-terminal truncation present in the splice-variant p^{44} (Schröder *et al.*, 2002) changes the dynamics of arrestin binding and release from rhodopsin (described in Appendix 1 of this dissertation). Finally, our novel method may also be extended in future studies to test arrestin's interaction with interesting rhodopsin mutants, such as those that are constitutively active (Rim and Oprian, 1995) or show extended amounts of Meta III formation. Arrestin-rhodopsin aggregates formed due to certain rhodopsin or arrestin mutations can be a cause of retinitis pigmentosa (Chuang *et al.*, 2004). The site-directed spectroscopic techniques described in this study will allow further investigation of these and other interesting questions.

2. 6 ACKNOWLEDGEMENTS

We thank J. Hugh McDowell and Anatol Arendt for synthesis of the phosphopeptide 7PP and Mary D. Barkley for advice regarding fluorescence lifetimes. We also thank Steven E. Mansoor for assistance in measuring fluorescence lifetimes. This work was supported in part by Grants EY12095 and DA14896 to (D.L. Farrens) and EY06225 (to W.C. Smith) from the National Institutes of Health, an unrestricted Grant from Research to Prevent Blindness (to Dept. Ophthalmology at U. Florida), a National Defense Science and Engineering Graduate Fellowship (to M.E. Sommer), and an N.L. Tartar Research Fellowship (to M.E. Sommer).

Table 2. 1 Mono- and double-exponential fluorescence lifetime analysis of bimane-labeled arrestin mutants I72C and S251C[a]

sample	α_1	τ_1 (ns)	α_2	τ_2 (ns)	χ^2	$\langle\tau\rangle$ (ns) [b]	$\bar{\tau}$ (ns) [b]
I72B	1.0	11.3			1.0	11.1 ± 0.1	11.1 ± .1
	1.0	11.2			0.8		
	1.0	11.0			1.0		
I72B + 7PP	1.0	10.9			1.2	10.6 ± 0.14	10.6 ± 0.14
	1.0	10.4			0.9		
	1.0	10.6			1.1		
I72B+ROS-P (dark)	1.0	10.6			1.0	10.5 ± 0.1	10.5 ± 0.1
	1.0	10.4			1.0		
I72B+ROS-P (+hν)	1.0	9.3			1.3	9.5 ± 0.2	9.5 ± 0.2
	1.0	9.7			0.9		
I72B+ROS-P (+NH_2OH)	1.0	10.4			1.0	10.4 ± 0.0	10.4 ± 0.0
	1.0	10.4			0.8		
S251B	0.27	7.8	0.73	1.6	0.9	2.9 ± 0.2	5.3 ± 0.2
	0.27	6.8	0.73	1.1	1.0		
	0.25	7.5	0.75	1.4	0.9		
S251B ± 7PP	0.34	6.1	0.66	0.86	0.9	2.7 ± 0.1	5.0 ± 0.1
	0.33	6.0	0.67	0.73	0.9		
	0.30	6.8	0.70	1.2	0.7		
S251B+ROS-P (dark)	0.29	6.1	0.71	0.94	0.7	2.6 ± 0.1	4.8 ± 0.1
	0.30	6.5	0.70	1.1	0.9		
S251B+ROS-P (+hν)	0.32	7.8	0.68	1.2	1.0	3.5 ± 0.2	6.0 ± 0.1
	0.39	7.3	0.61	1.5	0.9		
S251B+ROS-P (+NH_2OH)	0.28	6.5	0.72	1.1	0.8	2.6 ± 0.0	4.9 ± 0.1
	0.25	6.9	0.75	1.1	0.9		

[a] Lifetimes were measured as described in the Materials and Methods. Samples contained 500 nM I72B or S251B alone in buffer, in the presence of 100 μM phosphopeptide 7PP, or in the presence of 2 μM ROS-P (dark, after photo-activation (+hν), and after the addition of 50 mM hydroxylamine). Two or three sets of lifetime data from independent experiments are shown for each sample. τ_1 and τ_2 are the lifetimes in nanoseconds, and α_1 and α_2 are the fractional amplitudes of each lifetime τ_1 and τ_2, respectively (the sum of the pre-exponential factors α is normalized to 1).

[b] $\langle\tau\rangle = \alpha_1\tau_1+\alpha_2\tau_2$, or the amplitude-weighted average fluorescence lifetime, and $\bar{\tau} = (\alpha_1\tau_1^2+\alpha_1\tau_2^2) / (\alpha_1\tau_1+\alpha_2\tau_2)$, or the intensity-weighted average fluorescence lifetime (Ross *et al.*, 1992; Neyroz *et al.*, 1996; Zawadzki *et al.*, 2003). These values represent the mean of the two or three reported sets of lifetimes ± the standard error of the mean.

Table 2. 2 Summary of lifetime and quenching values for bimane-labeled arrestin mutants I72C and S251C.

Sample	$\bar{\tau}$ (ns) [a]	K_{SV} (M^{-1}) [b]	k_q [c] ($\times 10^9 M^{-1}s^{-1}$)
I72B	11.1 ± 0.1	26.7 ± 5.2	2.4
I72B + 7PP	10.6 ± 0.1	26.1 ± 4.5	2.5
I72B+ ROS-P (dark)	10.5 ± 0.1	25.6 ± 1.6	2.4
I72B+ROS-P (+hv)	9.5 ± 0.2	9.4 ± 2.3	1.0
S251B	5.3 ± 0.2	12.9 ± 1.4	2.4
S251B+7PP	5.0 ± 0.1	10.0 ± 0.7	2.0
S251B+ROS-P (dark)	4.8 ± 0.1	12.3 ± 2.0	2.5
S251B+ROS-P (+hv)	6.0 ± 0.1	5.5 ± 0.3	0.9

[a] $\bar{\tau}$ refers to the intensity-weighted average lifetime (Table 2. 1).

[b] K_{SV} values were derived as described in the Materials and Methods.

[c] The bimolecular quenching constant (k_q), which represents collisions per second between the fluorophore and the quencher, was derived using the relationship $K_{SV}=k_q*\tau_0$ (where τ_0 is the intensity-weighted average fluorescence lifetime in the absence of quencher) (Ross *et al.*, 1992; Neyroz *et al.*, 1996; Zawadzki *et al.*, 2003). Note that k_q is dependent on diffusion rates, and thus the reported k_q values may reflect not only a change in solvent accessibility but also a change in arrestin's rate of diffusion that occurs when it binds the ROS*-P vesicle.

Figure 2. 1 Model of rhodopsin and arrestin and the structures of the spectral probes used in this study. A) Model showing the putative interacting surfaces of rhodopsin and arrestin (Liang *et al.*, 2003; Gurevich and Gurevich, 2004; Ling *et al.*, 2004; Smith *et al.*, 2004). Both rhodopsin (*red*) and its hypothetical homodimer partner (*gray*) are shown in the membrane bilayer (Liang *et al.*, 2003). The N-domain of arrestin is colored in *blue*, and the C-domain is *orange*. Residues Ile^{72} (*magenta*) and Ser^{251} (*green*) are indicated with *spheres* at the position of their respective Cα carbons. Two tyrosine residues that lie close to Ser^{251}, Tyr^{67} of the N-domain and Tyr^{250} of the C-domain, are also indicated. The models were made using the program DS ViewerPro 5.0 (Accelrys, Inc.) using published coordinates deposited in the Protein Data Bank for the theoretical rhodopsin dimer model proposed by Liang *et al.* (Liang *et al.*, 2003) and the α-conformation of the Hirsch *et al.* (Hirsch *et al.*, 1999) arrestin crystal structure. **B)** Structure of the fluorescent probe monobromobimane. **C)** Structure of the methanethiosulfonate spin label (MTSL).

Figure 2. 1

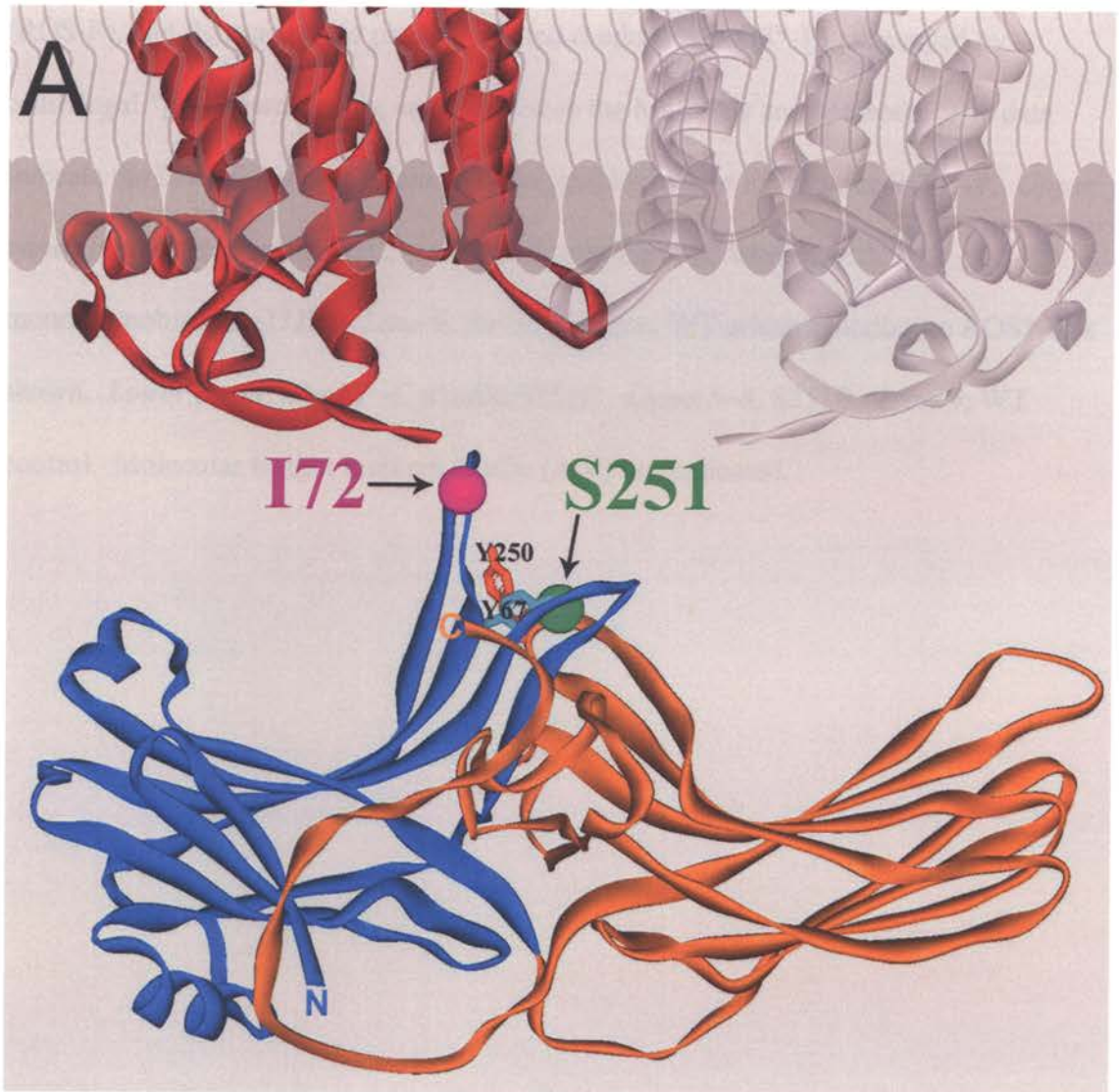

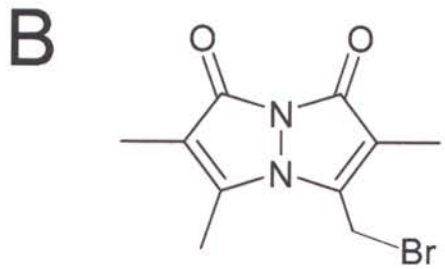

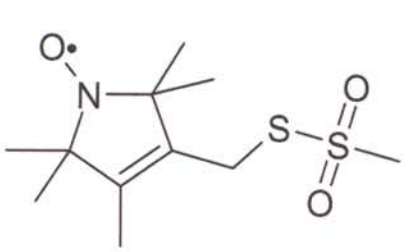

Figure 2. 2 Labeled arrestin mutants are functional. Arrestin affinity for dark rhodopsin (ROS), light-activated rhodopsin (ROS*), dark phosphorylated rhodopsin (ROS-P), and light-activated phosphorylated rhodopsin (ROS*-P) as assayed by centrifugal "pull-down" assay, as described in the Materials and Methods. The data indicate the labeled mutants retain WT-like specificity and affinity for ROS*-P. *Upper panel, lanes 1–4*, arrestin I72C. *Lanes 5–8*, arrestin I72C labeled with monobromobimane (I72B). *Lane 9*, for comparison, WT arrestin binding to ROS*-P is shown. *Lower panel, lanes 1–4*, arrestin S251C. *Lanes 5–8*, S251B. *Lane 9*, WT control. Molecular weight markers in kDa (*MW*) are indicated.

Figure 2. 2

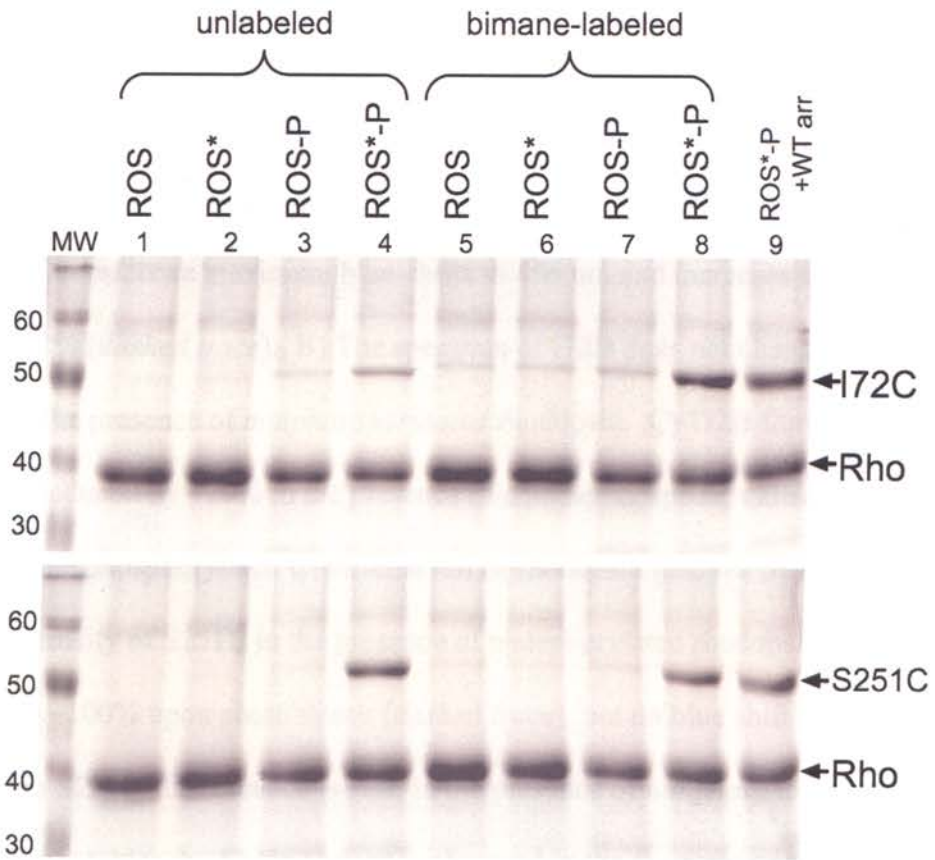
unlabeled
bimane-labeled
ROS
ROS*
ROS-P
ROS*-P
ROS
ROS*
ROS-P
ROS*-P
ROS*-P +WT arr
MW
1
2
3
4
5
6
7
8
9
60
50
40
30
I72C
Rho
60
50
40
30
S251C
Rho

Figure 2. 3 Fluorescence properties of arrestin I72B and S251B in the presence of ROS. The data indicate the fluorescence of bimane-labeled arrestin mutants change upon binding ROS*-P. **A)** I72B and sonicated ROS membranes containing phosphorylated rhodopsin (ROS-P) were mixed and loaded in the fluorimeter in the dark. In the dark, I72B shows a characteristic fluorescence maximum at ~470 nm (*black trace*). Upon light activation, the fluorescence maximum blue-shifts to 456 nm and increases in integrated intensity by ~12% (*dashed trace*). **B)** The spectrum of I72B does not change after photobleach in the presence of *nonphosphorylated* rhodopsin. **C)** I72B fluorescence (*solid trace*) is reduced by ~20% in the presence of a phosphopeptide, called 7PP, which corresponds to the phosphorylated C-terminal tail of rhodopsin (*dashed trace*). **D)** The fluorescence intensity of S251B in the presence of phosphorylated rhodopsin (*black trace*) increases ~100% upon photobleach (*dashed trace*), but no blue shift is observed. **E)** No change in S251B fluorescence is seen in the presence of *nonphosphorylated* rhodopsin after photobleach. **F)** No change is observed in the fluorescence of S251B in the absence (*solid trace*) or presence of phosphopeptide 7PP (*dashed trace*). The spectra represent normalized, background-subtracted data measured at 20 °C, as described in the Materials and Methods. In each experiment, 1 μM labeled arrestin and 4 μM rhodopsin (**A, B, D, E**) or 360 μM phosphopeptide 7PP (**C** and **F**) were used (10 mM HEPES, 150 mM NaCl, pH 7.4).

Figure 2. 3

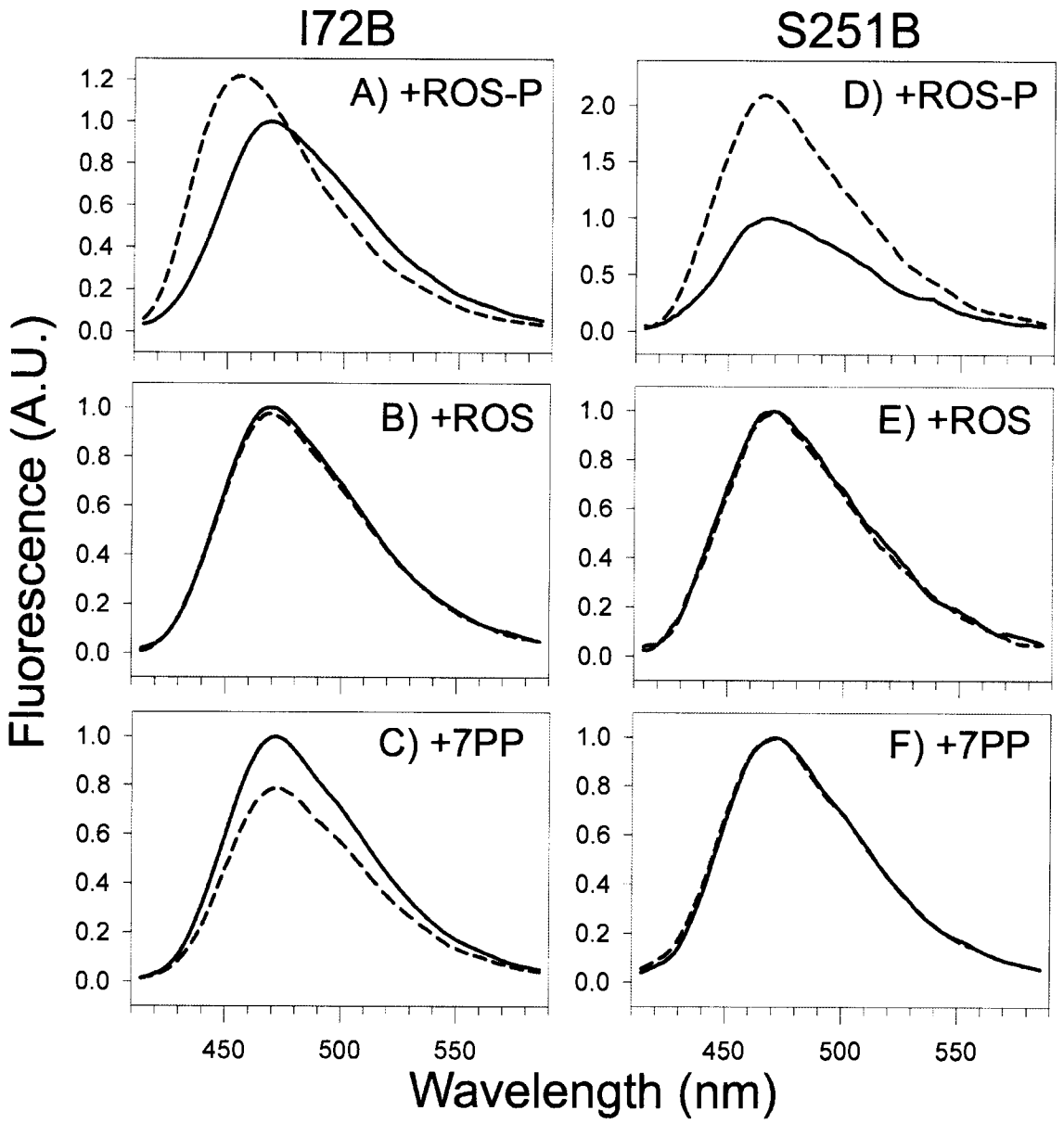
I72B
S251B
A) +ROS-P
D) +ROS-P
B) +ROS
E) +ROS
C) +7PP
F) +7PP
Fluorescence (A.U.)
Wavelength (nm)
450
500
550

Figure 2. 4 Kinetics of arrestin binding and release. The fluorescence changes in bimane-labeled arrestin mutants can be used to monitor binding and release from ROS*-P. **A)** Real-time monitoring of arrestin I72B binding to ROS*-P was carried out as described in the Materials and Methods. At time 0, the sample was irradiated (*left arrow*, hν1). Data from two independent experiments are shown (*open and closed circles*). The background-subtracted raw data are plotted (where F represents fluorescence and F_0 is dark state fluorescence) to show the relative change in fluorescence. A fit of the data (*solid line*) yields a rate constant k of $27.6 \pm 1.6 \times 10^{-3}$ s^{-1} ($t_{1/2} \sim 25$ s) for the binding of arrestin I72B to ROS*-P at 8 °C. Under these conditions, all of the arrestin is bound after the first flash, as indicated by the lack of fluorescence increase upon further photobleaching (*right arrow*, hν2, *gray circles*). **B)** Real-time monitoring of arrestin I72B release from ROS*-P. The fluorescence change at 456 nm due to I72B binding to ROS*-P reverses over time after the initial photobleach (*arrow*, hν). The *inset* shows the spectra of I72B in the dark (*thick black trace*) and after photobleach (*dashed trace*). The *thin black spectra* were measured at 5, 10, 15, 20, 30, 40, 60, 80, and 90 min after photobleach. The spectra were taken by combining I72B (1 μM) with a 4-fold excess of ROS-P in the dark at 20 °C and measured as described in the legend to Figure 2. 3.

Figure 2. 4

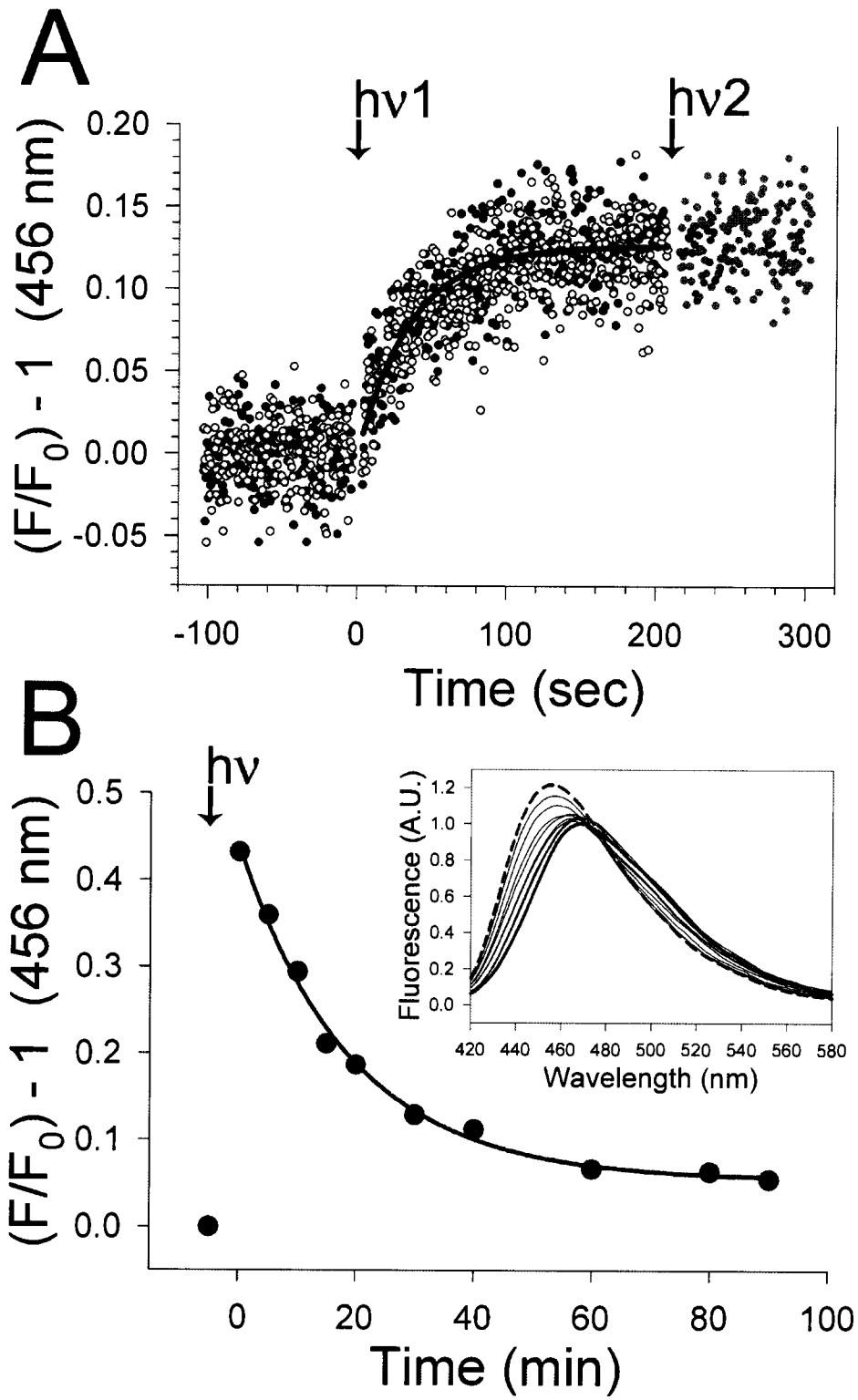
A
hν1
hν2
0.20
0.15
0.10
0.05
0.00
-0.05
(F/F0) - 1 (456 nm)
-100
0
100
200
300
Time (sec)
B
hν
0.5
0.4
0.3
0.2
0.1
0.0
(F/F0) - 1 (456 nm)
0
20
40
60
80
100
Time (min)
Fluorescence (A.U.)
1.2
1.0
0.8
0.6
0.4
0.2
0.0
420 440 460 480 500 520 540 560 580
Wavelength (nm)

Figure 2. 5 Temperature, pH, and arrestin dependence of retinal release from phosphorylated rhodopsin. Arrestin affects the rate and pH dependence of retinal release from ROS*-P. **A)** Using the fluorescence approach described in the Materials and Methods, retinal and arrestin release from ROS*-P can be monitored simultaneously. In this example, retinal release (λ_{ex} = 295 nm, λ_{em} = 330 nm, *black trace)* and arrestin release (λ_{ex} = 380 nm, λ_{em} = 456 nm, *gray trace*) from a sample of 4 μM I72B and 2 μM ROS-P was monitored at 25 °C. Rates were determined by fitting the buffer-subtracted raw data to a single exponential. The residuals demonstrate the goodness of fit. **B)** Arrestin slows retinal release from ROS*-P. Retinal (*atR*) release from ROS*-P in the absence of arrestin (*closed circles*), retinal release from ROS*-P in the presence of an excess of arrestin I72B (*open circles*), and arrestin release from ROS*-P (*triangles*) were measured at different temperatures (15–40 °C). The average of two independent experiments is shown for each point. **C)** Arrhenius analysis indicates that arrestin slows the rate of retinal release without dramatically affecting the energetics. The slopes of the plots indicate similar activation energies for retinal release from ROS*-P without arrestin (*closed circles*, E_a = 21.6 ± 0.9 kcal/mol), with arrestin (*open circles*, E_a = 19.4 ± 0.9 kcal/mol) and the release of arrestin from ROS*-P (*triangles*, E_a = 18.0 ± 0.7 kcal/mol) at pH 7.5. **D)** Arrestin abolishes the pH dependence of retinal release. The data show the effect of pH on retinal release from ROS*-P without arrestin (*closed circles*), retinal release from ROS*-P with an excess of arrestin I72B (*open circles*), and arrestin release from ROS*-P (*triangles*) at 35 °C. Each *point* represents data from two independent experiments.

Figure 2. 5

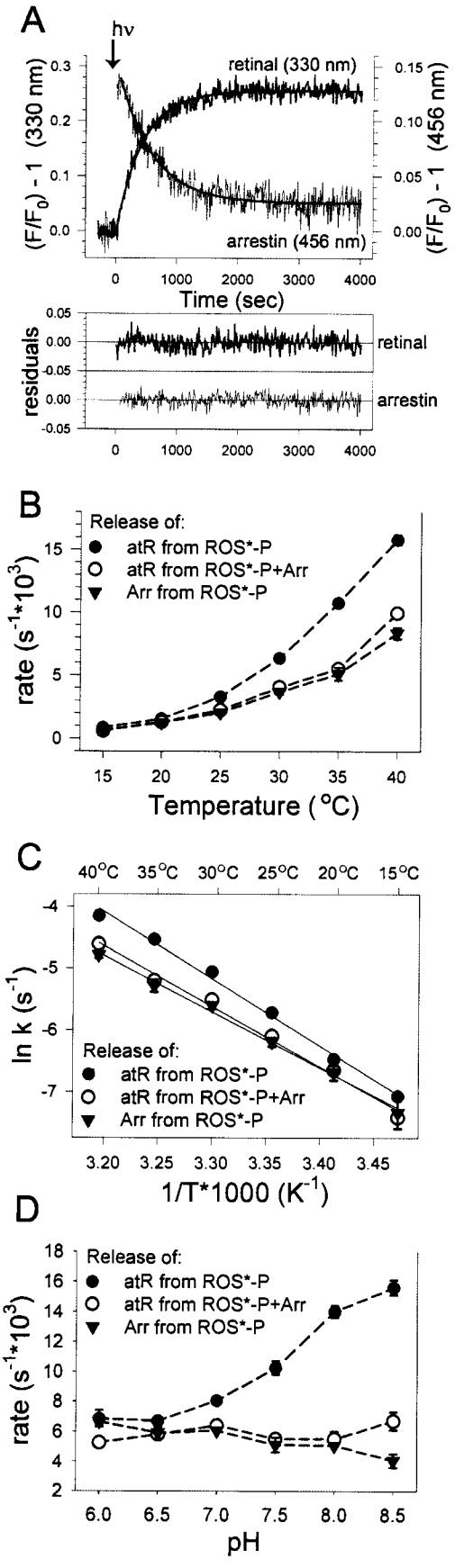
A
hv
retinal (330 nm)
arrestin (456 nm)
(F/F0) - 1 (330 nm)
(F/F0) - 1 (456 nm)
Time (sec)
residuals
retinal
arrestin
B
Release of:
atR from ROS*-P
atR from ROS*-P+Arr
Arr from ROS*-P
rate (s-1*10^3)
Temperature (°C)
C
40°C 35°C 30°C 25°C 20°C 15°C
ln k (s-1)
1/T*1000 (K-1)
D
rate (s-1*10^3)
pH

Figure 2. 6 A fraction of arrestin remains bound to rhodopsin after Meta II decay. Fluorescence and centrifugation studies both indicate that some arrestin remains bound to ROS-P after Meta II decay. **A)** After the initial increase after photoactivation (*arrow*), the fluorescence of arrestin I72B in the presence of ROS-P decreases as the arrestin dissociates, but it does not return to dark state levels and plateaus at ~20% of the starting state intensity. The addition of 10 mM hydroxylamine returns the fluorescence to dark state levels. *Inset*, a centrifugal pull-down assay also reveals that arrestin I72B remains bound to ROS-P long after Meta II decay. In this experiment, arrestin I72B and ROS-P were mixed in the dark and centrifuged at 90 s (*left lane*) or 1600 s after photobleach (*middle lane*). As a control, 10 mM hydroxylamine was added prior to centrifugation (*right lane*). The membrane pellets were subjected to SDS-PAGE, and the bimane labeled arrestin bands were visualized by fluorescence and quantified by densitometry. A significant amount of arrestin remains bound at 1600 s, corresponding to ~25% of the 90-s sample (subtracted for nonspecific pull-down seen in *far right lane*). Both experiments used 1 μM I72B and 4 μM ROS-P (pH 7, 35 °C). **B)** Fluorescence quenching analysis also indicates that a fraction of arrestin remains bound long after Meta II decay. Experiments similar to that shown in (A) were carried out with increasing concentrations of KI (0, 10, 20, 30, 50, 70, and 100 mM). Raw data (smoothed for the increase in noise due to the transformation) is plotted in three dimensions: time, KI concentration, and fractional change in fluorescence (where F represents fluorescence and F_0 is the fluorescence without quencher). Data from two independent experiments were used to derive Stern-Volmer constants of I72B in the presence of dark ROS-P (K_{SV} = 22.6 ± 0.4

M^{-1}) (*a*), after photoactivation (K_{SV} = 5.9 ± 0.6 M^{-1}) (*b*), and at the plateau (K_{SV} = 14.5 ± 1.5 M^{-1}) (*c*). The fits of F_0/F *versus* [KI] are indicated as *straight lines* in the *graph*.

Figure 2. 6

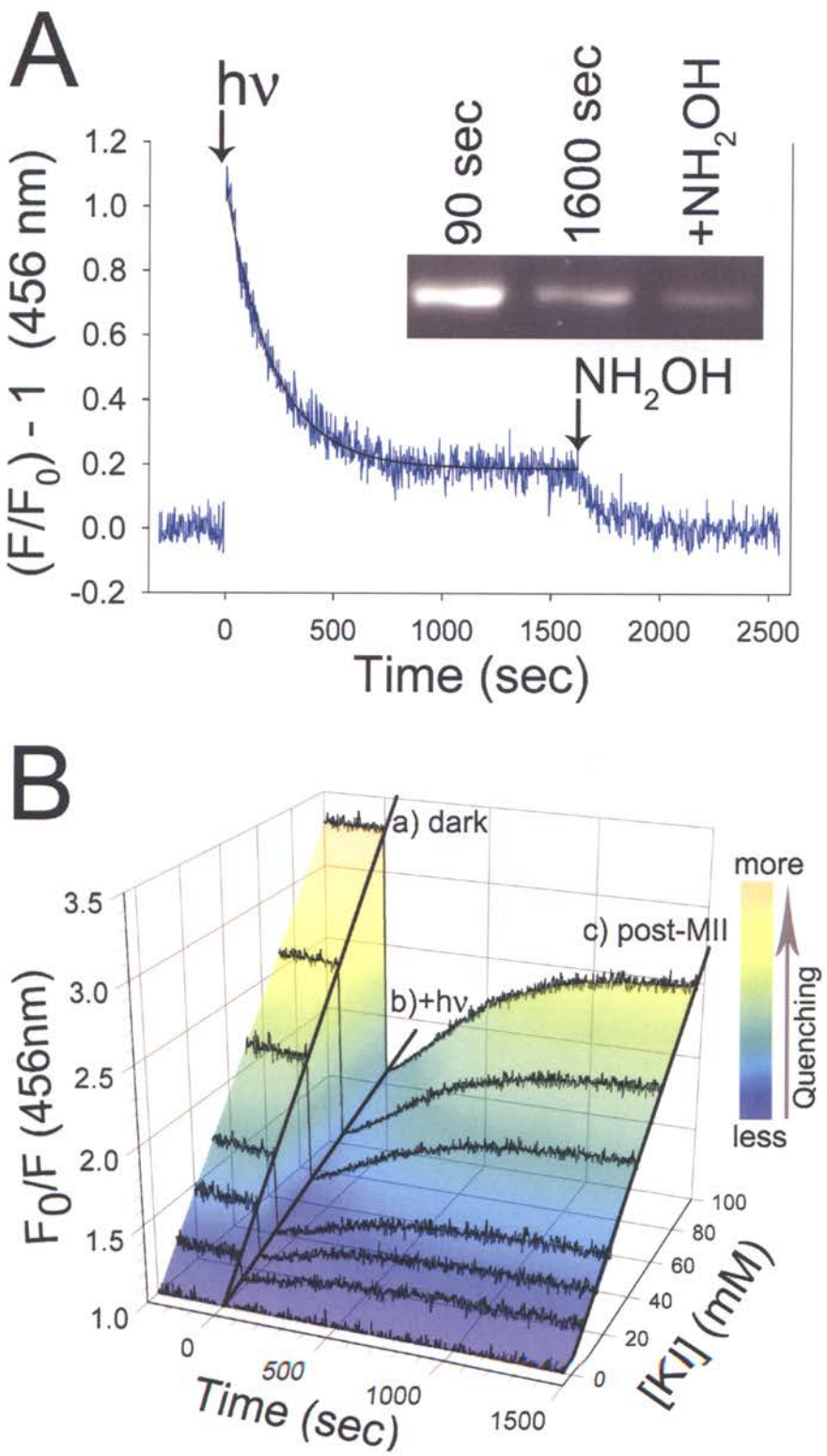
A
hν
90 sec
1600 sec
+NH2OH
NH2OH
(F/F0) - 1 (456 nm)
1.2
1.0
0.8
0.6
0.4
0.2
0.0
-0.2
0
500
1000
1500
2000
2500
Time (sec)
B
a) dark
b)+hν
c) post-MII
more
Quenching
less
F0/F (456nm)
3.5
3.0
2.5
2.0
1.5
1.0
0
500
1000
1500
Time (sec)
100
80
60
40
20
0
[K] (mM)

Figure 2. 7 EPR analysis of spin-labeled arrestin I72C. The nitroxide spin label at Ile^{72} is immobilized upon binding ROS*-P. **A)** Base line-corrected, unsmoothed EPR spectra of spin-labeled arrestin I72C (I72-SL) in the presence of an excess of ROS-P in the dark (*thick trace*), immediately (~2 min) after photoactivation (*thin trace*), and 90 min after photoactivation (*dotted trace*). EPR spectra represent four averaged scans of 50 μM I72-SL and 200 μM ROS-P (pH 7.5, 20 °C), except for the dark state scan, which represents nine averaged scans. **B)** The spectra of 50 μM I72-SL in the presence of 200 μM ROS-P or 20% Ficoll 400. *Bars*, 20 gauss.

Figure 2. 7

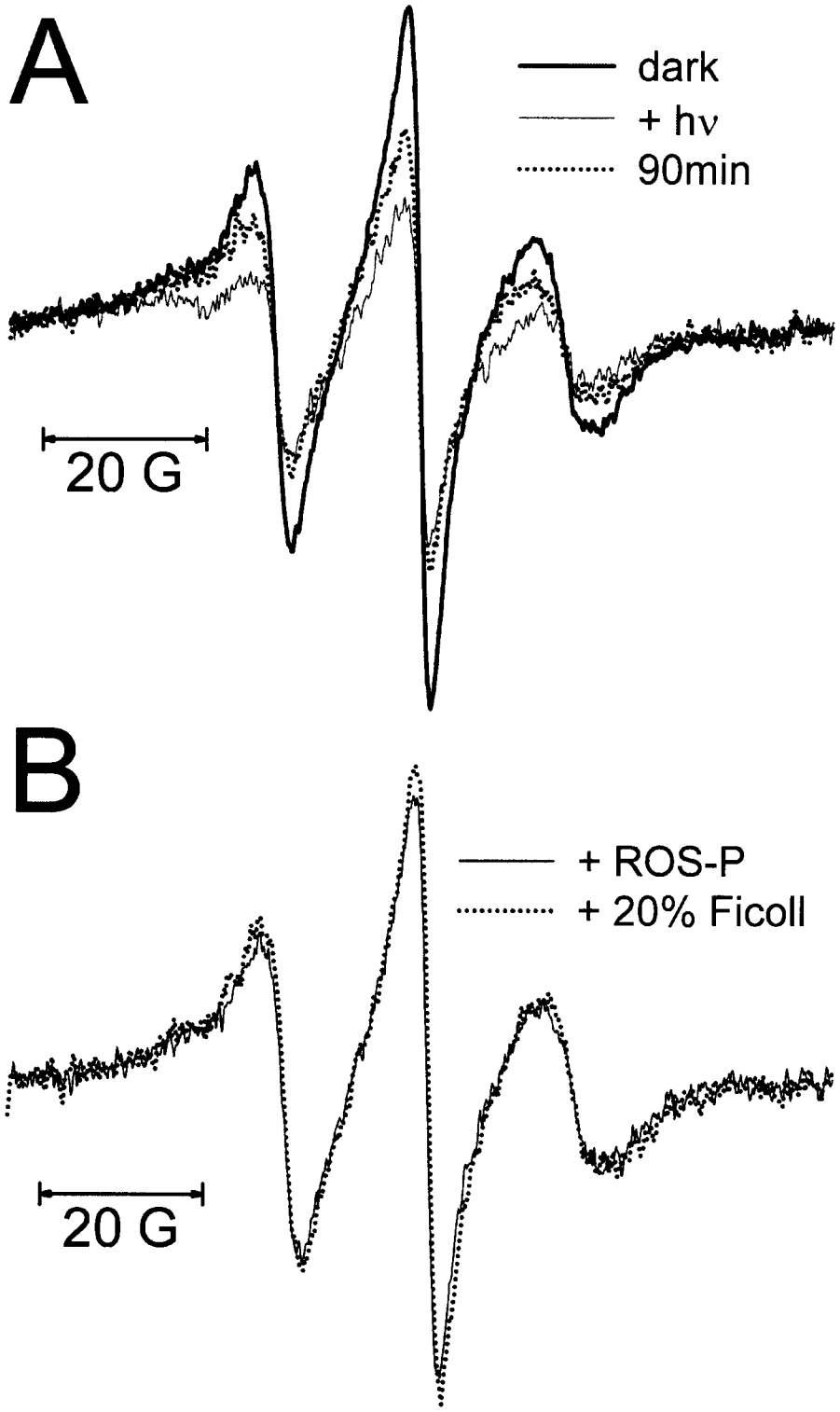

Figure 2. 8 Binding of arrestin to ROS-P after Meta II decay. ROS-P binds arrestin, even after Meta II has fully decayed. **A)** ROS-P membranes (10, 20, 30, and 40 μM) were photobleached at room temperature and allowed to decay at 35 °C for 12 min. At this time, arrestin I72B (1 μM) was added and allowed to incubate at room temperature for an additional 3 min. The samples were analyzed by a centrifugal pull-down assay, as described in the Materials and Methods. As a control, hydroxylamine (10 mM) was added prior to centrifugation in half of the samples and is seen to abolish the arrestin binding. The *far left lane* shows the amount of arrestin pulled down 90 s after photobleach at room temperature. **B)** Fluorescence analysis was used to derive normalized, background-subtracted values of bound arrestin from two independent experiments, as shown in (A). The arrestin that was pulled down in hydroxylamine containing samples represents the amount of nonspecific pull-down. A.U., arbitrary units.

Figure 2. 8

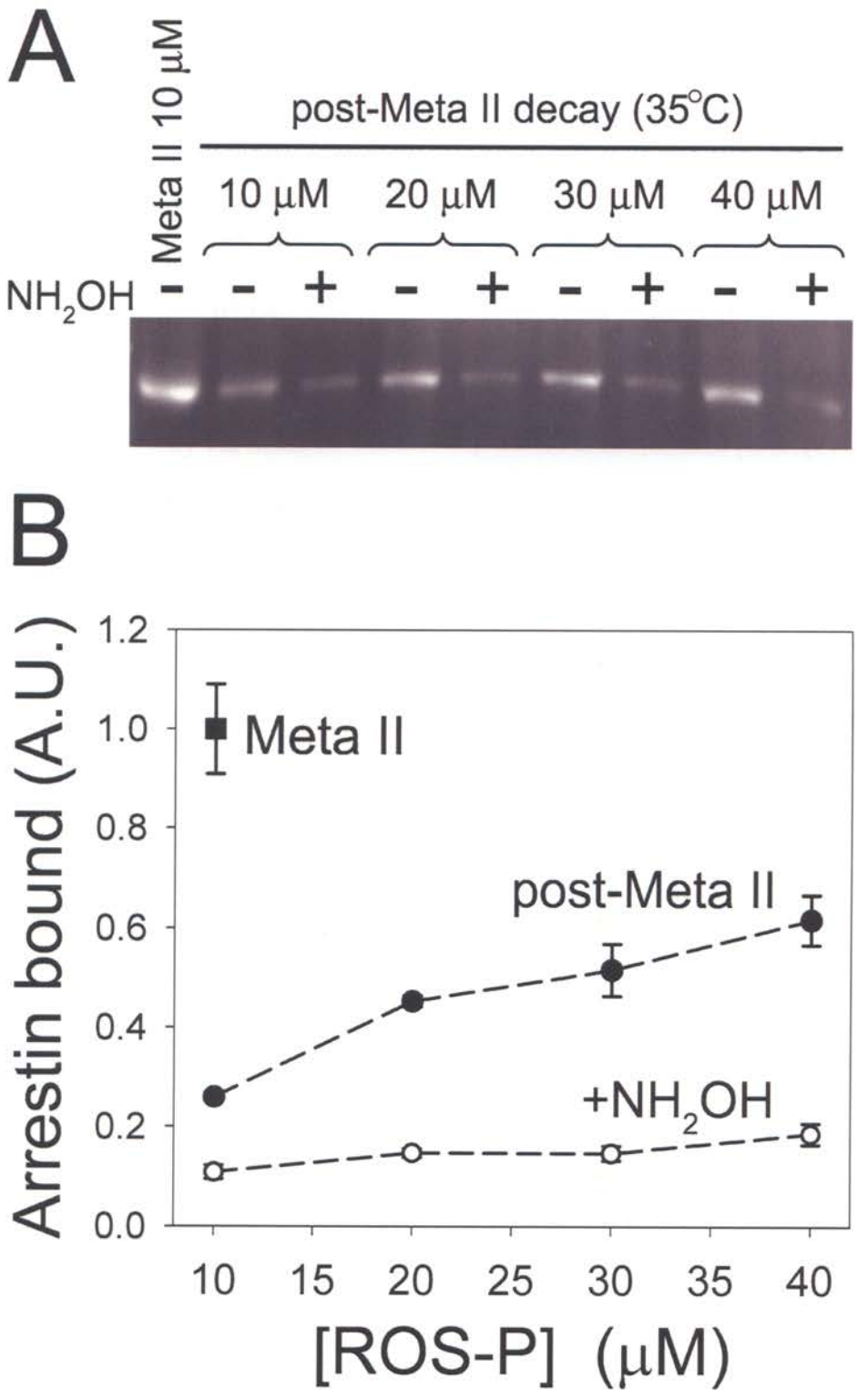
A
Meta II 10 μM
post-Meta II decay (35°C)
10 μM
20 μM
30 μM
40 μM
NH2OH - - + - + - + - +
B
Arrestin bound (A.U.)
1.2
1.0
0.8
0.6
0.4
0.2
0.0
Meta II
post-Meta II
+NH2OH
10 15 20 25 30 35 40
[ROS-P] (μM)

Figure 2. 9 Schematic of rhodopsin attenuation. This schematic diagram illustrates the relative time course of rhodopsin attenuation after photobleach and arrestin's possible interaction with the photodecay product Meta III. Dark state rhodopsin (*red*) absorbs light (hν) and converts within nanoseconds to Meta I and Meta II (*yellow*). Rhodopsin kinase (*RK*) phosphorylates the C-terminal tail of light-activated rhodopsin (Pulvermüller *et al.*, 1993; Maeda *et al.*, 2003). Meta II decays within seconds ($t_{1/2}$ = 65 s at 35 °C) to opsin (*gray*) and free retinal. If bound by arrestin, Meta II decay is slowed ($t_{1/2}$ = 126 s at 35 °C), and the arrestin and retinal release occur simultaneously. The Meta I/Meta II pool may also decay via Meta III and/or other photo-intermediates (*orange*) (Lewis *et al.*, 1997; Heck *et al.*, 2003a). Arrestin binds post-Meta II decay rhodopsin, producing a long lived complex. Arrestin may convert Meta III to Meta II when it binds (Hofmann *et al.*, 1992; Zimmermann *et al.*, 2004). Note that the timeline is not to scale, and events are placed along the timeline to show approximately when they occur after photoactivation.

Figure 2. 9

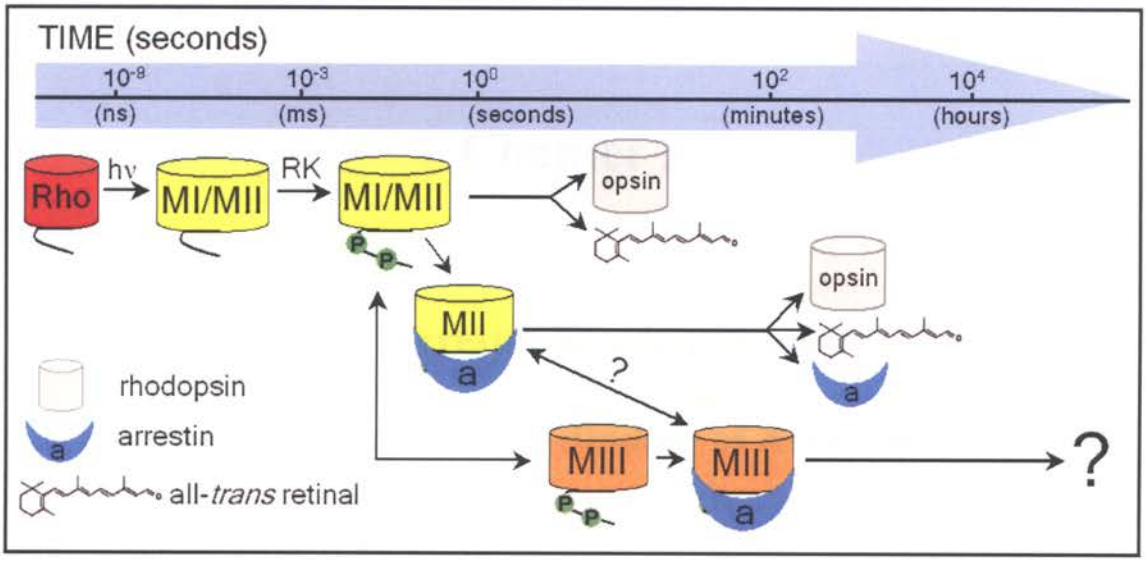
TIME (seconds)
10-8
(ns)
10-3
(ms)
100
(seconds)
102
(minutes)
104
(hours)
Rho
hν
MI/MII
RK
MI/MII
opsin
MII
opsin
a
?
rhodopsin
arrestin
all-trans retinal
MIII
MIII
a
?

Chapter 3

Dynamics of Arrestin-Rhodopsin Interactions: Acidic Phospholipids Enable Binding of Arrestin to Purified Rhodopsin in Detergent

Martha E. Sommer [‡], W. Clay Smith [§], and David L. Farrens [‡]

[‡] Department of Biochemistry and Molecular Biology, Oregon Health & Science University, Portland, OR 97239-3098, USA

[§] Departments of Ophthalmology and Neuroscience, University of Florida, Gainesville, FL 32610-0284, USA

3. 1 SUMMARY

We report acidic phospholipids can restore the binding of visual arrestin to purified rhodopsin solubilized in *n*-dodecyl-β-D-maltopyranoside (DM). We used this finding to investigate the interplay between arrestin binding and the status of the retinal chromophore ligand in the receptor binding pocket. Our results show that arrestin can stabilize Meta II and inhibit Meta III formation. Interestingly, in these mixed micelles, the release of retinal and arrestin is no longer directly coupled as it is in the native rod disk membrane. For example, up to ~50% of the retinal can be released even though arrestin remains bound to the receptor in a long-lived complex. We anticipate this new ability to study these proteins in a defined, purified system will facilitate further structural and dynamic studies of arrestin-rhodopsin interactions.

All sample preparation and experimental analysis reported in this chapter were performed by the author of this dissertation. Preliminary experiments utilized a purified arrestin sample from Dr. W. Clay Smith, but all subsequent experiments utilized arrestin mutants prepared by the author of this dissertation. Portions of this work have been published (Sommer, M.E., Smith, W.C., and Farrens, D.L. (2006) *J. Biological Chemistry* **281**: 9407-9417) and were recently presented (poster at the 50th Annual Biophysical Society Meeting, Salt Lake City, UT, 2006).

3. 2 INTRODUCTION

The integral membrane protein rhodopsin (Rho) enables the conversion of light to nerve signals in the rod cells, resulting in dim light vision (Pepe, 2001; Ridge *et al.*, 2003; Lamb and Pugh, 2004). In the dark, the chromophore (11-*cis*-retinal) is linked to Rho at Lys_{296} by a protonated Schiff base ($\lambda_{max} \sim 500$ nm). Light absorption isomerizes the chromophore to all-*trans*-retinal. Within milliseconds two photoproducts evolve, Meta I ($\lambda_{max} \sim 480$ nm) and Meta II ($\lambda_{max} \sim 380$ nm), which are in a pH- and temperature-sensitive equilibrium.

The ability of Meta II to bind and activate the G-protein transducin (Okada *et al.*, 2001) is terminated in several ways. Meta II can decay through hydrolysis of the Schiff base linkage and release of retinal, a process that takes ~1 min at physiological temperature and pH (Sommer *et al.*, 2005). Alternatively Meta II can decay to the long lived retinal storage photoproduct Meta III ($\lambda_{max} \sim 470$ nm) in which the Schiff base is intact and protonated (Lewis *et al.*, 1997; Heck *et al.*, 2003a; Vogel *et al.*, 2003; Vogel *et al.*, 2004b). Finally Rho signaling can be blocked through a series of protein-protein interactions that involves phosphorylation of the C-terminal tail of Rho by Rho kinase and binding of the protein arrestin (Gurevich and Gurevich, 2004).

As described in Chapter 2 of this dissertation, we found that these inactivation mechanisms are related for Rho in native ROS membranes. That is, arrestin release and retinal release appear to be directly linked events: both are described by similar activation energies, and arrestin slows the rate of retinal release ~2-fold at physiological temperatures. Intriguingly we also found that a fraction of the arrestin remains bound to ROS*-P long after "active" Meta II decay (Sommer *et al.*, 2005).

In the present work, we expanded upon these studies and made several surprising discoveries. First, we found that adding phospholipids restores arrestin binding to purified Rho*-P solubilized in *n*-dodecyl-β- D-maltopyranoside (DM). Second, we clearly established in the mixed micelle system that arrestin interacts with the post-Meta II photodecay product Meta III. Finally we found that arrestin and retinal release appear to be unlinked in mixed micelles with the acidic phospholipids PS, PI, and PA showing a more pronounced effect than the neutral phospholipids PC and PE (Figure 3. 1 shows a scheme of the different lipid head groups). Intriguingly with the acidic phospholipids, arrestin dissociation was nearly completely inhibited, yet approximately half of the retinal was released with the remainder trapped in the binding pocket.

3. 3 MATERIALS and METHODS

3. 3. 1 Materials

Frozen bovine retinas were purchased from Lawson and Lawson, Inc. (Lincoln, NE), and GBX red light filters were from Eastman Kodak Co. 11-*cis*-Retinal was a generous gift from Rosalie Crouch (Medical University of South Carolina and NEI, National Institutes of Health). Biomax centrifugal concentrators (10-kDa cutoff) were obtained from Millipore (Bedford, MA), and monobromobimane was purchased from Molecular Probes (Eugene, OR). Cuvettes were purchased from Uvonics (Plainview, NY), and band pass filters and long pass filters were obtained from Oriel (Stratford, CT). Acrylamide/bisacrylamide solution (37.5:1), and microcolumns were purchased from Bio-Rad. Concanavalin A-Sepharose, HiTrap heparin, and HiTrap Q prepacked columns were obtained from Amersham Biosciences. Spectroscopic grade buffers were from U.S.

Biochemical Corp. (Cleveland, OH). Asolectin was purchased from Fluka (Buchs, Switzerland), and DM was from Anatrace (Maumee, OH). Purified phospholipids 1,2 dioleoyl-*sn*-glycero-3-phosphocholine (PC), 1,2-dioleoyl-*sn*-glycero-3-phosphoethanolamine (PE), and 1,2-dioleoyl-*sn*-glycero-3-phosphoserine (PS), L-α-phosphatidylinositol (PI, from soy), and 1,2-dioleoyl-*sn*-glycero-3-phosphate (PA) were obtained from Avanti Polar Lipids (Alabaster, AL). All other chemicals and reagents were purchased from Sigma.

3. 3. 2 Buffers

Buffer A consisted of 137 mM NaCl, 2.7 mM KCl, 1.5 mM KH_2PO_4, 8 mM $NaHPO_4$, 2 mM $CaCl_2$, 2 mM $MgCl_2$, 2 mM $MnCl_2$, pH 6.0. Buffer B consisted of 20 mM HEPES, 2 mM $CaCl_2$, 2 mM $MgCl_2$, 2 mM $MnCl_2$, pH 6.5. Buffer C consisted of 20 mM HEPES, pH 7.4. Buffer D consisted of 10 mM Tris-HCl, 2mM EDTA, 100 mM NaCl, pH 7.5. Buffer E consisted of 10 mM Tris-HCl, 2 mM EDTA, pH 7.0. Buffer F consisted of 10 mM Tris-HCl, 2 mM EDTA, pH 8.5. Buffers A, B, and C were supplemented with 0.1 mM phenylmethylsulfonyl fluoride, and Buffers D, E, and F were supplemented with 1 mM dithiothreitol and protease inhibitor mixture (Sigma, for bacterial cell extracts) immediately before use.

3. 3. 3 Preparation of Rod Outer Segments and Purification of Rho

ROS and highly phosphorylated ROS were prepared from bovine retinas as described previously (Sommer *et al.*, 2005).

Rho was purified using concanavalin A. Briefly ROS containing 1 mg of Rho was solubilized in 14 ml of Buffer A containing 1% DM (mixing for 30 min at 4 °C) and then clarified by centrifugation (40,000 x *g* for 30 min). The supernatant was added to

concanavalin A-Sepharose (400 µl of settled beads, equilibrated with Buffer A plus 0.1% DM) and incubated overnight at 4 °C while mixing. Washing occurred batchwise: the beads were pelleted using a clinical centrifuge (2,000 rpm for 3 min), the supernatant was removed, fresh buffer was added, and the beads were mixed for 10 min (4 °C). The beads were washed three times with 15 ml of Buffer A plus 0.1% DM, three times with Buffer B plus 0.1% DM, and two times with Buffer C plus 0.05% DM. After transferring the beads to a microcolumn, Rho was eluted with Buffer C plus 0.05% DM and 0.3 M methyl α-D-mannopyranoside. Rho concentration was ascertained by absorbance at 500 nm (ε = 40,800 liters cm^{-1} mol^{-1}), and aliquots were snap frozen and stored at -80 °C. After thawing, Rho samples were centrifuged at 100,000 x *g* for 20 min, and the concentration was reassessed before use in experiments.

3. 3. 4 Construction, Expression, and Purification of Arrestin

The bovine visual arrestin cDNA with a single glycine inserted at residue 2 (a generous gift from V. V. Gurevich) was cloned in the pET15b vector (Invitrogen) for bacterial expression. Mutant constructs W194F and I72C/W194F were created using PCR, and the constructs were verified by DNA sequencing.

Arrestin was expressed in *Escherichia coli* BL21(DE3) cells and purified as described previously with some modifications (Schubert *et al.*, 1999; Gurevich and Benovic, 2000). A single colony was used to inoculate 400 ml of LB plus ampicillin (100 µg/ml), and this culture was grown while shaking at 37 °C overnight. This culture was then split between four flasks (each containing 1 liter of LB + ampicillin) and grown at 30 °C while shaking. Upon reaching an A_{595} of 0.6, the cultures were induced with 30 µM isopropyl 1-thio-β-D-galactopyranoside and grown for an additional 16–20 h. Cells

were harvested by centrifugation (6,000 x *g* for 15 min), resuspended in cold Buffer D, and lysed by two passes through a French press (20,000 p.s.i.). The lysate was cleared by centrifugation (27,000 x *g* for 30 min). Ammonium sulfate was added to a concentration of 0.32 g/ml, and the precipitated protein was collected by centrifugation (27,000 x *g* for 30 min). The pellet was resuspended in Buffer E and centrifuged again before being dialyzed overnight against Buffer E plus 0.1 M NaCl. The dialyzed lysate was loaded onto a HiTrap heparin column (20 ml) equilibrated with Buffer E plus 0.1 M NaCl. The column was washed with ~200 ml of Buffer E plus 0.1 M NaCl. After elution by a linear gradient of 0.1-0.5 M NaCl, the arrestin-containing fractions were determined by SDS-PAGE, pooled, and dialyzed overnight against Buffer F plus 0.1 M NaCl. The dialyzed fractions were loaded onto a HiTrap Q column (5 ml) equilibrated with Buffer F. The dialyzed fractions were diluted 1:10 with Buffer F while loading onto the column. The loaded column was washed with 50 ml of Buffer F, and arrestin was eluted with a two-step gradient: 0-0.1 M and 0.1-0.5 M NaCl. The arrestin-containing fractions were pooled and concentrated to ~2.5 mg/ml, snap frozen, and stored at -80 °C. The purity of the recombinant arrestin was >95% as ascertained by SDS-PAGE, and the yield was typically 5–6 mg of arrestin.

3. 3. 5 Labeling of Arrestin

Arrestin samples were labeled with monobromobimane as described previously (Sommer *et al.*, 2005) except that no His tag selection was used. Briefly arrestin samples were buffer exchanged (5 mM MES, 150 mM NaCl, pH 6.5) and concentrated, and monobromobimane was added in 10-fold molar excess to arrestin. After a 3 hour incubation at room temperature, the majority of the free label was removed by

ultrafiltration (Millipore Biomax). The labeled arrestin was then passed over a size exclusion column (500 µl, Sephadex G-15) to remove trace free label and buffer-exchanged into 20 mM HEPES, 150 mM NaCl, pH 7.4. The labeling efficiency was calculated as described previously (Sommer *et al.*, 2005); recombinant arrestin I72C/W194F labeled at ~92% efficiency, and recombinant arrestin W194F labeled at less than 2% efficiency. No free label contamination was detected in the labeled arrestin samples. Centrifugal pull-down analysis (Sommer *et al.*, 2005) showed arrestin W194F and bimane-labeled I72C/W194F to have essentially the same affinity for Rho*-P as that of wild-type arrestin (data not shown).

3. 3. 6 Preparation of Mixed Micelles

For experiments using mixed micelles of ROS phospholipids and DM, ROS containing 50 µM Rho-P was solubilized in 1% DM. The membranes were dispersed in the detergent by continuous sonication (25 °C for 2 min, Branson 1210) followed by centrifugation at 100,000 x *g* for 15 min to pellet the insoluble material. This stock of solubilized ROS-P was diluted into buffer containing different amounts of DM, and samples were sonicated briefly and incubated at 25 °C for 1 h to allow equilibration of the micelles.

For experiments using asolectin, an appropriate volume of 1% DM was added to a portion of powdered asolectin to yield a stock of 1% asolectin/DM. The solution was passed multiple times through a fine needle to disperse the phospholipids and was clarified by centrifugation (100,000 x *g* for 20 min) before use. For all experiments, DM and asolectin stocks were diluted in 20 mM HEPES, 150 mM NaCl, pH 7.4, to give a

final DM concentration of 0.02%. For molarity calculations of asolectin, an average phospholipid molecular mass of 750 g/mol was assumed.

For experiments using purified phospholipids, a measured volume of the chloroform stock corresponding to 1 mg of phospholipid (as supplied from Avanti) was dispersed into a glass test tube, and the chloroform was evaporated with a continuous stream of argon. The dried lipid film was then resuspended in a volume of 1% DM in buffer (20 mM HEPES, 150 mM NaCl, pH 7.4) by vortexing and multiple freeze-thaw cycles to give a final phospholipid concentration of 5 mM. All phospholipid suspensions were stored in the dark and handled under argon to avoid lipid oxidation, and lipid stocks were clarified by centrifugation (30,000 x *g* for 10 min) before use.

3. 3. 7 Fluorescence Spectroscopy

All steady-state and time-resolved fluorescence measurements were made as described previously (Sommer *et al.*, 2005). The tryptophanless arrestin mutant W194F was used, for it contributes less background while measuring opsin tryptophan fluorescence in samples of Rho and arrestin. Because asolectin exhibits some intrinsic fluorescence, background controls were measured and subtracted from appropriate fluorescence spectra.

3. 3. 8 UV-Visible Absorbance Spectroscopy

All UV-visible absorption spectra were recorded with a Shimadzu UV-1601 spectrophotometer using a bandwidth of 2 nm. For the photodecay experiments, the absorbance of 1 μM Rho-P (120 μl) was recorded in the dark after base-lining with the appropriate buffer. The sample was photoactivated using a 150-watt fiber optic light

source (>495 nm) for 20 s, and spectra were subsequently recorded every 90 s for 120 min. The presence of Schiff-base was ascertained by the addition of 5 µl of 0.8 N H_2SO_4.

3. 3. 9 $NaBH_4$ Reduction and V8 Proteolysis of Rho

Reduction of the Schiff-base in Rho with $NaBH_4$ results in the fluorescent *n*-retinylidene opsin species (λ_{ex} = 340 nm; λ_{em} = 480 nm) (Bownds and Wald, 1965; Farrens and Khorana, 1995). Samples of 3 µM Rho-P, with or without 6 µM arrestin, solubilized in 0.02% DM, 0.02% DM and 0.02% asolectin, or 0.02% DM and 100 µM purified phospholipid (20 µl) were photoactivated using a 150-watt fiber optic light source (>495 nm) for 20 s and allowed to decay at 20 °C in the dark. After 120 min, 5 µl of 1% $NaBH_4$ (made fresh in water) was added to each sample. After 10 min, 15 µl of 1 M sodium phosphate (pH 7.0) was added, each sample was split into two 20-µl aliquots, and 5 µl of 4.8 µM V8 protease was added to half the samples. Proteolysis occurred for 30 min at room temperature. To assess the amount of Schiff-base present in Meta II Rho immediately after activation, 1% NaBH4 was added to Rho-P (0.02% DM) in the dark. The sample was then photoactivated at 4 °C and immediately processed as described above. Bands were resolved by 15% Tris-Tricine SDS-PAGE, and gels were soaked in 30% methanol before visualization. The *n*-retinylidene opsin was excited with a short wave UV source (Alpha-Innotech FluorChem 5500 imaging system), and the fluorescent bands were detected by a charge-coupled device camera (535 ± 50 nm cutoff filter, 10 min exposure). AlphaEase FC software was used to quantify the fluorescence of the bands.

3. 4 RESULTS

Our results here indicate the following. 1) Phospholipids are required to enable Rho-arrestin interactions in detergent micelles. 2) In mixed DM/phospholipid micelles, arrestin interacts with Meta III and converts it to a Meta II-like species. 3) Arrestin release is significantly inhibited from Rho*-P in mixed micelles containing acidic phospholipids, while half of the retinal is trapped in the binding pocket. Details are given below.

3. 4. 1 Arrestin has Reduced Affinity for DM-purified Rho*-P

The binding of bimane-labeled arrestin I72C/W914F (I72B) to Rho*-P in native membranes resulted in an increase (~40%) and a blue shift (~15 nm) in fluorescence (Figure 3. 2A). However, when Rho-P was purified from ROS and solubilized in DM, the fluorescence changes were dramatically reduced, indicating a loss of arrestin binding (Figure 3. 2B).

3. 4. 2 Asolectin Stimulates Arrestin Binding to DM-purified Rho*-P

Adding asolectin (a mixture of phospholipids often used in Rho reconstitution (Niu *et al.*, 2002)), to DM-purified Rho-P restores I72B binding: the fluorescence increased ~70% and blue shifted ~15 nm after photoactivation (Figure 3. 2C).

3. 4. 3 Dilution of ROS Lipids with Detergent Inhibits Arrestin Binding to Rho*-P

We determined the effect of decreasing the apparent concentration of native ROS lipids on arrestin binding using DM (Figure 3. 2D). Rather than purify ROS lipids and add them back to purified Rho-P, we fully solubilized native ROS-P membranes and then added this mixture to buffer containing low to high concentrations of DM (0.02–1.0%). In this way, the relative Rho/phospholipid ratio was preserved, but the number of

micelles into which the phospholipids could segregate was increased. This process ensured that minimal oxidation or damage occurred to the ROS lipids. A similar approach has been used previously in control experiments involving ROS lipids (Gibson and Brown, 1993).

When this DM-solubilized ROS-P was added to 0.02% DM (micelle concentration, ~3 μM) [6], arrestin could bind as indicated by the ~70% increase and 15-nm blue shift in fluorescence. However, at higher DM concentrations, binding was dramatically inhibited (Figure 3. 2D). In 1% DM (micelle concentration, ~150 μM), the fluorescence of arrestin I72B increased only ~17% and blue shifted less than 2 nm after light activation. Assuming the ROS phospholipids distribute evenly to all micelles, we interpret this result to reflect the ability of DM to solubilized ROS phospholipids away from Rho. Although DM might directly inhibit arrestin binding, the addition of sufficient amounts of exogenous phospholipids, even at high DM concentrations, could rescue arrestin binding (see Figure 3. 2E, *inset*).

3. 4. 4 ~50 Phospholipids per Rho-P are Required for Arrestin Binding

We quantified the phospholipid effect by titrating asolectin in samples of DM-purified Rho-P (Figure 3. 2E). These studies indicate that ~0.015% asolectin, or ~200 μM phospholipid, is required to achieve maximal arrestin binding under conditions where there is roughly one Rho per micelle. This corresponds to ~67 phospholipids per Rho. Interestingly this is similar to the Rho/phospholipid ratio in the ROS where Rho composes half the volume of the tightly stacked membranous organelles (Anderson and Maude, 1970; Daemen, 1973; Molday, 1998). When 10-fold more DM was present,

[6] This calculation assumes that the aggregation number of 132 molecules of DM/micelle (Dupuy *et al.*, 1997) is not dramatically changed by the presence of ROS phospholipids.

correspondingly more phospholipid was required (0.1-0.12% asolectin) (Figure 3. 2E, *inset*). Again this value corresponds to ~50 phospholipids per micelle.

3. 4. 5 Some Retinal and Arrestin Release is Inhibited in Mixed Micelles

We used a fluorescence dual rate assay (Sommer *et al.*, 2005) to investigate the various dynamics of arrestin and retinal release. This assay monitors release of retinal as an increase in the tryptophan fluorescence of opsin (Farrens and Khorana, 1995) while simultaneously measuring dissociation of arrestin I72B as a decrease in bimane fluorescence. We determined the maximal and minimal fluorescence values possible for each process (the "plateaus") by adding hydroxylamine, a compound that cleaves the Schiff base and converts all remaining photoproducts to opsin and free retinaloxime.

Figures 3. 3A, 3C, and 3E, compare retinal and arrestin release from Rho*-P in pure DM micelles or mixed micelles containing ROS phospholipids or asolectin. The half-lives ($t_{1/2}$) of retinal and arrestin release and the relative levels of retinal trapping and arrestin binding are given in Tables 3. 1 and 3. 2. The data are briefly summarized below.

Mixed DM/ROS Phospholipid Micelles - In these samples, retinal release from Rho*-P ($t_{1/2}$ ~ 15 min) is slowed compared with intact native membranes by a factor of 2 (Sommer *et al.*, 2005). Adding hydroxylamine at the end of decay caused only a slight increase in fluorescence (Figure 3. 3A). In the presence of arrestin, retinal release was slowed by a factor of ~1.5 ($t_{1/2}$ ~ 23 min), and slightly more retinal appears to be trapped (~5%). Binding of arrestin I72B in these samples caused an increase (~50%) in bimane fluorescence, and the fluorescence decreased over time as arrestin dissociated at a slightly slower rate than retinal release ($t_{1/2}$ ~ 28 min) (Figure 3. 3A). The fluorescence plateaued

at~20% of the starting state intensity, indicating some arrestin remained bound. The addition of hydroxylamine returned the fluorescence to the starting state level. This pronounced residual post-Meta II binding is very similar to what we previously observed in native membranes (Table 3. 2) (Sommer *et al.*, 2005).

Pure DM Micelles - Retinal was released from these samples with a $t_{1/2} \sim 8$ min, and the tryptophan fluorescence increased a further ~20% upon the addition of hydroxylamine (Figure 3. 3C). Arrestin did not significantly affect either the rate of retinal release ($t_{1/2} \sim 9$ min) or the fluorescence plateau probably because little binding occurred. This sample showed only a small increase (~12%) in bimane fluorescence (Figure 3. 3C). We attribute the small amount of arrestin binding to DM-purified Rho-P to residual ROS phospholipids that were not removed during purification. Residual phospholipids are extremely difficult to remove with detergents (Aveldano, 1988; Aveldano, 1995; Cha *et al.*, 2000).

Mixed DM/Asolectin Micelles - The most striking effects were observed for these samples (Figure 3. 3E). Remarkably in the presence of arrestin, the tryptophan fluorescence of opsin plateaued at approximately half that seen in the absence of arrestin. Addition of hydroxylamine caused a dramatic increase in the opsin fluorescence to the same level as seen without arrestin. Arrestin binding to Rho*-P in these samples caused a ~50% increase in bimane fluorescence, and the rate of arrestin release ($t_{1/2} \sim 23$ min) was ~70% slower than retinal release (Figure 3. 3E). The bimane fluorescence plateaued at approximately half of the starting state intensity, and hydroxylamine returned the fluorescence to the starting state level.

3. 4. 6 Arrestin Blocks Meta III Formation

We also assessed the effect of the mixed micelles and arrestin on Rho-P photodecay by UV-visible absorption spectroscopy. In each type of micelle, dark state Rho-P exhibited a characteristic absorption maximum at 500 nm that shifted to 380 nm after light activation (Figure 3. 3B, 3D, and 3F, *upper panels*). Over time, the 380 nm absorbance decreased, whereas the absorbance between 440 and 480 nm increased. This latter increase could be due to both the appearance of Meta III (470 nm) and release of retinal from the binding pocket to form adducts with phospholipids (440–450 nm).

After photodecay, we looked for the presence of retinal Schiff base by acidifying the samples. A protonated retinal Schiff base adduct absorbs at 440 nm, and this property can be used to detect retinal attached to opsin or linked to phospholipid. These measurements showed very little Schiff base present for photodecayed Rho*-P in DM micelles (Figure 3. 3D, *upper panel*). In contrast, photodecayed Rho*-P in DM/ROS phospholipid and DM/asolectin mixed micelles gave a broadened red shifted absorbance (Figure 3. 3B and 3F, *upper panels*) that is typical for retinal adducts with PE (data not shown).

Not surprisingly (because it shows limited binding) arrestin did not affect the photodecay absorption spectra of Rho*-P in DM micelles (Figure 3. 3D, compare *upper* and *lower panels*). In contrast, arrestin caused substantial changes to the spectra of Rho*-P in mixed DM/ROS phospholipid and in DM/asolectin micelles (Figure 3. 3B and 3F). Both the absorbance loss at 380 nm and the increase between 440 nm and 480 nm were inhibited. Acidification produced a 440 nm absorbance peak indicative of protonated Schiff base. Together these data show that arrestin stabilizes Rho*-P as a

Meta II-like 380 nm-absorbing species in which retinal is covalently attached by a Schiff base.

3. 4. 7 Acidic Phospholipids Enhance Arrestin Binding and Inhibition of Retinal Release

We next assessed the effect of different phospholipids on arrestin's ability to trap retinal and inhibit Meta III formation. In these experiments, we used the dioleoyl form (except for PI, which contained a mixture of fatty acids). Experiments were carried out with a standard 100 μM phospholipid because in our experiments this was the maximal concentration at which all phospholipids were soluble in 0.02% DM.

Retinal release data with the different phospholipids are summarized in Table 3. 1. The neutral phospholipids PC and PE showed no significant difference in retinal trapping with or without arrestin. The absorbance data confirmed this result (Figure 3. 4). In contrast, significant differences in the ability of arrestin to trap retinal were seen using the acidic phospholipids PS, PI, and PA. With these lipids, approximately half of the retinal appeared to be trapped when arrestin was present, and the absorbance spectral changes were significantly reduced. Interestingly arrestin appeared to only affect the level at which opsin tryptophan fluorescence plateaued after photoactivation, not the rate of retinal release.

The effect of the different types of phospholipids on arrestin I72B binding and release to DM-purified Rho*-P is summarized in Table 3. 2. Qualitatively arrestin binding was only slightly enhanced by PC and PE but was significantly enhanced by PS, PI, and PA (Figure 3. 4). However, we are reluctant to read too much into the relative increases in arrestin I72B fluorescence. The bimane probe is sensitive to the polarity of

its environment (Kosower *et al.*, 1986; Mansoor *et al.*, 1999; Mansoor and Farrens, 2004), and we are unsure of how the different phospholipid head groups might alter the fluorescence intensity of the probe. However, we can conclude that PS, PI, and PA allow significant arrestin binding based on the fact that these phospholipids dramatically enhanced arrestin-dependent trapping of retinal and significantly slowed the rate of arrestin release. With these lipids, I72B fluorescence decreased only ~10% in the 2 hours after photoactivation. Most surprisingly, in contrast with ROS native membranes, the rates of arrestin and retinal release from mixed micelles were unlinked with the greatest difference seen with the acidic phospholipids. The significance of these results is explored in the Discussion.

We also tested the effects of docosahexaenoic acid-conjugated phospholipid because the ROS membrane is unusually enriched in this highly unsaturated long fatty acid (Anderson and Maude, 1970; Aveldano and Bazan, 1983; Aveldano, 1988). However, there were no significant differences in the data using this lipid compared with the dioleoyl forms (data not shown).

3. 4. 8 Biochemical Evidence that Arrestin Traps Retinal as a Schiff Base Adduct

We used the plateau level of tryptophan fluorescence to quantify the amount of trapped retinal as has been described by Heck *et al.* (Heck *et al.*, 2003a) (Figure 3. 5A and 5B). We also developed an independent assay to measure the amount of trapped retinal that exploits the fact that reducing the retinal Schiff base with $NaBH_4$ forms a fluorescent species, *n*-retinylidene opsin (Bownds and Wald, 1965; Farrens and Khorana, 1995). This new assay quantified the amount of trapped retinal in Rho*-P in different

micelles by $NaBH_4$ reduction 2 hours after photoactivation in the presence or absence of arrestin (Figure 3. 5C). Subsequent SDS-PAGE enabled the separation the *n*-retinylidene opsin from possible retinal-phospholipid adducts, and quantification of the fluorescent bands was plotted relative to the total amount of retinal Schiff base present in Meta II Rho*-P immediately after photobleaching (Figure 3. 5D).

The two methods reported very similar amounts of retinal trapping (Figure 3. 5, compare B and D). In pure DM micelles, ~20% of the original retinal population was attached to opsin after photodecay. This residual retinal may represent Meta III as well as retinal that is attached to peripheral lysines on Rho*-P after release from the binding pocket. In the presence of arrestin, the amount of fluorescence was not significantly changed.

Why is the trapping in DM/asolectin mixed micelles (~10%) lower than in DM alone? Presumably PE in asolectin competes with lysine residues for retinal (Sparrow *et al.*, 2003). This conclusion is supported by the presence of a low molecular weight fluorescent species seen on the gel (see Chapter 4, Figure 4. 3). Significantly arrestin caused ~60% of the retinal to remain attached to opsin (*lane 5*). In data not shown here (see Chapter 4, Figure 4. 3), V8 proteolysis analysis showed that most of this retinal (~80%) was attached to fragment F2 (residues 240–338, which contains Lys^{296} to which retinal is attached in dark state and Meta II Rho). These results confirm the fluorescence and absorption data in Figure 3. 3: in the presence of asolectin phospholipid, arrestin traps approximately half the retinal, presumably at Lys^{296}.

In mixed micelles containing the purified phospholipids, very little retinal was trapped by arrestin in the presence of PC or PE. In contrast, PS, PI, and PA allowed

significantly more retinal to be trapped when arrestin was present. Although generally the two methods for quantifying trapped retinal showed excellent agreement, samples with PS were unusual: they showed more retinal trapped as measured by tryptophan fluorescence (~57%) than that measured by $NaBH_4$ reduction (~22%). We are not sure of the cause of this discrepancy, but PS may somehow inhibit the reduction reaction.

3. 5 DISCUSSION

3. 5. 1 Mixed Micelles are Advantageous for Studying Arrestin

We found that acidic phospholipids could restore arrestin binding to DM-purified Rho*-P. This discovery opens the door for studying arrestin-Rho interactions in a soluble mixed micelle system [7]. Mixed micelles, because they are chemically defined, can be extremely helpful in the study of membrane proteins (Kragh-Hansen *et al.*, 1993; Kragh-Hansen *et al.*, 1998; Lichtenberg *et al.*, 2000; Seddon *et al.*, 2004). For example, they enable the purification of stable opsin from transfected COS cells (Rim and Oprian, 1995; Reeves *et al.*, 1999) and increase the affinity of transducin for Rho (Bubis, 1998). Mixed micelles exhibit similar advantages for studying arrestin, and we used our new system to carry out a more detailed examination of the interplay between arrestin and the retinal chromophore in Rho. The implications of our findings are discussed below.

3. 5. 2 Arrestin Stabilizes Spectral Meta II

Our studies showed that in mixed micelles containing asolectin, PS, PI, or PA, arrestin inhibited ~50% of the retinal release from Rho*-P. We confirmed this result

[7] Our conditions were well above the critical micelle concentration of DM, which is 0.006% at 0.2 M NaCl (unpublished measurements by Anatrace, Inc. in collaboration with R. M. Garavito). All experiments were carried out in a fully soluble system because samples could be centrifuged at 100,000 x *g* for 1 h with no loss of Rho-P absorbance.

using two independent methods: the tryptophan fluorescence retinal release assay and a new $NaBH_4$ reduction/SDS-PAGE method. Our results demonstrated that arrestin trapped this retinal in a Schiff base-linked form with a 380 nm absorbance (Figures 3. 3F and 4) with the retinal most likely still attached to Lys^{296} (data not shown) [8]. Cleaving the Schiff base retinal linkage with hydroxylamine released both the trapped retinal and arrestin from Rho*-P in mixed micelles (Figures 3. 3E and 4). Thus, we conclude arrestin can stabilize Meta II in a long-lived arrestin-Rho complex.

3. 5. 3 Why do Phospholipids Affect Arrestin Binding to Rho*-P?

It is unlikely that phospholipid-dependent effects on Rho photochemistry (Gibson and Brown, 1993; Litman *et al.*, 2001; Wang *et al.*, 2002; Alves *et al.*, 2005) explain the results presented here. The mixed micelles used in this study did not greatly affect the Meta I/Meta II equilibrium as the spectra of Rho*-P in the various mixed micelles were similar to those in pure DM micelles (see Figure 3. 4).

One possibility is that arrestin interacts directly with the phospholipids. Rho is certainly intimately associated with its surrounding phospholipids: it immobilizes ~25 phospholipids and induces a reorganization of these lipids upon light activation (Hessel *et al.*, 2001; Marsh and Pali, 2004). In fact, Rho and ROS phospholipids interact so tightly that it is very difficult to remove all lipids during Rho purification with detergents or even with organic solvents (Aveldano, 1988; Aveldano, 1995; Cha *et al.*, 2000). Our results may suggest that phospholipids compose a significant portion of the Rho arrestin

[8] Note that our results do not rule out the possibility that the retinal may have migrated to a secondary binding site, perhaps near Helix VIII, as has been proposed to occur during ligand channeling (Schädel *et al.*, 2003).

interface, and when phospholipids are removed from Rho-P by purification in detergent, the relative affinity decreases, and arrestin binding is severely diminished.

Interestingly our results may also imply that negative charges found on the phospholipid head groups are involved in a high affinity interface between arrestin and Rho*-P. In data not shown here, we found that free fatty acid or water-soluble short chain acidic lipids, like dioctanoyl phosphoserine, could enhance arrestin binding to DM purified Rho*-P. Conversely we also found that high concentrations of salt could inhibit arrestin binding to Rho*-P either in mixed micelles or native membranes. Together these results imply that ionic interactions may be involved in arrestin binding. However, it is difficult to interpret the effect of salt as it may alter the micelle structure or interactions with the phosphorylated tail and cytoplasmic loops of Rho*-P.

However, it is also possible that the phospholipids help stabilize a spectrally silent Rho conformation that interacts more tightly with arrestin. For example, Krishna *et al.* (Krishna *et al.*, 2002) suggest that the phospholipid PS induces helical structure in Helix VIII of Rho. Thus, arrestin may not bind to DM-purified Rho*-P because the structure of Helix VIII is perturbed. Addition of acidic phospholipids may restore the helical structure and enable arrestin binding.

3. 5. 4 Some Arrestin and Retinal Release Appear Unlinked in Mixed Micelles

Surprisingly we found that the rates of retinal and arrestin release differed in mixed phospholipid/detergent micelles in contrast with our previous findings with ROS membranes (Sommer *et al.*, 2005). The magnitude of the difference was dependent on the type of phospholipid. In mixed micelles containing ROS phospholipids, arrestin was released only ~20% more slowly than retinal; in micelles containing pure PC or PE,

arrestin was released ~40% more slowly. Remarkably in the presence of acidic phospholipids PS, PI, and PA, arrestin was released at least 10 times more slowly than retinal. We can rule out the possibility that this effect is merely due to nonspecific interaction of arrestin with the micelle based on our retinal trapping data (discussed below).

What could explain this anomaly? Is it related to the observation that adding detergent to membrane-bound Rho also affects retinal release and uptake, or "ligand channeling"? Some have proposed that a secondary retinal binding site is formed by Helix VIII of Rho (Sachs *et al.*, 2000a; Heck *et al.*, 2003a; Schädel *et al.*, 2003), and detergent may disrupt the interaction of the palmitoyl anchors of Helix VIII with the membrane. Because we found that arrestin and retinal release were decoupled in detergent, our results may imply a role for ligand channeling in arrestin release. Interestingly Kiselev and Subramaniam (Kiselev and Subramaniam, 1996) have found that addition of detergent to membrane extracts of *Drosophila* rhodopsin appears to decouple arrestin release and the rates of regeneration in the photocycle.

Note that the rates of arrestin and retinal release were more similar in micelles containing native ROS lipids than in those containing purified lipids. Perhaps some "special ingredient" present in the ROS might be responsible for coordinating these two events. ROS phospholipids are composed of ~45% PC, 42% PE, and 13% PS (Anderson and Maude, 1970; Aveldano and Bazan, 1983), and these phospholipids are enriched in the highly unsaturated long fatty acid docosahexaenoic acid (22:6*n*-3) (Anderson and Maude, 1970; Aveldano and Bazan, 1983; Aveldano, 1988). The ROS membrane also

contains a substantial amount of cholesterol (12–14%) (Anderson *et al.*, 1976; Stone *et al.*, 1979).

Perhaps the most intriguing anomaly in our results is that, although arrestin remained bound (~90%) using acidic phospholipids, only about half of the retinal was trapped. The cause of this discrepancy was not likely due to the presence of a large amount of nonphosphorylated Rho because our samples, at ~6 phosphates per Rho (Sommer *et al.*, 2005), were near the maximum of 7 (Maeda *et al.*, 2003). An intriguing (but highly speculative) possibility is that arrestin forms a long-lived complex when it interacts with a dimer of Rho*-P in which the retinal is able to dissociate from only one dimer partner. This possibility has obvious important implications for the function of arrestin and the structure of the complex (Liang *et al.*, 2003). Interestingly conditions that disfavor the association of Rho with native lipids, such as addition of high concentrations of DM to native membranes, inhibit Rho dimerization (Jastrzebska *et al.*, 2004). Perhaps arrestin binding is dependent on Rho dimerization, which is in turn dependent on the presence of phospholipid. We hope to address this possibility in future experiments.

3. 5. 5 Acidic Phospholipids Promote Stable Complexes of Arrestin and Rho*-P

The fact that long lived complexes of Rho*-P and arrestin can form in mixed micelles containing acidic phospholipids opens up new possibilities for studying the arrestin-Rho complex. At low temperature (8 °C) our assay indicated that arrestin and Rho*-P in DM/PA mixed micelles formed an extremely long-lived complex with a $t_{1/2}$ of ~85 h (Figure 3. S2). As seen at 20 °C, arrestin trapped approximately half of the retinal at low temperature. This finding should help enable long lived complexes, which may be

useful in crystallization, NMR, electron microscopy, or cross-linking experiments (see Figure 3. S3 for an example).

3. 5. 6 Possible Implications of these Results in the Visual Cycle

The interaction of visual arrestin with phospholipid may represent another level of regulation of arrestin function in the rod cell. For example, PS, which undergoes a light dependent translocation to the cytoplasmic side of the membrane (Hessel *et al.*, 2001), may interact specifically with arrestin in the native ROS as it appears to do with transducin (Hessel *et al.*, 2003). Intriguingly phosphoinositide has been implicated in the trafficking of *Drosophila* visual arrestin and recruitment of β-arrestin to clathrin-coated pits, although significant binding of phosphoinositide to visual arrestin has not been reported (Gaidarov *et al.*, 1999; Lee *et al.*, 2003). The molecular details of the interaction of arrestin with ROS phospholipids will be the focus of future study.

3. 5. 7 Summary

This chapter describes the surprising finding that arrestin requires phospholipids to bind rhodopsin. Using fluorescently labeled arrestin, we discovered that arrestin binding to purified phosphorylated rhodopsin in detergent is severely diminished. Addition of phospholipid rescues binding, and specifically, arrestin requires acidic phospholipids. In the presence of acidic phospholipids, arrestin traps some retinal in the binding pocket with an intact Schiff-base, and Meta III formation is inhibited. Importantly, mixed micelles of detergent and phospholipid represent a useful soluble system for the study of arrestin-rhodopsin interactions. In Chapter 4 of this dissertation, we use this system to more fully investigate the role of arrestin in regulating retinal release and photoproduct formation from rhodopsin.

3. 6 ACKNOWLEDGEMENTS

This work was supported in part by National Institutes of Health Grants DA14896 (to D. L. F.) and EY06225 and EY08571 (to W. C. S.), a grant from the Kirchgessner Foundation (to W. C. S.), an unrestricted grant from Research to Prevent Blindness (to the Department of Ophthalmology at the University of Florida), a National Defense Science and Engineering graduate fellowship (to M. E. S.), and an N. L. Tartar research fellowship (to M. E. S.).

Table 3. 1 Effect of arrestin on the rate of retinal release and amount of trapped retinal [a]

membrane or micelle	no arrestin		+ arrestin	
	$t_{1/2}$ retinal release (min) [b]	% retinal trapped [c]	$t_{1/2}$ retinal release (min) [b]	% retinal trapped [c]
native membranes	7.5 ± 0.3	N/D *	8.9 ± 0.7	N/D *
native membranes solubilized by DM	14.9 ± 0.5	5 ± 1	22.5 ± 0.3	11 ± 1
DM micelles	7.9 ± 0.3	19 ± 1	8.6 ± 0.2	20 ± 2
DM / asolectin micelles	12.3 ± 0.8	5 ± 0	13.2 ± 0.7	52 ± 4
DM / PC	12.0 ± 0.9	14 ± 2	14.0 ± 0.2	16 ± 1
DM / PE	12.4 ± 0.8	1 ± 0	14.0 ± 0.3	3 ± 1
DM / PS	12.6 ± 1.1	6 ± 3	12.8 ± 0.3	58 ± 4
DM / PI	13.2 ± 1.4	17 ± 3	13.6 ± 0.1	49 ± 1
DM / PA	8.8 ± 0.6	5 ± 1	11.1 ± 0.6	60 ± 3

[a] Values are derived from experiments described in Figures 3 and 4 and, for the native membrane sample, from previously published work (Sommer *et al.*, 2005). Values represent the average ± the S.E. from two independent experiments (20°C, pH 7.4).

[b] Single-exponential rates were measured and determined as described in the Materials and Methods and converted to $t_{1/2}$ values ($t_{1/2} = \ln 2/k$, where k is the rate constant in min^{-1}). In each experiment, 1 μM Rho-P ± 2 μM arrestin I72B was used, except for the native membrane sample, where 2 μM Rho-P ± 4 μM arrestin was used.

[c] The percent of trapped retinal was calculated from the Rho-P tryptophan fluorescence retinal release data (330 nm) as follows: [(c-a)/c]*100, where a is the $(F/F_0) - 1$ value before the addition of NH_2OH, and c is the $(F/F_0) - 1$ value after the addition of NH_2OH (see Figure 3. 5A for more details).

* Not determined, because of secondary fluorescence effects observed to occur when NH_2OH is added to native membranes.

Table 3. 2 Arrestin I72B fluorescence changes due to Rho*-P binding and release [a]

membrane or micelle	arrestin binding $(F/F_0) - 1$ (456 nm)	arrestin plateau $(F/F_0) - 1$ (456 nm)	% residual fluorescence [b]	$t_{1/2}$ of arrestin release (min) [c]
native membranes	0.42 ± 0.08 *	0.09 ± 0.02 *	21	9.4 ± 1.1
native membranes solubilized by DM	0.5 ± 0.1	0.1 ± 0.01	20	28.0 ± 0.7
DM micelles	0.12 ± 0.1	0.03 ± 0.02	25	8.1 ± 0.4
DM / asolectin micelles	0.5 ± 0.2	0.25 ± 0.02	50	23.4 ± 0.4
DM / PC	0.28 ± 0.2	0.06 ± 0.01	21	19.5 ± 1.3
DM / PE	0.24 ± 0.1	0.07 ± 0.01	29	19.8 ± 0.6
DM / PS	0.68 ± 0.1	0.62 ± 0.04	91	> 120
DM / PI	0.62 ± 0.1	0.55 ± 0.01	89	> 120
DM / PA	0.93 ± 0.1	0.87 ± 0.07	93	> 120

[a] Values are derived from experiments described in Figures 3 and 5 and, for the native membrane sample, from (Sommer *et al.*, 2005) and unpublished work. Values represent the average ± the S.E. from two independent experiments (20°C, pH 7.4).

[b] Determined from the average fluorescence intensity of arrestin I72B 120 min after light-activation (or 200 min for DM-solubilized ROS-P) divided by the average intensity immediately after light-activation.

[c] Single exponential rates were measured and determined as described in the Materials and Methods and converted to $t_{1/2}$ values ($t_{1/2} = \ln 2/k$, where k is the rate constant in min^{-1}). In each experiment, 1 μM Rho-P and 2 μM arrestin I72B was used, except for the native membrane sample, where 2 μM Rho-P and 4 μM arrestin was used.
Rates of arrestin release were measured during the same experiment in which retinal release was measured for Table 3. 1.

* The fluorescence intensity of arrestin I72B in the presence of native membranes is complicated by the variable amount of scatter generated by different membrane preparations.

Figure 3. 1 Structural models of rhodopsin, arrestin, and the detergents and lipids used in this study. A) Model showing rhodopsin (*red*) and its hypothetical dimer partner (*transparent red*) in a membrane bilayer (Liang *et al.*, 2003). The location Ile^{72} on arrestin is indicated by a *yellow sphere* at the site of the α-carbon. *Inset*, the structure of monobromobimane, which was attached to a mutant cysteine residue at site Ile^{72} (not to scale with the protein models). Models were created as described previously (Sommer *et al.*, 2005). **B)** Structure of the detergent DM. **C)** The structure of 1,2-dioleoyl-*sn*-glycero-3-phospholipid (*left*) and the various head groups used in this study (*X*, *right*). The full names of the phospholipids are given in the Materials and Methods.

Figure 3. 1

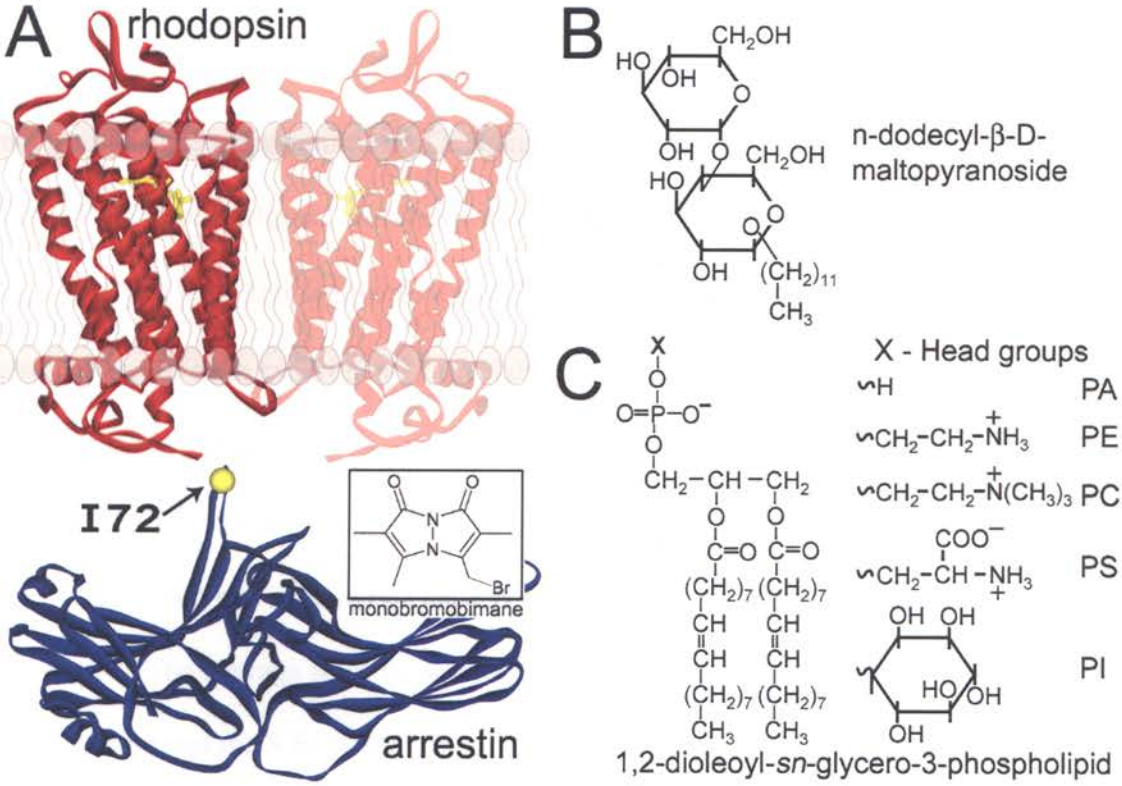
A
rhodopsin
I72
monobromobimane
arrestin
B
n-dodecyl-β-D-
maltopyranoside
C
X - Head groups
PA
PE
PC
PS
PI
1,2-dioleoyl-sn-glycero-3-phospholipid

Figure 3. 2 Phospholipids are required for arrestin binding to DM-purified Rho*-P. Fluorescence of bimane-labeled arrestin I72B is shown in the presence of Rho-P in native membranes (ROS-P) **(A)**, purified Rho-P solubilized in 0.02% DM **(B)**, and purified Rho-P solubilized in mixed micelles (0.02% DM and 0.02% asolectin) **(C)**. Spectra show before (*solid trace*) and after (*dashed trace*) light activation. **D)** The effect of increasing DM concentrations on I72B binding to solubilized Rho*-P in the presence of native ROS phospholipids. A scheme of how the samples were created is shown *above*. The dark state and light-activated ($+h\nu$) spectra at each DM concentration are labeled *below*. In each experiment, 1 μM labeled arrestin and 2 μM Rho-P were used. **E)** The relative fluorescence of 1 μM I72B at 470 nm (dark) and 456 nm (after light activation) was measured in the presence of a 3-fold excess of DM-solubilized, purified Rho-P (0.02% DM) and increasing amounts of asolectin. The experimental scheme is shown *above*. The average from three independent experiments is plotted *below*, and the *error bars* represent the S.E. The *inset* shows an example of the same experiment performed in 0.2% DM. All experiments were carried out at 20 °C in standard buffer (20 mM HEPES, 150 mM NaCl, pH 7.4) with 380-nm excitation. *Arr*, arrestin; *A.U.*, arbitrary units.

Figure 3. 2

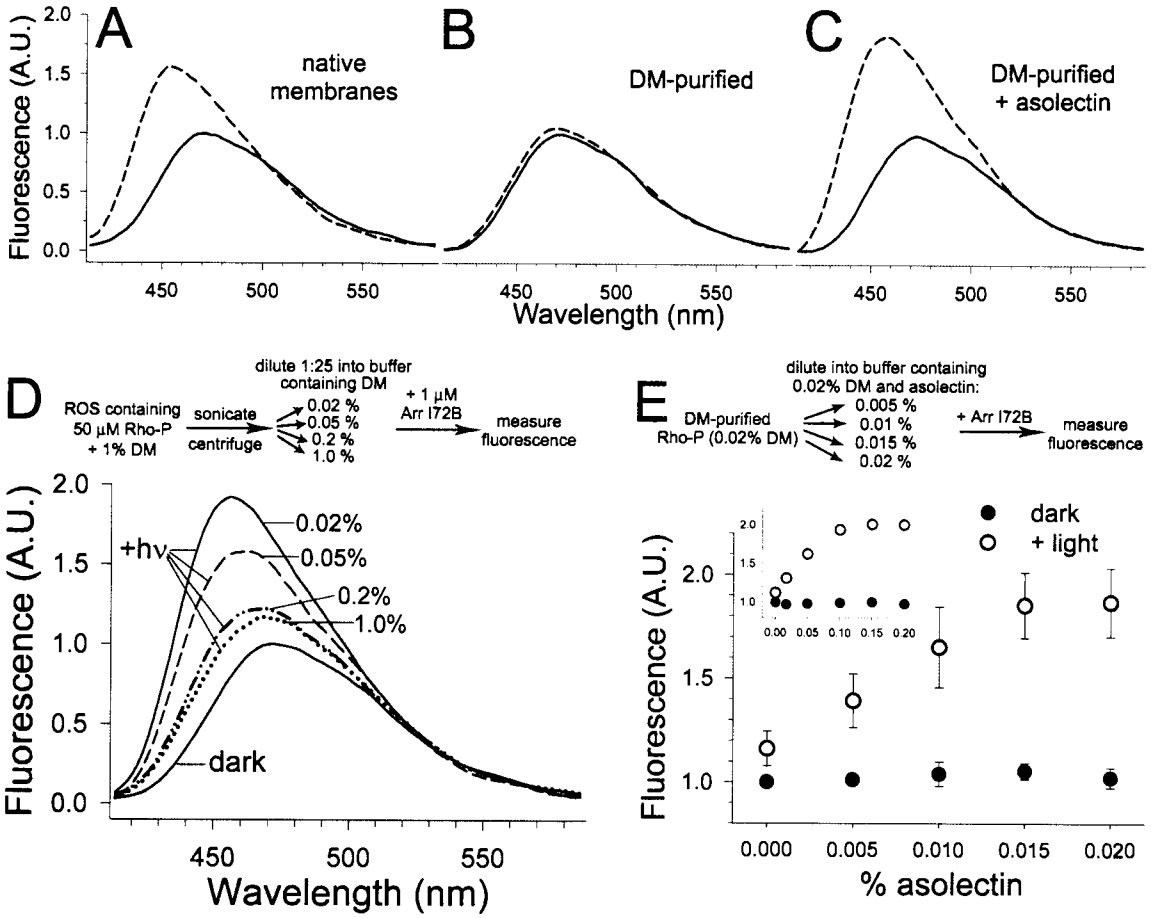
A
native membranes
B
DM-purified
C
DM-purified + asolectin
Fluorescence (A.U.)
Wavelength (nm)
D
ROS containing 50 µM Rho-P + 1% DM
sonicate
centrifuge
dilute 1:25 into buffer containing DM
0.02 %
0.05 %
0.2 %
1.0 %
+ 1 µM Arr I72B
measure fluorescence
+hν
0.02%
0.05%
0.2%
1.0%
dark
E
DM-purified Rho-P (0.02% DM)
dilute into buffer containing 0.02% DM and asolectin:
0.005 %
0.01 %
0.015 %
0.02 %
+ Arr I72B
measure fluorescence
dark
+ light
% asolectin

Figure 3. 3 Arrestin inhibits retinal release and Meta III formation in mixed micelles. The effect of arrestin on retinal release and Meta III formation was investigated by fluorescence and absorbance spectroscopy. **A)** Retinal release measured from solubilized Rho-P in mixed micelles of DM (0.02%) and native ROS phospholipids (prepared as described in Figure 3. 2). The assay monitored the increase in opsin tryptophan fluorescence (330 nm) in the absence (*dark blue*) or presence of a 2-fold excess of arrestin I72B (*light blue*). The sample was photo-activated at $t = 0$, and 10 mM hydroxylamine was added at $t = 210$ min. Arrestin binding and release was also monitored (456 nm, *green trace*) during the same experiment. **B)** The absorbance of solubilized Rho-P in DM/ROS phospholipid mixed micelles was observed in the dark (*red*) and after photoactivation (*blue*) both in the absence (*upper panel*) and presence (*lower panel*) of a 2-fold excess of arrestin. Spectra were recorded every 90 s after photoactivation (*black spectra*) for 120 min (the last spectrum is *orange*). The amount of retinal Schiff base remaining at the end of the experiment was assessed by adding H_2SO_4 (*green spectrum*). Experiments in **C**, **D**, **E**, and **F** were carried out as described for (A) and (B) except that purified Rho-P in pure DM micelles (**C** and **D**) or DM/asolectin mixed micelles (**E** and **F**) were used, and 10 mM hydroxylamine was added at 120 min (**C** and **E**). In each experiment, 1 μM Rho-P in 20 mM HEPES, 150 mM NaCl, pH 7.4, 0.02% DM ± 0.02% asolectin was used (20 °C).

Figure 3. 3

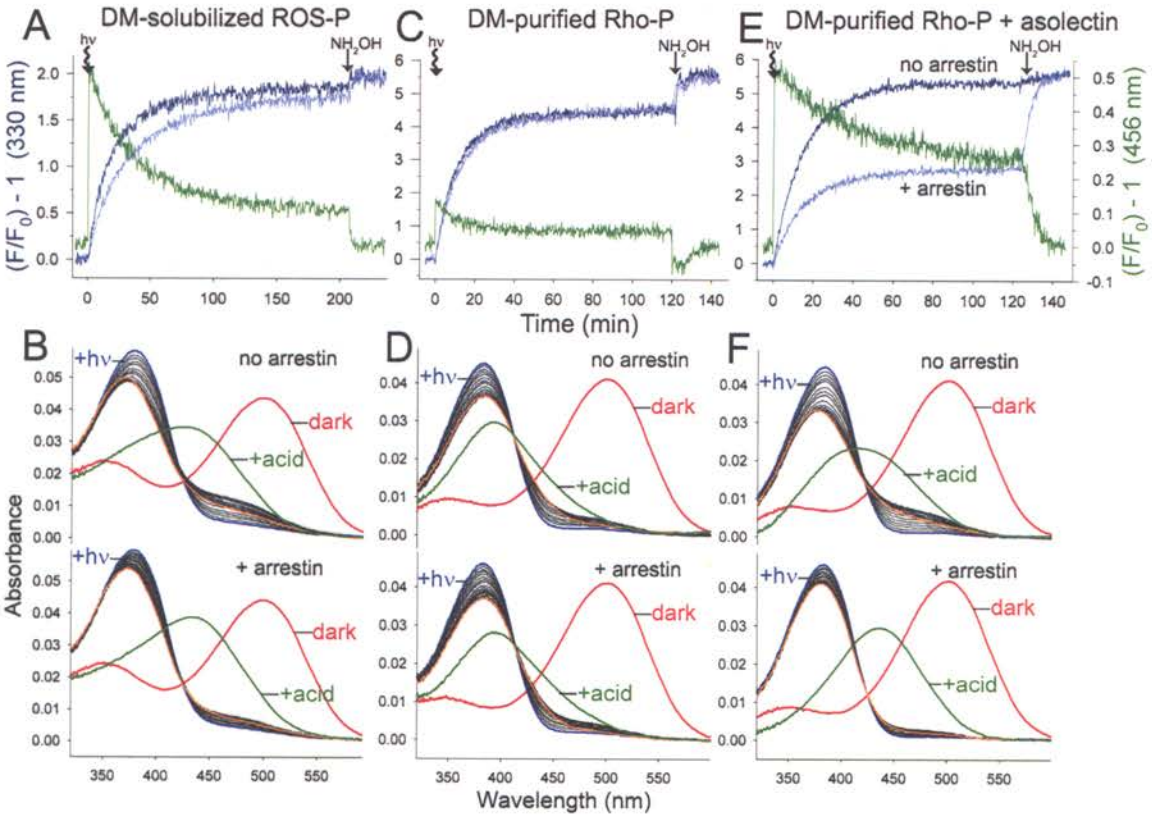
A
DM-solubilized ROS-P
C
DM-purified Rho-P
E
DM-purified Rho-P + asolectin
hν
NH2OH
no arrestin
+ arrestin
(F/F0) - 1 (330 nm)
(F/F0) - 1 (456 nm)
Time (min)
B
D
F
+hν
dark
+acid
Absorbance
Wavelength (nm)

Figure 3. 4 Arrestin binding is strongly enhanced by acidic phospholipids.

Fluorescence and absorption spectroscopy of DM-solubilized Rho-P in the presence of PC, PE, PS, PI, or PA (100 μM) is presented as shown in Figure 3. 3. Data obtained in the absence of phospholipid are shown for reference (DM). For fluorescence spectroscopy, retinal release in the absence (*dark blue*) or presence (*light blue*) of a 2-fold excess of arrestin I72B was monitored (330 nm). Arrestin binding and release was also monitored during the same experiment (*green trace*, 456 nm). Note that y-axis for the retinal release data (*left*) is not the same for (A) as for (C) and (E), due to the scatter present in the DM-solubilized ROS-P samples. The arrestin release axis (*far right*) is shared for parts (A), (C) and (E). The sample was photoactivated at $t = 0$, and 10 mM hydroxylamine was added at $t = 120$ min. For absorbance spectroscopy, spectra of DM-solubilized Rho-P in the presence of different phospholipids (100 μM) were measured as described in Figure 3. 3 in the absence or presence of a 2-fold excess of arrestin. In each experiment, 1 μM Rho-P in 20 mM HEPES, 150 mM NaCl, pH 7.4, 0.02% DM was used (20 °C).

Figure 3. 4

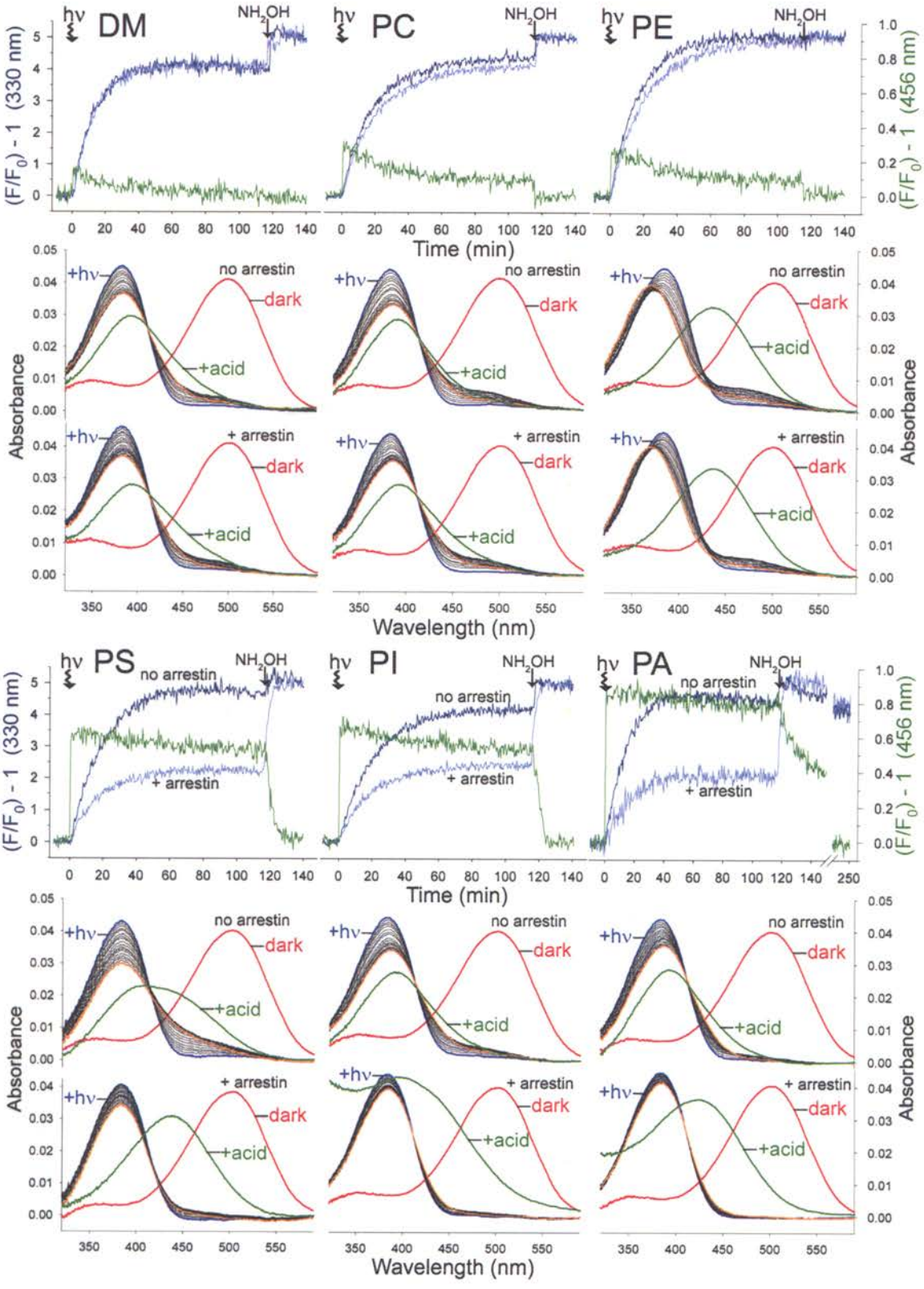
hν DM
NH2OH
hν PC
NH2OH
hν PE
NH2OH
(F/F0) - 1 (330 nm)
(F/F0) - 1 (456 nm)
Time (min)
+hν
no arrestin
dark
+acid
+ arrestin
Absorbance
Wavelength (nm)
hν PS
hν PI
hν PA

Figure 3. 5 Arrestin enhances trapping of retinal as a Schiff base adduct on Rho*-P. A) Trapped retinal, expressed as percentage of maximum fluorescence (*% of max fluorescence*), can be quantified from the plateau of the tryptophan fluorescence of Rho*-P and the increase that occurs after the addition of hydroxylamine. This scheme illustrates how this is calculated. **B)** Average change in the tryptophan fluorescence of Rho*-P that occurred after the addition of hydroxylamine, calculated as described above in (A). The analysis was carried out on the experiments described in Figures 3. 3 and 4, and Table 3. 1. The data represent two independent experiments ± S.E. **C)** Retinal trapping can also be measured by reduction with $NaBH_4$ followed by SDS-PAGE. The fluorescence of the bands indicates the amount of retinal covalently attached to opsin. Briefly, Rho-P solubilized in 0.02% DM (*lanes 2* and *3*), 0.02% DM and 0.02% asolectin (*lanes 4* and *5*), or 0.02% DM and a 100 μM concentration of the various purified phospholipids (*lanes 6–15*) without or with a 2-fold excess of arrestin was photoactivated, allowed to decay at 20 °C in the dark, reduced with $NaBH_4$ after 120 min, and then subjected to SDS-PAGE. The total amount of Schiff base-linked retinal was quantified by comparison to samples in which Meta II was reduced immediately after photoactivation (*lanes 1* and *16*). The fluorescence of the gels is shown in the *upper panels*, and the Coomassie-stained gels are shown in the *lower panels*. **D)** Plot of the average quantified fluorescence from four independent experiments as shown in (C); *error bars* represent the S.E. The fluorescence was measured as described under "Experimental Procedures" and is expressed as a percentage of the total Meta II fluorescence (*% max fluorescence*). All bands were compared with a Meta II control sample run on the same gel. *Arr*, arrestin; *aso*, asolectin.

Figure 3. 5

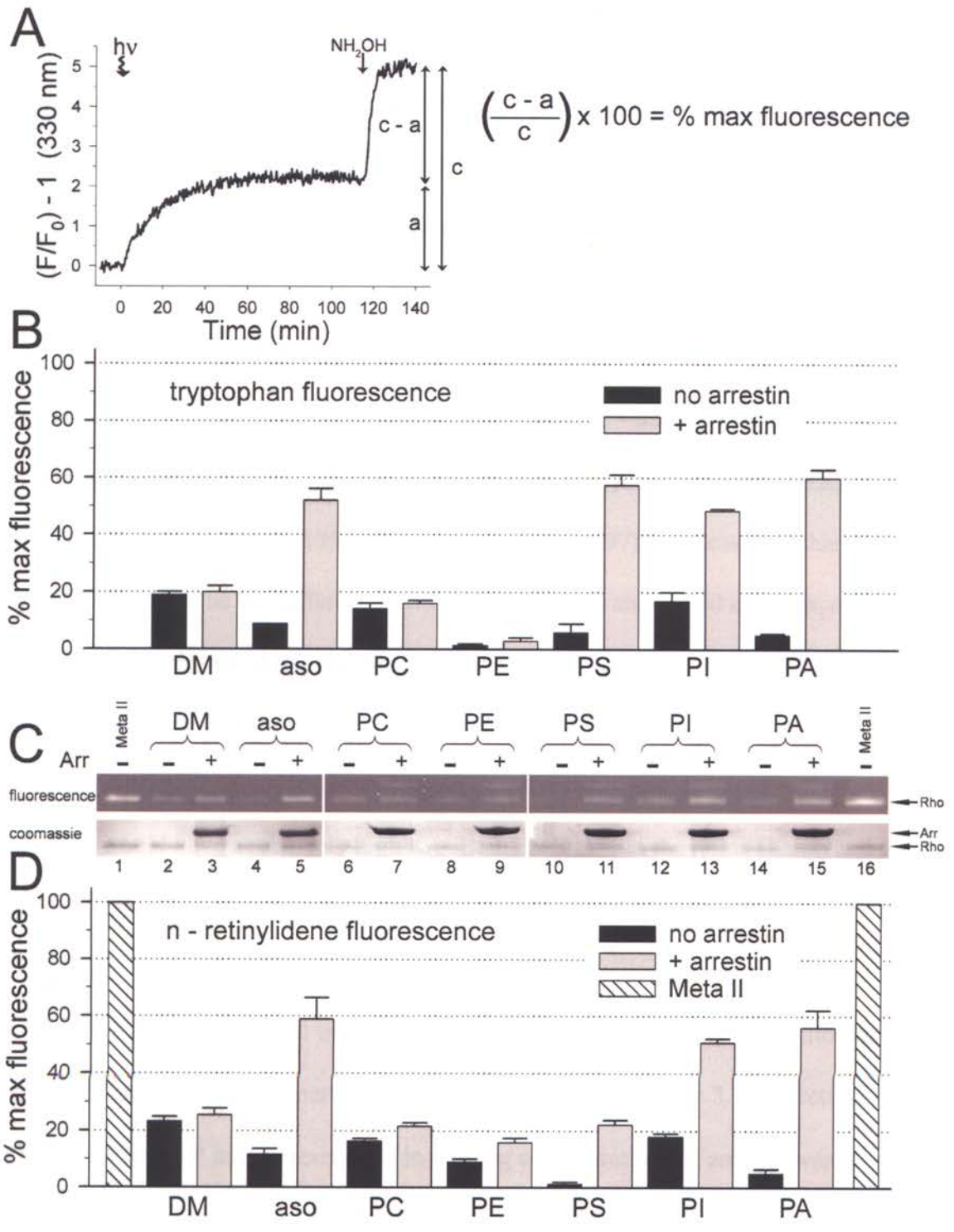
A
hν
NH2OH
(F/F0) - 1 (330 nm)
c - a
c
a
Time (min)
(c - a / c) x 100 = % max fluorescence
B
tryptophan fluorescence
no arrestin
+ arrestin
% max fluorescence
DM
aso
PC
PE
PS
PI
PA
C
Meta II
Arr
fluorescence
coomassie
Rho
Arr
D
n - retinylidene fluorescence
no arrestin
+ arrestin
Meta II
% max fluorescence

3. 7 SUPPLEMENTAL MATERIAL

3. 7. 1 Dissociation Constant of the Arrestin-Rhodopsin Complex in Mixed Micelles

We used the change in fluorescence that occurs upon arrestin I72B binding to assess the K_D of the arrestin-rhodopsin complex in mixed micelles. In this experiment, the arrestin concentration was varied over a range (0.25 μM to 4 μM), and the Rho-P concentration was kept constant at 1 μM (Figure 3. S1A). This approach was used to avoid possible inner filter effects that might occur if increasing concentrations of Rho-P are used. Assuming that the fluorescence change varies linearly with the amount of arrestin binding, the saturation binding curve yields a $K_D \sim 0.9$ μM (Figure 3. S1B). Previous quantitative studies using the extra-Meta II assay have reported the K_D to be 20 to 50 nM (Schleicher *et al.*, 1989; Pulvermüller *et al.*, 1997). The cause of this discrepancy might be the difference between membranes and mixed micelles, or the measuring techniques. Also, note that only one experimental data set containing a limited number of data points was used in the fit, which may cause some error in the determination of the K_D. However, it is not that surprising that the arrestin-rhodopsin complex would have a relatively high K_D. Being at 3 mM in the retina (Lamb and Pugh, 2004), a K_D of 1 μM would be sufficient to allow complete association, especially under bright-light conditions.

The percent of retinal trapped by arrestin is also a useful way to monitor arrestin binding. Using the same experimental samples as shown in Figure 3. S1A, retinal release from 1 μM Rho*-P in the presence of increasing concentrations of arrestin was measured (Figure 3. S1C). The amount of retinal trapped was calculated by comparing to the retinal release curve in the absence of arrestin. Interestingly, the plot of retinal trapping

versus arrestin concentration (Figure 3. S1D) yields a binding curve with a K_D of ~0.8 μM, which is about the same as found using arrestin I72B fluorescence. Note that these two methods for measuring arrestin binding are independent of one another, and the fact that they yield approximately the same K_D is consistent with previous data linking arrestin binding and retinal trapping.

Intriguingly, the maximum amount of retinal trapping seen, even with a four-fold excess of arrestin is still ~50% (Figure 3. S1D). Assuming a K_D of 0.9 μM and a binding ratio of 1:1, ~80% of the Rho*-P should be bound by arrestin at this concentration [9]. Thus, the high K_D does not fully explain why 50% retinal trapping is observed. A simple explanation for this effect would be that only ~50% of the rhodopsin is phosphorylated enough to interact with arrestin. Although we have not formally determined if most Rho*-P molecules in this experiment contain the 2 phosphates needed for arrestin binding (Kennedy *et al.*, 2001; Gurevich and Gurevich, 2006), we have determined with radio-labeled ATP that the population of Rho-P contains an average of 6 phosphates per rhodopsin (Sommer *et al.*, 2005). Thus, it is likely that most Rho-P molecules can bind arrestin. However, given this unknown, and because we cannot not formally relate I72B's fluorescence change to number of moles of arrestin bound, stoichiometry cannot be determined from this data.

[9] $K_D = [A][R]/[AR]$, where [A] is the concentration of free arrestin, [R] is the concentration of free Rho*-P, and [AR] is the concentration of the arrestin-rhodopsin complex. The total arrestin and rhodopsin concentrations are, respectively, $[A_{tot}]=[A]+[AR]$ and $[R_{tot}]=[R]+[AR]$. By solving for [A] and [R] using these equations and substituting into the K_D expression, the concentration of [AR] at any given $[A_{tot}]$ and $[R_{tot}]$ can be determined if the K_D is known: $[AR] = (p \pm \sqrt{(p^2 - 4q)})/ 2$, where $p = K_D+[A_{tot}]+[R_{tot}]$ and $q = [A_{tot}]\times[R_{tot}]$.

3. 7. 2 Example of Complex Stability at Low Temperature

The combination of mixed micelles containing acidic phospholipids and low temperature enables the formation of extremely long-lived arrestin-rhodopsin complexes. As shown in Figure 3. S2, less than 12% of arrestin is released within the first 20 hours after photoactivation at 8 °C. Note that in native membranes, this complex would be completely dissociated by 4 hours (Sommer *et al.*, 2005).

3. 7. 3 Preliminary Cross-linking Results Using Mixed Micelles

As described above in section **3. 5. 5**, the long-lived complexes of arrestin and Rho*-P in mixed micelles may be advantageous for future structural and biochemical experiments. Figure 3. S3 shows data from our preliminary cross-linking experiments. The ultimate goal of these studies would be to define the arrestin-rhodopsin stoichiometry. We used the lysine-specific cross-linker DSP [10], which was recently used to probe the oligomeric state of rhodopsin in native membranes (Jastrzebska *et al.*, 2004). DSP contains a disulfide in its linker region, so molecular cross-links can be broken with the addition of DTT. In our experiment, we added the cross-linker to Rho*-P-arrestin complexes in DM/PA micelles two hours after photo-activation. According to our fluorescence results, arrestin remains bound to the complex at this time-point, while half the retinal population has been released (Figure 3. 4).

We used two methods to detect cross-linked complexes. First, we reduced the complexes with $NaBH_4$, which results in a fluorescent *n*-retinylidene species if retinal is still trapped in the binding pocket (Figure 3. S3i). Second, we used fluorescently labeled arrestin (I72B) (Figure 3. S3ii). In this way, the cross-linked complexes could be

[10] Dithiobis(succinimidylpropionate), obtained from Pierce.

visualized after gel electrophoresis by fluorescence. Importantly, this detection method also reveals whether retinal and arrestin are present in the same bands.

When Meta II is $NaBH_4$-reduced immediately after photoactivation, multiple fluorescent bands result (Figure 3. S3A, *far left panel*). These bands may represent rhodopsin monomers (Rho_1), dimers (Rho_2), and higher order oligomers (Rho_3 and Rho_4), although we have not formally shown this. After photodecay (2 hours, 20 °C), the fluorescent bands disappear, probably because of Meta II decay (Figure 3. S3A, *middle panel*). In the presence of arrestin, $NaBH_4$-reduction results in fluorescent bands (Figure 3. S3A, *far right panel*). Densitometry analysis reports that the total amount of fluorescence in this lane is ~half that seen in the Meta II lane, suggesting that arrestin traps ~half of retinal, just as we have observed before (Figure 3. 5). Although the signal intensity is weak, it appears as though a majority of the fluorescence is located in the Rho_2 band. When DTT is added to these samples (Figure 3. S3C), the higher-molecular weight bands disappear. Note that not all the high molecular weight "Meta II" bands disappear, probably because of Rho's tendancy to aggregate during SDS PAGE.

Figure 3. S3B compares the cross-linked complexes formed with fluorescent arrestin in dark or light-activated samples. In this non-reducing gel, arrestin I72B tends to run as a diffuse band with a lower apparent molecular weight that is similar Rho. Interestingly, with light-activation, multiple higher molecular weight fluorescent bands appear. Furthermore, these bands have approximately the same mobility as the $NaBH_4$-reduced Rho bands. When DTT is added to the samples, cross-linked complexes disappear (Figure 3. S3D).

To summarize, these preliminary data suggest that DSP can cross-link Rho*-P and arrestin in DM/PA micelles. Both the $NaBH_4$-reduced samples and the arrestin I72B samples report that the majority of cross-linked samples run at approximately same molecular weight as the "Rho_2" band. Since in non-reducing conditions, arrestin has about the same apparent molecular weight as rhodopsin, this cross-linked band could represent a 1:1 complex of arrestin and rhodopsin. However, at least three more higher molecular weight complexes exist, which may imply that arrestin binds rhodopsin oligomers. Furthermore, this cross-linking appears to be dependent on the presence of phospholipid, since no cross-linked species were observed using Rho*-P in pure DM micelles (data not shown). However, several unresolved issues remain with this experiment, and this data does not indicate the stoichiometry of the complex. Future experiments will focus on this question by quantifying the amounts of rhodopsin and arrestin present in the bands, perhaps by quantitative Western blot or mass spectrometry.

Figure 3. S1 Dissociation constant of the arrestin-rhodopsin complex in mixed micelles. A) The fluorescence spectra of increasing concentrations of arrestin were measured in the presence of 1 μM Rho-P in DM/asolectin mixed micelles, before (*solid traces*) and after (*dashed traces*) light-activation (*red* - 0.25 μM, *blue* - 0.5 μM; *green* - 1.0 μM, *orange* - 2.0 μM, and *purple* - 4.0 μM arrestin I72B). Spectra were measured as described in Figure 3. 2 at 25 °C. **B)** The change in arrestin I72B's integrated fluorescence intensity (photoactivated intensity minus dark-state intensity) is plotted against arrestin concentration to give a saturation binding curve with a K_D of ~0.9 μM. **C)** Retinal release from 1 μM Rho*-P was monitored during the same experiment described in (A), and the fluorescence traces follow the same color scheme (retinal release in the absence of arrestin is shown in *gray*). In each case, retinal release occurred at about the same rate, with a $t_{1/2}$ of ~5 min. Retinal release was monitored as described in Figure 3. 3 at 25 °C. **D)** The amount of retinal trapped in (C), which was calculated as described in Figure 3. 5, is plotted against arrestin concentration, and the calculated K_D is ~0.8 μM. Plots in (B) and (D) were fit using a one-site saturation ligand binding equation in the program Sigma Plot, $y = (B_{max}*[Arr]) / (K_D+[Arr])$, where [Arr] is the arrestin concentration (μM), K_D is the dissociation constant, and B_{max} is a constant that describes the plateau of the binding curve.

Figure 3. S1

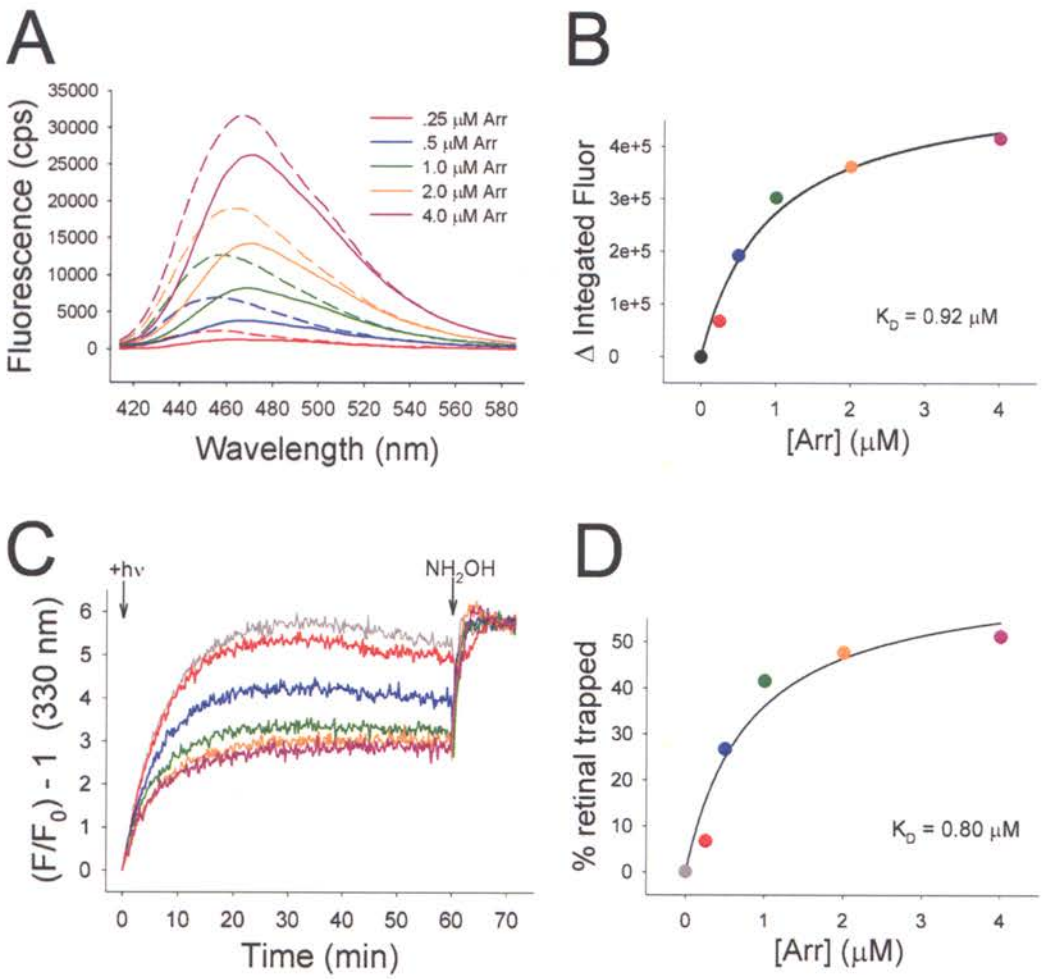
A
Fluorescence (cps)
35000
30000
25000
20000
15000
10000
5000
0
.25 μM Arr
.5 μM Arr
1.0 μM Arr
2.0 μM Arr
4.0 μM Arr
420 440 460 480 500 520 540 560 580
Wavelength (nm)
B
Δ Integated Fluor
4e+5
3e+5
2e+5
1e+5
0
K_D = 0.92 μM
0 1 2 3 4
[Arr] (μM)
C
+hν
NH_2OH
(F/F_0) - 1 (330 nm)
0 1 2 3 4 5 6
0 10 20 30 40 50 60 70
Time (min)
D
% retinal trapped
50
40
30
20
10
0
K_D = 0.80 μM
0 1 2 3 4
[Arr] (μM)

Figure 3. S2 The arrestin-rhodopsin complex at low temperature. Retinal (*upper panel*) and arrestin (*lower panel*) release from Rho*-P in DM/PA mixed micelles (8 °C) was monitored as described in Figure 3. 4 (note that the time scale is in hours). Rate analysis indicates that retinal was released from Rho*-P, in the absence or presence of arrestin, with a $t_{1/2}$ of ~90 min. As noted at 20 °C, about half the retinal is trapped in the presence of arrestin. The fluorescence (456 nm) indicative of arrestin release drops less than 12% during the 20 hours of the experiment, which corresponds to a $t_{1/2}$ of arrestin release of ~85 hours.

Figure 3. S2

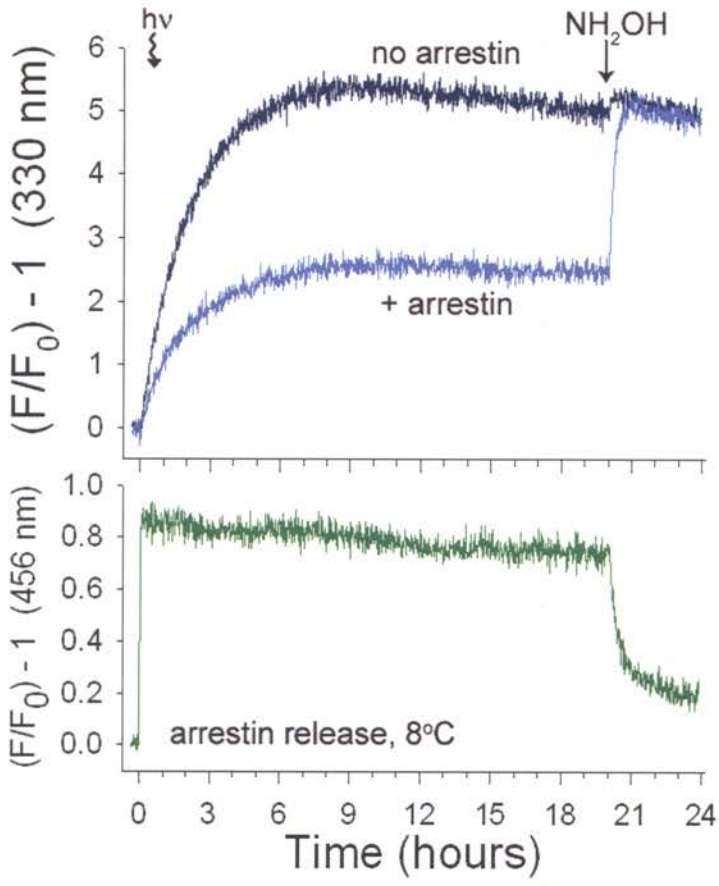
hν
NH2OH
no arrestin
+ arrestin
(F/F0) - 1 (330 nm)
(F/F0) - 1 (456 nm)
arrestin release, 8°C
Time (hours)

Figure 3. S3 Preliminary cross-linking experiment using mixed micelles. i) Experimental scheme showing how cross-linked complexes can be detected by $NaBH_4$-reduction of the retinal Schiff-base. **ii)** Experimental scheme showing how cross-linked complexes can be detected using fluorescently labeled arrestin. **A)** Samples in the *middle* and *far right* panels were processed as described in scheme (i). For comparison, $NaBH_4$-reduced Meta II (in the absence of arrestin) is shown in the *far left* panel. Note that multiple fluorescent bands are present for Meta II (labeled with *arrows* on the *left*). In the presence of arrestin, multiple fluorescent bands are also present for photo-decayed Rho*-P (labeled with *arrows* on the *right*). **B)** Samples in this part were processed as described in scheme (ii). Note that with the addition of light, multiple high-molecular weight complexes containing arrestin I72B are present (labeled with *arrows* on the *right*). **C)** and **D)** Same as parts (A) and (B), except that 5 mM DTT was added to the gel-loading buffer. The fluorescence image of the gels is reversed for easier visualization of the bands, and MW markers (kDa) are indicated between the panels. Note that arrestin runs lower than its apparent molecular weight in non-reducing conditions. In each experiment, 1 μM Rho-P in DM/PA micelles (0.02% DM, 100 μM PA) was used, with or without 2 μM wild-type arrestin (A and C) or arrestin I72B (B and D) (20 mM HEPES, 150 mM NaCl, pH 7.4). After photodecay, the pH of the samples was raised to 8.5 with Na_2HPO_4, and DSP was added (3.2 mM). After two hours on ice, the pH was lowered to 7.5 with Tris-HCl, and then 0.1% $NaBH_4$ was added to the samples for part (A). Samples were divided in two, loading buffer with or without DTT was added to each, and samples were subjected to SDS PAGE electrophoresis (10%). The "Meta II" sample in part (A) was treated the same, except that photo-activation occurred after the addition of $NaBH_4$.

Figure 3. S3

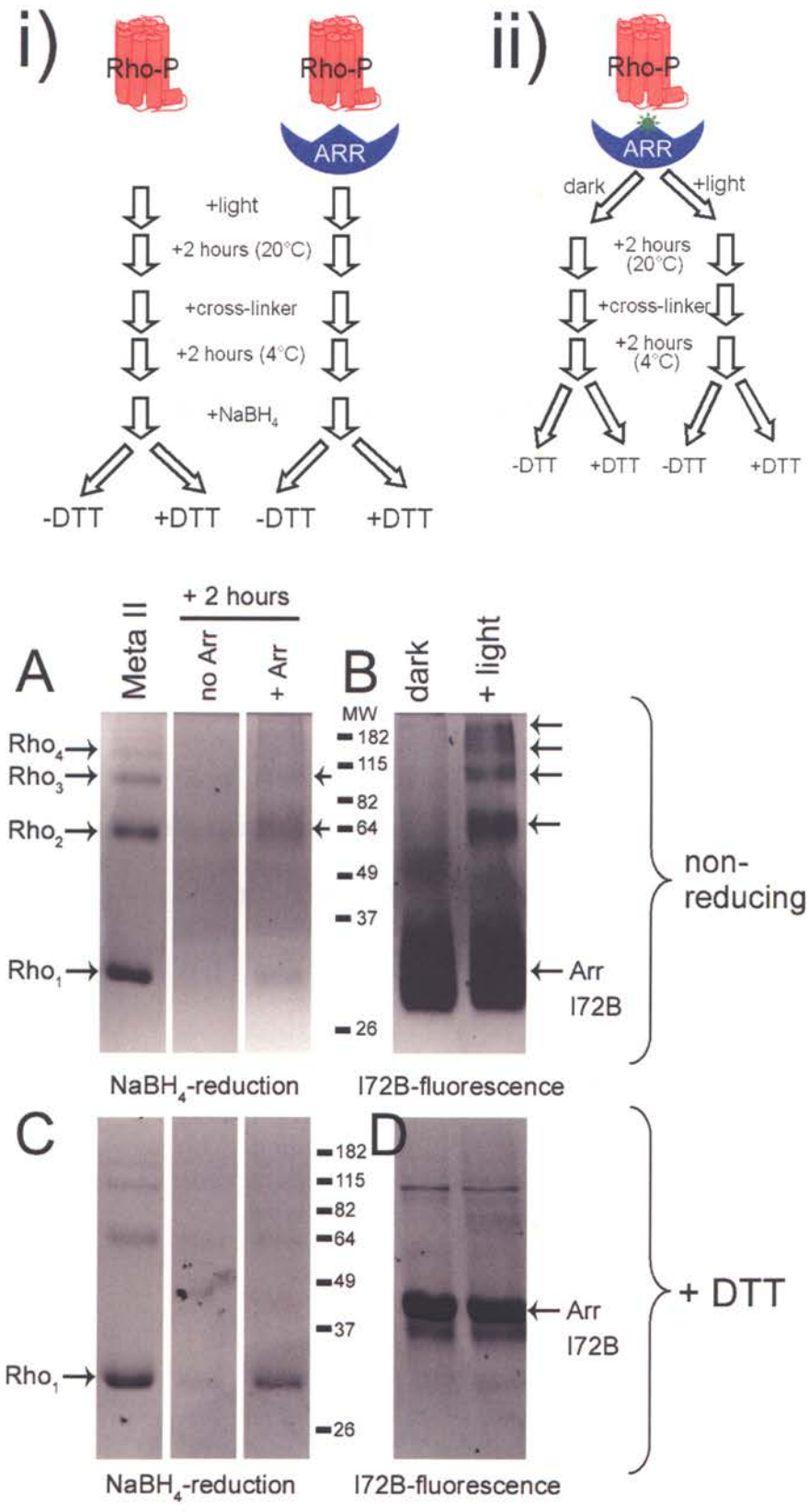
i)
Rho-P
Rho-P
ARR
+light
+2 hours (20°C)
+cross-linker
+2 hours (4°C)
+NaBH4
-DTT
+DTT
-DTT
+DTT
ii)
Rho-P
ARR
dark
+light
+2 hours (20°C)
+cross-linker
+2 hours (4°C)
-DTT
+DTT
-DTT
+DTT
A
Meta II
+ 2 hours
no Arr
+ Arr
B
dark
+ light
MW
182
115
82
64
49
37
26
Rho4
Rho3
Rho2
Rho1
Arr
I72B
non-reducing
NaBH4-reduction
I72B-fluorescence
C
D
182
115
82
64
49
37
26
Rho1
Arr
I72B
+ DTT
NaBH4-reduction
I72B-fluorescence

Chapter 4

Regulation of Rhodopsin Photochemistry by Arrestin

Martha E. Sommer and David L. Farrens

Department of Biochemistry and Molecular Biology, Oregon Health & Science University, Portland, OR 97239-3098, USA

4. 1 SUMMARY

This chapter describes new findings regarding the ability of visual arrestin to regulate retinal release and late photoproduct formation from rhodopsin. Our experiments employ a fluorescently-labeled arrestin mutant and a soluble system that enables arrestin-rhodopsin interactions. We find that arrestin traps ~half of the population of retinal in the binding pocket with an absorbance characteristic of Meta II and the retinal Schiff-base intact. Furthermore, arrestin can convert Metarhodopsin III (formed either by thermal decay or blue-light irradiation) to a Meta II-like absorbing species. Together, our results suggest that arrestin may play a more complex role in the rod cell besides simply quenching transducin activity and may explain why arrestin deficiency leads to stationary night blindness (Oguchi disease) and retinal degeneration.

All sample preparation and experimental analysis reported in this chapter were performed by the author of this dissertation. Part of this work (Figure 4. 5) has been published (Sommer, M.E., Smith, W.C., and Farrens, D.L. (2006) *J. Biological Chemistry* **281**: 9407-9417), and the remaining part will be submitted for publication (*Vision Research).* This work was recently presented (poster at the 50th Annual Biophysical Society Meeting, Salt Lake City, UT, 2006).

4. 2 INTRODUCTION

Within the rod cells of the retina, the membrane bound photoreceptor rhodopsin composes half the volume of the tightly packed membranous rod disks (Molday, 1998). In the dark-state, rhodopsin's chromophore 11-*cis* retinal is covalently attached to Lys^{296} by a protonated Shiff-base (λ_{max} ~ 500 nm). Upon absorption of light, the chromophore isomerizes to all-*trans* retinal and two photoproducts evolve in equilibrium, Meta I (λ_{max} ~ 480 nm) and Meta II (λ_{max} ~ 380 nm).

Meta II, the active signaling form of the receptor, couples with the G-protein transducin to induce the downstream signaling cascade (Burns and Baylor, 2001; Ridge *et al.*, 2003). The retinal Schiff-base of Meta II is sensitive to cleavage, and eventually Meta II decays to opsin and free retinal (Farrens and Khorana, 1995). Fast deactivation of Meta II-signaling involves phosphorylation of the C-terminal tail by rhodopsin kinase, followed by binding of visual arrestin (Kühn, 1982; Wilden *et al.*, 1986; Gurevich and Gurevich, 2004).

Another major late retinal photoproduct, Meta III (λ_{max}~470 nm), results from the thermal decay of Meta I (Vogel *et al.*, 2003; Vogel *et al.*, 2004b). In bright-light, up to half of the rhodopsin in the human retina may be converted to this long-lived photoproduct (Lewis *et al.*, 1997), which may exist for retinal storage purposes (Heck *et al.*, 2003a). Recent work has also shown that Meta III has some signaling ability, for it interacts with transducin (Zimmermann *et al.*, 2004).

Blue-light (<420 nm) absorption by Meta II also forms Meta III (Ritter *et al.*, 2004), as well as the photoproduct P500 (λ_{max}~500 nm) (Arnis and Hofmann, 1995).

P500 appears to be similar to dark-state rhodopsin in its activity, although it most likely binds an all-*trans* retinal (Bartl *et al.*, 2001).

The focus of this chapter is how arrestin affects the formation and decay of these photoproducts. These questions are important for understanding the visual photocycle, especially in bright-light conditions where the rod cell is nonfunctional. Recent work has documented arrestin's remarkable translocation from the rod inner segment to the outer segment upon exposure to light that is near the upper limit of rod cell responsiveness (Strissel *et al.*, 2006). Intriguingly, transducin migrates in the opposite direction (Elias *et al.*, 2004). These phenomena may suggest that in the photo-bleached rod, arrestin serves not just to inhibit transducin signaling, but also to interact with the late photoproducts of rhodopsin.

As described in Chapters 2 and 3 of this dissertation, our recent characterization of a fluorescently labeled arrestin mutant (Sommer *et al.*, 2005) and development of a functional solubilized system for the study of arrestin-rhodopsin interactions (Sommer *et al.*, 2006) has allowed us to gain new insight into arrestin's regulation of rhodopsin photochemistry. In this chapter, we present data that show arrestin stabilizes Meta II, both by inhibiting retinal release and Meta III formation. Our results imply that arrestin serves a biological role to limit retinal release in the photo-bleached retina, which may protect the cell from long-term oxidative damage (Sparrow *et al.*, 2003).

4. 3 MATERIALS and METHODS

4. 3. 2 Materials

Frozen bovine retinas were obtained from Lawson and Lawson, Inc. (Lincoln,

NE), and 11-*cis* retinal was a generous gift from Rosalie Crouch (Medical University of South Carolina and National Eye Institute). Except where noted below, all reagents were obtained from Sigma (St. Louis, MO). Monobromobimane was purchased from Molecular Probes (Eugene, OR), and spectroscopic-grade buffers were from USB Corporation (Cleveland, OH). Acrylamide / bisacrylamine solution (37:5:1) was purchased from Bio-Rad, and Concavalin A Sepharose was obtained from Amersham (Piscataway, NJ). Asolectin was purchased from Fluka (Buchs, Switzerland), and n-dodecyl-β-D-maltopyranoside (DM) was from Anatrace (Maumee, OH). For experiments using asolectin/DM mixed micelles, a stock of 1% asolectin and 1% DM was made by dispersing the powdered asolectin into solution with a syringe and needle. The solution was clarified by centrifugation (100,000 x g, 20 min) before use.

4. 3. 2 Purification of Native Rhodopsin and Recombinant Arrestin

ROS and highly phosphorylated ROS were prepared from bovine retinas, and rhodopsin was purified from ROS using ConA and solubilized in DM as described previously (Sommer *et al.*, 2005; Sommer *et al.*, 2006). Mutant arrestin constructs W194F and I72C/W194F were created from the bovine visual arrestin cDNA cloned in the pET15b vector (Invitrogen). All constructs were verified by DNA sequencing, arrestin was expressed and purified from *Escherichia coli* BL21(DE3) cells, and arrestin samples were subsequently labeled with monobromobimane as described (Sommer *et al.*, 2006). Recombinant arrestin I72C/W194F labeled at ~92% efficiency; recombinant arrestin W194F labeled at less than 2% efficiency. No free label contamination was detected in the labeled arrestin samples.

4. 3. 3 Fluorescence Spectroscopy

All steady-state and time-resolved fluorescence measurements were made using a Photon Technologies steady-state spectrophotometer with a single excitation source (DeltaRam) and two emission detectors (T format). Excitation slits were set <0.25 nm to avoid bleaching of rhodopsin, and emission slits were set at 15 nm band pass. For emission scans, the sample was excited at 380 nm, and emission was measured from 400 to 600 nm using 2 nm increments (0.25 second integration per point). For simultaneous monitoring of retinal and arrestin release, the sample was excited for 1 second at 295 nm, followed by 1 second at 380 nm. Emission was detected at 330 nm and 456 nm, and the shutter was closed for 8 seconds between measurements. Samples were photoactivated using a 150-watt fiber optic light source (>495 nm). Background fluorescence was subtracted from all data, and steady-state scans were smoothed using the program Felix (Sommer *et al.*, 2005; Sommer *et al.*, 2006).

4. 3. 4 UV-Visible Absorbance Spectroscopy

All UV-visible absorption spectra were recorded with a Shimadzu UV-1601 spectrophotometer (bandwidth of 2 nm) (Sommer *et al.*, 2006). For the photodecay experiments, the absorbance of 1 μM Rho-P was recorded in the dark after base-lining the spectrophotometer with the appropriate buffer. The sample was photoactivated (>495 nm) for 20 seconds, and spectra were subsequently recorded every 90 seconds for 120 min. For blue-light experiments, the sample was illuminated by a Machine Vision Strobe light source filtered through a 400 ± 20 nm band pass filter for 20 seconds. The presence of Schiff-base was ascertained by the addition of 5 μl of 0.8 N H_2SO_4 to the sample.

4. 3. 5 $NaBH_4$ Reduction and V8 Proteolysis of Rhodopsin

The fluorescent *n*-retinylidene opsin species (λ_{ex} = 340 nm, λ_{em} = 480 nm) results from reduction of the Schiff-base in rhodopsin with $NaBH_4$ (Bownds and Wald, 1965; Farrens and Khorana, 1995). Samples of 3 μM Rho-P, with or without 6 μM arrestin W194F, solubilized in 0.02% DM or 0.02% DM and 0.02% asolectin (20 μl) were photo-activated (>495 nm, 20 seconds, 20 °C), incubated in the dark for 120 minutes, and then 5 μl of 1% $NaBH_4$ was added to each sample. After 10 minutes, 15 μl of 1 M sodium phosphate (pH 7.0) was added, each sample was split into two 20 μl aliquots, and 5 μl of 4.8 μM V8 protease was added to half the samples. Proteolysis occurred for 30 minutes at 20 °C. To assess the amount of Schiff-base present in Meta II rhodopsin immediately after activation, 1% $NaBH_4$ was added to Rho-P (0.02% DM) in the dark. The sample was then photo-activated at 4 °C and immediately processed as described above. Bands were resolved by 15% Tris-Tricine SDS PAGE, and gels were soaked in 30% methanol before visualization. The n-retinylidene opsin was excited with a short wave UV source (Alpha-Innotech FluorChem 5500 gel-doc), and the fluorescent bands were detected by a CCD camera (535 ± 50 nm cut-off filter; 10 minute exposure). AlphaEase FC software was used to quantify the fluorescence of the bands.

4. 3. 6 Arrestin Functional "Pull-down" Assay

Arrestin's ability to bind Rho-P in native membranes (ROS-P) was performed as described previously with some modifications (Sommer *et al.*, 2005). Briefly, a single sample of sonicated ROS-P (15 μM) was mixed with arrestin W194F/I72B (3 μM) in the dark (120 μl, 20 mM HEPES, 150 mM NaCl, pH 7.4, 20 °C). 20 μl aliquots were removed and immediately placed on ice in the dark, after green light illumination (>495

nm, 60 sec), after subsequent blue-light illumination (<420 nm, 60 sec), after subsequent green light illumination (60 sec), and after the addition of 10 mM hydroxylamine. The sample was illuminated from the top to prevent the plastic tube from filtering the light. The samples were then diluted 10-fold with ice-cold buffer, centrifuged at 100,000 x *g* for 10 min (4 °C), and the pellets were solubilized in loading buffer and subjected to SDS PAGE (10%). The gel was visualized as described above using a gel-doc apparatus, and bands were quantified using the AlphaEase FC software.

4. 4 RESULTS

4. 4. 1 Fluorescent Arrestin Binding to Rhodopsin in Mixed Micelles

Previously, we showed that arrestin binding and release from light-activated phosphorylated rhodopsin (Rho*-P) in native membranes can be monitored with fluorescently labeled arrestin mutants (Sommer *et al.*, 2005). Specifically, bimane-labeled arrestin I72C (I72B) exhibits a blue-shift and increase in fluorescence upon binding Rho*-P, and this fluorescence change is most likely due to a burying of the bimane probe in a protein-protein or a protein-lipid interface. Figure 4. 1A illustrates the location of the fluorescent probe on arrestin and the likely binding interfaces between rhodopsin and arrestin.

Using this fluorescent arrestin, we also discovered that arrestin binding is abolished when Rho-P is purified out of the native membrane and solubilized in *n*-dodecyl-β-D-maltopyranoside (DM) (Sommer *et al.*, 2006). Interestingly, arrestin binding can be restored with the addition of exogenous phospholipids in the form of asolectin (an inexpensive mixture of soybean phospholipids used to reconstitute purified

rhodopsin (Niu *et al.*, 2002)) (Figure 4. 1B). Furthermore, we have showed that acidic phospholipids (phosphatidylserine, phosphatidylinositol, and phosphatidic acid) specifically enable arrestin binding (Sommer *et al.*, 2006). The high phosphatidylinositol content (~30%) of asolectin [11] probably explains why it serves as a good enhancer of arrestin binding to DM-purified Rho-P.

Importantly, Rho-P solubilized in mixed DM/asolectin micelles represents a functional soluble system in which to study the dynamics of arrestin's interaction with the major photoproducts of rhodopsin and how arrestin influences the release of the retinal chromophore from the binding pocket. Our results are described below.

4. 4. 2 Arrestin Traps a Population of Retinal in Mixed Micelles

We measured retinal release from Rho*-P solubilized in mixed DM/asolectin micelles by monitoring the increase in native opsin tryptophan fluorescence that occurs when retinal is released from the binding pocket (Farrens and Khorana, 1995) (Figure 4. 2A). The data show that retinal is released from Rho*-P in mixed micelles with a $t_{1/2}$ = 12.3 ± 0.8 min, which is ~60% slower compared to native ROS membranes (Sommer *et al.*, 2006). The addition of hydroxylamine, a compound that cleaves the Schiff-base, results in a small (~5%) increase in fluorescence.

Strikingly, in the presence of a two-fold excess of arrestin, the tryptophan fluorescence plateaus at ~half that seen in the absence of arrestin, implying that arrestin traps ~half of the retinal population in the binding pocket (Heck *et al.*, 2003a). The addition of hydroxylamine causes the fluorescence to increase to the same level as seen in the absence of arrestin. Interestingly, arrestin appears to only affect the plateau of

[11] Product information listed in the Sigma catalogue.

tryptophan fluorescence and not the rate at which the fluorescence increases ($t_{1/2}$ = 13.2 ± 0.7 min).

The fluorescent arrestin I72B allows observation of arrestin binding and release during the same experiment described above (Figure 4. 2B). Arrestin binding to Rho*-P in mixed micelles results in a ~50% increase in bimane fluorescence. The rate of arrestin release is significantly slower ($t_{1/2}$ ~ 25 min) compared to retinal release, and the bimane fluorescence plateaus at ~70% of the starting state intensity [12]. Hydroxylamine returns the fluorescence to the starting-state level. To summarize, these results suggest that while arrestin remains bound in the complex, ~half of the retinal population is trapped.

4. 4. 3 Arrestin Traps Retinal as a Schiff-base Adduct

In order to determine if the retinal trapping observed in Figure 4. 2 represents a Schiff-base linked form, we quantified the amount of retinal covalently attached to opsin after photodecay by reducing the Schiff-base with $NaBH_4$, resulting in the fluorescent n-retinylidene species (Bownds and Wald, 1965; Farrens and Khorana, 1995). Subsequent SDS PAGE enables the separation the n-retinylidene opsin from possible retinal-phospholipid adducts. We also digested the reduced opsin with V8 protease to reveal the relative location of the covalently attached retinal on the protein. V8 cleaves opsin in the third cytoplasmic loop, resulting in two fragments. The larger fragment F1 (~27 kDa) contains transmembrane helices 1-5, and the smaller fragment F2 (~15 kDa) consists of transmembrane helices 6 and 7 and Lys^{296} (Farrens *et al.*, 1996), to which retinal is attached in dark-state and Meta II rhodopsin (Palczewski *et al.*, 2000).

---

[12] Note that this plateau is higher than observed in Figure 3. 3E (~50%), even though both experiments used DM/asolectin mixed micelles. Some variation in arrestin plateau levels are observed using asolectin, probably due to the hetergenous nature of this phospholipid source. However, retinal release consistently plateaus at 50%.

When Rho-P in DM-micelles is reduced immediately after photo-activation (Meta II), the majority of the retinal is clearly attached to F2 (Figure 4. 3B, *lane 1*). Two hours after photo-activation, ~25% of the original retinal population is attached to opsin (Figure 4. 3A, *lane 2*). The V8 proteolysis assay reveals that this retinal is attached to both F1 and F2 of Rho-P (Figure 4. 3B). This residual retinal may represent Meta III as well as retinal which attached to peripheral lysines on Rho*-P after release from the binding pocket. Note that the fluorescence of the V8 protease implies that retinal may react with this protein as well. In the presence of arrestin (*lane 3*), slightly more retinal (~10%) remains attached to opsin on F2.

In DM/asolectin mixed micelles, only ~10% of retinal remains attached to opsin after photodecay (Figure 4. 3A, *lane 4*). Why is this value lower than in DM alone? Phosphatidylethanolamine in asolectin may compete with lysine residues for retinal (Sparrow *et al.*, 2003), and this conclusion is supported by the presence of a low molecular-weight fluorescence species (Figure 4. 3B, *lanes 4 and 5*). Significantly, arrestin causes ~60% of the retinal to remain attached to opsin, and most of this retinal (~80%) is attached to F2 (*lane 5*). Besides illustrating the phospholipid-dependence of retinal trapping by arrestin, these results confirm that arrestin traps ~half the retinal in opsin as observed in Figure 2A. In addition, it appears that arrestin traps retinal on F2 of rhodopsin, possibly at Lys^{296}.

4. 4. 4 Arrestin Traps Spectral Meta II and Blocks Meta III Formation

The photo-intermediates of Rho-P in DM/asolectin micelles were monitored using UV-visible absorption spectroscopy (Figure 4. 4A). Dark-state Rho-P exhibits a characteristic absorption maximum at 500 nm that shifts to 380 nm after photo-activation.

Over time, there is a loss of absorbance at 380 nm and an increase in absorbance between 450 nm and 480 nm. This event can be explained as the conversion of Meta II (380 nm) to Meta III (470 nm) and release of retinal from the binding pocket to form adducts with phospholipid head-groups (440-450 nm). The blue-shift of the 380 nm absorbance in Figure 4. 4A is characteristic of all-*trans* retinal in the presence of asolectin (data not shown).

With an excess of arrestin present, the photodecay absorption spectra of Rho-P are dramatically different (Figure 4. 4B). There is a significant inhibition of the absorbance loss at 380 nm, and the increase of absorbance between 450 and 480 nm is inhibited. These data suggest that arrestin stabilizes rhodopsin in a Meta II-like state and inhibits retinal release and Meta III formation.

The presence of Schiff-base was ascertained by acidification after photodecay in the experiments described above. Protonated Schiff-bases absorb at 440 nm and are indicative of retinal attached to opsin (as in the case of Meta II and Meta III) or linked to phospholipid. In the absence of arrestin, a broadened absorbance ($\lambda_{max} \sim 416$ nm, Figure 4. 4C) that is typical for retinal adducts with asolectin phospholipids results. In the presence of arrestin, acidification results in a 440 nm absorbance peak that verifies the $NaBH_4$-reduction data (Figure 4. 3): arrestin traps retinal in a Schiff-base linked form.

4. 4. 5 Arrestin Converts Thermal Meta III to Spectral Meta II

The above results clearly show that arrestin can prevent accumulation of Meta III. We next tested whether Meta III could interact with arrestin directly (Figure 4. 5), as has been shown for transducin (Zimmermann *et al.*, 2004). Note that this experiment is greatly facilitated with our functional solubilized system, since it allows clear observation

of rhodopsin's spectral intermediates free of scattering artifacts. With membranes, the data would be complicated by the fact that arrestin binding to vesicles results in a significant increase in scattering.

Adding arrestin to Rho*-P 27 minutes after photoactivation (20 °C) results in a clear decrease at 470 nm (Meta III) and increase at 380 nm (Figure 4. 5A). This 380 nm species is characterized by an intact Schiff-base, and is thus likely Meta II (Figure 4. 5A, *inset*). Although some decay of Meta III in the absence of arrestin is observed, arrestin clearly speeds its depletion (Figure 4. 5B). Furthermore, in the absence of arrestin, no significant increase in absorbance at 380 nm is observed as Meta III decays, because Meta II is not stabilized (data not shown). Note that in the presence of arrestin, the absorbance at 475 nm does not return to the starting state levels, probably because retinal-phospholipid adducts absorbing in that region were formed before the addition of arrestin.

4. 4. 6 Arrestin Interacts with the Blue-light Photoproduct P470 but not P500

We next explored arrestin's interaction with the blue-light photoproducts P470 and P500. The properties of these photoproducts are illustrated in Figures 4. 6A and B. When Meta II (Figure 4. 6A, curve ii) is illuminated with blue light (<420 nm), two absorbance peaks result (Figure 4. 6A, curve iii): unconverted Meta II ($\lambda_{max} \sim 380$ nm) and the "P-products" P470 and P500 ($\lambda_{max} \sim 480$ nm). When hydroxylamine is added to these photoproducts (Figure 4. 6B, curve iv), absorbance peaks corresponding to retinaloxime ($\lambda_{max} \sim 365$ nm) and P500 ($\lambda_{max} \sim 500$ nm) are observed. These data indicate that while P470 is hydroxylamine-sensitive, P500 is thermally stable and resistant to hydroxylamine. When P500 is illuminated with green light in the presence of

hydroxylamine, retinaloxime results (Figure 4. 6B, curve v), suggesting that green light coverts P500 to a form that is hydroxylamine sensitive, like Meta II.

After the blue-light irradiation of Meta II, there is a gradual loss of 470 nm absorbance and gain of 380 nm absorbance over time (Figure 4. 6C). We interpret this event as the thermal decay of P470 to Meta II and/or opsin and free retinal. Since P470 is equivalent to Meta III (Ritter *et al.*, 2004), we were curious if arrestin would also interact with P470. To this end, we added arrestin to a sample of blue-light irradiated Meta II. Interestingly, arrestin speeds the conversion of the ~470 nm species to a Meta II-like species (λ_{max} ~ 380 nm) (Figure 4. 6D). Furthermore, we note that the relative intensity of the 380 nm peak two hours after illumination is much greater in the presence of arrestin than in its absence. Since Meta II is more absorptive than free retinal, this result suggests that arrestin can interact with P470 and convert it to Meta II, which it stabilizes. In the absence of arrestin, P470 appears to decay ultimately to opsin and free retinal.

Our data also suggest that arrestin is unable to interact with P500, since a hydroxylamine-insensitive peak (λ_{max} ~ 500 nm) remains even after arrestin is added to blue-light irradiated Meta II (data not shown). In order to explore this possibility further, we monitored arrestin I72B binding after blue-light illumination of Meta II (Figure 4. 6E). Blue-light irradiation of arrestin-bound Meta II causes a dramatic drop in arrestin's fluorescence, suggesting that blue light releases a significant fraction of arrestin. Arrestin binding can be restored by subsequent green-light illumination (note the increase in fluorescence), and hydroxylamine-catalyzed decay of Meta II returns the fluorescence to the dark-state intensity. We confirmed these results by assaying the effect of blue-light

on ROS-P membranes' ability to "pull-down" arrestin (Figure 4. 6F). Interestingly, the fluorescence profile in Figure 4. 6F closely mirrors that in Figure 4. 6E.

Finally, we have observed by absorption spectroscopy that when arrestin-bound Meta II is illuminated with blue light, a similar distribution of species results as in the absence of arrestin, suggesting that arrestin cannot inhibit the conversion of Meta II to the P-products (data not shown), although arrestin may affect the rate of photo-conversion as has been shown for transducin (Ernst *et al.*, 2000). These results collectively suggest that blue-light irradiation of arrestin-bound Meta II causes dissociation of arrestin, because arrestin cannot bind P500. However, because arrestin can bind P470, some arrestin remains bound after blue-light illumination. Furthermore, green-light illumination of P500 converts it to a form which arrestin can bind.

4. 5 DISCUSSION

4. 5. 1 Overview of Chapter

We used the discovery that arrestin binds to Rho*-P in mixed DM/phospholipid micelles to observe arrestin-rhodopsin interactions in a soluble system. This approach enabled us to assess several important aspects of arrestin's regulation of rhodopsin photochemistry that were not previously observable using membrane-bound rhodopsin.

Our findings are summarized in Figure 4. 7. Briefly, we have found that arrestin can stabilize ~half the population of retinal in a Schiff-base linked form with a Meta II-like absorbance (Figures 4. 2, 3 and 4). In this stabilized form, retinal is likely attached to Lys^{296}, although our results do not exclude the possibility that retinal may have migrated to another site, perhaps near Helix VIII (Schädel *et al.*, 2003).

Using the optically clear mixed micelle system, we have also firmly established that arrestin can interact with Meta III and convert it to a species with Meta II-like characteristics (Figure 4. 5) [13]. The fast conversion of Meta III to Meta II may explain why very little Meta III forms when arrestin is present (Figure 4. 4). An alternative explanation is that arrestin favors Meta II at the expense of Meta I (Schleicher *et al.*, 1989), which is the precursor to Meta III (Vogel *et al.*, 2004b).

Finally, our studies indicate that arrestin does not interact with the blue-light photoproduct P500, but green-light can convert P500 to a form to which arrestin can bind (Figure 4. 6). The implications of our results in the visual photo-cycle are discussed below.

4. 5. 2 Long-lived Complexes Might Drive Arrestin Translocation

Several recent studies have begun to explore the mechanisms of the massive light-dependent translocation of arrestin, which is no doubt important for light adaptation in the rod cell (Elias *et al.*, 2004; Nair *et al.*, 2004; Strissel *et al.*, 2006). In the dark-adapted rod cell, arrestin is normally sequestered in the inner segment, where microtubules probably serve as a "sink" for arrestin binding (Nair *et al.*, 2004; Hanson *et al.*, 2006a). Upon exposure to light, arrestin translocates from the inner segment to the outer segment, where it remains until the removal of light (Elias *et al.*, 2004). Recently, Nair *et al.* have shown that this translocation is ATP-independent and may be governed by passive diffusion, and arrestin's affinity for Rho*-P keeps it in the outer segment (Nair *et al.*, 2004). Remarkably, there is enough arrestin in the rod to bind the entire pool of

[13] Note that in our studies with mixed micelles we define Meta III as a rhodopsin photoproduct absorbing at 470 nm. We have not formally established that this photoproduct is identical to the Meta III that forms in membranes (Lewis *et al.*, 1997; Heck *et al.*, 2003a; Vogel *et al.*, 2003; Vogel *et al.*, 2004b).

rhodopsin in a completely photobleached cell (Strissel *et al.*, 2006). Since little regeneration of rhodopsin probably takes place under constant illumination (Palczewski *et al.*, 1999), the persistence of arrestin in the outer segment suggests that it might be interacting with a long-lived photoproduct of rhodopsin. This possibility is supported by the results presented in this chapter.

However, a recent paper by Strissel *et al.* suggests that the translocation of arrestin may be governed by a more complex mechanism (Strissel *et al.*, 2006). The authors find that with the minimal light-intensity needed to trigger arrestin translocation, the amount of arrestin that translocates to the outer segement is in 30-fold excess to photo-activated rhodopsin. This finding implies that arrestin's interaction with Rho*-P is not solely driving translocation and that downstream signaling events might be involved.

In any case, it is worth noting that the experiments presented in this chapter, which involved complete photo-bleaching of rhodopsin and an excess of arrestin, mirror the state of the rod cell in bright light. Based on the fact that arrestin only enters the rod outer segment in bright light, when the rod cell becomes nonfunctional, arrestin is probably not playing the classical role of signal terminator. It is more likely that p44, the short splice variant of arrestin, regulates rhodopsin signaling in the dim-light operational range of the rod cell (Langlois *et al.*, 1996). Consistent with this role, p44 is present in the outer segment even in the dark (Smith *et al.*, 1994) and is expressed at only ~1 to 10% the levels of arrestin, which would be more than sufficient to bind the limited number of Rho* produced by dim light (Palczewski *et al.*, 1994a). As described below, the role of arrestin in the rod cell is more likely to be a regulator of late-photoproducts and retinal release.

4. 5. 3 Arrestin Interacts with Metarhodopsin III

A form of stationary night blindness called Oguchi disease is a recessive genetic disorder caused by mutations in either rhodopsin kinase or arrestin. Patients with Oguchi disease require 5 to 7 hours to dark-adapt, much longer than the normal 40 minutes (Dryja, 2000; Lamb and Pugh, 2004). This phenomenon suggests that arrestin activity is necessary for proper dark adaptation, which involves the removal of all metarhodopsin species from the rod cells and the regeneration of rhodopsin with 11-*cis* retinal. In bright light conditions, up to half of the rhodopsin in the human retina is estimated to be converted to Meta III (Lewis *et al.*, 1997). It has been hypothesized that Oguchi disease is caused by a build-up of Meta III, which decays much slower in the absence of arrestin and thus prevents regeneration (Lamb and Pugh, 2004).

Our results support this hypothesis, since we have shown that phosphorylated Meta III is bound by arrestin and stabilized as Meta II. Arrestin-bound Meta II may be more accessible to the regeneration machinery, which begins with the reduction of all-*trans* retinal by retinal dehydrogenase (Hofmann *et al.*, 1992), than Meta III. Furthermore, arrestin may serve to attenuate Meta III signaling by competing with transducin (Zimmermann *et al.*, 2004).

4. 5. 4 Arrestin May Limit Retinal Release to Prevent Retinal Degeneration

Some patients with Oguchi disease suffer retinal degeneration (Dryja, 2000; Hao *et al.*, 2002). This phenomenon is not caused by excessive transducin-mediated signaling, since Hao *et al.* demonstrated that under very bright light conditions, retinal degeneration in arrestin knock-out mice is independent of transducin (Hao *et al.*, 2002). Furthermore, retinal degeneration is characterized by an induction of the transcription

factor AP-1, which suggests that oxidative stress might be the cause (Reme, 2005). How might bright light trigger this pro-apototic redox-sensitive transcription factor? Under these conditions, the concentration of free all-*trans* retinal may become quite high, because the relatively slow rate of retinal dehydrogenase activity becomes limiting (Saari *et al.*, 1998). High levels of free retinal can lead to di-retinal conjugates with phosphatidylethanolamine (A2E). Light-dependent oxidation of A2E yields dangerous epoxides, which may be a causative agent in both age-related (AMD) and Stargardt's macular degeneration (Sparrow *et al.*, 2003; Radu *et al.*, 2004; Wenzel *et al.*, 2005). The fact that animals that lack arrestin are highly sensitive to bright light suggests that arrestin serves a protective role in the rod cell. Our data supports this hypothesis, in that we observe that arrestin limits the release of retinal and traps it in stabilized Meta II.

4. 5. 5 Possible Roles of the Blue-light Photoproducts

Rod cell exposure to full-spectrum light might generate P500 as well as Meta III (Arnis and Hofmann, 1995; Bartl *et al.*, 2001). Although Meta III appears to have some activity, since it is bound by both transducin and arrestin, P500 seems to be similar to dark-state rhodopsin in its activity. Thus P500 might represent another storage form of the protein. Since P500 can undergo light-dependent activation to a Meta II-like species, this photoproduct might serve to preserve some light-sensitive pigment in the rod cells after being exposed to high-bleaching conditions. This mechanism would allow the cell to maintain some sensitivity when transitioning from bright to dim light conditions before dark adaptation has occurred.

4. 5. 6 Summary

The studies described here were made possible by the development of fluorescently labeled arrestin and a functional soluble system, as described in Chapters 2 and 3 of this dissertation. In this chapter, we have found the following: 1) Arrestin inhibits ~50% of retinal release from rhodopsin by trapping it in a Schiff-base linked form, most likely at Lys^{296}, with an absorbance characteristic of Meta II (380 nm). 2) Arrestin can interact with Meta III, formed either by thermal decay or blue-light irradiation, and convert it to a Meta II-like species. 3) Arrestin does not interact with the blue-light photoproduct P500, but green light can convert P500 to a form which arrestin binds. Together, these observations suggest that arrestin's true role in the rod cell might be to limit retinal release and regulate Meta III, which is consistent with recent physiological evidence supporting this hypothesis.

4. 6 ACKNOWLEDMENTS

This work was supported in part by National Institutes of Health Grant DA14896 (to D. L. F.), a National Defense Science and Engineering graduate fellowship (to M. E. S.), and an N. L. Tartar research fellowship (to M. E. S.).

Figure 4. 1 Fluorescently labeled arrestin can be used to monitor arrestin binding to Rho*-P in mixed micelles. A) Structural models of rhodopsin (*dark gray*) and its hypothetical dimer partner (*light gray*) in a membrane bilayer. Arrestin is also shown, and the location of I72 on arrestin is indicated by a black sphere at the site of the α-carbon. *Inset* – The structure of monobromobimane, which was attached to a mutant cysteine residue at site I72 (not to scale with the protein models). from: (Sommer *et al.*, 2006) **B)** The fluorescence of bimane-labeled arrestin mutant I72C (I72B) in the presence of dark-state Rho-P (*solid spectrum*) and after light-activation (*dashed spectrum*). In this experiment, 1 μM arrestin I72B and a two-fold excess of Rho-P solubilized in mixed micelles (0.02% DM and 0.02% asolectin) was used (20 mM HEPES, 150 mM NaCl, pH 7.4, 20 °C).

Figure 4. 1

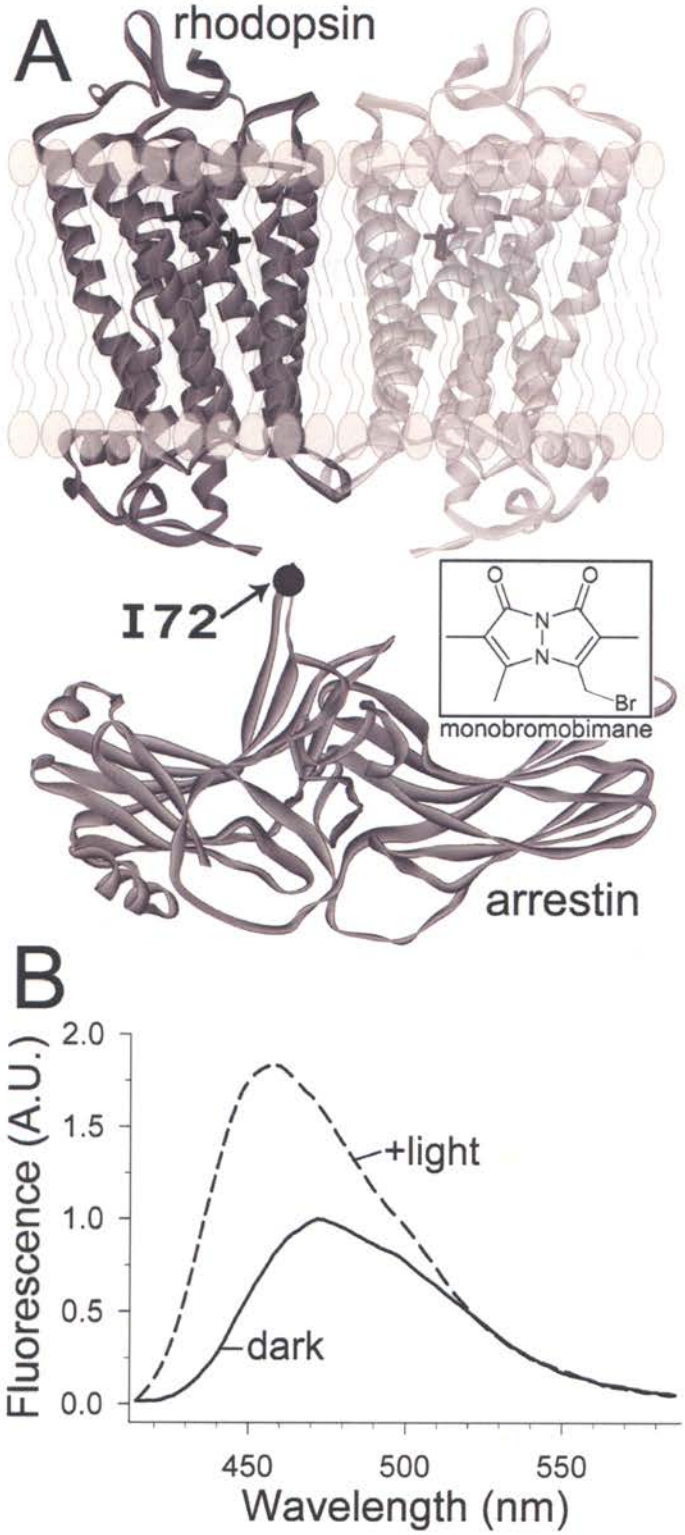
A
rhodopsin
I72
monobromobimane
Br
arrestin
B
Fluorescence (A.U.)
2.0
1.5
1.0
0.5
0.0
+light
dark
450
500
550
Wavelength (nm)

Figure 4. 2 **Arrestin traps ~half of the retinal population in opsin.** **A)** Retinal release from Rho-P in mixed micelles measured as an increase in opsin tryptophan fluorescence (λ_{ex} = 295 nm, λ_{em} = 330 nm). Photoactivation occurred at t = 0 min, and 10 mM hydroxylamine was added at t = 120 min. Samples contained 1 μM Rho-P (0.02% DM and 0.02% asolectin) with or without a two-fold excess of arrestin I72B (20 mM HEPES, 150 mM NaCl, pH 7.4, 20 °C). **B)** Arrestin binding and release measured during the same experiment as described in (A) (λ_{ex} = 380 nm, λ_{em} = 456 nm).

Figure 4. 2

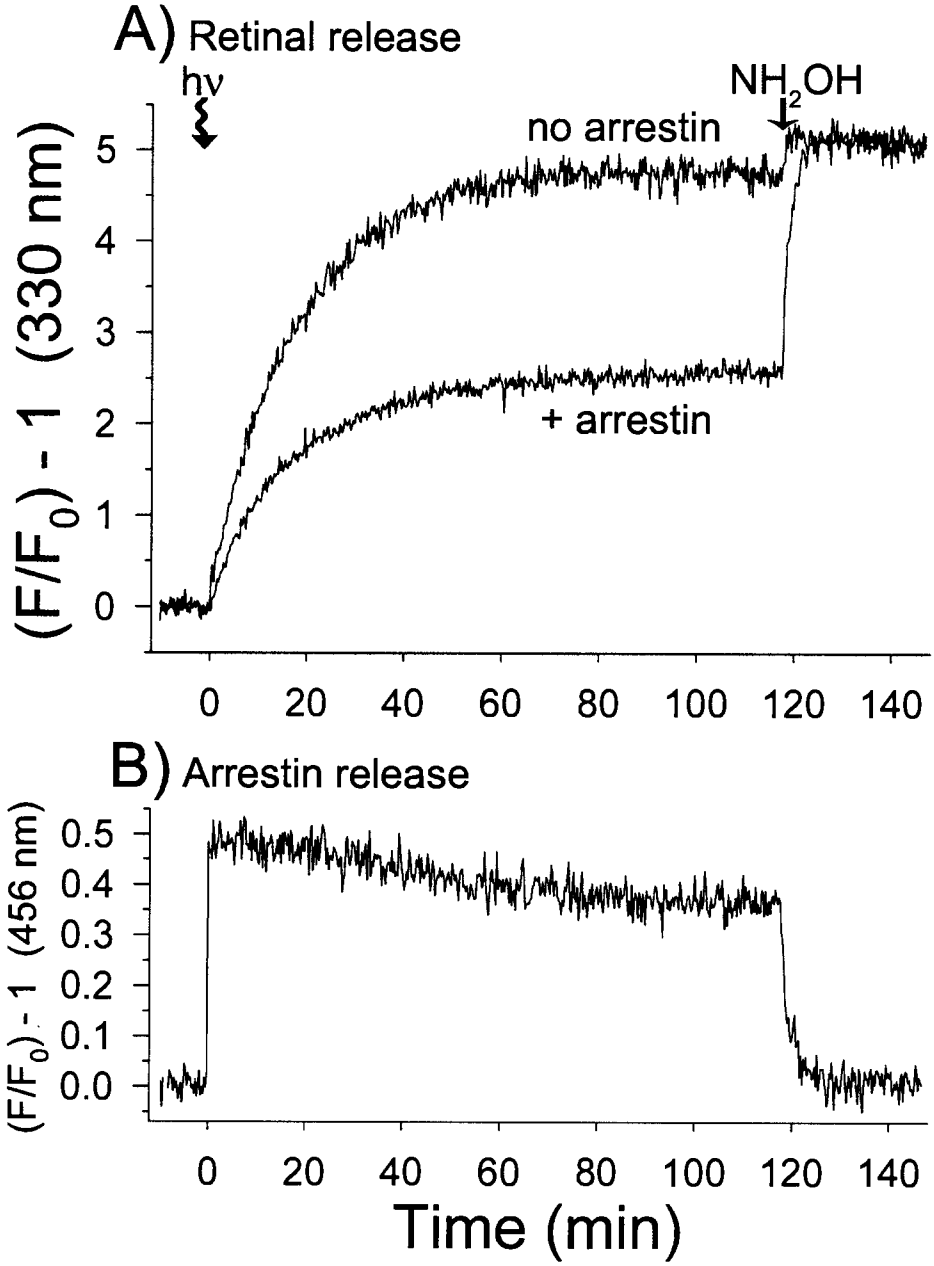
A) Retinal release
hν
NH2OH
no arrestin
+ arrestin
(F/F0) - 1 (330 nm)
0
1
2
3
4
5
0
20
40
60
80
100
120
140
B) Arrestin release
(F/F0) - 1 (456 nm)
0.0
0.1
0.2
0.3
0.4
0.5
0
20
40
60
80
100
120
140
Time (min)

Figure 4. 3 Arrestin traps retinal as a Schiff-base adduct on F2 of Rho*-P. A) Reducing the retinal Schiff-base with $NaBH_4$ produces a fluorescent Rho*-P that indicates the amount of retinal covalently attached to opsin. Briefly, Rho-P solubilized in 0.02% DM or 0.02% DM and 0.02% asolectin, without or with a two-fold excess of arrestin (*lanes 2-5*), was photoactivated, allowed to decay at 20 °C in the dark, reduced after 120 minutes, and then subjected to SDS PAGE. The total amount of Schiff-base linked retinal was assessed by the reduction of Meta II Rho immediately after bleach (*lane 1*). **B)** The same samples as described in (A) were subjected to V8 proteolysis. Molecular weight markers (kDa) are indicated on the left. In both (A) and (B), the Coomassie-stain (*left*) and fluorescence (*right*) of each gel is shown, and *arrows* on the right identify the bands: arrestin (Arr), rhodopsin (Rho), Rho fragments resulting from V8 proteolysis (F1 and F2), the V8 protease (V8), and asolectin phospholipids (PL). **C)** Plot of the average quantified fluorescence from four independent experiments as shown in (A). The fluorescence is expressed as a percent of the total "Meta II" fluorescence, and the error bars represent the standard error.

Figure 4. 3

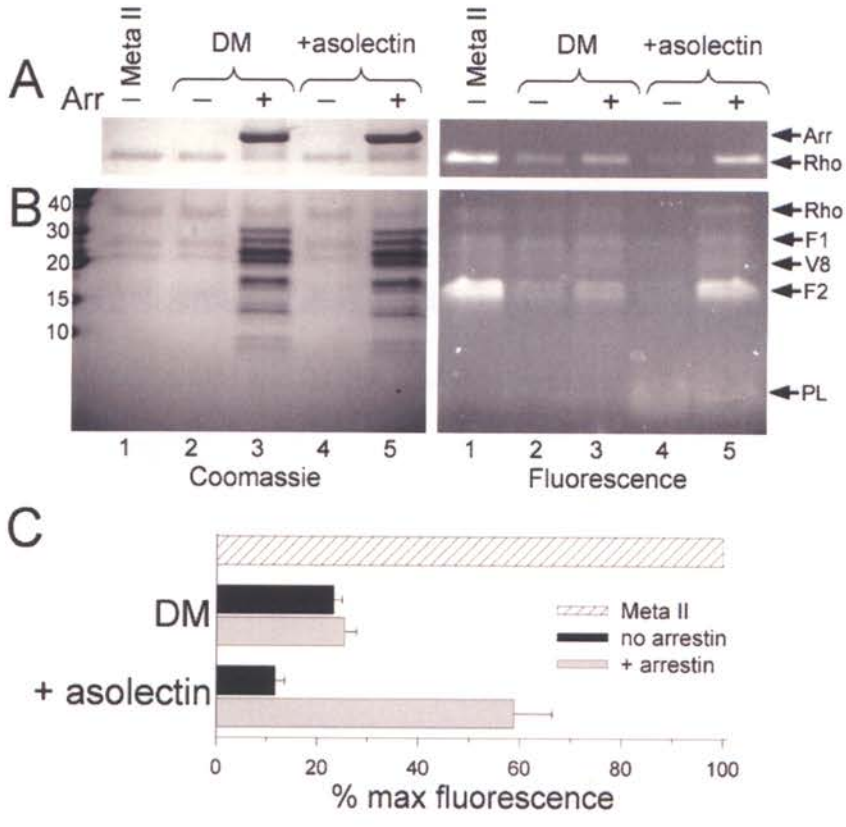
A
Arr
Meta II
DM
+asolectin
Meta II
DM
+asolectin
Arr
Rho
B
40
30
20
15
10
Rho
F1
V8
F2
PL
1 2 3 4 5
Coomassie
1 2 3 4 5
Fluorescence
C
DM
+ asolectin
Meta II
no arrestin
+ arrestin
0 20 40 60 80 100
% max fluorescence

Figure 4. 4 Arrestin stabilizes Meta II and inhibits Meta III formation. A) The absorbance of Rho-P in DM/asolectin mixed micelles was observed in the dark (*thick solid spectrum*) and after photoactivation (*dashed spectrum*). Spectra were subsequently recorded every three minutes (*thin solid spectra*) for 120 minutes (the last spectrum is *thick*). The arrows indicate the loss of absorbance at 380 nm and the increase in absorbance at 440 – 480 nm over time. **B)** The same experiment as described in (A) in the presence of a two-fold excess of arrestin. **C**) The amount of retinal Schiff-base remaining at the end of the experiments described in (A) and (B) was assessed by adding H_2SO_4 (protonated Schiff-bases absorb at 440 nm). In each experiment, 1 μM Rho-P in mixed micelles (0.02% DM and 0.02% asolectin) was used (20 mM HEPES, 150 mM NaCl, pH 7.4, 20 °C).

Figure 4. 4

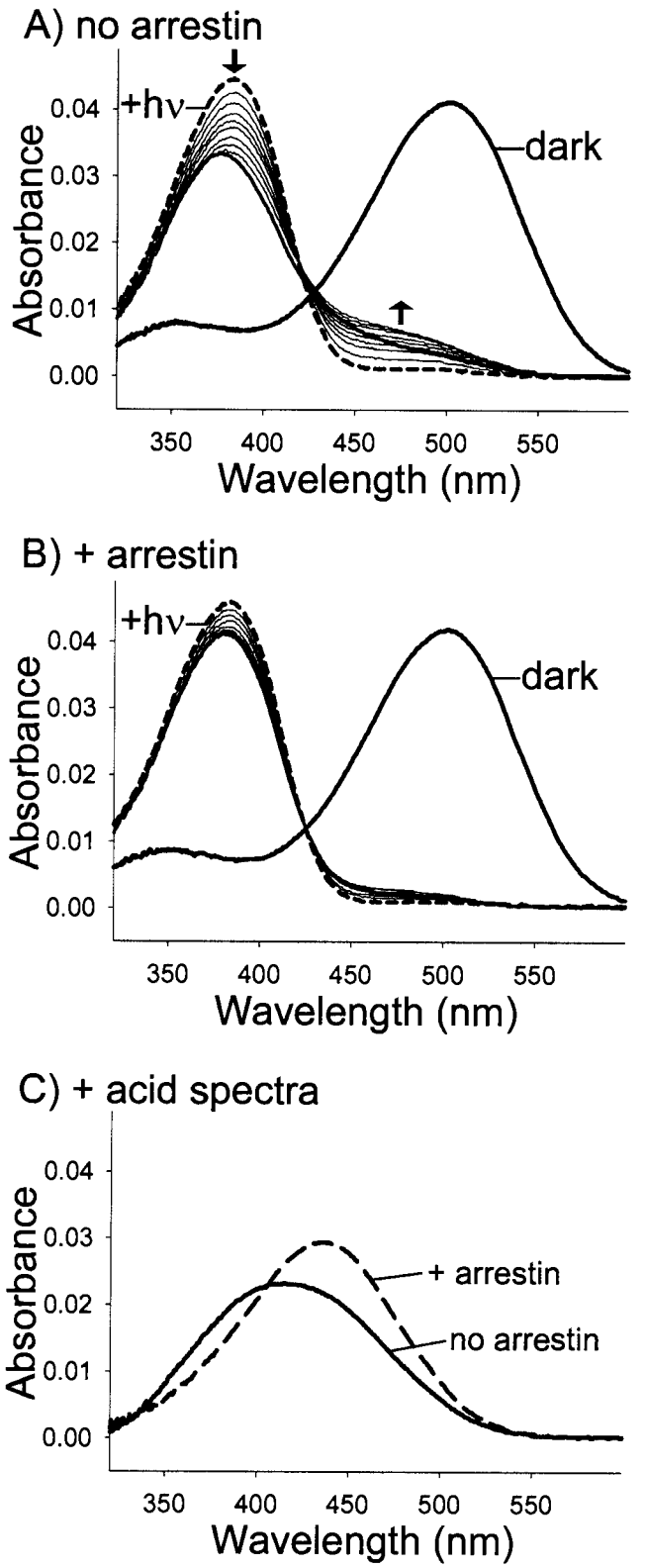
A) no arrestin
+hν
dark
Absorbance
0.04
0.03
0.02
0.01
0.00
350
400
450
500
550
Wavelength (nm)
B) + arrestin
+hν
dark
Absorbance
0.04
0.03
0.02
0.01
0.00
350
400
450
500
550
Wavelength (nm)
C) + acid spectra
+ arrestin
no arrestin
Absorbance
0.04
0.03
0.02
0.01
0.00
350
400
450
500
550
Wavelength (nm)

Figure 4. 5 Arrestin converts Meta III to spectral Meta II. Rho-P in mixed micelles was photoactivated (>495 nm), and after 27 min either arrestin or an equal volume of buffer (control) was added to the cuvette, and absorbance spectra were recorded every 90 seconds. **A)** Difference spectra representing the conversion of ~470 nm absorbance to ~380 nm absorbance after the addition of arrestin. The base-line spectrum (the first spectrum of Rho*-P after the addition of buffer) was subtracted from spectra that had been recorded at 1, 2.5, 4, 8.5, 17.5, 50, and 90 min after the addition of arrestin. The first and last spectra are labeled. *Inset*, the increased 380 nm absorbance is most likely due to an increase in Meta II because acidification at the end of the experiment yielded more of the 440 nm species (indicating Schiff base) compared with the control in which no arrestin was added. **B)** Addition of arrestin caused a decrease in Meta III absorbance (475 nm) over time. The *arrow* marks the time at which buffer (*closed circles*) or arrestin (*open circles*) was added. The data points represent the average from three independent experiments, and the *error bars* represent the S.E. In each experiment, 1 μM Rho-P in 20mM HEPES, 150 mM NaCl, pH 7.4, 0.02% DM, 0.02% asolectin was used (20 °C), and arrestin was added to a final concentration of 1.5 μM. Figure is taken from (Sommer *et al.*, 2006).

Figure 4. 5

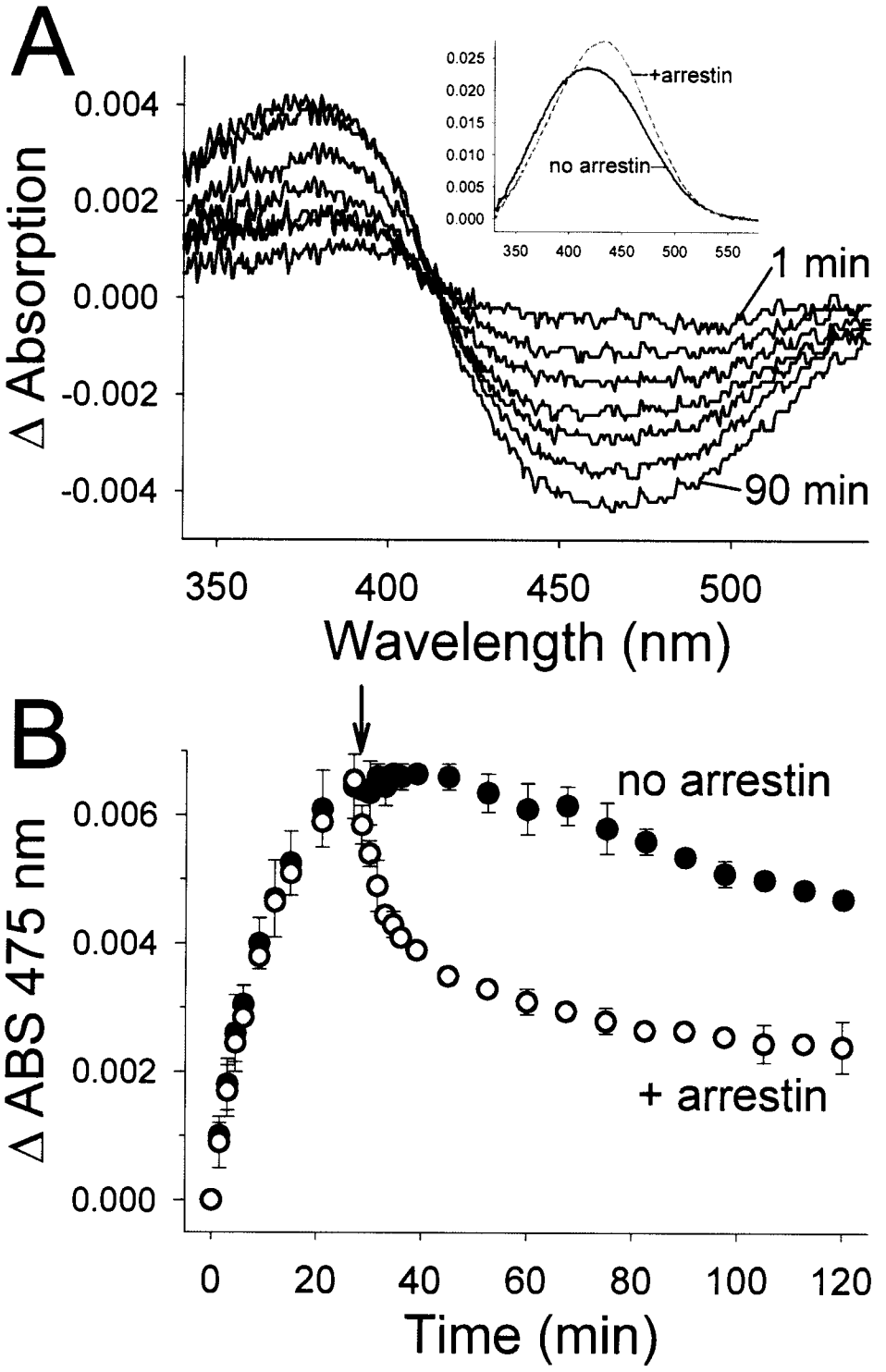
A
0.004
0.002
0.000
-0.002
-0.004
Δ Absorption
350
400
450
500
Wavelength (nm)
1 min
90 min
0.025
0.020
0.015
0.010
0.005
0.000
350
400
450
500
550
+arrestin
no arrestin
B
0.006
0.004
0.002
0.000
Δ ABS 475 nm
0
20
40
60
80
100
120
Time (min)
no arrestin
+ arrestin

Figure 4. 6 Arrestin interacts with the blue-light photoproduct P470 but not P500. **A)** The absorbance spectra of Rho-P were recorded i) in the dark state, ii) after illumination with green light (>495 nm, 20 sec), and iii) after subsequent illumination with blue light (<420 nm, 20 sec), which results in a mixtures of the products P470 (Meta III) and P500. **B)** The same sample as described in (A), iv) after the addition of 10 mM hydroxylamine, and v) after subsequent illumination with green light (20 sec). **C and D)** Rho-P was illuminated with green light followed by blue light, as described in (A), and spectra were subsequently recorded at 1.5, 3, 4.5, 7.5, and 10.5 minutes after the addition of 2 μM arrestin (D) or and equal volume of buffer (C). Difference spectra were calculated by subtracting the first spectrum after blue-light irradiation from all subsequent spectra after the addition of arrestin or buffer. In each experiment, 1 μM Rho-P in 20 mM HEPES, 150 mM NaCl, pH 7.4, 0.02% DM, 0.02% asolectin was used (20 °C). **E)** Fluorescence of arrestin I72B (1 μM) in the presence of a 2-fold excess of Rho-P (0.02% DM, 0.02% asolectin). The sample was illuminated at the indicated times with green or blue light (20 sec), and 15 minutes after the initial illumination, 10 mM hydroxylamine was added. The sample was excited at 380 nm (20 °C). **F)** The ability of ROS-P to "pull-down" arrestin in the dark (*lane 1*), after green-light illumination (*lane 2*), after subsequent blue-light illumination (*lane 3*), after subsequent green-light illumination (*lane 4*), and after the addition of 10 mM hydroxylamine (*lane 5*). The *upper panel* shows the fluorescence of the pulled-down arrestin resolved by SDS PAGE, and in the *lower panel*, the fluorescence of the bands is plotted as a percent of the total arrestin present.

Figure 4. 6

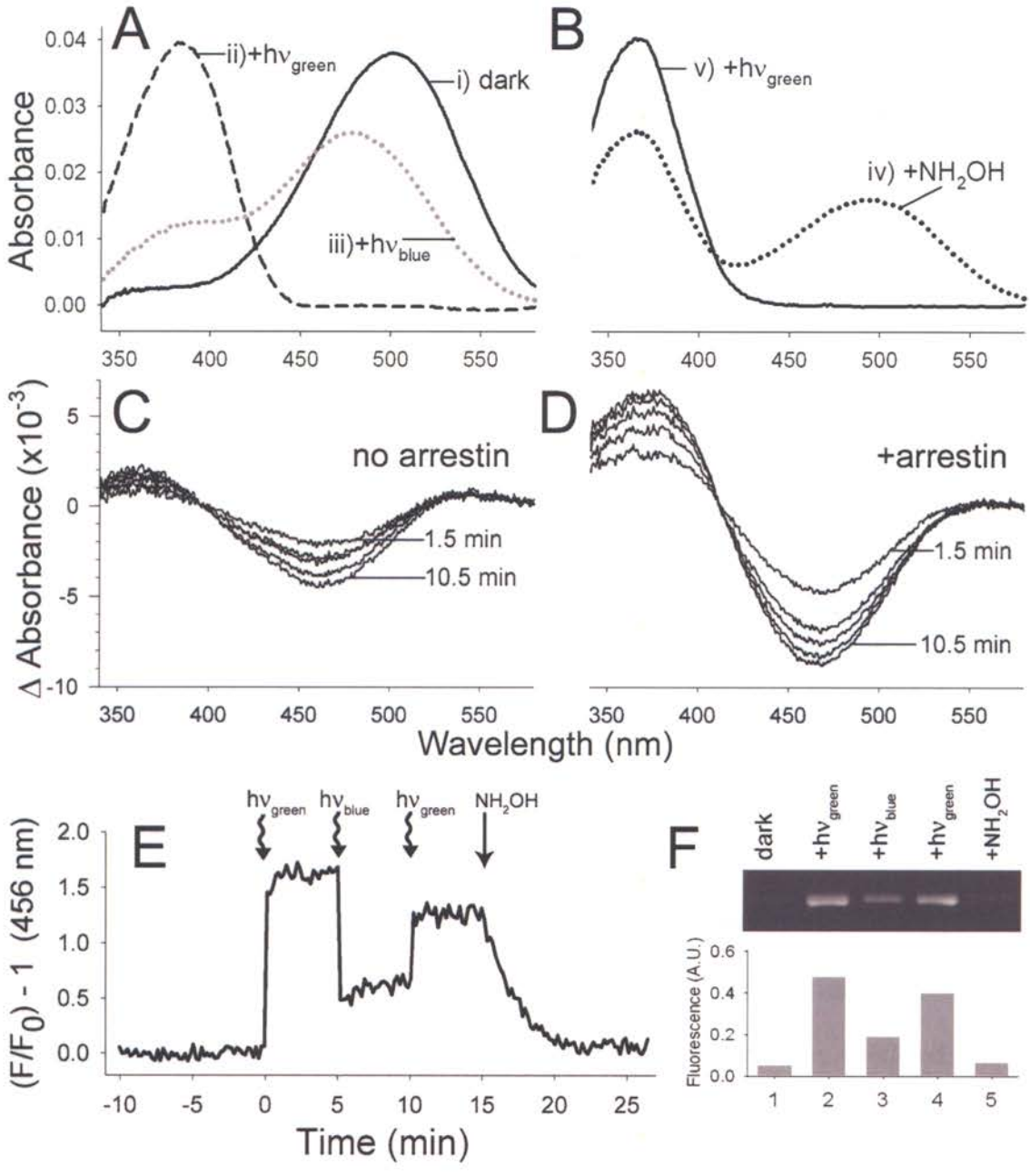
A
ii)+hν green
i) dark
iii)+hν blue
Absorbance
B
v) +hν green
iv) +NH2OH
C
no arrestin
1.5 min
10.5 min
D
+arrestin
1.5 min
10.5 min
Δ Absorbance (x10-3)
Wavelength (nm)
E
hν green
hν blue
hν green
NH2OH
(F/F0) - 1 (456 nm)
Time (min)
F
dark
+hν green
+hν blue
+hν green
+NH2OH
Fluorescence (A.U.)

Figure 4. 7 A cartoon representation of how arrestin can interact with the major photoproducts of phosphorylated rhodopsin. Dark state rhodopsin (Rho) is converted by green light (>495 nm) to Meta I (MI), which is in equilibrium with Meta II (MII), and can decay to Meta III (MIII) (Vogel *et al.*, 2004b). Meta II decays ultimately to opsin and all-*trans* retinal (atR), and Meta III slowly decays to opsin and atR as well (Zimmermann *et al.*, 2004), although it is not known if this happens directly or through additional intermediates. Blue-light irradiation (<420 nm) of Meta II leads to two photoproducts, P470 (Meta III) and P500 (Arnis and Hofmann, 1995). Green light can convert P500 back to Meta II (Bartl *et al.*, 2001). The conformation of the chromophore and the protonation state of the Schiff-base (*blue proton*) is illustrated for each photoproduct, including the isomerization around the Schiff base that occurs during Meta III formation (Vogel *et al.*, 2003; Vogel *et al.*, 2004a; Vogel *et al.*, 2004b; Zimmermann *et al.*, 2004). Although it has been shown that P500 most likely binds an all-*trans* retinal (Bartl *et al.*, 2001), the exact nature of this photoproduct has not been determined. The selectivity of arrestin for the photoproducts is also illustrated: arrestin does not bind dark state Rho-P, P500, or opsin. Arrestin stabilizes Meta II at the expense of Meta I, yielding "extra Meta II" (Schleicher *et al.*, 1989), and we have shown that arrestin will interact with Meta III/P470 and convert it to Meta II. Arrestin-bound Meta II is stabilized, and its decay to opsin and free retinal is inhibited. In the figure, the *filled and empty arrows* represent conversions that occur in the absence and presence of arrestin, respectively. Note that the protein models are not to scale, and possible binding stoichiometries (does arrestin bind a dimer of rhodopsin?) are not considered.

Figure 4. 7

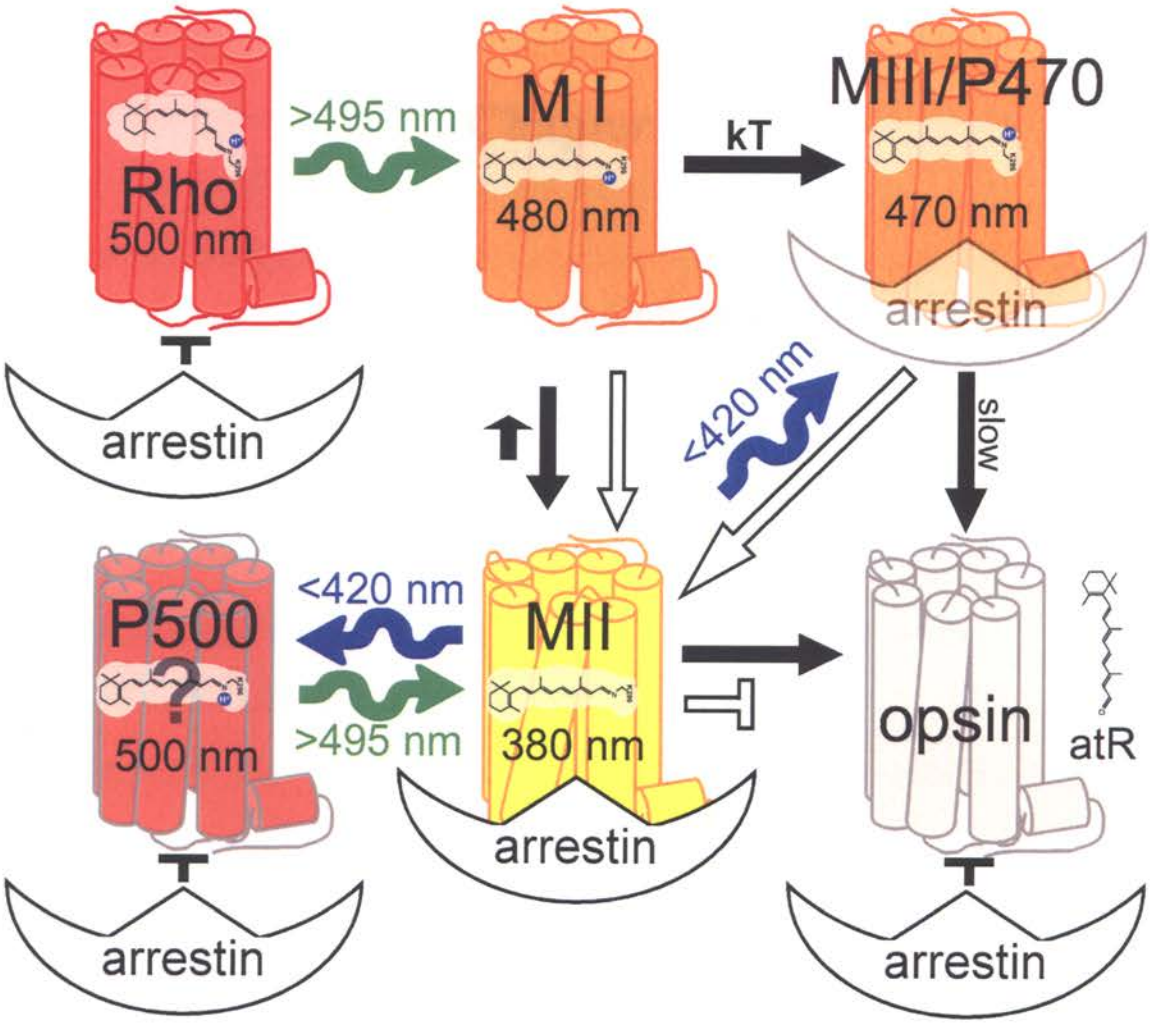
Rho
500 nm
>495 nm
M I
480 nm
kT
MIII/P470
470 nm
arrestin
arrestin
<420 nm
slow
P500
?
500 nm
<420 nm
>495 nm
MII
380 nm
opsin
atR
arrestin
arrestin

Chapter 5

Summary and Conclusions

This dissertation reports how the interaction between arrestin and rhodopsin affects retinal release and photoproduct formation from rhodopsin. These studies were enabled by the development of a fluorescent assay to monitor arrestin binding to rhodopsin, which then led to the discovery that acidic phospholipids enable arrestin-rhodopsin interactions in a soluble system. The main findings and conclusions of these studies, as well as their physiological implications, are briefly summarized below.

5. 1 Fluorescently Labeled Arrestin Mutants can be used to Monitor Arrestin Binding and Release

Many of the experiments presented in this dissertation employed a fluorescently labeled arrestin, I72B. The fluorescence of I72B increases and blue-shifts in intensity upon binding light-activated, phosphorylated rhodopsin (Rho*-P). Fluorescence quenching, steady-state anisotropy, as well as EPR analysis of a spin-probe at this site indicate that this change in fluorescence is likely because the probe is buried in a protein-protein interface. Furthermore, the loop to which the probe is attached likely undergoes a folded to extended conformational change upon binding Rho*-P (see Appendix 2). Importantly, these fluorescence changes can be used to directly monitor arrestin's binding and release in real time. When combined with a previously established fluorescence assay for monitoring retinal release, arrestin I72B provides a valuable tool for addressing questions about the dynamics and mechanisms of arrestin-rhodopsin interactions.

5. 2 Acidic Phospholipids Enable Arrestin Binding to Purified Rhodopsin in Detergent

Using fluorescently labeled arrestin, we discovered that arrestin binding is severely diminished when Rho*-P is purified out of the native membrane and solubilized

in detergent. Surprisingly, we found that the addition of acidic phospholipids to detergent-solubilized Rho*-P can restore arrestin binding. Why are acidic phospholipids necessary for arrestin-rhodopsin interactions? The negatively charged phospholipid head groups may contribute critical ionic interactions between arrestin and the membrane. Alternatively, phospholipids may be necessary to stabilize a spectrally silent conformation of rhodopsin, or they might be necessary for rhodopsin dimerization. Either of these possibilities could affect arrestin function.

Interestingly, there is evidence that the acidic phospholipid phosphatidylserine (PS) is flipped from the intradiskal to the cytoplasmic side of the membrane upon rhodopsin activation (Hessel *et al.*, 2001), and transducin may interact specifically with this PS when it binds Rho* (Hessel *et al.*, 2003). It is reasonable to speculate that arrestin binding might be regulated by a similar mechanism.

5. 3 Arrestin Regulates Retinal Release

Using arrestin I72B we discovered that retinal and arrestin release appear directly linked in ROS membranes. Arrestin and retinal release occur at the same time with the same energy of activation (~20 kcal/mol), and arrestin slows retinal release from native membranes ~2 fold at physiological temperatures. Interestingly, these studies also suggested that some arrestin forms a long-lived complex with rhodopsin. In later experiments using mixed micelles of detergent and acidic phospholipids, we found further evidence for the long-lived complexes. Although arrestin appeared to remain bound to the complex, we consistently observed that up to ~50% of retinal was trapped in the binding pocket, and ~50% of retinal was released. Furthermore, this retinal was

released at the same rate as in the absence of arrestin. Thus, arrestin and retinal release appear unlinked in mixed micelles.

Several potential explanations exist for this phenomenon. 1) *Low levels of Rho phosphorylation.* If only 50% of the Rho-P in these experiments was phosphorylated enough to interact with arrestin, we would expect to see this result. Since quantitation of our phosphorylation efficiency indicates that an average of ~6 phosphates per Rho are present, so this possibility seems unlikely. However, we have not verified that our subsequent purification procedure does not hydrolyze phosphates from Rho-P. 2) *Low K_D in mixed micelles.* Using I72B's fluorescence change, we determined the K_D for the arrestin-rhodopsin complex to be ~0.9 μM (see section **3. 7. 1** in Chapter 3). Since our retinal trapping experiments were done with ~1 μM protein, this may mean that only ~50% of Rho*-P was actually bound by arrestin at this concentration (assuming 100% arrestin activity in these samples). However, even when we used 4 fold excess arrestin, which should bind ~80% of Rho*-P, we still observed only 50% retinal trapping (Figure 3. S1C). Note that previous studies report the K_D to be 20-50 nM using membrane-bound Rho*-P (Schleicher *et al.*, 1989; Pulvermüller *et al.*, 1997). 3) *Possible contribution of Rho dimers.* Our preliminary cross-linking data suggest that arrestin binds rhodopsin oligomers (see section **3. 7. 3** in Chapter 3). A highly speculative explanation for the 50% retinal trapping is that arrestin binds a dimer of rhodopsin, and that retinal is released from one dimer partner but trapped in the other. Clearly, resolving the cause of this interesting phenomenon requires further study.

Another intriguing question raised from this dissertation is, why are arrestin and retinal both released from Rho*-P in native ROS membranes, but "stuck" in mixed

micelles containing acidic phospholipids? Perhaps there is some membrane constituent or structure necessary for arrestin release that is lacking in micelles. For example, the unidirectional movement of retinal through opsin, or "ligand-channeling", is thought to be disrupted by the presence of detergent (Sachs *et al.*, 2000b; Heck *et al.*, 2003b). Interestingly, the proposed "exit site" for retinal, which is on the cytoplasmic surface of rhodopsin between Helix VIII and the C-terminal tail (Schädel *et al.*, 2003), is in an ideal position to communicate with arrestin. Finally, in ROS membranes, PS is only ~10% of the total phospholipid (Anderson and Maude, 1970; Aveldano and Bazan, 1983). Thus, the relatively high concentrations of acidic phospholipids present in our mixed micelles may substantially decrease the off-rate of arrestin simply because of increased ionic interactions. In support of this idea, we found that mixed micelles containing a physiological ratio of phospholipids were similar to intact membranes in regards to retinal and arrestin release.

Clearly, arrestin regulates retinal release, by both slowing the rate of its release as well as trapping some retinal in a long-lived complex [14]. How could this be important in the rod cell? Recent studies have indicated that arrestin is normally sequestered in the rod inner segment in the dark and only translocates to the outer segment when the light intensity approaches the limit of rod cell function (~3% photobleaching) (Strissel *et al.*, 2006). Our results suggest that the purpose of this translocation is to bind all photo-activated rhodopsin and prevent the massive release of retinal that would occur otherwise. Retinal is known to form toxic oxidative compounds that damage the rod cell

[14] Note that arrestin likely traps a population of retinal in native membranes as well. In Chapter 2 we see that ~20% of arrestin remains bound to ROS*-P, long after Meta II decay. Although we could not determine if this "stuck" arrestin traps retinal, our later results with mixed micelles suggest that it does.

(Fishkin *et al.*, 2003; Dillon *et al.*, 2004), and the build-up of these compounds in the elderly or in patients with certain mutations is likely a contributing factor in macular degeneration (Sparrow *et al.*, 2003; Wenzel *et al.*, 2005).

5. 4 Arrestin Interacts with Meta III

The data presented in this dissertation also show that arrestin binds the post-Meta II photodecay product Meta III and converts it to a Meta II-like species, which it stabilizes. This discovery is particularly interesting considering that up to half the human retina is converted to Meta III in bright-light conditions (Lewis *et al.*, 1997). In addition, arrestin makes a dramatic translocation into the rod outer segment in bright-light conditions (Elias *et al.*, 2004), and recent measurements suggest that arrestin is present at stoichiometric levels to rhodopsin (Strissel *et al.*, 2006). Hence, in bright-light conditions, arrestin most likely binds the large pool of Meta III and converts it to a stabilized Meta II. When arrestin function is absent, such as in patients with Oguchi disease, dark-adaptation after exposure to bright-light is severely inhibited, probably due to a build-up of Meta III (Lamb and Pugh, 2004). Thus, our results imply that another physiological role of arrestin is to clear Meta III during dark-adaptation.

5. 5 A Revision of Arrestin-Mediated Visual Signal Attenuation

Ever since the discovery that arrestin quenches phosphodiesterase activity in the rod cell (Kühn *et al.*, 1984; Wilden *et al.*, 1986), the paradigm for visual signal attenuation is that arrestin binds Rho*-P to block transducin activation. However, this dissertation proposes that arrestin plays a more complex role of regulating retinal release and photoproduct formation. Furthermore, regulation of retinal release may be arrestin's major role in the rod cell, since arrestin does not enter the outer segment until the rod cell

becomes nonfunctional in bright light (Strissel *et al.*, 2006). In contrast, p44, the alternative splice of arrestin, is localized to the outer segment in dim light when the rod cell is operational, probably due to its high affinity for residual phosphorylated rhodopsin (see Appendix 1). Thus, p44 is likely the fast quencher of visual signal transduction in dim light, and arrestin is a protective protein that inhibits retinal release in bright light and clears Meta III photoproducts during dark adaptation.

5. 6 Future Directions

The results presented in this dissertation raise several questions for future study. For example, where does the Ile^{72}-loop bind on rhodopsin? Could the hydrophobic cleft opened by Helix VI movement in rhodopsin be this binding site, or does this loop insert into the membrane? Furthermore, why are phospholipids required for arrestin binding? Does a phospholipid-binding site exist on arrestin, or is the effect localized to rhodopsin? What is the mechanism of arrestin release, and how is this coordinated with retinal release in the membrane? And finally, what is the cause of the 50% trapping of retinal we observe in mixed micelles? Is this effect related to possible rhodopsin dimerization, and what is the stoichiometry of the arrestin-rhodopsin complex? Answers to these questions will undoubtedly be interrelated and are necessary to understand fully the true structure and function of the arrestin-rhodopsin complex.

5. 7 Concluding Remarks

This dissertation contributes to a better biochemical understanding of arrestin function in the rod cell and also describes new structural details of the arrestin-rhodopsin interaction. Furthermore, this work defines a novel fluorescence assay and soluble system that will be useful in future arrestin-rhodopsin studies. These findings may also

be extended to the larger field of GPCRs and understanding the role of β-arrestin in modulating receptor affinity for ligand and the mechanisms of desensitization, which is ultimately necessary for the design of better therapeutics.

References

Altenbach, C., K. Yang, D.L. Farrens, Z.T. Farahbakhsh, H.G. Khorana, and W.L. Hubbell. (1996) "Structural features and light-dependent changes in the cytoplasmic interhelical E-F loop region of rhodopsin: a site-directed spin-labeling study". *Biochemistry*. **35**: 12470-8.

Alves, I.D., G.F. Salgado, Z. Salamon, M.F. Brown, G. Tollin, and V.J. Hruby. (2005) "Phosphatidylethanolamine enhances rhodopsin photoactivation and transducin binding in a solid supported lipid bilayer as determined using plasmon-waveguide resonance spectroscopy". *Biophys J.* **88**: 198-210.

Anderson, D.H., and S.K. Fisher. (1975) "Disc shedding in rodlike and conelike photoreceptors of tree squirrels". *Science*. **187**: 953-5.

Anderson, R.E., and M.B. Maude. (1970) "Phospholipids of bovine outer segments". *Biochemistry*. **9**: 3624-8.

Anderson, R.E., D.J. Landis, and P.A. Dudley. (1976) "Essential fatty acid deficiency and renewal of rod outer segments in the albino rat". *Invest Ophthalmol.* **15**: 232-6.

Angers, S., A. Salahpour, and M. Bouvier. (2002) "Dimerization: an emerging concept for G protein-coupled receptor ontogeny and function". *Annu Rev Pharmacol Toxicol.* **42**: 409-35.

Arnis, S., K. Fahmy, K.P. Hofmann, and T.P. Sakmar. (1994) "A conserved carboxylic acid group mediates light-dependent proton uptake and signaling by rhodopsin". *J Biol Chem.* **269**: 23879-81.

Arnis, S., and K.P. Hofmann. (1995) "Photoregeneration of bovine rhodopsin from its signaling state". *Biochemistry*. **34**: 9333-40.

Arshavsky, V.Y. (2002) "Rhodopsin phosphorylation: from terminating single photon responses to photoreceptor dark adaptation". *Trends Neurosci*. **25**: 124-6.

Arshavsky, V.Y., T.D. Lamb, and E.N. Pugh, Jr. (2002) "G proteins and phototransduction". *Annu Rev Physiol*. **64**: 153-87.

Ascano, M., and P.R. Robinson. (2006) "Differential phosphorylation of the rhodopsin cytoplasmic tail mediates the binding of arrestin and its splice variant, p44". *Biochemistry*. **45**: 2398-407.

Aton, B.R. (1986) "Illumination of bovine photoreceptor membranes causes phosphorylation of both bleached and unbleached rhodopsin molecules". *Biochemistry*. **25**: 677-80.

Aveldano, M.I., and N.G. Bazan. (1983) "Molecular species of phosphatidylcholine, -ethanolamine, -serine, and -inositol in microsomal and photoreceptor membranes of bovine retina". *J Lipid Res*. **24**: 620-7.

Aveldano, M.I. (1988) "Phospholipid species containing long and very long polyenoic fatty acids remain with rhodopsin after hexane extraction of photoreceptor membranes". *Biochemistry*. **27**: 1229-39.

Aveldano, M.I. (1995) "Phospholipid solubilization during detergent extraction of rhodopsin from photoreceptor disk membranes". *Arch Biochem Biophys*. **324**: 331-43.

Balla, T. (2005) "Inositol-lipid binding motifs: signal integrators through protein-lipid and protein-protein interactions". *J Cell Sci*. **118**: 2093-104.

Bartfai, T., J.L. Benovic, J. Bockaert, R.A. Bond, M. Bouvier, A. Christopoulos, O. Civelli, L.A. Devi, S.R. George, A. Inui, B.K. Kobilka, R. Leurs, R. Neubig, J.-P. Pin, R. Quirion, B.P. Roques, T.P. Sakmar, R. Seifert, R. Stenkamp, and P.G. Strange. (2004) "THE STATE OF GPCR RESEARCH IN 2004". *Nat Rev Drug Discov.* **3**: 577-626.

Bartl, F.J., E. Ritter, and K.P. Hofmann. (2001) "Signaling states of rhodopsin: absorption of light in active metarhodopsin II generates an all-trans-retinal bound inactive state". *J Biol Chem.* **276**: 30161-6.

Binder, B.M., T.M. O'Connor, M.D. Bownds, and V.Y. Arshavsky. (1996) "Phosphorylation of non-bleached rhodopsin in intact retinas and living frogs". *J Biol Chem.* **271**: 19826-30.

Blazynski, C., and S.E. Ostroy. (1984) "Pathways in the hydrolysis of vertebrate rhodopsin". *Vision Res.* **24**: 459-70.

Bockaert, J., and J.P. Pin. (1999) "Molecular tinkering of G protein-coupled receptors: an evolutionary success". *Embo J.* **18**: 1723-9.

Botelho, A.V., N.J. Gibson, R.L. Thurmond, Y. Wang, and M.F. Brown. (2002) "Conformational energetics of rhodopsin modulated by nonlamellar-forming lipids". *Biochemistry.* **41**: 6354-68.

Bownds, D., and G. Wald. (1965) "Reaction of the Rhodopsin Chromophore with Sodium Borohydride". *Nature.* **205**: 254-7.

Brannock, M.T., K. Weng, and P.R. Robinson. (1999) "Rhodopsin's carboxyl-terminal threonines are required for wild-type arrestin-mediated quench of transducin activation in vitro". *Biochemistry.* **38**: 3770-7.

Bridges, C.D., R.A. Alvarez, and S.L. Fong. (1982) "Vitamin A in human eyes: amount, distribution, and composition". *Invest Ophthalmol Vis Sci.* **22**: 706-14.

Bubis, J. (1998) "Effect of detergents and lipids on transducin photoactivation by rhodopsin". *Biol Res.* **31**: 59-71.

Buczylko, J., J.C. Saari, R.K. Crouch, and K. Palczewski. (1996) "Mechanisms of opsin activation". *J Biol Chem.* **271**: 20621-30.

Burns, M.E., and D.A. Baylor. (2001) "Activation, deactivation, and adaptation in vertebrate photoreceptor cells". *Annu Rev Neurosci.* **24**: 779-805.

Burns, M.E., and V.Y. Arshavsky. (2005) "Beyond counting photons: trials and trends in vertebrate visual transduction". *Neuron.* **48**: 387-401.

Burns, M.E., A. Mendez, C.K. Chen, A. Almuete, N. Quillinan, M.I. Simon, D.A. Baylor, and J. Chen. (2006) "Deactivation of phosphorylated and nonphosphorylated rhodopsin by arrestin splice variants". *J Neurosci.* **26**: 1036-44.

Cai, K., Y. Itoh, and H.G. Khorana. (2001) "Mapping of contact sites in complex formation between transducin and light-activated rhodopsin by covalent crosslinking: use of a photoactivatable reagent". *Proc Natl Acad Sci U S A.* **98**: 4877-82.

Carter, J.M., V.V. Gurevich, E.R. Prossnitz, and J.R. Engen. (2005) "Conformational differences between arrestin2 and pre-activated mutants as revealed by hydrogen exchange mass spectrometry". *J Mol Biol.* **351**: 865-78.

Celver, J., S.A. Vishnivetskiy, C. Chavkin, and V.V. Gurevich. (2002) "Conservation of the phosphate-sensitive elements in the arrestin family of proteins". *J Biol Chem.* **277**: 9043-8.

Cha, K., P.J. Reeves, and H.G. Khorana. (2000) "Structure and function in rhodopsin: destabilization of rhodopsin by the binding of an antibody at the N-terminal segment provides support for involvement of the latter in an intradiscal tertiary structure". *Proc Natl Acad Sci U S A.* **97**: 3016-21.

Chabre, M., and M. le Maire. (2005) "Monomeric G-protein-coupled receptor as a functional unit". *Biochemistry.* **44**: 9395-403.

Chen, J., M.I. Simon, M.T. Matthes, D. Yasumura, and M.M. LaVail. (1999) "Increased susceptibility to light damage in an arrestin knockout mouse model of Oguchi disease (stationary night blindness)". *Invest Ophthalmol Vis Sci.* **40**: 2978-82.

Chuang, J.Z., C. Vega, W. Jun, and C.H. Sung. (2004) "Structural and functional impairment of endocytic pathways by retinitis pigmentosa mutant rhodopsin-arrestin complexes". *J Clin Invest.* **114**: 131-40.

Claing, A., S.A. Laporte, M.G. Caron, and R.J. Lefkowitz. (2002) "Endocytosis of G protein-coupled receptors: roles of G protein-coupled receptor kinases and beta-arrestin proteins". *Prog Neurobiol.* **66**: 61-79.

Cohen, G.B., D.D. Oprian, and P.R. Robinson. (1992) "Mechanism of activation and inactivation of opsin: role of Glu113 and Lys296". *Biochemistry.* **31**: 12592-601.

Cone, R.A. (1972) "Rotational diffusion of rhodopsin in the visual receptor membrane". *Nat New Biol.* **236**: 39-43.

Cooper, A., M. Dixon, M. Nutley, and J. Robb. (1987) "Mechanism of Retinal Schiff Base Formation and Hydrolyisis in Relation to Visual Pigment Photolysis and Regeneration: Resonance Raman Spectroscopy of a Tetrahedral Carbinolamine

Intermediate and Oxygen-18 Labeling of Retinal at the Metarhodopsin Stage in Photoreceptor Membranes". *J Am Chem Soc.* **109**: 7254-7263.

Daemen, F.J. (1973) "Vertebrate rod outer segment membranes". *Biochim Biophys Acta.* **300**: 255-88.

DeGrip, W.L., and K.J. Rothschild. (2000) "Strcuture and Mechanism of vertebrate visual pigments" in *Molecular Mechanisms in Visual Transduction.* E.N. Pugh, Jr., editor. Elsevier, Amsterdam. 3-54.

Dillon, J., Z. Wang, L.B. Avalle, and E.R. Gaillard. (2004) "The photochemical oxidation of A2E results in the formation of a 5,8,5',8'-bis-furanoid oxide". *Exp Eye Res.* **79**: 537-42.

Dinculescu, A., J.H. McDowell, S.A. Amici, D.R. Dugger, N. Richards, P.A. Hargrave, and W.C. Smith. (2002) "Insertional mutagenesis and immunochemical analysis of visual arrestin interaction with rhodopsin". *J Biol Chem.* **277**: 11703-8.

Dizhoor, A.M. (2000) "Regulation of cGMP synthesis in photoreceptors: role in signal transduction and congenital diseases of the retina". *Cell Signal.* **12**: 711-9.

Dryja, T.P. (2000) "Molecular genetics of Oguchi disease, fundus albipunctatus, and other forms of stationary night blindness: LVII Edward Jackson Memorial Lecture". *Am J Ophthalmol.* **130**: 547-63.

Dunham, T.D., and D.L. Farrens. (1999) "Conformational changes in rhodopsin. Movement of helix f detected by site-specific chemical labeling and fluorescence spectroscopy". *J Biol Chem.* **274**: 1683-90.

Dupuy, C., X. Auvray, and C. Petipas. (1997) "Anomeric Effects on the Structure of Micelles of Alkyl Maltosides in Water". *Langmuir.* **13**: 3965.

Elias, R.V., S.S. Sezate, W. Cao, and J.F. McGinnis. (2004) "Temporal kinetics of the light/dark translocation and compartmentation of arrestin and alpha-transducin in mouse photoreceptor cells". *Mol Vis.* **10**: 672-81.

Emeis, D., and K.P. Hofmann. (1981) "Shift in the relation between flash-induced metarhodopsin I and metarhodpsin II within the first 10% rhodopsin bleaching in bovine disc membranes". *FEBS Lett.* **136**: 201-7.

Ernst, O.P., C.K. Meyer, E.P. Marin, P. Henklein, W.Y. Fu, T.P. Sakmar, and K.P. Hofmann. (2000) "Mutation of the fourth cytoplasmic loop of rhodopsin affects binding of transducin and peptides derived from the carboxyl-terminal sequences of transducin alpha and gamma subunits". *J Biol Chem.* **275**: 1937-43.

Farrens, D.L., and H.G. Khorana. (1995) "Structure and function in rhodopsin. Measurement of the rate of metarhodopsin II decay by fluorescence spectroscopy". *J Biol Chem.* **270**: 5073-6.

Farrens, D.L., C. Altenbach, K. Yang, W.L. Hubbell, and H.G. Khorana. (1996) "Requirement of rigid-body motion of transmembrane helices for light activation of rhodopsin". *Science.* **274**: 768-70.

Farrens, D.L. (1999) "Site-Directed Spin-Labeling (SDSL) Studies of the G Protein-coupled Receptor Rhodopsin" in *Structure-Function Analysis of G Protein-Coupled Receptors*. J. Wess, editor. Wiley-Liss, New York. 289-314.

Feller, S.E., K. Gawrisch, and T.B. Woolf. (2003) "Rhodopsin exhibits a preference for solvation by polyunsaturated docosohexaenoic acid". *J Am Chem Soc.* **125**: 4434-5.

Feller, S.E., and K. Gawrisch. (2005) "Properties of docosahexaenoic-acid-containing lipids and their influence on the function of rhodopsin". *Curr Opin Struct Biol.* **15**: 416-22.

Ferguson, S.S., and M.G. Caron. (1998) "G protein-coupled receptor adaptation mechanisms". *Semin Cell Dev Biol.* **9**: 119-27.

Filipek, S., R.E. Stenkamp, D.C. Teller, and K. Palczewski. (2003a) "G protein-coupled receptor rhodopsin: a prospectus". *Annu Rev Physiol.* **65**: 851-79.

Filipek, S., D.C. Teller, K. Palczewski, and R. Stenkamp. (2003b) "The crystallographic model of rhodopsin and its use in studies of other G protein-coupled receptors". *Annu Rev Biophys Biomol Struct.* **32**: 375-97.

Fisher, S.K., D.H. Anderson, P.A. Erickson, C.J. Guerin, G.P. Lewis, and K.A. Linberg. (1993) "Light and Electron Microscopy of Vertebrate Photoreceptors" in *Methods in Neurosciences: Photoreceptor Cells*. Vol. 15. P.A. Hargrave, editor. 3-36.

Fishkin, N., Y.P. Jang, Y. Itagaki, J.R. Sparrow, and K. Nakanishi. (2003) "A2-rhodopsin: a new fluorophore isolated from photoreceptor outer segments". *Org Biomol Chem.* **1**: 1101-5.

Fotiadis, D., Y. Liang, S. Filipek, D.A. Saperstein, A. Engel, and K. Palczewski. (2003) "Atomic-force microscopy: Rhodopsin dimers in native disc membranes". *Nature.* **421**: 127-8.

Francis, D.J., S.M. Hanson, V.V. Gurevich, W.L. Hubbell, and C.S. Klug. (2006). "Structural dynamics of visual arrestin upon binding rhodopsin". *in* the 50th Annual Biophysical Society Meeting, Salt Lake City, Utah.

Frank, R.N., H.D. Cavanagh, and K.R. Kenyon. (1973) "Light-stimulated phosphorylation of bovine visual pigments by adenosine triphosphate". *J Biol Chem.* **248**: 596-609.

Frazier, A.A., M.A. Wisner, N.J. Malmberg, K.G. Victor, G.E. Fanucci, E.A. Nalefski, J.J. Falke, and D.S. Cafiso. (2002) "Membrane orientation and position of the C2 domain from cPLA2 by site-directed spin labeling". *Biochemistry.* **41**: 6282-92.

Fredriksson, R., M.C. Lagerstrom, L.G. Lundin, and H.B. Schioth. (2003) "The G-protein-coupled receptors in the human genome form five main families. Phylogenetic analysis, paralogon groups, and fingerprints". *Mol Pharmacol.* **63**: 1256-72.

Fuchs, S., M. Nakazawa, M. Maw, M. Tamai, Y. Oguchi, and A. Gal. (1995) "A homozygous 1-base pair deletion in the arrestin gene is a frequent cause of Oguchi disease in Japanese". *Nat Genet.* **10**: 360-2.

Fukuda, M.N., D.S. Papermaster, and P.A. Hargrave. (1979) "Rhodopsin carbohydrate. Structure of small oligosaccharides attached at two sites near the NH2 terminus". *J Biol Chem.* **254**: 8201-7.

Gaidarov, I., J.G. Krupnick, J.R. Falck, J.L. Benovic, and J.H. Keen. (1999) "Arrestin function in G protein-coupled receptor endocytosis requires phosphoinositide binding". *Embo J.* **18**: 871-81.

Gether, U., and B.K. Kobilka. (1998) "G protein-coupled receptors. II. Mechanism of agonist activation". *J Biol Chem.* **273**: 17979-82.

Getmanova, E., A.B. Patel, J. Klein-Seetharaman, M.C. Loewen, P.J. Reeves, N. Friedman, M. Sheves, S.O. Smith, and H.G. Khorana. (2004) "NMR spectroscopy

of phosphorylated wild-type rhodopsin: mobility of the phosphorylated C-terminus of rhodopsin in the dark and upon light activation". *Biochemistry*. **43**: 1126-33.

Gibson, N.J., and M.F. Brown. (1993) "Lipid headgroup and acyl chain composition modulate the MI-MII equilibrium of rhodopsin in recombinant membranes". *Biochemistry*. **32**: 2438-54.

Gibson, S.K., J.H. Parkes, and P.A. Liebman. (2000) "Phosphorylation modulates the affinity of light-activated rhodopsin for G protein and arrestin". *Biochemistry*. **39**: 5738-49.

Giniger, R., D. Huppert, and E.M. Kosower. (1985) "Correlation of the Corrected Solvent Dielectric Relaxation Time with the Rate of Conformational Isomerization in Excited States of Syn-9,10-Dioxabimanes". *Chem Phys Letters*. **118**: 240-245.

Golobokova, E.Y., and V.I. Govardovskii. (2006) "Late stages of visual pigment photolysis in situ: Cones vs. rods". *Vision Res.*

Granit, R., T. Holmberg, and M. Zewi. (1938) "On the mode of action of visual purple on the rod cell". *J Physiol.* **94**: 430-440.

Granzin, J., U. Wilden, H.W. Choe, J. Labahn, B. Krafft, and G. Buldt. (1998) "X-ray crystal structure of arrestin from bovine rod outer segments". *Nature*. **391**: 918-21.

Gray-Keller, M.P., P.B. Detwiler, J.L. Benovic, and V.V. Gurevich. (1997) "Arrestin with a single amino acid substitution quenches light-activated rhodopsin in a phosphorylation-independent fashion". *Biochemistry*. **36**: 7058-63.

Grossfield, A., S.E. Feller, and M.C. Pitman. (2006) "A role for direct interactions in the modulation of rhodopsin by {omega}-3 polyunsaturated lipids". *Proc Natl Acad Sci U S A.*

Gurevich, V.V., and J.L. Benovic. (1992) "Cell-free expression of visual arrestin. Truncation mutagenesis identifies multiple domains involved in rhodopsin interaction". *J Biol Chem.* **267**: 21919-23.

Gurevich, V.V., and J.L. Benovic. (1993) "Visual arrestin interaction with rhodopsin. Sequential multisite binding ensures strict selectivity toward light-activated phosphorylated rhodopsin". *J Biol Chem.* **268**: 11628-38.

Gurevich, V.V., C.Y. Chen, C.M. Kim, and J.L. Benovic. (1994) "Visual arrestin binding to rhodopsin. Intramolecular interaction between the basic N terminus and acidic C terminus of arrestin may regulate binding selectivity". *J Biol Chem.* **269**: 8721-7.

Gurevich, V.V., and J.L. Benovic. (1995) "Visual arrestin binding to rhodopsin. Diverse functional roles of positively charged residues within the phosphorylation-recognition region of arrestin". *J Biol Chem.* **270**: 6010-6.

Gurevich, V.V., and J.L. Benovic. (1997) "Mechanism of phosphorylation-recognition by visual arrestin and the transition of arrestin into a high affinity binding state". *Mol Pharmacol.* **51**: 161-9.

Gurevich, V.V., R. Pals-Rylaarsdam, J.L. Benovic, M.M. Hosey, and J.J. Onorato. (1997) "Agonist-receptor-arrestin, an alternative ternary complex with high agonist affinity". *J Biol Chem.* **272**: 28849-52.

Gurevich, V.V. (1998) "The selectivity of visual arrestin for light-activated phosphorhodopsin is controlled by multiple nonredundant mechanisms". *J Biol Chem.* **273**: 15501-6.

Gurevich, V.V., and J.L. Benovic. (2000) "Arrestin: mutagenesis, expression, purification, and functional characterization". *Methods Enzymol.* **315**: 422-37.

Gurevich, V.V., and E.V. Gurevich. (2004) "The molecular acrobatics of arrestin activation". *Trends Pharmacol Sci.* **25**: 105-11.

Gurevich, V.V., and E.V. Gurevich. (2006) "The structural basis of arrestin-mediated regulation of G-protein-coupled receptors". *Pharmacol Ther.*

Hamm, H.E. (1998) "The many faces of G protein signaling". *J Biol Chem.* **273**: 669-72.

Hamm, H.E. (2001) "How activated receptors couple to G proteins". *Proc Natl Acad Sci U S A.* **98**: 4819-21.

Han, M., V.V. Gurevich, S.A. Vishnivetskiy, P.B. Sigler, and C. Schubert. (2001) "Crystal structure of beta-arrestin at 1.9 A: possible mechanism of receptor binding and membrane Translocation". *Structure.* **9**: 869-80.

Hanson, S.M., D.J. Francis, S.A. Vishnivetskiy, C.S. Klug, and V.V. Gurevich. (2006a) "Visual arrestin binding to microtubules involves a distinct conformational change". *J Biol Chem.* **in press**.

Hanson, S.M., D.J. Francis, S.A. Vishnivetskiy, E.A. Kolobova, W.L. Hubbell, C.S. Klug, and V.V. Gurevich. (2006b) "Differential interaction of spin-labeled arrestin with inactive and active phosphorhodopsin". *Proc Natl Acad Sci U S A.*

Hanson, S.M., and V.V. Gurevich. (2006) "The differential engagement of arrestin surface charges by the various functional forms of the receptor". *J Biol Chem.* **281**: 3458-62.

Hao, W., A. Wenzel, M.S. Obin, C.K. Chen, E. Brill, N.V. Krasnoperova, P. Eversole-Cire, Y. Kleyner, A. Taylor, M.I. Simon, C. Grimm, C.E. Reme, and J. Lem. (2002) "Evidence for two apoptotic pathways in light-induced retinal degeneration". *Nat Genet.* **32**: 254-60.

Heck, M., S.A. Schädel, D. Maretzki, F.J. Bartl, E. Ritter, K. Palczewski, and K.P. Hofmann. (2003a) "Signaling states of rhodopsin. Formation of the storage form, metarhodopsin III, from active metarhodopsin II". *J Biol Chem.* **278**: 3162-9.

Heck, M., S.A. Schädel, D. Maretzki, and K.P. Hofmann. (2003b) "Secondary binding sites of retinoids in opsin: characterization and role in regeneration". *Vision Res.* **43**: 3003-10.

Hessel, E., P. Muller, A. Herrmann, and K.P. Hofmann. (2001) "Light-induced reorganization of phospholipids in rod disc membranes". *J Biol Chem.* **276**: 2538-43.

Hessel, E., M. Heck, P. Muller, A. Herrmann, and K.P. Hofmann. (2003) "Signal transduction in the visual cascade involves specific lipid-protein interactions". *J Biol Chem.* **278**: 22853-60.

Hill, S.J. (2006) "G-protein-coupled receptors: past, present and future". *Br J Pharmacol.* **147 Suppl 1**: S27-37.

Hirsch, J.A., C. Schubert, V.V. Gurevich, and P.B. Sigler. (1999) "The 2.8 A crystal structure of visual arrestin: a model for arrestin's regulation". *Cell.* **97**: 257-69.

Hofmann, K.P., A. Pulvermüller, J. Buczylko, P. Van Hooser, and K. Palczewski. (1992) "The role of arrestin and retinoids in the regeneration pathway of rhodopsin". *J Biol Chem.* **267**: 15701-6.

Hsieh, C., S. Brown, C. Derleth, and K. Mackie. (1999) "Internalization and recycling of the CB1 cannabinoid receptor". *J Neurochem.* **73**: 493-501.

Hsu, Y.T., and R.S. Molday. (1994) "Interaction of calmodulin with the cyclic GMP-gated channel of rod photoreceptor cells. Modulation of activity, affinity purification, and localization". *J Biol Chem.* **269**: 29765-70.

Hubbell, W.L., D.S. Cafiso, and C. Altenbach. (2000) "Identifying conformational changes with site-directed spin labeling". *Nat Struct Biol.* **7**: 735-9.

Hubbell, W.L., C. Altenbach, C.M. Hubbell, and H.G. Khorana. (2003) "Rhodopsin structure, dynamics, and activation: a perspective from crystallography, site-directed spin labeling, sulfhydryl reactivity, and disulfide cross-linking". *Adv Protein Chem.* **63**: 243-90.

Huber, T., K.M. Gunnison, M.A. Kazmi, B.S.W. Chang, and T.P. Sakmar. (2006). "Closing the visual cycle - exit and entry of retinal in opsin". *in* the 50th Annual Biophysical Society Meeting, Salt Lake City, Utah.

Hurley, J.B., M. Spencer, and G.A. Niemi. (1998) "Rhodopsin phosphorylation and its role in photoreceptor function". *Vision Res.* **38**: 1341-52.

Imamoto, Y., C. Tamura, H. Kamikubo, and M. Kataoka. (2003) "Concentration-dependent tetramerization of bovine visual arrestin". *Biophys J.* **85**: 1186-95.

Imanishi, Y., M.L. Batten, D.W. Piston, W. Baehr, and K. Palczewski. (2004) "Noninvasive two-photon imaging reveals retinyl ester storage structures in the eye". *J Cell Biol.* **164**: 373-83.

Itoh, Y., K. Cai, and H.G. Khorana. (2001) "Mapping of contact sites in complex formation between light-activated rhodopsin and transducin by covalent crosslinking: use of a chemically preactivated reagent". *Proc Natl Acad Sci U S A.* **98**: 4883-7.

Jäger, S., K. Palczewski, and K.P. Hofmann. (1996) "Opsin/all-trans-retinal complex activates transducin by different mechanisms than photolyzed rhodopsin". *Biochemistry.* **35**: 2901-8.

Janz, J.M., J.F. Fay, and D.L. Farrens. (2003) "Stability of dark state rhodopsin is mediated by a conserved ion pair in intradiscal loop E-2". *J Biol Chem.* **278**: 16982-91.

Janz, J.M., and D.L. Farrens. (2004a) "Rhodopsin activation exposes a key hydrophobic binding site for the transducin alpha-subunit C terminus". *J Biol Chem.* **279**: 29767-73.

Janz, J.M., and D.L. Farrens. (2004b) "Role of the retinal hydrogen bond network in rhodopsin Schiff base stability and hydrolysis". *J Biol Chem.* **279**: 55886-94.

Jastrzebska, B., T. Maeda, L. Zhu, D. Fotiadis, S. Filipek, A. Engel, R.E. Stenkamp, and K. Palczewski. (2004) "Functional characterization of rhodopsin monomers and dimers in detergents". *J Biol Chem.* **279**: 54663-75.

Jin, S., M.C. Cornwall, and D.D. Oprian. (2003) "Opsin activation as a cause of congenital night blindness". *Nat Neurosci.* **6**: 731-5.

Karnik, S.S., C. Gogonea, S. Patil, Y. Saad, and T. Takezako. (2003) "Activation of G-protein-coupled receptors: a common molecular mechanism". *Trends Endocrinol Metab.* **14**: 431-7.

Kefalov, V., Y. Fu, N. Marsh-Armstrong, and K.W. Yau. (2003) "Role of visual pigment properties in rod and cone phototransduction". *Nature.* **425**: 526-31.

Kefalov, V.J., M.E. Estevez, M. Kono, P.W. Goletz, R.K. Crouch, M.C. Cornwall, and K.W. Yau. (2005) "Breaking the covalent bond--a pigment property that contributes to desensitization in cones". *Neuron.* **46**: 879-90.

Keith, D.E., B. Anton, S.R. Murray, P.A. Zaki, P.C. Chu, D.V. Lissin, G. Monteillet-Agius, P.L. Stewart, C.J. Evans, and M. von Zastrow. (1998) "mu-Opioid receptor internalization: opiate drugs have differential effects on a conserved endocytic mechanism in vitro and in the mammalian brain". *Mol Pharmacol.* **53**: 377-84.

Kennedy, M.J., K.A. Lee, G.A. Niemi, K.B. Craven, G.G. Garwin, J.C. Saari, and J.B. Hurley. (2001) "Multiple phosphorylation of rhodopsin and the in vivo chemistry underlying rod photoreceptor dark adaptation". *Neuron.* **31**: 87-101.

Kieffer, B.L., and C.J. Evans. (2002) "Opioid tolerance-in search of the holy grail". *Cell.* **108**: 587-90.

Kieselbach, T., K.D. Irrgang, and H. Ruppel. (1994) "A segment corresponding to amino acids Val170-Arg182 of bovine arrestin is capable of binding to phosphorylated rhodopsin". *Eur J Biochem.* **226**: 87-97.

Kim, Y.M., and J.L. Benovic. (2002) "Differential roles of arrestin-2 interaction with clathrin and adaptor protein 2 in G protein-coupled receptor trafficking". *J Biol Chem.* **277**: 30760-8.

Kiselev, A., and S. Subramaniam. (1996) "Modulation of arrestin release in the light-driven regeneration of Rh1 Drosophila rhodopsin". *Biochemistry*. **35**: 1848-55.

Kisselev, O.G., M.A. Downs, J.H. McDowell, and P.A. Hargrave. (2004a) "Conformational changes in the phosphorylated C-terminal domain of rhodopsin during rhodopsin arrestin interactions". *J Biol Chem*. **279**: 51203-7.

Kisselev, O.G., J.H. McDowell, and P.A. Hargrave. (2004b) "The arrestin-bound conformation and dynamics of the phosphorylated carboxy-terminal region of rhodopsin". *FEBS Lett*. **564**: 307-11.

Kisselev, O.G. (2005) "Focus on molecules: rhodopsin". *Exp Eye Res*. **81**: 366-7.

Kochendoerfer, G.G., S.W. Lin, T.P. Sakmar, and R.A. Mathies. (1999) "How color visual pigments are tuned". *Trends Biochem Sci*. **24**: 300-5.

Kolb, H., E. Fernandez, R. Nelson, and B.W. Jones. (2006). "Sagittal section of the adult human eye". http://webvision.med.utah.edu/imageswv/sagitta2.jpeg, editor.

Kolesnikov, A.V., E.Y. Golobokova, and V.I. Govardovskii. (2003) "The identity of metarhodopsin III". *Vis Neurosci*. **20**: 249-65.

Kosower, E.M., R. Giniger, A. Radkowsky, D. Hebel, and A. Shusterman. (1986) "Bimanes. 22. Flexible Fluorescent Molecules. Solvent Effects on the Photophysical Properties of syn-Bimanes". *J Phys Chem*. **90**: 5552-5557.

Kota, P., P.J. Reeves, U.L. Rajbhandary, and H.G. Khorana. (2006) "Opsin is present as dimers in COS1 cells: identification of amino acids at the dimeric interface". *Proc Natl Acad Sci U S A*. **103**: 3054-9.

Kragh-Hansen, U., M. le Maire, J.P. Noel, T. Gulik-Krzywicki, and J.V. Moller. (1993) "Transitional steps in the solubilization of protein-containing membranes and liposomes by nonionic detergent". *Biochemistry*. **32**: 1648-56.

Kragh-Hansen, U., M. le Maire, and J.V. Moller. (1998) "The mechanism of detergent solubilization of liposomes and protein-containing membranes". *Biophys J.* **75**: 2932-46.

Krishna, A.G., S.T. Menon, T.J. Terry, and T.P. Sakmar. (2002) "Evidence that helix 8 of rhodopsin acts as a membrane-dependent conformational switch". *Biochemistry*. **41**: 8298-309.

Krupnick, J.G., V.V. Gurevich, T. Schepers, H.E. Hamm, and J.L. Benovic. (1994) "Arrestin-rhodopsin interaction. Multi-site binding delineated by peptide inhibition". *J Biol Chem*. **269**: 3226-32.

Krupnick, J.G., O.B. Goodman, Jr., J.H. Keen, and J.L. Benovic. (1997) "Arrestin/clathrin interaction. Localization of the clathrin binding domain of nonvisual arrestins to the carboxy terminus". *J Biol Chem*. **272**: 15011-6.

Kühn, H., and W.J. Dreyer. (1972) "Light dependent phosphorylation of rhodopsin by ATP". *FEBS Lett*. **20**: 1-6.

Kühn, H. (1978) "Light-regulated binding of rhodopsin kinase and other proteins to cattle photoreceptor membranes". *Biochemistry*. **17**: 4389-95.

Kühn, H. (1982) "Light-regulated binding of proteins to photoreceptor membranes and its use for the purification of several rod cell proteins". *Methods Enzymol*. **81**: 556-64.

Kühn, H., and U. Wilden. (1982) "Assay of phosphorylation of rhodopsin in vitro and in vivo". *Methods Enzymol.* **81**: 489-96.

Kühn, H., S.W. Hall, and U. Wilden. (1984) "Light-induced binding of 48-kDa protein to photoreceptor membranes is highly enhanced by phosphorylation of rhodopsin". *FEBS Lett.* **176**: 473-8.

Kühne, W. (1879) "Chemische vorgänge in der netzhaut" in *Handbuch der Physiologie.* L. Hermann, editor. Vogel, Leipzig.

Lakowicz, J.R. (1999). *Principles of Fluorescence Spectroscopy.* Kluwer Academic, New York.

Lamb, T.D., and E.N. Pugh, Jr. (2004) "Dark adaptation and the retinoid cycle of vision". *Prog Retin Eye Res.* **23**: 307-80.

Langen, R., K. Cai, C. Altenbach, H.G. Khorana, and W.L. Hubbell. (1999) "Structural features of the C-terminal domain of bovine rhodopsin: a site-directed spin-labeling study". *Biochemistry.* **38**: 7918-24.

Langlois, G., C.K. Chen, K. Palczewski, J.B. Hurley, and T.M. Vuong. (1996) "Responses of the phototransduction cascade to dim light". *Proc Natl Acad Sci U S A.* **93**: 4677-82.

Laporte, S.A., R.H. Oakley, J.A. Holt, L.S. Barak, and M.G. Caron. (2000) "The interaction of beta-arrestin with the AP-2 adaptor is required for the clustering of beta 2-adrenergic receptor into clathrin-coated pits". *J Biol Chem.* **275**: 23120-6.

Lee, S.J., H. Xu, L.W. Kang, L.M. Amzel, and C. Montell. (2003) "Light adaptation through phosphoinositide-regulated translocation of Drosophila visual arrestin". *Neuron.* **39**: 121-32.

Lefkowitz, R.J., and S.K. Shenoy. (2005) "Transduction of receptor signals by beta-arrestins". *Science.* **308**: 512-7.

Leskov, I.B., V.A. Klenchin, J.W. Handy, G.G. Whitlock, V.I. Govardovskii, M.D. Bownds, T.D. Lamb, E.N. Pugh, Jr., and V.Y. Arshavsky. (2000) "The gain of rod phototransduction: reconciliation of biochemical and electrophysiological measurements". *Neuron.* **27**: 525-37.

Lewis, J.W., F.J. van Kuijk, J.A. Carruthers, and D.S. Kliger. (1997) "Metarhodopsin III formation and decay kinetics: comparison of bovine and human rhodopsin". *Vision Res.* **37**: 1-8.

Li, J., P.C. Edwards, M. Burghammer, C. Villa, and G.F. Schertler. (2004) "Structure of bovine rhodopsin in a trigonal crystal form". *J Mol Biol.* **343**: 1409-38.

Li, T., W.K. Franson, J.W. Gordon, E.L. Berson, and T.P. Dryja. (1995) "Constitutive activation of phototransduction by K296E opsin is not a cause of photoreceptor degeneration". *Proc Natl Acad Sci U S A.* **92**: 3551-5.

Liang, Y., D. Fotiadis, S. Filipek, D.A. Saperstein, K. Palczewski, and A. Engel. (2003) "Organization of the G protein-coupled receptors rhodopsin and opsin in native membranes". *J Biol Chem.* **278**: 21655-62.

Lichtenberg, D., E. Opatowski, and M.M. Kozlov. (2000) "Phase boundaries in mixtures of membrane-forming amphiphiles and micelle-forming amphiphiles". *Biochim Biophys Acta.* **1508**: 1-19.

Liebman, P.A., and G. Entine. (1974) "Lateral diffusion of visual pigment in photorecptor disk membranes". *Science.* **185**: 457-9.

Lin, S.W., and T.P. Sakmar. (1996) "Specific tryptophan UV-absorbance changes are probes of the transition of rhodopsin to its active state". *Biochemistry*. **35**: 11149-59.

Ling, Y., M. Ascano, P. Robinson, and S.K. Gregurick. (2004) "Experimental and computational studies of the desensitization process in the bovine rhodopsin-arrestin complex". *Biophys J*. **86**: 2445-54.

Litman, B.J., S.L. Niu, A. Polozova, and D.C. Mitchell. (2001) "The role of docosahexaenoic acid containing phospholipids in modulating G protein-coupled signaling pathways: visual transduction". *J Mol Neurosci*. **16**: 237-42; discussion 279-84.

Lodowski, D.T., J.A. Pitcher, W.D. Capel, R.J. Lefkowitz, and J.J. Tesmer. (2003) "Keeping G proteins at bay: a complex between G protein-coupled receptor kinase 2 and Gbetagamma". *Science*. **300**: 1256-62.

Lu, Z.L., J.W. Saldanha, and E.C. Hulme. (2002) "Seven-transmembrane receptors: crystals clarify". *Trends Pharmacol Sci*. **23**: 140-6.

Luttrell, L.M., and R.J. Lefkowitz. (2002) "The role of beta-arrestins in the termination and transduction of G-protein-coupled receptor signals". *J Cell Sci*. **115**: 455-65.

Maeda, T., Y. Imanishi, and K. Palczewski. (2003) "Rhodopsin phosphorylation: 30 years later". *Prog Retin Eye Res*. **22**: 417-34.

Mansoor, S.E., H.S. McHaourab, and D.L. Farrens. (1999) "Determination of protein secondary structure and solvent accessibility using site-directed fluorescence labeling. Studies of T4 lysozyme using the fluorescent probe monobromobimane". *Biochemistry*. **38**: 16383-93.

Mansoor, S.E., H.S. McHaourab, and D.L. Farrens. (2002) "Mapping proximity within proteins using fluorescence spectroscopy. A study of T4 lysozyme showing that tryptophan residues quench bimane fluorescence". *Biochemistry*. **41**: 2475-84.

Mansoor, S.E., and D.L. Farrens. (2004) "High-throughput protein structural analysis using site-directed fluorescence labeling and the bimane derivative (2-pyridyl)dithiobimane". *Biochemistry*. **43**: 9426-38.

Mansoor, S.E., K. Palczewski, and D.L. Farrens. (2006) "Rhodopsin self-associates in asolectin liposomes". *Proc Natl Acad Sci U S A*. **103**: 3060-5.

Marchese, A., C. Chen, Y.M. Kim, and J.L. Benovic. (2003) "The ins and outs of G protein-coupled receptor trafficking". *Trends Biochem Sci*. **28**: 369-76.

Marion, S., R.H. Oakley, K.M. Kim, M.G. Caron, and L.S. Barak. (2006) "A beta-arrestin binding determinant common to the second intracellular loops of rhodopsin family G protein-coupled receptors". *J Biol Chem*. **281**: 2932-8.

Marsh, D., and T. Pali. (2004) "The protein-lipid interface: perspectives from magnetic resonance and crystal structures". *Biochim Biophys Acta*. **1666**: 118-41.

Mata, N.L., R.A. Radu, R.C. Clemmons, and G.H. Travis. (2002) "Isomerization and oxidation of vitamin a in cone-dominant retinas: a novel pathway for visual-pigment regeneration in daylight". *Neuron*. **36**: 69-80.

Matthews, R.G., R. Hubbard, P.K. Brown, and G. Wald. (1963) "Tautomeric forms of metarhodopsin". *Journal of General Physiology*. **47**: 215-240.

McBee, J.K., K. Palczewski, W. Baehr, and D.R. Pepperberg. (2001) "Confronting complexity: the interlink of phototransduction and retinoid metabolism in the vertebrate retina". *Prog Retin Eye Res*. **20**: 469-529.

McDowell, J.H., J.P. Nawrocki, and P.A. Hargrave. (1993) "Phosphorylation sites in bovine rhodopsin". *Biochemistry*. **32**: 4968-74.

McDowell, J.H., W.C. Smith, R.L. Miller, M.P. Popp, A. Arendt, G. Abdulaeva, and P.A. Hargrave. (1999) "Sulfhydryl reactivity demonstrates different conformational states for arrestin, arrestin activated by a synthetic phosphopeptide, and constitutively active arrestin". *Biochemistry*. **38**: 6119-25.

Medina, R., D. Perdomo, and J. Bubis. (2004) "The hydrodynamic properties of dark- and light-activated states of n-dodecyl beta-D-maltoside-solubilized bovine rhodopsin support the dimeric structure of both conformations". *J Biol Chem*. **279**: 39565-73.

Melia, T.J., Jr., C.W. Cowan, J.K. Angleson, and T.G. Wensel. (1997) "A comparison of the efficiency of G protein activation by ligand-free and light-activated forms of rhodopsin". *Biophys J*. **73**: 3182-91.

Mendez, A., M.E. Burns, A. Roca, J. Lem, L.W. Wu, M.I. Simon, D.A. Baylor, and J. Chen. (2000) "Rapid and reproducible deactivation of rhodopsin requires multiple phosphorylation sites". *Neuron*. **28**: 153-64.

Menon, S.T., M. Han, and T.P. Sakmar. (2001) "Rhodopsin: structural basis of molecular physiology". *Physiol Rev*. **81**: 1659-88.

Milano, S.K., Y.M. Kim, F.P. Stefano, J.L. Benovic, and C. Brenner. (2006) "Nonvisual arrestin oligomerization and cellular localization are regulated by inositol hexakisphosphate binding". *J Biol Chem*.

Mitchell, D.C., M. Straume, and B.J. Litman. (1992) "Role of sn-1-saturated,sn-2-polyunsaturated phospholipids in control of membrane receptor conformational

equilibrium: effects of cholesterol and acyl chain unsaturation on the metarhodopsin I in equilibrium with metarhodopsin II equilibrium". *Biochemistry.* **31**: 662-70.

Mitchell, D.C., S.L. Niu, and B.J. Litman. (2001) "Optimization of receptor-G protein coupling by bilayer lipid composition I: kinetics of rhodopsin-transducin binding". *J Biol Chem.* **276**: 42801-6.

Mitchell, D.C., S.L. Niu, and B.J. Litman. (2003) "Enhancement of G protein-coupled signaling by DHA phospholipids". *Lipids.* **38**: 437-43.

Moiseyev, G., Y. Chen, Y. Takahashi, B.X. Wu, and J.X. Ma. (2005) "RPE65 is the isomerohydrolase in the retinoid visual cycle". *Proc Natl Acad Sci U S A.* **102**: 12413-8.

Molday, R.S. (1998) "Photoreceptor membrane proteins, phototransduction, and retinal degenerative diseases. The Friedenwald Lecture". *Invest Ophthalmol Vis Sci.* **39**: 2491-513.

Nair, K.S., S.M. Hanson, M.J. Kennedy, J.B. Hurley, V.V. Gurevich, and V.Z. Slepak. (2004) "Direct Binding of Visual Arrestin to Microtubules Determines the Differential Subcellular Localization of Its Splice Variants in Rod Photoreceptors". *J Biol Chem.* **279**: 41240-41248.

Nair, K.S., S.M. Hanson, A. Mendez, E.V. Gurevich, M.J. Kennedy, V.I. Shestopalov, S.A. Vishnivetskiy, J. Chen, J.B. Hurley, V.V. Gurevich, and V.Z. Slepak. (2005) "Light-dependent redistribution of arrestin in vertebrate rods is an energy-independent process governed by protein-protein interactions". *Neuron.* **46**: 555-67.

Nathans, J. (1992) "Rhodopsin: structure, function, and genetics". *Biochemistry*. **31**: 4923-31.

Neyroz, P., C. Menna, E. Polverini, and L. Masotti. (1996) "Intrinsic fluorescence properties and structural analysis of p13(suc1) from Schizosaccharomyces pombe". *J Biol Chem*. **271**: 27249-58.

Niu, L., J.M. Kim, and H.G. Khorana. (2002) "Structure and function in rhodopsin: asymmetric reconstitution of rhodopsin in liposomes". *Proc Natl Acad Sci U S A*. **99**: 13409-12.

Niu, S.L., D.C. Mitchell, and B.J. Litman. (2001) "Optimization of receptor-G protein coupling by bilayer lipid composition II: formation of metarhodopsin II-transducin complex". *J Biol Chem*. **276**: 42807-11.

Oakley, R.H., S.A. Laporte, J.A. Holt, M.G. Caron, and L.S. Barak. (2000) "Differential affinities of visual arrestin, beta arrestin1, and beta arrestin2 for G protein-coupled receptors delineate two major classes of receptors". *J Biol Chem*. **275**: 17201-10.

Ohguro, H., K. Palczewski, L.H. Ericsson, K.A. Walsh, and R.S. Johnson. (1993) "Sequential phosphorylation of rhodopsin at multiple sites". *Biochemistry*. **32**: 5718-24.

Ohguro, H., R.S. Johnson, L.H. Ericsson, K.A. Walsh, and K. Palczewski. (1994a) "Control of rhodopsin multiple phosphorylation". *Biochemistry*. **33**: 1023-8.

Ohguro, H., K. Palczewski, K.A. Walsh, and R.S. Johnson. (1994b) "Topographic study of arrestin using differential chemical modifications and hydrogen/deuterium exchange". *Protein Sci*. **3**: 2428-34.

Ohguro, H., J.P. Van Hooser, A.H. Milam, and K. Palczewski. (1995) "Rhodopsin phosphorylation and dephosphorylation in vivo". *J Biol Chem.* **270**: 14259-62.

Okada, T., O.P. Ernst, K. Palczewski, and K.P. Hofmann. (2001) "Activation of rhodopsin: new insights from structural and biochemical studies". *Trends Biochem Sci.* **26**: 318-24.

Okada, T., M. Sugihara, A.N. Bondar, M. Elstner, P. Entel, and V. Buss. (2004) "The retinal conformation and its environment in rhodopsin in light of a new 2.2 A crystal structure". *J Mol Biol.* **342**: 571-83.

Palczewski, K., P.A. Hargrave, J.H. McDowell, and T.S. Ingebritsen. (1989a) "The catalytic subunit of phosphatase 2A dephosphorylates phosphoopsin". *Biochemistry.* **28**: 415-9.

Palczewski, K., J.H. McDowell, S. Jakes, T.S. Ingebritsen, and P.A. Hargrave. (1989b) "Regulation of rhodopsin dephosphorylation by arrestin". *J Biol Chem.* **264**: 15770-3.

Palczewski, K., J. Buczylko, N.R. Imami, J.H. McDowell, and P.A. Hargrave. (1991a) "Role of the carboxyl-terminal region of arrestin in binding to phosphorylated rhodopsin". *J Biol Chem.* **266**: 15334-9.

Palczewski, K., A. Pulvermüller, J. Buczylko, and K.P. Hofmann. (1991b) "Phosphorylated rhodopsin and heparin induce similar conformational changes in arrestin". *J Biol Chem.* **266**: 18649-54.

Palczewski, K., J.H. Riazance-Lawrence, and W.C. Johnson, Jr. (1992) "Structural properties of arrestin studied by chemical modification and circular dichroism". *Biochemistry.* **31**: 3902-6.

Palczewski, K., J. Buczylko, H. Ohguro, R.S. Annan, S.A. Carr, J.W. Crabb, M.W. Kaplan, R.S. Johnson, and K.A. Walsh. (1994a) "Characterization of a truncated form of arrestin isolated from bovine rod outer segments". *Protein Sci.* **3**: 314-24.

Palczewski, K., S. Jäger, J. Buczylko, R.K. Crouch, D.L. Bredberg, K.P. Hofmann, M.A. Asson-Batres, and J.C. Saari. (1994b) "Rod outer segment retinol dehydrogenase: substrate specificity and role in phototransduction". *Biochemistry.* **33**: 13741-50.

Palczewski, K., and J.C. Saari. (1997) "Activation and inactivation steps in the visual transduction pathway". *Curr Opin Neurobiol.* **7**: 500-4.

Palczewski, K., J.P. Van Hooser, G.G. Garwin, J. Chen, G.I. Liou, and J.C. Saari. (1999) "Kinetics of visual pigment regeneration in excised mouse eyes and in mice with a targeted disruption of the gene encoding interphotoreceptor retinoid-binding protein or arrestin". *Biochemistry.* **38**: 12012-9.

Palczewski, K., T. Kumasaka, T. Hori, C.A. Behnke, H. Motoshima, B.A. Fox, I. Le Trong, D.C. Teller, T. Okada, R.E. Stenkamp, M. Yamamoto, and M. Miyano. (2000) "Crystal structure of rhodopsin: A G protein-coupled receptor". *Science.* **289**: 739-45.

Papac, D.I., J.E. Oatis, Jr., R.K. Crouch, and D.R. Knapp. (1993) "Mass spectrometric identification of phosphorylation sites in bleached bovine rhodopsin". *Biochemistry.* **32**: 5930-4.

Papermaster, D.S. (1982) "Preparation of retinal rod outer segments". *Methods Enzymol.* **81**: 48-52.

Park, P.S., S. Filipek, J.W. Wells, and K. Palczewski. (2004) "Oligomerization of G protein-coupled receptors: past, present, and future". *Biochemistry.* **43**: 15643-56.

Parkes, J.H., S.K. Gibson, and P.A. Liebman. (1999) "Temperature and pH dependence of the metarhodopsin I-metarhodopsin II equilibrium and the binding of metarhodopsin II to G protein in rod disk membranes". *Biochemistry*. **38**: 8598.

Pepe, I.M. (2001) "Recent advances in our understanding of rhodopsin and phototransduction". *Prog Retin Eye Res*. **20**: 733-59.

Perry, S.J., and R.J. Lefkowitz. (2002) "Arresting developments in heptahelical receptor signaling and regulation". *Trends Cell Biol*. **12**: 130-8.

Peterson, J.J., B.M. Tam, O.L. Moritz, C.L. Shelamer, D.R. Dugger, J.H. McDowell, P.A. Hargrave, D.S. Papermaster, and W.C. Smith. (2003) "Arrestin migrates in photoreceptors in response to light: a study of arrestin localization using an arrestin-GFP fusion protein in transgenic frogs". *Exp Eye Res*. **76**: 553-63.

Pierce, K.L., and R.J. Lefkowitz. (2001) "Classical and new roles of beta-arrestins in the regulation of G-protein-coupled receptors". *Nat Rev Neurosci*. **2**: 727-33.

Pierce, K.L., R.T. Premont, and R.J. Lefkowitz. (2002) "Seven-transmembrane receptors". *Nat Rev Mol Cell Biol*. **3**: 639-50.

Pitman, M.C., A. Grossfield, F. Suits, and S.E. Feller. (2005) "Role of cholesterol and polyunsaturated chains in lipid-protein interactions: molecular dynamics simulation of rhodopsin in a realistic membrane environment". *J Am Chem Soc*. **127**: 4576-7.

Polans, A., W. Baehr, and K. Palczewski. (1996) "Turned on by Ca2+! The physiology and pathology of Ca(2+)-binding proteins in the retina". *Trends Neurosci*. **19**: 547-54.

Polozova, A., and B.J. Litman. (2000) "Cholesterol dependent recruitment of di22:6-PC by a G protein-coupled receptor into lateral domains". *Biophys J.* **79**: 2632-43.

Poo, M., and R.A. Cone. (1974) "Lateral diffusion of rhodopsin in the photoreceptor membrane". *Nature.* **247**: 438-41.

Puig, J., A. Arendt, F.L. Tomson, G. Abdulaeva, R. Miller, P.A. Hargrave, and J.H. McDowell. (1995) "Synthetic phosphopeptide from rhodopsin sequence induces retinal arrestin binding to photoactivated unphosphorylated rhodopsin". *FEBS Lett.* **362**: 185-8.

Pulvermüller, A., K. Palczewski, and K.P. Hofmann. (1993) "Interaction between photoactivated rhodopsin and its kinase: stability and kinetics of complex formation". *Biochemistry.* **32**: 14082-8.

Pulvermüller, A., D. Maretzki, M. Rudnicka-Nawrot, W.C. Smith, K. Palczewski, and K.P. Hofmann. (1997) "Functional differences in the interaction of arrestin and its splice variant, p44, with rhodopsin". *Biochemistry.* **36**: 9253-60.

Pulvermüller, A., K. Schröder, T. Fischer, and K.P. Hofmann. (2000) "Interactions of metarhodopsin II. Arrestin peptides compete with arrestin and transducin". *J Biol Chem.* **275**: 37679-85.

Radu, R.A., N.L. Mata, A. Bagla, and G.H. Travis. (2004) "Light exposure stimulates formation of A2E oxiranes in a mouse model of Stargardt's macular degeneration". *Proc Natl Acad Sci U S A.* **101**: 5928-33.

Raman, D., S. Osawa, and E.R. Weiss. (1999) "Binding of arrestin to cytoplasmic loop mutants of bovine rhodopsin". *Biochemistry.* **38**: 5117-23.

Raman, D., S. Osawa, V.V. Gurevich, and E.R. Weiss. (2003) "The interaction with the cytoplasmic loops of rhodopsin plays a crucial role in arrestin activation and binding". *J Neurochem.* **84**: 1040-50.

Rando, R.R. (1996) "Polyenes and vision". *Chem Biol.* **3**: 255-62.

Rattner, A., H. Sun, and J. Nathans. (1999) "Molecular genetics of human retinal disease". *Annu Rev Genet.* **33**: 89-131.

Reeves, P.J., J. Hwa, and H.G. Khorana. (1999) "Structure and function in rhodopsin: kinetic studies of retinal binding to purified opsin mutants in defined phospholipid-detergent mixtures serve as probes of the retinal binding pocket". *Proc Natl Acad Sci U S A.* **96**: 1927-31.

Reme, C.E. (2005) "The dark side of light: rhodopsin and the silent death of vision the proctor lecture". *Invest Ophthalmol Vis Sci.* **46**: 2672-82.

Resek, J.F., Z.T. Farahbakhsh, W.L. Hubbell, and H.G. Khorana. (1993) "Formation of the meta II photointermediate is accompanied by conformational changes in the cytoplasmic surface of rhodopsin". *Biochemistry.* **32**: 12025-32.

Ridge, K.D., N.G. Abdulaev, M. Sousa, and K. Palczewski. (2003) "Phototransduction: crystal clear". *Trends Biochem Sci.* **28**: 479-87.

Rieke, F., and D.A. Baylor. (1998) "Origin of reproducibility in the responses of retinal rods to single photons". *Biophys J.* **75**: 1836-57.

Rim, J., and D.D. Oprian. (1995) "Constitutive activation of opsin: interaction of mutants with rhodopsin kinase and arrestin". *Biochemistry.* **34**: 11938-45.

Ritter, E., K. Zimmermann, M. Heck, K.P. Hofmann, and F.J. Bartl. (2004) "Transition of rhodopsin into the active metarhodopsin II state opens a new light-induced pathway linked to Schiff base isomerization". *J Biol Chem.* **279**: 48102-11.

Ross, J.B., H.R. Wyssbrod, R.A. Porter, G.P. Schwartz, C.A. Michaels, and W.R. Laws. (1992) "Correlation of tryptophan fluorescence intensity decay parameters with 1H NMR-determined rotamer conformations: [tryptophan2]oxytocin". *Biochemistry.* **31**: 1585-94.

Ruprecht, J.J., T. Mielke, R. Vogel, C. Villa, and G.F. Schertler. (2004) "Electron crystallography reveals the structure of metarhodopsin I". *Embo J.* **23**: 3609-20.

Saari, J.C., G.G. Garwin, J.P. Van Hooser, and K. Palczewski. (1998) "Reduction of all-trans-retinal limits regeneration of visual pigment in mice". *Vision Res.* **38**: 1325-33.

Saari, J.C. (2000) "Biochemistry of visual pigment regeneration: the Friedenwald lecture". *Invest Ophthalmol Vis Sci.* **41**: 337-48.

Sachs, K., D. Maretzki, and K.P. Hofmann. (2000a) "Assays for activation of opsin by all-trans-retinal". *Methods Enzymol.* **315**: 238-51.

Sachs, K., D. Maretzki, C.K. Meyer, and K.P. Hofmann. (2000b) "Diffusible ligand all-trans-retinal activates opsin via a palmitoylation-dependent mechanism". *J Biol Chem.* **275**: 6189-94.

Salem, N., Jr., B. Litman, H.Y. Kim, and K. Gawrisch. (2001) "Mechanisms of action of docosahexaenoic acid in the nervous system". *Lipids.* **36**: 945-59.

Sallese, M., L. Iacovelli, A. Cumashi, L. Capobianco, L. Cuomo, and A. De Blasi. (2000) "Regulation of G protein-coupled receptor kinase subtypes by calcium sensor proteins". *Biochim Biophys Acta.* **1498**: 112-21.

Sato, E., M. Sakashita, Y. Kanaoka, and E.M. Kosower. (1988) "Organic Fluorescent Reagents". *Bioorg. Chem.* **16**: 298-306.

Schädel, S.A., M. Heck, D. Maretzki, S. Filipek, D.C. Teller, K. Palczewski, and K.P. Hofmann. (2003) "Ligand channeling within a G-protein-coupled receptor. The entry and exit of retinals in native opsin". *J Biol Chem.* **278**: 24896-903.

Schertler, G.F. (2005) "Structure of rhodopsin and the metarhodopsin I photointermediate". *Curr Opin Struct Biol.* **15**: 408-15.

Schleicher, A., H. Kühn, and K.P. Hofmann. (1989) "Kinetics, binding constant, and activation energy of the 48-kDa protein-rhodopsin complex by extra-metarhodopsin II". *Biochemistry.* **28**: 1770-5.

Schröder, K., A. Pulvermüller, and K.P. Hofmann. (2002) "Arrestin and its splice variant Arr1-370A (p44). Mechanism and biological role of their interaction with rhodopsin". *J Biol Chem.* **277**: 43987-96.

Schubert, C., J.A. Hirsch, V.V. Gurevich, D.M. Engelman, P.B. Sigler, and K.G. Fleming. (1999) "Visual arrestin activity may be regulated by self-association". *J Biol Chem.* **274**: 21186-90.

Seddon, A.M., P. Curnow, and P.J. Booth. (2004) "Membrane proteins, lipids and detergents: not just a soap opera". *Biochim Biophys Acta.* **1666**: 105-17.

Shi, G.W., J. Chen, F. Concepcion, K. Motamedchaboki, P. Marjoram, and R. Langen. (2005) "Light causes phosphorylation of nonactivated visual pigments in intact mouse rod photoreceptor cells". *J Biol Chem.* **280**: 41184-91.

Shi, W., C.D. Sports, D. Raman, S. Shirakawa, S. Osawa, and E.R. Weiss. (1998) "Rhodopsin arginine-135 mutants are phosphorylated by rhodopsin kinase and bind arrestin in the absence of 11-cis-retinal". *Biochemistry.* **37**: 4869-74.

Shichi, H., and R.L. Somers. (1978) "Light-dependent phosphorylation of rhodopsin. Purification and properties of rhodopsin kinase". *J Biol Chem.* **253**: 7040-6.

Shilton, B.H., J.H. McDowell, W.C. Smith, and P.A. Hargrave. (2002) "The solution structure and activation of visual arrestin studied by small-angle X-ray scattering". *Eur J Biochem.* **269**: 3801-9.

Slep, K.C., M.A. Kercher, W. He, C.W. Cowan, T.G. Wensel, and P.B. Sigler. (2001) "Structural determinants for regulation of phosphodiesterase by a G protein at 2.0 A". *Nature.* **409**: 1071-7.

Smith, W.C., A.H. Milam, D. Dugger, A. Arendt, P.A. Hargrave, and K. Palczewski. (1994) "A splice variant of arrestin. Molecular cloning and localization in bovine retina". *J Biol Chem.* **269**: 15407-10.

Smith, W.C., J.H. McDowell, D.R. Dugger, R. Miller, A. Arendt, M.P. Popp, and P.A. Hargrave. (1999) "Identification of regions of arrestin that bind to rhodopsin". *Biochemistry.* **38**: 2752-61.

Smith, W.C., A. Dinculescu, J.J. Peterson, and J.H. McDowell. (2004) "The surface of visual arrestin that binds to rhodopsin". *Mol Vis.* **10**: 392-8.

Sommer, M.E., W.C. Smith, and D.L. Farrens. (2005) "Dynamics of arrestin-rhodopsin interactions: arrestin and retinal release are directly linked events". *J Biol Chem.* **280**: 6861-71.

Sommer, M.E., W.C. Smith, and D.L. Farrens. (2006) "Dynamics of arrestin-rhodopsin interactions: acidic phospholipids enable binding of arrestin to purified rhodopsin in detergent". *J Biol Chem.* **281**: 9407-9417.

Sparrow, J.R., N. Fishkin, J. Zhou, B. Cai, Y.P. Jang, S. Krane, Y. Itagaki, and K. Nakanishi. (2003) "A2E, a byproduct of the visual cycle". *Vision Res.* **43**: 2983-90.

Stenkamp, R.E., S. Filipek, C.A. Driessen, D.C. Teller, and K. Palczewski. (2002) "Crystal structure of rhodopsin: a template for cone visual pigments and other G protein-coupled receptors". *Biochim Biophys Acta.* **1565**: 168-82.

Stone, W.L., C.C. Farnsworth, and E.A. Dratz. (1979) "A reinvestigation of the fatty acid content of bovine, rat and frog retinal rod outer segments". *Exp Eye Res.* **28**: 387-97.

Straume, M., and M.L. Johnson. (1992) "Analysis of residuals: criteria for determining goodness-of-fit". *Methods Enzymol.* **210**: 87-105.

Strissel, K.J., M. Sokolov, L.H. Trieu, and V.Y. Arshavsky. (2006) "Arrestin translocation is induced at a critical threshold of visual signaling and is superstoichiometric to bleached rhodopsin". *J Neurosci.* **26**: 1146-53.

Stryer, L. (1988) "Molecular basis of visual excitation". *Cold Spring Harb Symp Quant Biol.* **53 Pt 1**: 283-94.

Sun, H., R.S. Molday, and J. Nathans. (1999) "Retinal stimulates ATP hydrolysis by purified and reconstituted ABCR, the photoreceptor-specific ATP-binding cassette transporter responsible for Stargardt disease". *J Biol Chem.* **274**: 8269-81.

Sutton, R.B., S.A. Vishnivetskiy, J. Robert, S.M. Hanson, D. Raman, B.E. Knox, M. Kono, J. Navarro, and V.V. Gurevich. (2005) "Crystal structure of cone arrestin at 2.3A: evolution of receptor specificity". *J Mol Biol.* **354**: 1069-80.

Teller, D.C., T. Okada, C.A. Behnke, K. Palczewski, and R.E. Stenkamp. (2001) "Advances in determination of a high-resolution three-dimensional structure of rhodopsin, a model of G-protein-coupled receptors (GPCRs)". *Biochemistry.* **40**: 7761-72.

Teller, D.C., R.E. Stenkamp, and K. Palczewski. (2003) "Evolutionary analysis of rhodopsin and cone pigments: connecting the three-dimensional structure with spectral tuning and signal transfer". *FEBS Lett.* **555**: 151-9.

Tsao, P., T. Cao, and M. von Zastrow. (2001) "Role of endocytosis in mediating downregulation of G-protein-coupled receptors". *Trends Pharmacol Sci.* **22**: 91-6.

Vishnivetskiy, S.A., C.L. Paz, C. Schubert, J.A. Hirsch, P.B. Sigler, and V.V. Gurevich. (1999) "How does arrestin respond to the phosphorylated state of rhodopsin?" *J Biol Chem.* **274**: 11451-4.

Vishnivetskiy, S.A., C. Schubert, G.C. Climaco, Y.V. Gurevich, M.G. Velez, and V.V. Gurevich. (2000) "An additional phosphate-binding element in arrestin molecule. Implications for the mechanism of arrestin activation". *J Biol Chem.* **275**: 41049-57.

Vishnivetskiy, S.A., J.A. Hirsch, M.G. Velez, Y.V. Gurevich, and V.V. Gurevich. (2002) "Transition of arrestin into the active receptor-binding state requires an extended interdomain hinge". *J Biol Chem.* **277**: 43961-7.

Vishnivetskiy, S.A., M.M. Hosey, J.L. Benovic, and V.V. Gurevich. (2004) "Mapping the arrestin-receptor interface. Structural elements responsible for receptor specificity of arrestin proteins". *J Biol Chem.* **279**: 1262-8.

Vogel, R., F. Siebert, G. Mathias, P. Tavan, G. Fan, and M. Sheves. (2003) "Deactivation of rhodopsin in the transition from the signaling state meta II to meta III involves a thermal isomerization of the retinal chromophore C[double bond]D". *Biochemistry.* **42**: 9863-74.

Vogel, R., S. Ludeke, I. Radu, F. Siebert, and M. Sheves. (2004a) "Photoreactions of metarhodopsin III". *Biochemistry.* **43**: 10255-64.

Vogel, R., F. Siebert, X.Y. Zhang, G. Fan, and M. Sheves. (2004b) "Formation of Meta III during the decay of activated rhodopsin proceeds via Meta I and not via Meta II". *Biochemistry.* **43**: 9457-66.

Wald, G. (1951) "The chemistry of rod vision". *Science.* **113**: 287-91.

Wald, G. (1968) "Molecular basis of visual excitation". *Science.* **162**: 230-9.

Wang, Y., A.V. Botelho, G.V. Martinez, and M.F. Brown. (2002) "Electrostatic properties of membrane lipids coupled to metarhodopsin II formation in visual transduction". *J Am Chem Soc.* **124**: 7690-701.

Weng, J., N.L. Mata, S.M. Azarian, R.T. Tzekov, D.G. Birch, and G.H. Travis. (1999) "Insights into the function of Rim protein in photoreceptors and etiology of Stargardt's disease from the phenotype in abcr knockout mice". *Cell.* **98**: 13-23.

Wenzel, A., C. Grimm, M. Samardzija, and C.E. Reme. (2005) "Molecular mechanisms of light-induced photoreceptor apoptosis and neuroprotection for retinal degeneration". *Prog Retin Eye Res.* **24**: 275-306.

Wess, J. (1997) "G-protein-coupled receptors: molecular mechanisms involved in receptor activation and selectivity of G-protein recognition". *Faseb J.* **11**: 346-54.

Wettschureck, N., and S. Offermanns. (2005) "Mammalian G proteins and their cell type specific functions". *Physiol Rev.* **85**: 1159-204.

Wey, C.L., R.A. Cone, and M.A. Edidin. (1981) "Lateral diffusion of rhodopsin in photoreceptor cells measured by fluorescence photobleaching and recovery". *Biophys J.* **33**: 225-32.

Whelan, J.P., and J.F. McGinnis. (1988) "Light-dependent subcellular movement of photoreceptor proteins". *J Neurosci Res.* **20**: 263-70.

Wilden, U., S.W. Hall, and H. Kühn. (1986) "Phosphodiesterase activation by photoexcited rhodopsin is quenched when rhodopsin is phosphorylated and binds the intrinsic 48-kDa protein of rod outer segments". *Proc Natl Acad Sci U S A.* **83**: 1174-8.

Wilden, U. (1995) "Duration and amplitude of the light-induced cGMP hydrolysis in vertebrate photoreceptors are regulated by multiple phosphorylation of rhodopsin and by arrestin binding". *Biochemistry.* **34**: 1446-54.

Wilson, C.J., and R.A. Copeland. (1997) "Spectroscopic characterization of arrestin interactions with competitive ligands: study of heparin and phytic acid binding". *J Protein Chem.* **16**: 755-63.

Wise, A., S.C. Jupe, and S. Rees. (2004) "The identification of ligands at orphan G-protein coupled receptors". *Annu Rev Pharmacol Toxicol.* **44**: 43-66.

Xiao, K., S.K. Shenoy, K. Nobles, and R.J. Lefkowitz. (2004) "Activation-dependent conformational changes in {beta}-arrestin 2". *J Biol Chem.* **279**: 55744-53.

Xu, J., R.L. Dodd, C.L. Makino, M.I. Simon, D.A. Baylor, and J. Chen. (1997) "Prolonged photoresponses in transgenic mouse rods lacking arrestin". *Nature.* **389**: 505-9.

Yan, E.C., M.A. Kazmi, S. De, B.S. Chang, C. Seibert, E.P. Marin, R.A. Mathies, and T.P. Sakmar. (2002) "Function of extracellular loop 2 in rhodopsin: glutamic acid 181 modulates stability and absorption wavelength of metarhodopsin II". *Biochemistry.* **41**: 3620-7.

Yan, E.C., M.A. Kazmi, Z. Ganim, J.M. Hou, D. Pan, B.S. Chang, T.P. Sakmar, and R.A. Mathies. (2003) "Retinal counterion switch in the photoactivation of the G protein-coupled receptor rhodopsin". *Proc Natl Acad Sci U S A.* **100**: 9262-7.

Zawadzki, K.M., C.P. Pan, M.D. Barkley, D. Johnson, and S.S. Taylor. (2003) "Endogenous tryptophan residues of cAPK regulatory subunit type IIbeta reveal local variations in environments and dynamics". *Proteins.* **51**: 552-61.

Zhang, L., C.D. Sports, S. Osawa, and E.R. Weiss. (1997) "Rhodopsin phosphorylation sites and their role in arrestin binding". *J Biol Chem.* **272**: 14762-8.

Zhu, X., A. Li, B. Brown, E.R. Weiss, S. Osawa, and C.M. Craft. (2002) "Mouse cone arrestin expression pattern: light induced translocation in cone photoreceptors". *Mol Vis.* **8**: 462-71.

Zhu, X., B. Brown, A. Li, A.J. Mears, A. Swaroop, and C.M. Craft. (2003) "GRK1-dependent phosphorylation of S and M opsins and their binding to cone arrestin during cone phototransduction in the mouse retina". *J Neurosci.* **23**: 6152-60.

Zimmermann, K., E. Ritter, F.J. Bartl, K.P. Hofmann, and M. Heck. (2004) "Interaction with transducin depletes metarhodopsin III: a regulated retinal storage in visual signal transduction?" *J Biol Chem.* **279**: 48112-9.

Appendix 1

Dynamics of p44 - Rhodopsin Interactions

Martha E. Sommer [‡], W. Clay Smith [§], and David L. Farrens [‡]

[‡] Department of Biochemistry and Molecular Biology, Oregon Health & Science University, Portland, OR 97239-3098, USA

[§] Departments of Ophthalmology and Neuroscience, University of Florida, Gainesville, FL 32610-0284, USA

A1. 1 SUMMARY

This appendix reports preliminary characterization of the arrestin splice variant p44, using a p44 mutant fluorescently labeled with monobromobimane at I72C (p44/I72B). As reported in earlier literature, p44 shows constitutive activity, in that it binds dark-state phosphorylated rhodopsin (Rho-P). The results presented here show that p44/I72B bound to dark-state Rho-P exhibits quenched fluorescence, which may be due to energy transfer from the bimane probe to the 11-*cis* retinal chromophore. Upon light-activation, the energy transfer is relieved and the fluorescence of p44/I72B increases and blue-shifts in intensity as observed for arrestin I72B. Importantly, the mobility and solvent accessibility of the bimane probe on p44/I72B suggest that p44 does not bind Rho-P in the same way as Rho*-P. Surprisingly, p44 does not have the same stringent phospholipid requirement as arrestin. p44 binds purified, DM-solubilized Rho-P and is able to inhibit some retinal release (~25%) from Rho*-P in DM micelles. However, in mixed micelles of DM and phospholipid, p44 is similar to full-length arrestin, in that it traps up to ~50% of retinal. p44 is also able to convert Meta III to Meta II, and blue-light irradiation results in similar binding dynamics for p44 as for full-length arrestin.

All experiments reported in this appendix were performed by the author of this dissertation. Purified arrestin and p44 mutant proteins were supplied by Dr. W. Clay Smith.

A1. 2 INTRODUCTION

Among G-protein coupled receptors, the dim-light photoreceptor rhodopsin is renowned for its sensitivity and efficacy as a signal transducer. Dark-state rhodopsin (Rho) exhibits an extremely low activity (Melia *et al.*, 1997), which is achieved by the covalent attachment of an inverse agonist, 11-*cis* retinal. Upon the absorption of a photon of light, 11-*cis* retinal isomerizes to the all-*trans* conformation, which induces activating conformational changes within the protein within milliseconds (Rho*) (Burns and Baylor, 2001). The G-protein transducin, which is located close to the receptor since it is associated with the membrane, binds Rho* (Hamm, 2001). Subsequent dissociation of transducin's subunits leads to the activation of phosphodiesterase (PDE), which depletes cellular cGMP (Ridge *et al.*, 2003). The net effect of these interactions is an enormous amplification of the signal. A single Rho* can activate hundreds of PDE molecules in a single second (Leskov *et al.*, 2000), and the impressive catalytic efficiency of PDE translates to a substantial decrease in the local cGMP concentration (Stryer, 1988; Burns and Arshavsky, 2005). Hence, rod cells can detect single photons of light (Rieke and Baylor, 1998).

However, visual acuity depends not only on fast and efficient activation, but also on fast and efficient deactivation. Signal termination begins with phosphorylation of the C-terminal tail of Rho* by rhodopsin kinase (Hurley *et al.*, 1998; Maeda *et al.*, 2003). Subsequent binding by arrestin blocks further interaction of Rho*-P with transducin (Kühn *et al.*, 1984; Wilden *et al.*, 1986). However, this classic paradigm of rhodopsin deactivation may need revising, since recent studies have reported that arrestin is normally sequestered within the inner segment of the rod cell in the dim-light operational

range of the rod cell (Elias *et al.*, 2004; Nair *et al.*, 2005; Strissel *et al.*, 2006). Surprisingly, arrestin translocates to the outer segment when light intensities approach saturation levels (~3% photobleaching) (Strissel *et al.*, 2006).

However, arrestin is not the only quencher of Rho* activity. A short splice variant of arrestin, p44 (Palczewski *et al.*, 1994a), results from a retained intron in the arrestin mRNA that causes the last 35 amino acids to be replaced by a single alanine residue (Smith *et al.*, 1994). p44 is only present at ~1% the level of rhodopsin, and it localizes in the outer segment (Palczewski *et al.*, 1994a; Smith *et al.*, 1994). Previous characterization of p44 found that it is constitutively active. In contrast to full-length arrestin, p44 will bind both Rho* and dark-state Rho-P (Palczewski *et al.*, 1994a; Pulvermüller *et al.*, 1997). p44 binds faster and tighter to Rho*-P than arrestin (Schröder *et al.*, 2002), and hence p44 is probably responsible for the fast and efficient termination of rhodopsin signaling in the operational rod cell (Langlois *et al.*, 1996).

This appendix reports preliminary experiments using a fluorescently labeled p44, analogous to the arrestin I72B that is the focus of much of this dissertation. For the most part, these experiments have confirmed previously published findings and provide further evidence for the dark-state association of p44 with the ROS membrane, which facilitates its fast quenching ability.

A1. 3 MATERIALS and METHODS

A1. 3. 1 Materials

For materials used in this study, see sections **3. 3. 1** and **4. 3. 1** in Chapters 3 and 4.

A1. 3. 2 Purification of Native Rhodopsin and Recombinant Arrestin and p44

For information regarding the purification of the proteins used in this study, see sections **2. 3. 2** , **2. 3. 4**, and **3. 3. 3** in Chapters 2 and 3.

A1. 3. 3 Bimane-Labeling of Arrestin and p44

For protocols regarding the fluorescent labeling of arrestin I72C and p44/I72C, see sections **2. 3. 5** and **3. 3. 5** in Chapters 2 and 3. For determination of p44 concentration, an extinction coefficient of ε_{280} = 25,080 liters M^{-1} cm^{-1} was used, for p44 lacks Tyr^{391} of full-length arrestin (the extinction coefficient of full-length arrestin is ε_{280} = 26,360 liters M^{-1} cm^{-1}). p44 also aggregates much more than full-length arrestin, so labeling yields were lower (<50% of p44 recovered after labeling *versus* >90% of full-length arrestin). p44 stocks were always centrifuged (100,000 x *g*, 15 min) before use in experiments.

A1. 3. 4 Functional Pull-down Assay

The functional pull-down assay is described in section **2. 3. 6** in Chapter 2.

A1. 3. 5 Fluorescence Spectroscopy

For details concerning steady-state experiments, see sections **2. 3. 7**, **3. 3. 7**, and **4. 3. 3** in Chapters 2, 3, and 4. For information regarding time-based fluorescence experiments, see sections **2. 3. 10** and **4. 3. 3** in Chapters 2 and 4.

A1. 3. 6 Steady-State Fluorescence Anisotropy Measurements

The steady-state fluorescence anisotropy, which is a measure of the rotational diffusion of a fluorophore (Lakowicz, 1999), was measured on a Photon Technologies QM-1 steady-state fluorescence spectrophotometer. Polarizers were fitted over the

excitation source and the emission detector and used to vary the polarization of the light. Anisotropy (r) is defined as:

$$r = \frac{I_{\parallel} - GI_{\perp}}{I_{\parallel} + 2GI_{\perp}}$$

$I_{\parallel}$ and $I_{\perp}$ are the intensities of the fluorescence emission parallel and perpendicular to the plane of the excitation light, respectively. The G-factor, which is a term that corrects for the different sensitivities of the emission detector for vertically and horizontally polarized light, was determined before measuring the anisotropy. In a typical experiment, the fluorescence emission of 1 μM bimane-labeled arrestin (200 μl sample volume, 15 °C) was measured at 475 nm (380 nm excitation) for 15 seconds (1 second integration per point). The average of the 15 points was used for $I_{\parallel}$ and $I_{\perp}$, and measurements were done in triplicate. Excitation slits were set at 1 nm, and emission slits were set at 10 nm. These settings caused <1% rhodopsin bleaching in samples containing ROS, as measured by absorbance spectroscopy. Background fluorescence of buffer or ROS was subtracted where appropriate before the calculation of anisotropy.

A1. 3. 7 KI Quenching Analysis

KI quenching analysis was performed as described in section **2. 3. 9** in Chapter 2.

A1. 3. 8 Fluorescence Lifetime Analysis

For information regarding the measurement and analysis of fluorescence lifetimes, see section **2. 3. 8** in Chapter 2.

A1. 3. 9 UV-Visible Absorbance Spectroscopy

For information regarding absorbance spectroscopy, see sections **3. 3. 8** and **4. 3. 4** in Chapters 3 and 4.

A1. 4 RESULTS

The experiments presented in this appendix examine the differences between arrestin and the splice variant p44 using similar approaches as described in Chapters 2, 3 and 4 of this dissertation. To this end, a mutant cysteine was engineered into p44 at Ile^{72}, and the fluorescent probe monobromobimane was attached to this site (Figure A1. 1).

A1. 4. 1 Fluorescently Labeled p44 is Constitutively Active

Before making any fluorescence measurements, we first carried out centrifugal pull-down analysis in order to determine if the bimane-labeled p44 (p44/I72B) was functional and to compare its binding profile to full-length arrestin I72B (Figure A1. 2 and Table A1. 1). Arrestin I72B shows strict selectivity for light-activated, phosphorylated rhodopsin (ROS*-P). In contrast, p44 has a moderate basal affinity for ROS membranes that is at least 10-times greater than arrestin I72B [15], but this affinity is not changed much by rhodopsin activation (only ~7% more p44 is pulled down upon light-activation of ROS). Strikingly, p44 binds all forms of phosphorylated rhodopsin with high affinity, and it does not discriminate between light-activated and dark-state, as has been reported previously (Pulvermüller *et al.*, 1997; Schröder *et al.*, 2002).

A1. 4. 2 Spectral Properties of arrestin I72B and p44/I72B

Figure A1. 3 shows the fluorescence emission spectra of arrestin I72B and p44/I72B in the presence of rhodopsin. Since p44 demonstrates some binding to dark-state rhodopsin, we normalized these spectra to those of identical samples in the absence

[15] This figure was obtained as follows: in the absence of any ROS membranes, 2% of arrestin I72B and 6% of p44/I72B is pulled-down. This represents non-specific pull-down and should be subtracted as background. In the presence of ROS membranes containing opsin, ~2% more arrestin I72B is pulled down, while ~20% more p44/I72B is pulled down. Thus, p44 binds ROS membranes at least 10-times better than arrestin.

of rhodopsin. In this way, any fluorescence changes due to the interaction of p44/I72B with ROS membranes may be detected [16].

In the presence of nonphosphorylated rhodopsin (ROS), the fluorescence of arrestin I72B does not change upon light-activation (Figure A1. 3A). Note that the fluorescence of p44/I72B is slightly increased and blue-shifted in the presence of dark ROS (Figure A1. 3E), and this may be due to a change in the environment of the bimane probe or an increase in scattering when p44 binds the ROS membrane vesicles [17]. Upon light-activation, there is only a small change in p44/I72B's fluorescence.

In the presence of phosphorylated rhodopsin (ROS-P), the fluorescence of arrestin I72B displays a large increase and blue-shift in intensity upon light-activation (Figure A1. 3B). Curiously, the fluorescence of p44/I72B is slightly quenched in the presence of dark ROS-P (Figure A1. 3F). From the results of the centrifugal pull-down experiment (Figure A1. 2), we can surmise that some of the p44/I72B in this experiment is bound to ROS-P. Why would its fluorescence be quenched? Since dark-state rhodopsin absorbs at 500 nm, it is possible that energy transfer might occur between the bimane probe on p44/I72B and the 11-*cis* retinal chromophore. Upon light activation, the fluorescence of p44/I72B increases and blue-shifts as seen for arrestin I72B (Figure A1. 3F). After the addition of hydroxylamine, which cleaves the retinal Schiff base and converts all rhodopsin photoproducts to opsin and free retinal oxime, the fluorescence of p44/I72B decreases. However, the fluorescence remains elevated and slightly blue-shifted

---

[16] Note that the fluorescence intensities of arrestin I72B (Figure A1. 3, *right panels*) all normalize to 1.0, since little interaction of I72B with dark-state rhodopsin occurs.

[17] This possibility is supported by the fact that the fluorescence emission of p44/I72B (Figure A1. 3B) is elevated at the bluer wavelengths compared to the emission of I72B (Figure A1. 3A).

compared to p44/I72B in the absence of ROS-P. This difference may be due to the interaction of p44 with phosphorylated opsin.

A1. 4. 3 Steady-state Anisotropy of Arrestin I72B and p44/I72B

When a fluorophore absorbs polarized light, its rotational diffusion dictates how depolarized the emitted fluorescence will be. A probe that is tumbling quickly in solution will emit highly depolarized light and will have a low anisotropy, whereas an immobilized probe will have a higher anisotropy. The rotational diffusion of a fluorophore can be affected by attaching to a larger molecule, or by placing it in a restricted space, such as the interior of a protein. As arrestin I72B binding involves a burying of the bimane probe in a protein-protein (or protein-lipid) interface (Sommer *et al.*, 2005), steady-state anisotropy represents another valuable method for observing this fluorescently labeled arrestin mutant.

Table A1. 1 reports the steady-state anisotropy values of arrestin I72B and p44/I72B in buffer alone or in the presence of various functional forms of membrane-bound rhodopsin. The probe on arrestin I72B has a low anisotropy (~0.06) that is not changed much in the presence of opsin membranes. Intriguingly, the anisotropy increases slightly in the presence of dark ROS or ROS-P (~0.09), implying that I72B interacts with the dark-state ROS membrane. The largest increase in I72B anisotropy occurs, expectedly, upon light-activation of ROS-P (~0.17).

In buffer alone, p44/I72B has a slightly higher anisotropy than arrestin I72B (~0.08), and this difference may reflect some local conformational change in the protein due to the truncation of the C-tail. As expected, p44/I72B has a high anisotropy in the presence of opsin-P and dark ROS-P (~0.14), and this increases (~0.18) upon light-

activation of ROS-P. However, it is curious that nearly the same amount of p44 is pulled-down with ROS-P and ROS*-P, and yet they impose different anisotropies on the probe. As discussed below, this difference might reflect different modes of p44 binding (or different binding affinities).

In summary, the anisotropies generally reflect the results seen in the pull-down experiment (Table A1. 1). The differences seen, such as arrestin's interaction with dark ROS membranes, may be due to the different sensitivities of these two methods.

A1. 4. 4 Fluorescence Lifetime Analysis

The fluorescence decay lifetimes (τ) of arrestin I72B and p44/I72B were measured and analyzed using a two-component fit. The average lifetimes are reported in Table A1. 1. Briefly, both arrestin I72B and p44/I72B have a similar amplitude-weighted average fluorescence lifetime, $\langle\tau\rangle$, of 11 ns, and this value does not change significantly upon binding rhodopsin. The $\langle\tau\rangle$ of p44/I72B is slightly shorter in the presence of ROS-P (9 ns), which might be due to the quenching of the bimane probe on p44/I72B by the dark-state retinal chromophore (Figure A1. 3F). However, because these lifetime measurements were done with ROS membranes, which introduce a significant amount of scatter, we are reluctant to draw too many conclusions from this data. Future measurements using Rho-P in optically-clear mixed micelles will be needed to better explain this potential energy transfer.

A1. 4. 5 KI Quenching Analysis

The relative accessibility of the bimane probe to the quencher I^-, described by the Stern-Volmer constant (K_{SV}) and the bimolecular quenching constant (k_q), can reliably report whether arrestin I72B is free in solution or bound to ROS*-P (Sommer *et al.*,

2005). K_{SV} and k_q values for arrestin I72B and p44/I72B are reported in Table A1. 1, and these values are consistent with centrifugal pull-down and anisotropy results.

A1. 4. 6 p44/I72B Does not Require Phospholipids to Bind Detergent-solubilized Rho*-P

As discussed in Chapter 3 of this dissertation, the removal of phospholipids from Rho-P by purification in detergent severely inhibits arrestin I72B binding (Figure A1. 3C). Binding can be rescued by the addition of asolectin phospholipid (Figure A1. 3D). Surprisingly, p44/I72B appears to be able to bind DM-solubilized Rho*-P in the absence of phospholipid (Figure A1. 3G). Interestingly, in the presence of dark Rho-P in DM/asolectin micelles, the fluorescence of p44/I72B is similarly quenched as seen with dark ROS-P (Figure A1. 3H). Upon light-activation of Rho-P, the fluorescence increases and blue-shifts, and the addition of hydroxylamine results in p44/I72B fluorescence that is elevated compared to that in the absence of rhodopsin.

A1. 4. 7 p44/I72B Inhibits Some Retinal Release from Rho*-P in DM micelles

Since p44/I72B is able to bind Rho*-P in pure DM micelles, we were curious if it would be able to inhibit retinal release in this system. We investigated this possibility by fluorescence and absorbance spectroscopy (Figure A1. 4). Since detailed descriptions of this type of data were given in Chapters 3 and 4 of the dissertation, a detailed explanation is not given here. To summarize, the data report that p44/I72B traps ~25% of the retinal in DM micelles. In contrast, no retinal is trapped by arrestin I72B, because it does not interact significantly with DM-solubilized Rho*-P.

A1. 4. 8 p44 Inhibits Retinal Release and Meta III Formation in Mixed Micelles

The dynamics of retinal release and rhodopsin photoproduct formation from Rho*-P in DM/asolectin mixed micelles are shown in Figure A1. 5. To briefly summarize, p44 is similar to full-length arrestin in its ability to trap ~50% of retinal and inhibit Meta III formation.

A1. 4. 9 p44 Converts Meta III to Spectral Meta II

As shown in Figure 4. 5 of Chapter 4 of this dissertation, arrestin can interact with Meta III and convert it to a Meta II-like species with a 380 nm absorbance and an intact retinal Schiff-base. The same experiment was performed with p44, and a similar result was obtained (Figure A1 .6).

A1. 4. 10 Blue-light Effects on the Interaction of Arrestin and p44 with Rho*-P

As described in Figure 4. 6 of Chapter 4 of this dissertation, blue-light irradiation of Meta II forms two photoproducts, Meta III and P500. Arrestin can interact with Meta III, but it does not bind P500. Hence, blue-light irradiation of Meta II-bound arrestin causes a partial dissociation of arrestin. Subsequent illumination with green light causes arrestin to rebind. As shown in Figure A1. 7, p44/I72B behaves similarly. Note that the fluorescence of p44/I72B in the presence of dark-state Rho-P is quenched, and upon green-light illumination, it appears to bind faster than arrestin I72B. p44 may also affect the efficiency of blue-light photoproduct formation (note the differences in the fluorescence of arrestin I72B and p44/I72B after blue-light irradiation), but this possibility has not been fully investigated here.

A1. 5 DISCUSSION

A1. 5. 1 Appendix Overview

This work employed several different quantitative methods to compare full-length arrestin and p44 function. Centrifugal pull-down analysis indicates p44 has a higher basal affinity for the ROS membrane than arrestin I72B, but p44 does not discriminate significantly between inactive and active Rho. p44 binds avidly to all forms of phosphorylated rhodopsin, while arrestin I72B shows strict selectivity for light-activated phosphorylated rhodopsin. Steady-state anisotropy and fluorescence quenching measurements are, for the most part consistent with the pull-down data (Table A1. 1). However, these data may suggest that arrestin interacts with dark ROS and ROS-P to a greater extent than implied by the pull-down analysis.

The fluorescence emission spectra of p44/I72B also indicate some interaction of p44 with the dark-state ROS membrane (Figure A1. 3). Curiously, we consistently see that p44/I72B's fluorescence is quenched in the presence of dark ROS-P (or even purified Rho-P in micelles). The cause of this quenching is still unclear, but it could be due to energy transfer from the bimane probe to the retinal chromophore. Alternatively, the structure of p44 could differ, putting the probe at Ile^{72} into a different environment. Upon light-activation, p44/I72B's fluorescence displays the same increase and blue-shift as seen for arrestin I72B.

Surprisingly, p44 does not have the same stringent phospholipid requirement for binding purified Rho*-P as arrestin, and in pure DM micelles, p44 can trap ~25% of retinal (Figure A1. 4). In mixed DM/asolectin micelles, the behavior of p44/I72B is nearly identical to arrestin I72B, with respect to retinal trapping and inhibition of Meta III

(Figures A1. 5 and 6). The only differences worth noting are the quenched fluorescence of p44/I72B in the presence of dark Rho-P and that it appears to bind faster after light-activation (Figure A1. 7). The structural and physiological implications of these results are discussed below.

A1. 5. 2 The Functional Role of Arrestin's C-tail

Structurally, p44 and arrestin are identical except for the missing C-tail in p44 (Palczewski *et al.*, 1994a; Smith *et al.*, 1994). The C-tail is hypothesized to be important in "locking" arrestin in an inactive conformation (Gurevich and Gurevich, 2004). When the C-tail is displaced by the phosphorylated tail of rhodopsin, arrestin can "switch" to an active form that is capable of binding Meta II (see section **1. 4. 2** in Chapter 1 for more details). Because the C-tail is missing in p44, the paradigm is that it is already "pre-activated" to bind. However, the data presented here show that p44 does not bind Rho* much better than Rho. Consistent with this result, the affinity of p44 for Rho* has been reported to be a full order of magnitude less than arrestin's affinity for Rho*-P (Pulvermüller *et al.*, 1997). Although the loss of the C-tail may be insufficient for tight binding to Meta II, it could possibly free the amphipathic α-helix 1 of arrestin, which has been hypothesized to serve as a membrane anchor for activated arrestin (Han *et al.*, 2001). This possibility might explain p44's ability to be pulled down with membranes containing dark Rho or opsin.

p44 binds all forms of phosphorylated rhodopsin (opsin-P, Rho-P and Rho*-P) with similar high affinity. This result implies that the loss of the C-tail exposes critical binding sites for the phosphorylated tail of rhodopsin. This interaction is sufficient to tether p44 to the membrane even in the absence of activated rhodopsin.

A1. 5. 3 p44 binds Rho-P Differently than Rho*-P

Although nearly the same amount of p44/I72B is pulled-down with dark ROS-P as ROS*-P, the steady-state anisotropy and quenching studies report that the bimane probe is more mobile and exposed in the presence of ROS-P than ROS*-P (Table A1. 1). This result implies that rhodopsin must be activated to bury the probe fully in the interface. However, the probe is still more immobile and less exposed with ROS-P than in its absence. Hence, p44 may interact with dark ROS-P in a more "peripheral" way that does not bury the probe to the same extent as when arrestin binds ROS*-P.

A1. 5. 4 Comparison of p44 and Arrestin Binding to Rho*-P

All the data presented here suggest that p44 binds ROS*-P in the same way as arrestin, in that their anisotropies, k_q's, and fluorescence emission spectra are all very similar. Thus, it is not that surprising that p44 behaves similarly as arrestin in its ability to inhibit retinal release and convert Meta III to Meta II in mixed micelles.

However, we do find that p44 does not require phospholipids for binding detergent-purified Rho*-P, in sharp contrast to arrestin. As described in Chapter 3 of this dissertation, phospholipids might compose part of the interface between arrestin and rhodopsin. Alternatively, they may be required to stabilize a spectrally silent conformation of Meta II or might be necessary for rhodopsin dimerization. In any case, the cause of this difference between p44 and arrestin is unclear. It could be that the affinity of p44 for the phosphorylated tail of Rho-P is so high that is sufficient to overcome whatever barriers are imposed by the absence of phospholipids. It is interesting to note that p44 can only trap ~half as much retinal in the absence of phospholipids as in their presence, so p44 is still sensitive to the loss of phospholipid.

Finally, we observe that p44/I72B binds to Rho*-P faster than arrestin I72B, and this fact has been reported previously (Pulvermüller *et al.*, 1997). The cause of p44's faster rate of binding might be its lower activation energy of binding (~70 kJ/mol compared to ~140 kJ/mol for arrestin) (Pulvermüller *et al.*, 1997), as well as the fact that it is pre-localized to the membrane or micelles because of its interaction with Rho-P (Schröder *et al.*, 2002).

A1. 5. 5 Physiological Implications

All reported *in vitro* and *in vivo* evidence suggest that p44 serves to quench Rho* activity in the dim-light operational range of the rod cell, when arrestin is still sequestered in the inner segment (Smith *et al.*, 1994; Langlois *et al.*, 1996; Pulvermüller *et al.*, 1997; Schröder *et al.*, 2002; Strissel *et al.*, 2006). Schröder *et al.* have published a detailed description of how p44 is functionally adapted to this role (Schröder *et al.*, 2002), which we will briefly summarize here and in Figure A1. 8. In the dark rod cell, about 1% of rhodopsin is phosphorylated (Binder *et al.*, 1996), which together with p44's residual affinity for the ROS membrane, is sufficient to bind up all the p44 present (Palczewski *et al.*, 1994a). When a photon is absorbed by the rod, it will most likely activate a nonphosphorylated rhodopsin. Rho* has the opportunity to interact with transducin for a time until it is phosphorylated by rhodopsin kinase. Once phosphorylated, it is quickly bound by p44, which is already localized to the membrane by its interaction with Rho-P. Consistent with this idea, Langlois *et al.* found that p44 can never eliminate the 0.2-0.5 sec initial rise in activity that occurs upon light absorption, but it does deactivate this signaling 10-times faster than arrestin (Langlois *et al.*, 1996). Although it might be tempting to suppose that p44's slight affinity for Rho* is

responsible for the fast quench, a recent study using transgenic mice found that p44 was unable to quench the photo-response in the absence of rhodopsin phosphorylation (Burns *et al.*, 2006).

In this study we also found that p44 can inhibit retinal release and Meta III formation like arrestin. However, it is unlikely that this "arrestin-like" ability of p44 is useful for the rod cell in dim-light. As opposed to bright-light conditions, retinal dehydrogenase activity would not be limiting (Palczewski *et al.*, 1994b), and Meta III would not be present at any significant concentration.

A1. 5. 6 Summary and Future Directions

For the most part, the experiments in this appendix illustrate what was already known about p44: loss of the C-tail increases p44's affinity for the ROS membrane and phosphorylated opsin. However, the present work using fluorescently labeled proteins did yield some new information regarding the difference in the way p44 binds dark Rho-P and Rho*-P. Future experiments will address more of the details of p44's interaction with the ROS membrane. First, the energy transfer between p44/I72B and the retinal chromophore should be better quantified, as this might yield some distance information. Secondly, it will be important to address whether p44 activity is modulated by the extent of rhodopsin phosphorylation (Ascano and Robinson, 2006). And finally, can the transfer of p44 from Rho-P to a distant Rho*-P be measured, perhaps using a spin-labeled p44 and near-physiological concentrations of rhodopsin? What implication does this have on the possibility of rhodopsin dimerization? Such quantitative *in vitro* experiments will contribute greatly to our understanding of p44 and dim-light photo-transduction.

AI. 6 ACKNOWLEDGEMENTS

The work was supported by the same funding as described in section **3. 6** in Chapter 3. We thank Steven E. Mansoor for assistance in measuring fluorescence lifetimes.

Table A1. 1 Fluorescence characteristics of Arr I72B and p44 / I72B in the presence of different forms of rhodopsin (native membranes).

	sample	% pull down[a]	anisotropy[b]	K_{sv} (M^{-1})[c]	$\langle\tau\rangle$ (ns)[d]	$\bar{\tau}$ (ns)[d]	k_q[e] ($x10^9 M^{-1}s^{-1}$)
I72B	buffer alone	2	0.0559 ± 0.0034	24.9 ± 2.1	11.2 ± 0.2	12.6 ± 0.2	2.0
	+ opsin	4	0.0532 ± 0.0026	n.d.[f]	n.d.	n.d.	n.d.
	+ opsin-P	6	0.0686 ± 0.0029	n.d.	n.d.	n.d.	n.d.
	+ ROS (dark)	4	0.0895 ± 0.0010	19.9	8.4 ± 0.4	11.1 ± 0.1	1.8
	+ ROS* (+hν)	5	0.0956 ± 0.0002	19.1	9.7 ± 1.5	12.0 ± 1.3	1.6
	+ ROS* ($+NH_2OH$)	3	0.0803 ± 0.0020	n.d.	9.1 ± 1.5	11.5 0.5	n.d.
	+ ROS-P (dark)	5	0.0898 ± 0.0031	24.0 ± 1.5	10.5 ± 0.8	12.7 ± 0.8	1.9
	+ ROS*-P (+hν)	60	0.1751 ± 0.0028	6.9 ± 0.3	10.2 ± 0.9	12.5 ± 0.9	0.5
	+ ROS*-P ($+NH_2OH$)	4	0.0972 ± 0.0028	23.5 ± 1.8	10.7 ± 0.2	12.3 ± 0.0	1.9
p44 / I72B	buffer alone	6	0.0785 ± 0.0026	25.9 ± 1.7	10.8 ± 0.0	13.0 ± 0.0	2.0
	+ opsin	27	0.0726 ± 0.0057	n.d.	n.d.	n.d.	n.d.
	+ opsin-P	69	0.1369 ± 0.0020	n.d.	n.d	n.d.	n.d.
	+ ROS (dark)	32	0.0902 ± 0.0013	16.0 ± 0.5	10.1 ± 0.3	12.4 ± 0.4	1.3
	+ ROS* (+hν)	39	0.1101 ± 0.0015	14.6 ± 1.0	7.9 ± 1.0	11.5 ± 0.3	1.3
	+ ROS* ($+NH_2OH$)	26	0.0991 ± 0.0040	14.8 ± 0.8	9.4 ± 0.1	12.2 ± 0.6	1.2
	+ ROS-P (dark)	71	0.1437 ± 0.0047	11.1 ± 0.7	9.0 ± 0.1	12.2 ± 0.2	0.9
	+ ROS*-P (+hν)	74	0.1853 ± 0.0049	8.0 ± 0.5	7.6 ± 0.6	11.6 ± 0.5	0.7
	+ ROS*-P ($+NH_2OH$)	62	0.1475 ± 0.0040	10.7 ± 1.3	8.6 ± 0.2	12.2 ± 0.1	0.9

See next page for table details.

[a] The amount of arrestin pulled-down by a four-fold excess of ROS membranes in a centrifugal assay (see Figure A1. 2). The fluorescence of the bands was quantified by densitometry and is expressed as a percentage of the total amount of arrestin present in the assay (3 μM).

[b] The steady-state anisotropy of the bimane probe was measured as described in the Materials and Methods. The mean ± the S.E. from three measurements (15 °C).

[c] K_{SV}, the Stern-Volmer constant, was derived as described in the Materials and Methods. The mean ± the S.E. from two independent experiments (20 °C).

[d] Lifetimes were measured as described in the Materials and Methods (20 °C). The data were used for double exponential lifetime analysis, and the χ^2 value for each fit was between 0.8 and 1.2. The average lifetimes were calculated from this data: $\langle\tau\rangle = \alpha_1\tau_1+\alpha_2\tau_2$, or the amplitude-weighted average fluorescence lifetime, and $\bar{\tau} = (\alpha_1\tau_1^2+\alpha_1\tau_2^2) / (\alpha_1\tau_1+\alpha_2\tau_2)$, or the intensity-weighted average fluorescence lifetime (Ross *et al.*, 1992; Neyroz *et al.*, 1996; Zawadzki *et al.*, 2003). These values represent the mean of two independent sets of lifetimes ± the S.E.

[e] The bimolecular quenching constant (k_q), which represents collisions per second between the fluorophore and the quencher, was derived using the relationship $K_{SV}=k_q*\tau_0$ (where τ_0 is the intensity-weighted average fluorescence lifetime in the absence of quencher) (Ross *et al.*, 1992; Neyroz *et al.*, 1996; Zawadzki *et al.*, 2003).

[f] n.d., not determined.

Figure A1. 1 Structural models of rhodopsin, the arrestin splice variant p44, and the fluorescent probe used in this study. The figure shows rhodopsin (*red*) and its hypothetical dimer partner (*transparent red*) in a membrane bilayer (Liang *et al.*, 2003). The domains of p44 are colored (*blue*, N-domain; *orange*, C-domain), and the approximate site of p44's C-terminal truncation (Ala^{370}) is indicated (Palczewski *et al.*, 1994a). The C-tail of arrestin, which is missing in p44, is shown in *transparent green*. The location of Ile^{72} is shown by a *yellow sphere* at the site of the α-carbon. *Inset* – structure of the fluorescent probe monobromobimane, which was attached to a mutant cysteine at site Ile^{72} (not to scale with the protein models). Models were created as described previously (Sommer *et al.*, 2005).

Figure A1. 1

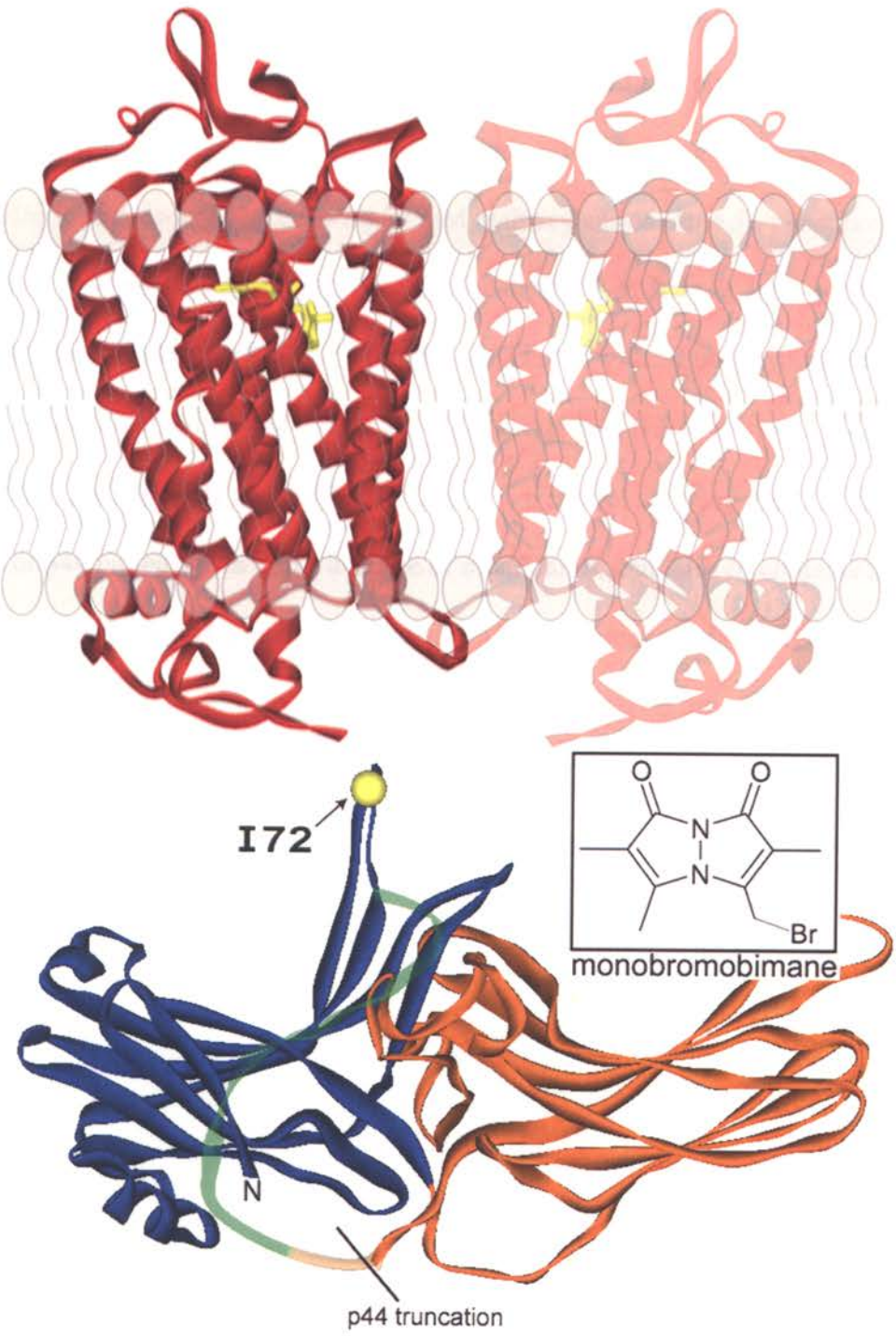

Figure A1. 2 Functional pull-down analysis of arrestin I72B and p44 / I72B. The relative affinities of bimane-labeled arrestin I72B and p44 / I72B for ROS membranes containing difference forms of the receptor rhodopsin were determined by a centrifugal "pull-down" assay. Briefly, ROS membranes containing 12 μM opsin (*lane 2*), nonphosphorylated rhodopsin (ROS, *lane 3*), light-activated nonphosphorylated rhodopsin (ROS*, *lane 4*), ROS* with 50 mM hydroxylamine (*lane 5*), phosphorylated opsin (*lane 6*), dark-state phosphorylated rhodopsin (ROS-P, *lane 7*), light-activated phosphorylated rhodopsin (ROS*-P, *lane 8*), or ROS*-P with 50 mM hydroxylamine (*lane 9*) were mixed with 3 μM of arrestin (*left gels*) or p44 (*right gels*) and processed as described in the Materials and Methods. *Lane 1* is a control showing the amount of arrestin or p44 pulled-down in the absence of membranes, and *lane 10* contains the total amount of arrestin or p44 present in the assay. The fluorescence of the gels is shown *above*, and the Coomassie stain is shown *below*. The arrows on the *right* point to the locations of rhodopsin (Rho), p44, and arrestin (Arr). The amount of arrestin or p44 in each lane was quantified by densitometry of the fluorescent bands and is reported in Table A I. 1.

Figure A1. 2

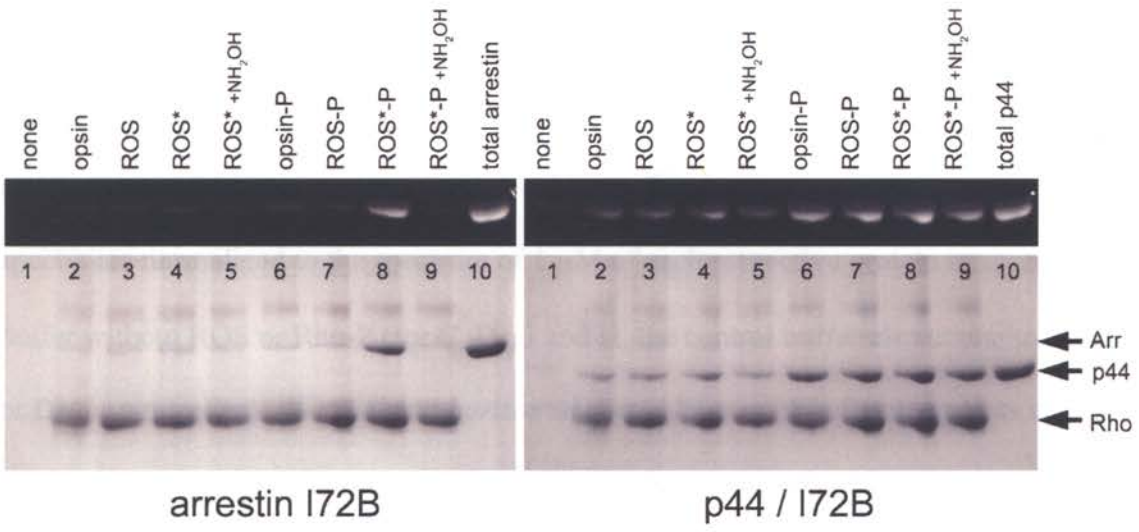
none
opsin
ROS
ROS*
ROS* +NH2OH
opsin-P
ROS-P
ROS*-P
ROS*-P +NH2OH
total arrestin
1 2 3 4 5 6 7 8 9 10
arrestin I72B
none
opsin
ROS
ROS*
ROS* +NH2OH
opsin-P
ROS-P
ROS*-P
ROS*-P +NH2OH
total p44
1 2 3 4 5 6 7 8 9 10
p44 / I72B
Arr
p44
Rho

Figure A1. 3 Steady-state fluorescence spectra of arrestin I72B and p44 / I72B in the presence of rhodopsin. The fluorescence of 1 μM I72B (A, B, C and D) or p44 / I72B (E, F, G and H) was measured in the presence of ROS (A and E), ROS-P (B and F), purified Rho-P in DM micelles (C and G), or purified Rho-P in DM/asolectin micelles (D and H). In each panel, the dark-state (*solid trace*), light-activated (*dashed trace*) and "+ hydroxylamine" (*dotted trace*) spectra are shown. The background-subtracted, smoothed spectra are normalized to the spectrum of 1 μM of each respective protein in appropriate buffer without ROS or Rho-P (for C, D, G and H, the control buffer also contained DM or DM/aso micelles). *Vertical* and *horizontal dotted lines* mark reference points at 470 nm and the normalized fluorescence intensity of 1.0, respectively. Note that the while the fluorescence of arrestin I72B in the presence of dark ROS-P or ROS*-P+NH_2OH normalizes to 1, the fluorescence of p44/I72B varies. These differences could be due to interaction of p44/I72B with ROS and ROS-P, which might contribute to a different environment for the probe, a change in the scatter of the sample, or energy transfer to the dark-state chromophore (see text for more details). In parts A, B, E and F, a four-fold excess of rhodopsin or phosphorylated rhodopsin in ROS native membranes was used, and in parts C, D, G and H, a two-fold excess of Rho-P in 0.02% DM with or without 0.02% asolectin was used (20 mM HEPES, 150 mM NaCl, pH 7.4, 20 °C).

Figure A1. 3

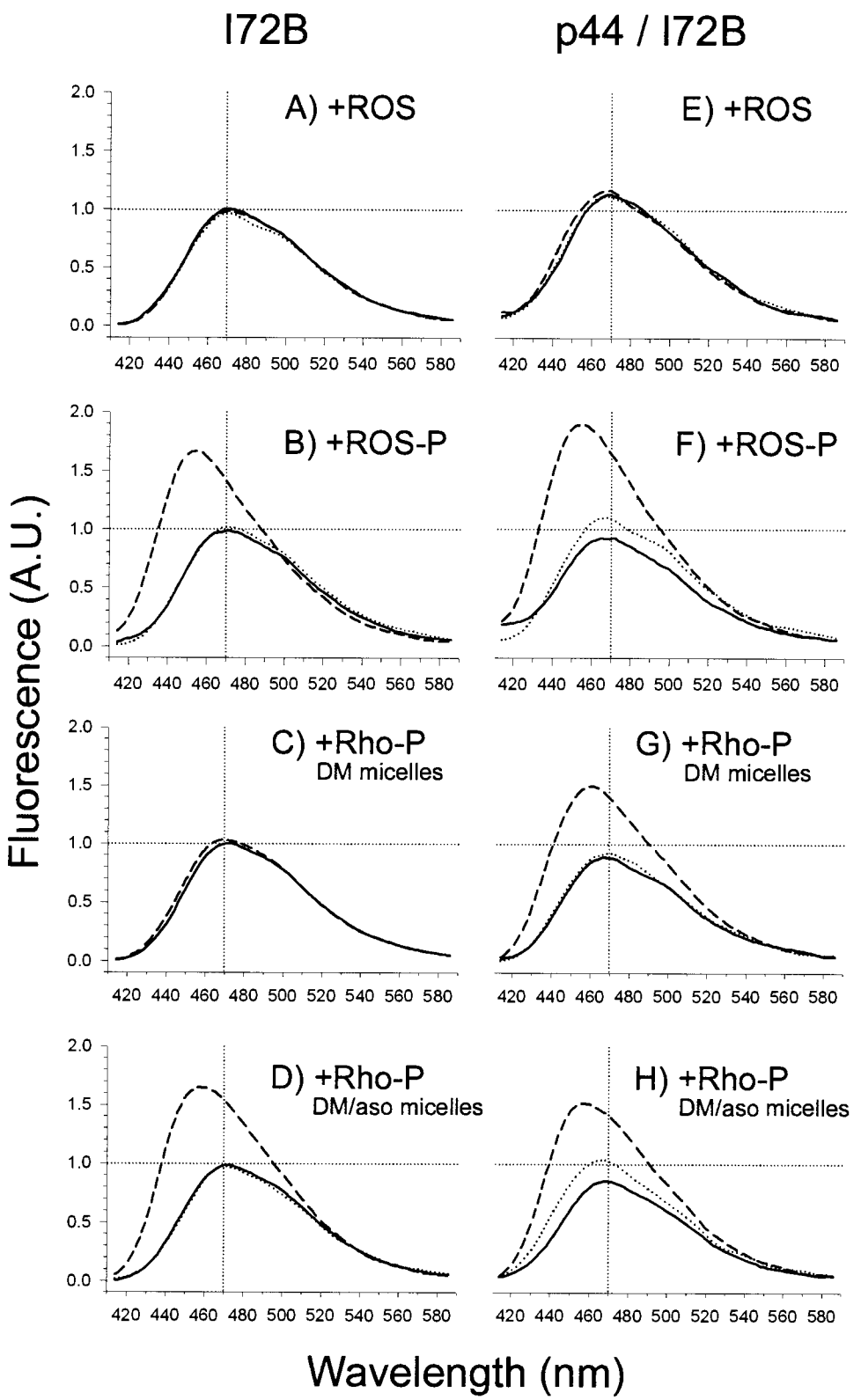
I72B
p44 / I72B
A) +ROS
E) +ROS
B) +ROS-P
F) +ROS-P
C) +Rho-P
DM micelles
G) +Rho-P
DM micelles
D) +Rho-P
DM/aso micelles
H) +Rho-P
DM/aso micelles
Fluorescence (A.U.)
Wavelength (nm)
2.0
1.5
1.0
0.5
0.0
420 440 460 480 500 520 540 560 580

Figure A1. 4 p44 inhibits some retinal release from Rho*-P in DM micelles. The effect of arrestin and p44 on retinal release in pure DM micelles was investigated by fluorescence and absorbance spectroscopy. **A)** Retinal release measured from 1 μM purified Rho-P in DM micelles as the increase in opsin tryptophan fluorescence (330 nm) in the presence of a 2-fold excess of arrestin (*dark blue trace*) or p44 (*light blue trace*). The sample was photoactivated at t=0 (>495 nm), and 10 mM hydroxylamine was added at ~120 min. p44/I72B binding and release was also monitored (456 nm, *green trace*) during the same experiment. The p44 fluorescence is normalized to an F_0 value determined from the fluorescence emission (456 nm) of an identical p44 sample without Rho-P. Note that the relative fluorescence of p44/I72B after the addition of NH_2OH in this experiment is different from the steady-state data shown in Figure A1. 3G. This difference may be due to experimental noise or the fact that fluorescence was monitored at 456 nm, not 470. **B)** The absorbance of purified Rho-P in DM micelles was observed in the dark (*red*) and after photoactivation (*blue*) in the presence of 2-fold excess arrestin. Spectra were recorded every 90 seconds after photoactivation (*black spectra*) for 120 minutes (the last spectrum is *orange*). The amount of retinal Schiff base remaining at the end of the experiment was assessed by adding H_2SO_4 (*green spectrum*). **C)** Same as (B), except a 2-fold excess of p44 was used. Note the differences in the loss of 380 nm absorbance and the "+acid" spectra (B) and (C). These differences also imply that p44 traps some amount of retinal in pure DM micelles. In each experiment, 1 μM Rho-P in 20 mM HEPES, 150 mM NaCl, pH 7.4, 0.02% DM was used (20 °C).

Figure A1. 4

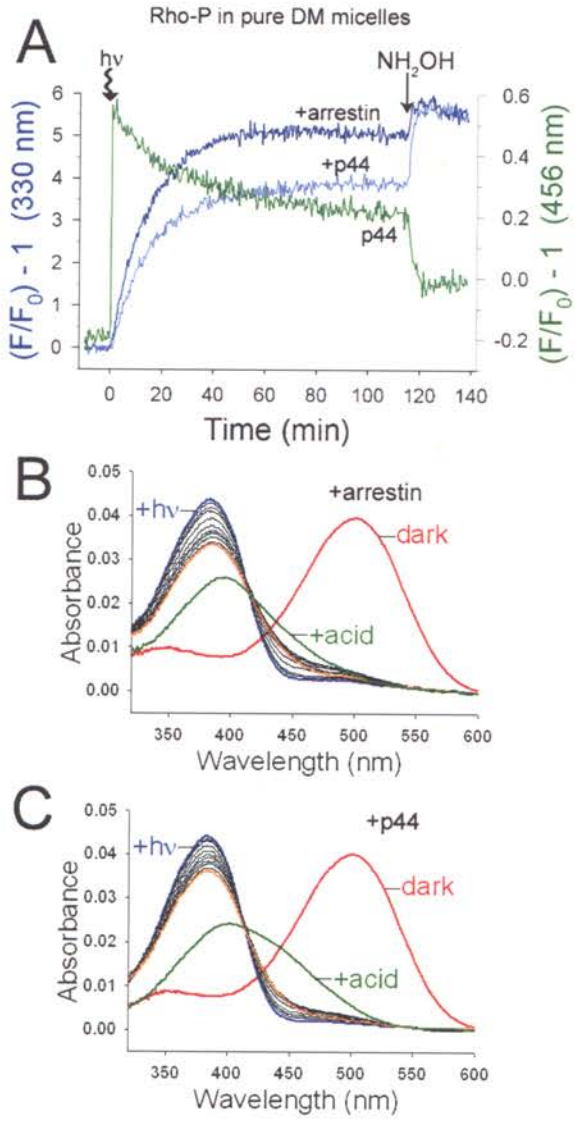
A
Rho-P in pure DM micelles
hν
NH2OH
+arrestin
+p44
p44
(F/F0) - 1 (330 nm)
(F/F0) - 1 (456 nm)
Time (min)
B
+arrestin
+hν
dark
+acid
Absorbance
Wavelength (nm)
C
+p44
+hν
dark
+acid
Absorbance
Wavelength (nm)

Figure A1. 5 p44 inhibits retinal release and Meta III formation in mixed micelles. The effect of arrestin and p44 on retinal release in DM/asolectin micelles was investigated by fluorescence and absorbance spectroscopy. **A)** Retinal release measured from 1 μM purified Rho-P in DM/asolectin micelles as the increase in opsin tryptophan fluorescence (330 nm, *blue trace*). The sample was photoactivated at t=0 (>495 nm), and 10 mM hydroxylamine was added at ~120 min. **B)** The absorbance of purified Rho-P in DM/asolectin micelles was observed as described in Figure A I. 4B. Experiments in **C**, **D**, **E** and **F** were carried out as described for (A) and (B), except that a two-fold excess of arrestin (C and D) or p44 (E and F) was present. The binding and release of arrestin I72B (C) and p44/I72B (E) was monitored (456 nm, *green trace*) at the same time as retinal release. The I72B and p44/I72B fluorescence traces are normalized to F_0 values determined from the fluorescence emission (456 nm) of identical I72B and p44/I72B samples without Rho-P. Note that the fluorescence of p44/I72B is quenched in the dark and remains elevated after the addtion of NH_2OH. These variations were also observed in the steady-state spectra in Figure A1. 3H. In each experiment, 1 μM Rho-P in 20 mM HEPES, 150 mM NaCl, pH 7.4, 0.02% DM and 0.02% asolectin was used (20 °C).

Figure A1. 5

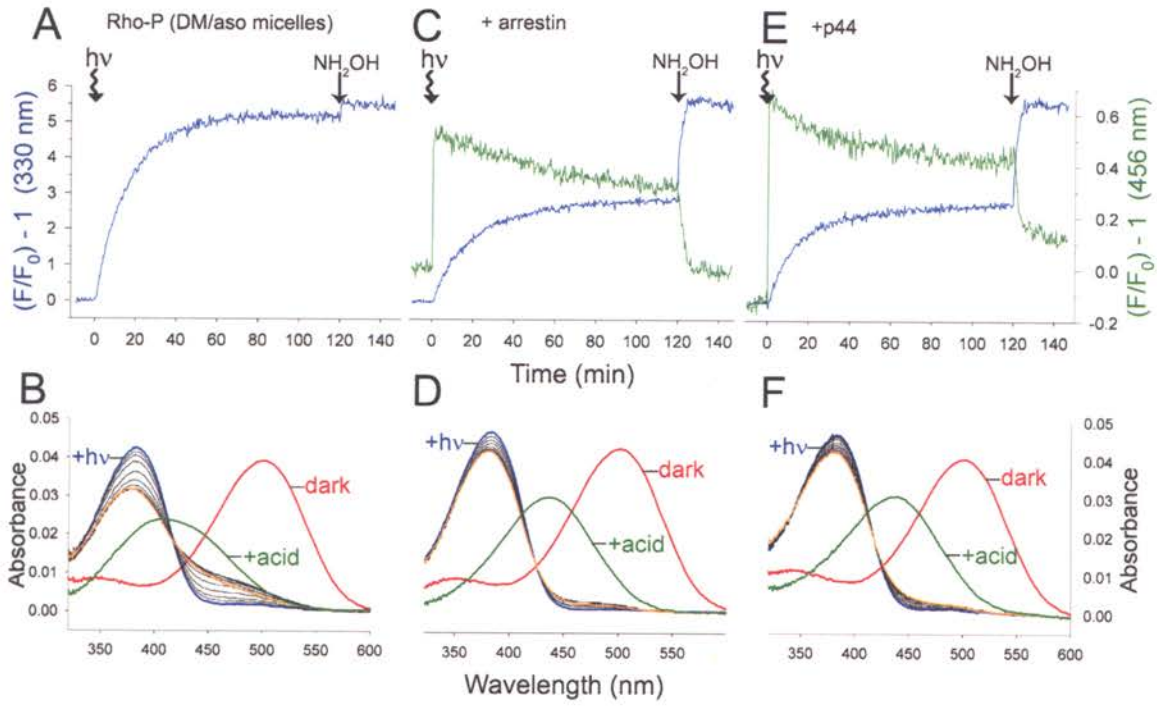
A
Rho-P (DM/aso micelles)
hν
NH2OH
(F/F0) - 1 (330 nm)
C
+ arrestin
E
+p44
(F/F0) - 1 (456 nm)
Time (min)
B
D
F
+hν
dark
+acid
Absorbance
Wavelength (nm)

Figure A1. 6 p44 converts Meta III to spectra Meta II. As shown previously for arrestin, p44 can interact with Meta III and convert it to a species with Meta II-like absorbance and an intact Schiff base. **A)** Difference spectra representing the conversion of ~470 nm absorbance to ~380 nm absorbance at 1.5, 4, 6, 26, 54 and 90 minutes after the addition of p44 (the first and the last spectra are labeled). p44 was added to photo-decayed Rho*-P 27 minutes after photoactivation, and absorbance spectra were subsequently recorded. Difference spectra were calculated by subtracting a base-line spectrum derived from a control experiment in which an equal volume of buffer was added at t=27 min after photoactivation. *Inset* – The converted species (380 nm) is most likely Meta II, since acidification at 90 minutes after the addition of p44 yields more of the 440 nm absorbance (indicative of retinal Schiff base) than the control where no p44 was added. **B)** p44 speeds the depletion of the 475 nm species over time. The arrow marks the time at which buffer (*closed circles*) or p44 (*open circles*) was added. In each experiment, 1 μM Rho-P in 20 mM HEPES, 150 mM NaCl, pH 7.4, 0.02% DM, 0.02% asolectin was used (20 °C), and p44 was added to a final concentration of 1.5 μM.

Figure A1. 6

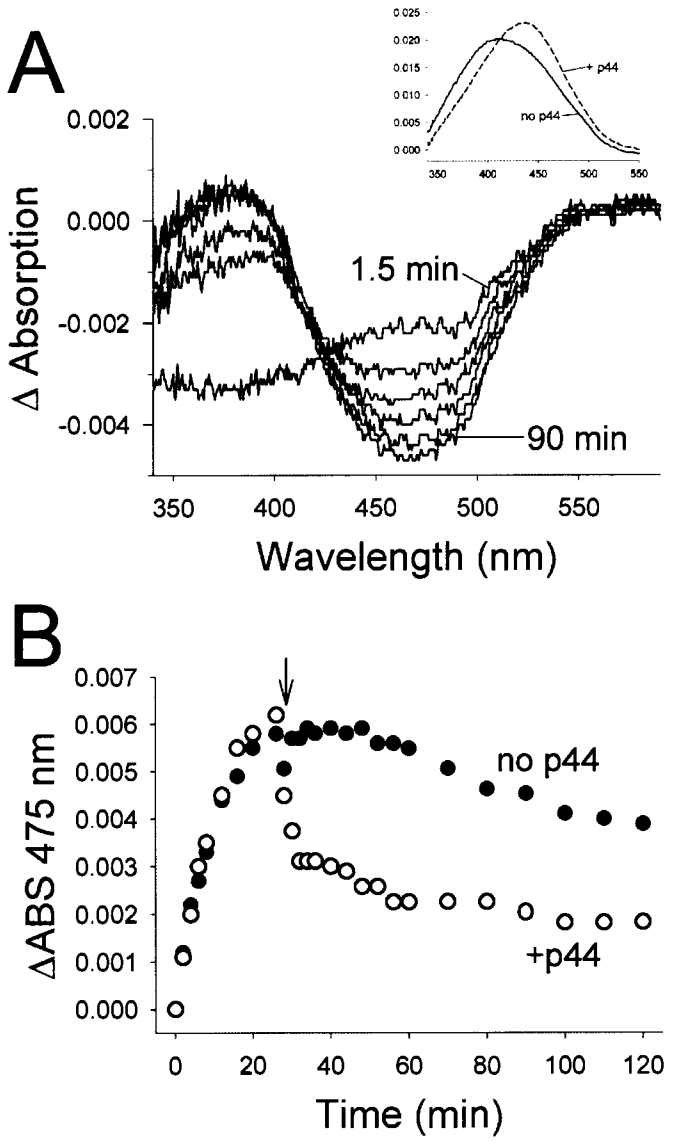
A
0.002
0.000
-0.002
-0.004
Δ Absorption
1.5 min
90 min
350
400
450
500
550
Wavelength (nm)
+ p44
no p44
B
0.007
0.006
0.005
0.004
0.003
0.002
0.001
0.000
ΔABS 475 nm
no p44
+p44
0
20
40
60
80
100
120
Time (min)

Figure A1. 7 Effect of blue-light on the interaction of arrestin and p44 with Rho*-P. Fluorescence of 1 μM arrestin I72B (*red*) and p44 (*blue*) in the presence a two-fold excess of Rho-P (DM/asolectin mixed micelles). The samples were illuminated at the indicated times with green or blue light (20 sec), and 15 minutes after the initial illumination, 10 mM hydroxylamine was added. The samples were excited at 380 nm (20 °C). The I72B and p44/I72B fluorescence traces are normalized to F_0 values determined from the fluorescence emission (456 nm) of identical I72B and p44/I72B samples in DM/asolectin buffer without Rho-P.

Figure A1. 7

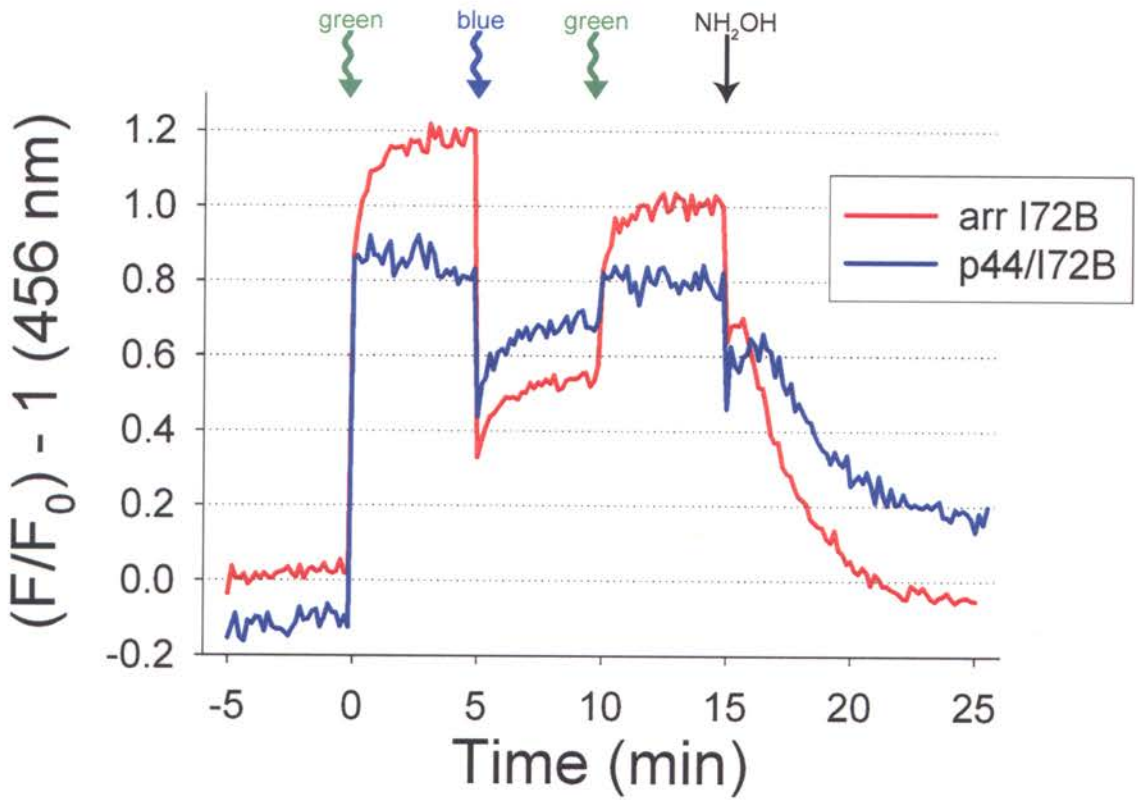
green
blue
green
NH2OH
1.2
1.0
0.8
0.6
0.4
0.2
0.0
-0.2
(F/F0) - 1 (456 nm)
-5
0
5
10
15
20
25
Time (min)
arr I72B
p44/I72B

Figure A1. 8 Model of light-dependent attenuation of Rho* by p44 and arrestin. In the dark-adapted rod disk (*upper panel*), p44 (*light blue*) is "tethered" to the membrane by its interaction with Rho-P (*red*), which comprises ~1% of the dark-state rhodopsin population (Binder *et al.*, 1996). Transducin (G_t, *blue, green, and orange subunits*) and rhodopsin kinase (RK, *purple*) are also localized to the membrane by lipid membrane anchors (for simplicity, the interactions of RK with recoverin and $G_{\beta\gamma}$ are ignored in this schematic). Upon exposure to dim light (*middle panels*), a single rhodopsin molecule (*red*) is converted to Meta II (*yellow*). **1)** G_t binds Meta II, is activated, and the $G_t\alpha$ subunit dissociates and activates PDE (not shown). **2)** Meta II is phosphorylated by RK. **3)** p44 binds phosphorylated Meta II and blocks further G_t activation. It is not known exactly how p44 "hops" from Rho-P to Rho*-P, but diffusion in the membrane may facilitate this process. Furthermore, the role of rhodopsin dimerization in this process is an intriguing possibility (Schröder *et al.*, 2002). Note that the different modes of p44 binding to Rho-P and Rho*-P are illustrated. Upon exposure to bright light (*lowest panel*), which results in complete rhodopsin bleaching, arrestin (*dark blue*) translocation from the inner segment provides an pool of protein sufficient to bind up every photo-activated receptor (Strissel *et al.*, 2006). In the figure, rhodopsin dimers and a binding stoichiometry of 2 arrestin to 2 Rho*-P are shown, although this issue is still unresolved.

Figure A1. 8

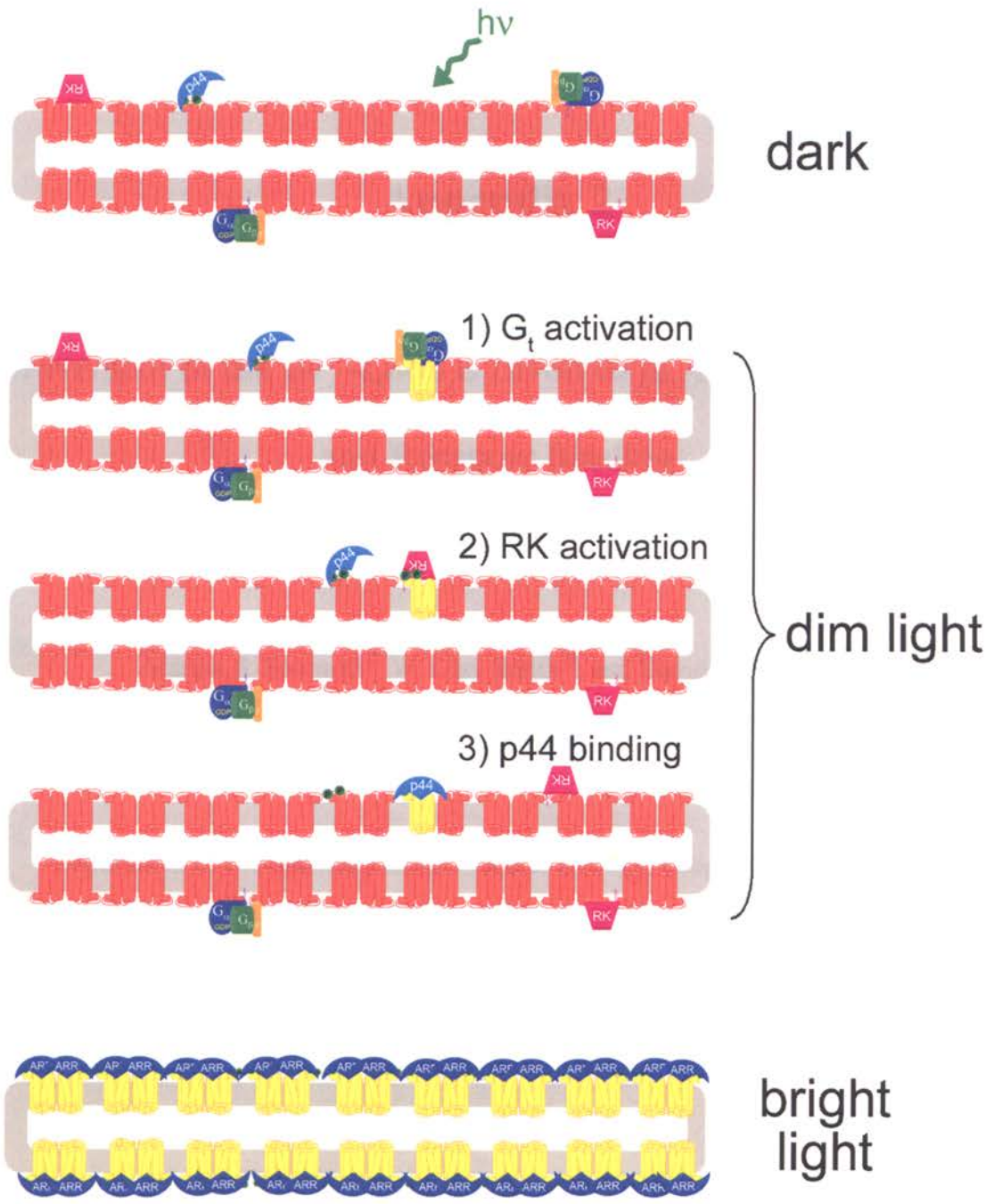
hν
dark
1) G_t activation
2) RK activation
3) p44 binding
dim light
bright light

Appendix 2

Movement of the Ile^{72}-Loop is Involved in Arrestin Activation and Receptor Binding

Martha E. Sommer [‡], W. Clay Smith [§], and David L. Farrens [‡]

[‡] Department of Biochemistry and Molecular Biology, Oregon Health & Science University, Portland, OR 97239-3098, USA

[§] Departments of Ophthalmology and Neuroscience, University of Florida, Gainesville, FL 32610-0284, USA

A2. 1 SUMMARY

This appendix presents spectroscopic evidence that suggests the loop containing Ile^{72} (Ile^{72}-loop) in arrestin undergoes a folded to extended conformational change upon activation and binding to rhodopsin. The approach used a bimane probe placed on the loop at Ile^{72} and tryptophan residues on the arrestin N- and C-domains. Nearby tryptophan residues quench bimane fluorescence and can thus yield relative distance information. The data indicate that tryptophan residues at Glu^{148} and Lys^{298} quench bimane fluorescence statically in inactive arrestin, and the quenching is relieved upon arrestin binding to rhodopsin or an activating phosphopeptide. These results imply that movement of the Ile^{72}-loop is important in arrestin activation and binding to rhodopsin.

All experiments reported in this appendix were performed by the author of this dissertation. Purified arrestin mutant proteins were supplied by Dr. W. Clay Smith.

A2. 2 INTRODUCTION

The arrestin loop structure containing Ile^{72} (Ile^{72}-loop) is highly conserved among the different arrestins (Han *et al.*, 2001) and is clearly important in receptor binding (Dinculescu *et al.*, 2002; Smith *et al.*, 2004; Vishnivetskiy *et al.*, 2004; Sommer *et al.*, 2005; Hanson *et al.*, 2006b). The crystal structure of arrestin shows that the Ile^{72}-loop is flexible and can adopt different conformations (Figure A2. 1). In this work, we directly tested the movement of this loop by monitoring the ability of a bimane probe on the Ile^{72}-loop to be quenched by introduced Trp residues in the N- and C-domains of arrestin.

This work was initiated when our collaborator, Dr. W. Clay Smith, discovered that cross-linking Ile^{72} to a cysteine residue in the C-domain of arrestin, K298C, significantly diminishes arrestin's ability to bind Rho*-P. In addition, limited trypsin proteolysis suggests that conformational changes induced in native arrestin by either Rho*-P or the phosphopeptide analog of rhodopsin's C-terminus (7PP) are blocked in the cross-linked arrestin mutant. As described below, our spectroscopic data also suggest that movement of the Ile^{72}-loop is involved in arrestin activation and binding to Rho*-P.

A2. 3 MATERIALS and METHODS

A2. 3. 1 Materials

For materials used in this study see sections **3. 3. 1** and **4. 3. 1** in Chapters 3 and 4.

A2. 3. 2 Preparation of ROS and Recombinant Arrestin Mutants

For information regarding the purification of the proteins used in this study, see sections **2. 3. 2** and **2. 3. 4** in Chapter 2. All arrestin mutants were created in minimal cysteine (C63A, C143A) and tryptophan-less (W194F) mutant background.

A2. 3. 3 Bimane-Labeling of Arrestin

For protocols regarding the fluorescent labeling of arrestin mutants (I72C, I72C/K298W, I72C/K298F, I72C/E148W, I72C/E148F), see sections **2. 3. 5** and **3. 3. 5** in Chapters 2 and 3. For determination of the concentration of tryptophan-less arrestin mutants, a modified extinction coefficient was used (ε_{280} = 20,760 liters M^{-1} cm^{-1}).

A2. 3. 4 Synthesis of Synthetic Phosphopeptide 7PP

The 19-amino acid-long peptide analogous to the fully phosphorylated C-terminal tail of rhodopsin was synthesized and purified as described previously (Puig *et al.*, 1995).

A2. 3. 5 Functional Pull-down Assay

The functional pull-down assay is described in section **2. 3. 6** in Chapter 2.

A2. 3. 6 Fluorescence Spectroscopy

For details concerning steady-state experiments, see sections **2. 3. 7**, **3. 3. 7**, and **4. 3. 3** in Chapters 2, 3, and 4. Determination of accurate excitation and emission λ_{max} values was done as described previously (Mansoor *et al.*, 1999).

A2. 3. 7 Quantum Yield Measurements

The quantum yield (ϕ) of each labeled arrestin mutant was determined as described previously (Mansoor *et al.*, 1999). Briefly, the optical density at 360 nm (OD) and integrated fluorescence intensity (F) (λ_{ex}: 360 nm; λ_{em}: 370-700 nm) of each arrestin were compared to that of a standard with a known quantum yield (0.55), quinine sulfate in 1 N H_2SO_4, using the relation:

$$\phi_A = \phi_S * \frac{F_A}{F_S}\frac{OD_S}{OD_A}$$

where the subscripts A and S stand for the arrestin sample and the standard, respectively.

A2. 3. 8 Steady-State Fluorescence Anisotropy Measurements

Steady-state anisotropies were measured as described in section **A1. 3. 6** in Appendix 1.

A2. 3. 9 Fluorescence Lifetime Analysis

For information regarding the measurement and analysis of fluorescence lifetimes, see section **2. 3. 8** in Chapter 2.

A2. 4 RESULTS

A2. 4. 1 Rational for Mutant Design

The bimane-labeled arrestin mutant I72C (I72B) has been well characterized (Sommer *et al.*, 2005; Sommer *et al.*, 2006) and is an ideal position to measure the relative movement of the Ile^{72}-loop using Trp-bimane quenching. Comparison of the α and β conformers of structure show that the distance between Ile^{72} and residues Glu^{148} and Lys^{298} is >20 Å in the α-conformer, while it is only ~10 Å in the β conformer [18] (Figure A2. 1). Since Trp-bimane quenching only occurs when the two groups are within near-contact distance (<15 Å) (Mansoor *et al.*, 2002), these residues are ideal for this methodology. To assess any potential effects of mutating Glu^{148} and Lys^{298} on arrestin function, we also placed Phe at these sites as a control. Phe is bulky like Trp but does not quench bimane fluorescence.

A2. 4. 2 Labeled Arrestin Mutants are Functional

We first tested if these bimane-labeled arrestin mutants are functional by a centrifugal pull-down assay (Figure A2. 2). The data indicate that all mutants have wild-

[18] These are the distances between the α-carbons of these residues. The actual distances between bimane and tryptophan at these sites might be much less.

type specificity for Rho*-P binding. All mutants also bind Rho*-P with wild-type affinity, except for I72B/K298F, which pulls-down at ~70% the levels of wild-type.

A2. 4. 3 Trp-containing Mutants Exhibit Bimane Quenching

We next characterized the fluorescence properties of the arrestin mutants (Table A2. 1). Note that I72B/K298W and I72B/E148W have significantly diminished quantum yields compared to I72B and the controls I72B/K298F and I72B/E148F. Interestingly, the quantum yield of I72B/E148F is actually 37% higher than that of I72B, which may be because the E148F mutation increases the local hydrophobicity around the probe.

The amplitude-weighted average fluorescence lifetime, $\langle\tau\rangle$, of arrestin I72B is ~10 ns (Table A2. 1). Both Trp-containing mutants have similar $\langle\tau\rangle$ values. The fact that I72B/K298W and I72B/E148W have significantly reduced quantum yields but similar $\langle\tau\rangle$ values as the Trp-less controls implies that bimane probe is being quenched statically (Lakowicz, 1999). Furthermore, this means that the bimane and the Trp residue in these mutants are "very close" (5-10 Å) [19] (Mansoor *et al.*, 2002). This static quenching is also reflected in the red-shifted absorbance λ_{max} of these two mutants (Table A2. 1). Note that the lifetime of I72B/E148F is significantly longer (14.5 ns) than I72B, which explains why its quantum yield is higher and is consistent with it being in a more hydrophobic environment [20].

A2. 4. 4 Bimane Quenching is Relieved by ROS*-P Binding

The steady-state fluorescence spectra of the I72B mutants in the presence of ROS and ROS-P are shown in Figure A2. 3. In the presence of ROS, none of the mutants

---

[19] Static quenching occurs when the two groups are so close they are "touching" at the moment of light-excitation and thus form a ground-state nonfluorescent complex.

[20] S.E. Mansoor and D.L. Farrens, unpublished results.

exhibit significant fluorescence changes upon light-activation. In the presence of ROS-P, the fluorescence of each mutant increases and blue-shifts in intensity upon light-activation (λ_{max} values and relative increases in intensity are summarized in Table A2. 2). Interestingly, upon light activation, the intensities of the Trp-containing mutants I72B/K298W and I72B/E148W increases >200% to a level similar to that of I72B. This result suggests that binding to ROS*-P relieves the Trp-bimane quenching in these mutants. Arrestin I72B/K298F exhibits a diminished fluorescence change compared to I72B, probably because it has lower affinity for ROS*-P (as suggested by pull-down analysis, Figure A2. 2). Note arrestin I72B/E148F exhibits only a ~30% increase in intensity, compared to ~60% for I72B, because its dark-state fluorescence intensity is higher.

The fluorescence anisotropy of each bimane-labeled arrestin mutant, except I72B/K298F, is higher in the presence of dark ROS*-P (Table A2. 2) than in its absence (Table A2. 1). This result suggests that arrestin interacts with dark ROS-P, and this interaction is perturbed by the K298F mutation. Upon light-activation, the anisotropy of each mutant increases, as expected when arrestin binds. The addition of hydroxylamine returns the anisotropies to lower values.

Finally, the fluorescence lifetime values of the bimane labeled mutants do not change significantly upon ROS*-P binding (Table A2. 2), except for I72B/E148F, which goes from ~14 ns in the dark to 11 ns upon light-activation.

A2. 4. 5 Bimane Quenching is Somewhat Relieved by 7PP

The phosphopeptide 7PP represents the fully phosphorylated C-terminal tail of rhodopsin and has been shown to induce activating conformational changes in arrestin

(Puig *et al.*, 1995; McDowell *et al.*, 1999). We measured the fluorescence spectra of the bimane-labeled arrestin mutants in the presence of saturating amounts of 7PP [21] (Figure A2. 4). The fluorescence of arrestin I72B decreases ~30% upon addition of 7PP, which is similar to what we observed previously (Chapter 2, Figure 2. 3C). In contrast, the fluorescence of I72B/K298W increases (~30%), and the fluorescence of I72B/E148W only decreases ~9%. The fluorescence intensities of the controls I72B/K298F and I72B/E148F decrease ~17% and ~46%, respectively. These results suggest that 7PP may induce conformational changes in arrestin that allow the probe at Ile^{72} to move away from Trp residues at Lys^{298} and Glu^{148}.

A2. 5 DISCUSSION

A2. 5. 1 Appendix Overview

In this work Trp-bimane quenching was used to directly test whether the variation in the placement of the Ile^{72}-loop seen in the crystal structure conformers of arrestin represents a functional conformational change. To summarize, in free arrestin the probe at Ile^{72} is statically quenched by Trp residues at Glu^{148} and Lys^{298}, and this quenching appears to be relieved upon binding ROS*-P. This is consistent with Ile^{72} being very close (5-10 Å) to Glu^{148} and Lys^{298} in inactive arrestin, and then moving away from these residues upon binding ROS*-P. The data also show that the proximity of these sites can be affected by binding of the phosphopeptide 7PP. Note that while the fluorescence of I72B/K298W and I72B/E148W indicate a movement of the Trp residues away from the

[21] 360 μM, which is ten-times the published K_D of 36 μM (Puig *et al.*, 1995).

probe at Ile^{72}, no mutant exhibits a blue-shift in fluorescence upon binding 7PP. This means the blue-shift in fluorescence is specific for p44/I72B's interaction with ROS*-P.

Interestingly, our data also provide evidence that Lys^{298} might be involved in binding ROS*-P. Centrifugal pull-down and fluorescence experiments indicate that the K298F mutation decreases arrestin affinity for ROS*-P by ~30%. Furthermore, the anisotropy of I72B/K298F is lower in the presence of dark ROS-P than I72B, suggesting a loss of dark-state binding. Finally, the fluorescence of I72B/K298F in the presence of 7PP only drops half as much as that of I72B, which may be because it does not bind 7PP as well. However, it is curious that the K298W mutant has wild-type affinity for ROS*-P. In data not shown here, we find that the K298F mutation nearly eliminates binding to Rho*-P in DM/PA micelles, and the K298W only binds ~half as well as wild-type. Thus, mutation of Lys^{298} appears to perturb phosphorylation-dependent binding, and this effect is further enhanced by solubilization of Rho*-P in detergent.

Finally, the increased quantum yield of mutant I72B/E148F also provides evidence of the close proximity of Ile^{72} and Glu^{148} in inactive arrestin. Since the quantum yield of bimane increases with the hydrophobicity of its environment (Mansoor *et al.*, 1999), the increased fluorescence of I72B/E148F is likely due Phe creating a hydrophobic "patch" for bimane, thus enhancing its fluorescence and lengthening its lifetime. In addition, depending on how the two groups interact, the Phe might also protect the bimane from solvent quenching. Finally, we cannot rule out the possibility that Glu^{148} quenches bimane in I72B, although bimane quenching by Glu residues has not been reported (Sato *et al.*, 1988).

A2. 5. 2 Implications of these Results on the Mechanism of Arrestin Activation

The Ile^{72}-loop of arrestin is obviously important for binding to ROS*-P. The region is highly conserved among the different arrestins (Han *et al.*, 2001), and substitution of hydrophobic residues in this region with cysteines dramatically diminishes binding (Sommer *et al.*, 2005; Hanson *et al.*, 2006b). In a recent EPR study of arrestin binding to ROS*-P using spin-labeled single cysteine mutants of arrestin, Hanson *et al.* present evidence that may suggest that the two-concave surfaces of arrestin bind dark ROS-P, and upon light-activation, only probes on the Ile^{72}-loop are dramatically more immobilized (Hanson *et al.*, 2006b), which is consistent with our previous analysis of spin-labeled arrestin I72C (Sommer *et al.*, 2005). In this work, we show that the Ile^{72}-loop likely undergoes a folded to extended conformational change upon arrestin binding to ROS*-P. Hanson *et al.* suggest that light-activation of ROS-P must expose some rhodopsin element that binds the Ile^{72}-loop. It is tempting to hypothesize that this element is the cytoplasmic hydrophobic cleft that is opened by Helix VI movement (Altenbach *et al.*, 1996; Farrens *et al.*, 1996; Janz and Farrens, 2004a). Furthermore, Ile^{72} on arrestin is flanked on either side by Asp residues. Could these Asp residues interact with certain charged residues in rhodopsin, such a Arg^{135} of the E(D)RY sequence, which is exposed upon rhodopsin activation (Hamm, 2001)? These possibilities remain speculative and will be the subject of future investigations.

A2. 5. 3 Future Directions

Although only Lys^{298} and Glu^{148} have been tested in this work [22], they have yielded convincing evidence of an important conformational change of the Ile^{72}-loop, as first suggested by the crystal structure conformers (Granzin *et al.*, 1998; Hirsch *et al.*, 1999). In future studies, we will introduce Trp into other close sites, as well as reverse the Trp-bimane locations (for example, I72W/K298B). Furthermore, double cysteine mutants will be spin-labeled and characterized by EPR, since spin-spin interactions can yield distance information (Farrens, 1999; Hubbell *et al.*, 2000). Finally, we will investigate why the Ile^{72}-loop is important for binding. That is, where in rhodopsin does it bind? Firstly, we will try to delineate the size of the binding pocket by attaching various sized-groups to I72C and quantifying binding. In addition, we may be able to map where Ile^{72} contact rhodopsin using the cross-linking/mass spectrometry approach of the Khorana group (Cai *et al.*, 2001; Itoh *et al.*, 2001).

A2. 6 ACKNOWLEDGEMENTS

The work was supported by the same funding as described in section **3. 6** in Chapter 3. We also thank J. Hugh McDowell and Anatol Arendt for synthesis of the phosphopeptide 7PP and Steven E. Mansoor for assistance in measuring fluorescence lifetimes and advice regarding bimane quenching.

[22] Lys^{300} has also been tested, but the K300W mutation resulted in ~50% loss of affinity and it did not show dramatic I72B quenching, since it is >13Å away from Ile^{72}.

Table A2. 1 Fluorescence characteristics of bimane-labeled arrestin I72C mutants

Mutant	absorbance λ_{max} (nm)	excitation [a] λ_{max} (nm)	emission [b] λ_{max} (nm)	quantum yield (ϕ)	$\langle\tau\rangle$ (ns)[c]	anisotropy [d]
I72B	392	396.5	470.5	0.19	10.1 ± 0.3	0.0637 ± 0.006
I72B K298W	398	396.5	471.7	0.09	9.7 ± 0.4	0.0559 ± 0.0026
I72B K298F	392	396.5	470.9	0.17	8.7 ± 0.8	0.0604 ± 0.005
I72B E148W	394	396.5	470.4	0.10	8.7 ± 0.5	0.0634 ± 0.0022
I72B E148F	392	396.5	468.5	0.26	14.5 ± 0.2	0.0718 ± 0.003

[a] Emission collected at 490 nm (20 °C).

[b] Excitation at 381 nm (20 °C).

[c] $\langle\tau\rangle = \alpha_1\tau_1+\alpha_2\tau_2$, or the amplitude-weighted average fluorescence lifetime. The mean ± the S.E. from three fluorescence lifetime measurements and two-component analysis (20 °C). The χ^2 value for each fit was between 0.8 and 1.2.

[d] The steady-state anisotropy of the bimane probe. (14 °C).

Table A2. 2 Fluorescence characteristics of bimane-labeled arrestin I72C mutants in the presence of membrane-bound Rho-P

Mutant	+ ROS-P	emission [a] λmax (nm)	increase in integrated intensity	anisotropy [b]	⟨τ⟩ (ns)[c]	χ^{2} [d]
I72B	dark	470		0.099 ±0.007	9.2	0.9
	+light	453	63 %	0.165 ± 0.003	9.8	1.0
	+NH_2OH	n.d.[f]		0.081 ± 0.005	10.7	0.9
I72B K298W	dark	468		0.103 ± 0.003	8.5	0.9
	+light	456	240 %	0.146 ± 0.005	8.6	1.0
	+NH_2OH	n.d.		0.045 ± 0.016	9.1	0.9
I72B K298F	dark	470		0.070 ± 0.003	10.5	0.9
	+light	460	45 %	0.112 ± 0.007	10.0	0.8
	+NH_2OH	n.d.		0.045 ± 0	10.5	1.0
I72B E148W	dark	473		0.153 ± 0.009	9.1	0.8
	+light	455	200 %	0.190 ± 0.007	8.1	1.0
	+NH_2OH	n.d.		0.064 ± 0.009	9.2	0.9
I72B E148F	dark	467		0.113 ± 0.004	13.5	1.3
	+light	454	31 %	0.166 ± 0.008	10.7	0.8
	+NH_2OH	n.d.		0.085 ± 0.006	12.3	1.0

[a] Excitation at 380 nm (20 °C).
[b] The steady-state anisotropy of the bimane probe. The mean ± the S.E. from two measurements (14 °C).
[c] Derived from two-component fluorescence lifetime analysis (20 °C). $\langle\tau\rangle = \alpha_1\tau_1+\alpha_2\tau_2$, or the amplitude-weighted average fluorescence lifetime.
[d] The chi-squared value describes the goodness of the fit (or the deviance of the residuals) for the two-component lifetime analysis.
[f] n.d., not determined.

Figure A2. 1 Structural models of arrestin conformers and the sites mutated in this study. The two crystallographic conformers of arrestin, α and β, are shown, and the arrestin domains are color-coded: N-domain, *blue*; C-domain, *orange*; C-tail, *green*. The location of Ile^{72}, which was mutated to cysteine and labeled with bimane in this study, is indicated by a *yellow sphere*. Residues Glu^{148} (*violet*) and Lys^{298} (*red*) were each mutated to tryptophan in this study and are modeled as such in the figure. In the α conformer, the distance between Ile^{72} and Glu^{148} is ~27 Å, and the distance from Ile^{72} to Lys^{298} is ~21 Å. In the β conformer, these distances are shortened to ~10 Å. E148W and K298W mutations were introduced into the arrestin structure using the program Deep View/Swiss-PDB Viewer (GlaxoSmithKline) and the published coordinates (Hirsch *et al.*, 1999). The rotamer conformation of each mutated Trp residue was selected by energy minimization. Subsequent mutant PDB coordinates were imported into the program DS Viewer Pro 5.0 (Accelrys, Inc.) to make the ribbon models.

Figure A2. 1

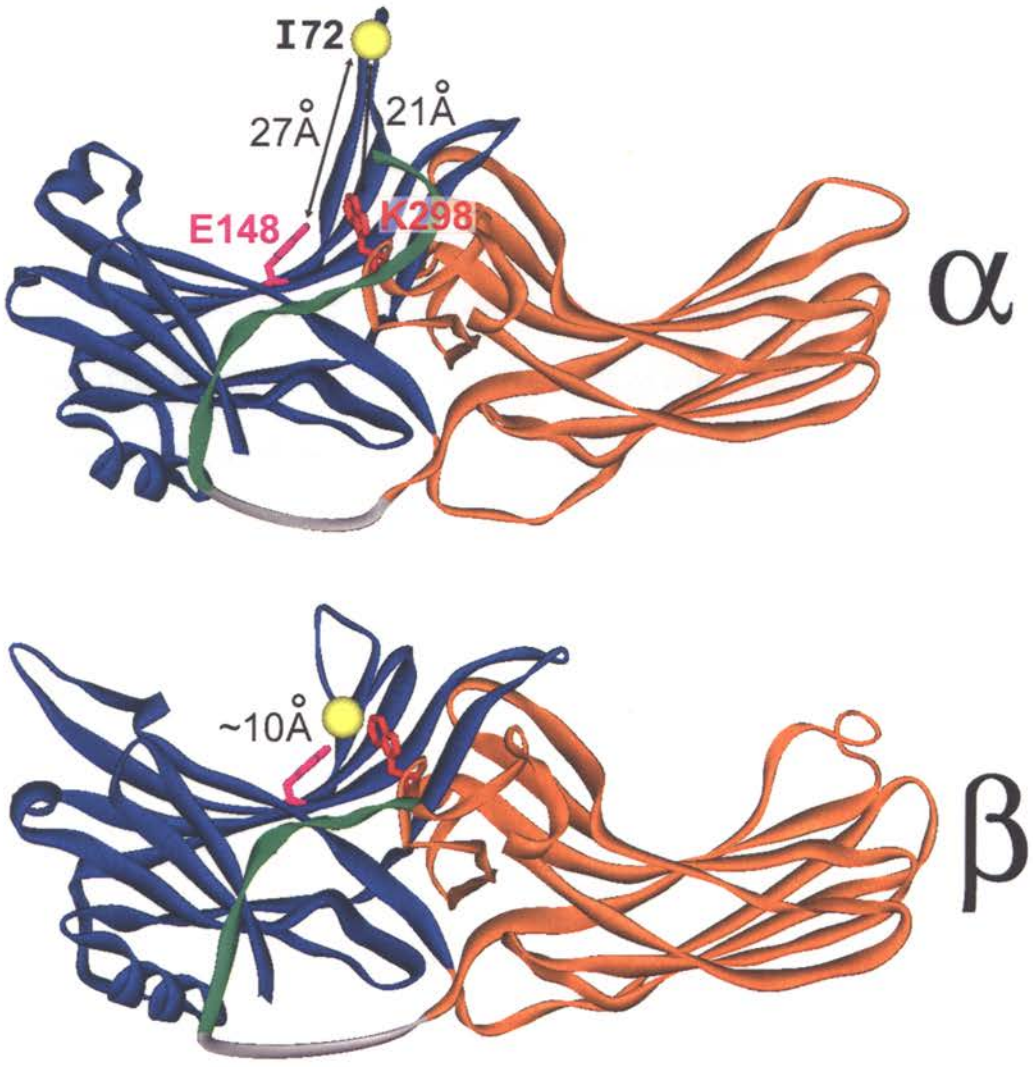

Figure A2. 2 Bimane-labeled arrestin I72C mutants are functional. Arrestin affinity for dark rhodopsin (R), light-activated rhodopsin (R*), dark phosphorylated rhodopsin (RP), and light-activated phosphorylated rhodopsin (R*P) was assayed by a centrifugal pull-down experiment. The fluorescence of each gel is shown in the *upper panels*, and the Coomassie stains are shown in the *lower panels*. Molecular weight (MW) markers are defined in kDa in the space between the two gels, and the far right lane on each gel contains a wild-type arrestin + R*P control. The data indicate that arrestin mutants I72B/K298W, I72B/E148W, and I72B/E148F have essentially wild-type affinity for R*P, while arrestin I72B/K298F has reduced affinity (~70% of wild-type). Note that because of different regeneration efficiencies during sample preparation, the R bands appear darker than the RP bands. Although the R bands contain more protein (opsin), the total amount of dark-state rhodopsin (A_{500}=0.48) was equalized for each sample.

Figure A2. 2

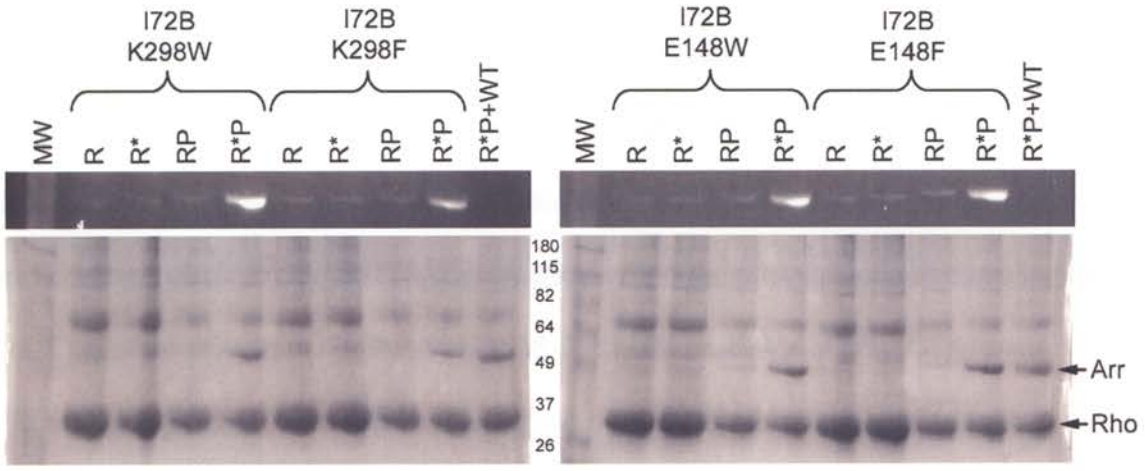
I72B
K298W
I72B
K298F
I72B
E148W
I72B
E148F
MW
R
R*
RP
R*P
R
R*
RP
R*P
R*P+WT
MW
R
R*
RP
R*P
R
R*
RP
R*P
R*P+WT
180
115
82
64
49
37
26
Arr
Rho

Figure A2. 3 Steady-state fluorescence of bimane-labeled arrestin I72C mutants in the presence of rhodopsin. The fluorescence spectra of identical amounts of arrestin mutants I72B (A), I72B/K298W (B), I72B/K298F (C), I72B/E148W (D), and I72B/E148F (E) were measured in the presence of membrane-bound Rho (ROS, *left column*) and Rho-P (ROS-P, *right column*) before (*solid traces*) and after light-activation (*dashed traces*). Arrestin mutants I72B/K298W and I72B/E148W exhibit quenched fluorescence compared to I72B, while I72B/E148F exhibits increased fluorescence. For each mutant, no fluorescence changes are observed in the presence of nonphosphorylated ROS. Remarkably, in the presence of ROS-P, the fluorescence of arrestin mutants I72B/K298W and I72B/E148W increases and blue-shifts after light-activation to approximately the same level as the control I72B. Arrestin I72B/K298F shows a less dramatic change in fluorescence, probably because it has reduced affinity for ROS*-P. Arrestin I72B/E148F also shows a less dramatic fluorescence changes, because it has a higher dark-state fluorescence than arrestin I72B. In each experiment, 1 μM arrestin and a four-fold excess of ROS or ROS-P were used (20 mM HEPES, 150 mM NaCl, pH 7.4, 20 °C, λ_{ex}: 380 nm). The spectra represent smoothed and buffer-subtracted raw data and are plotted on the same scale for comparison.

Figure A2. 3

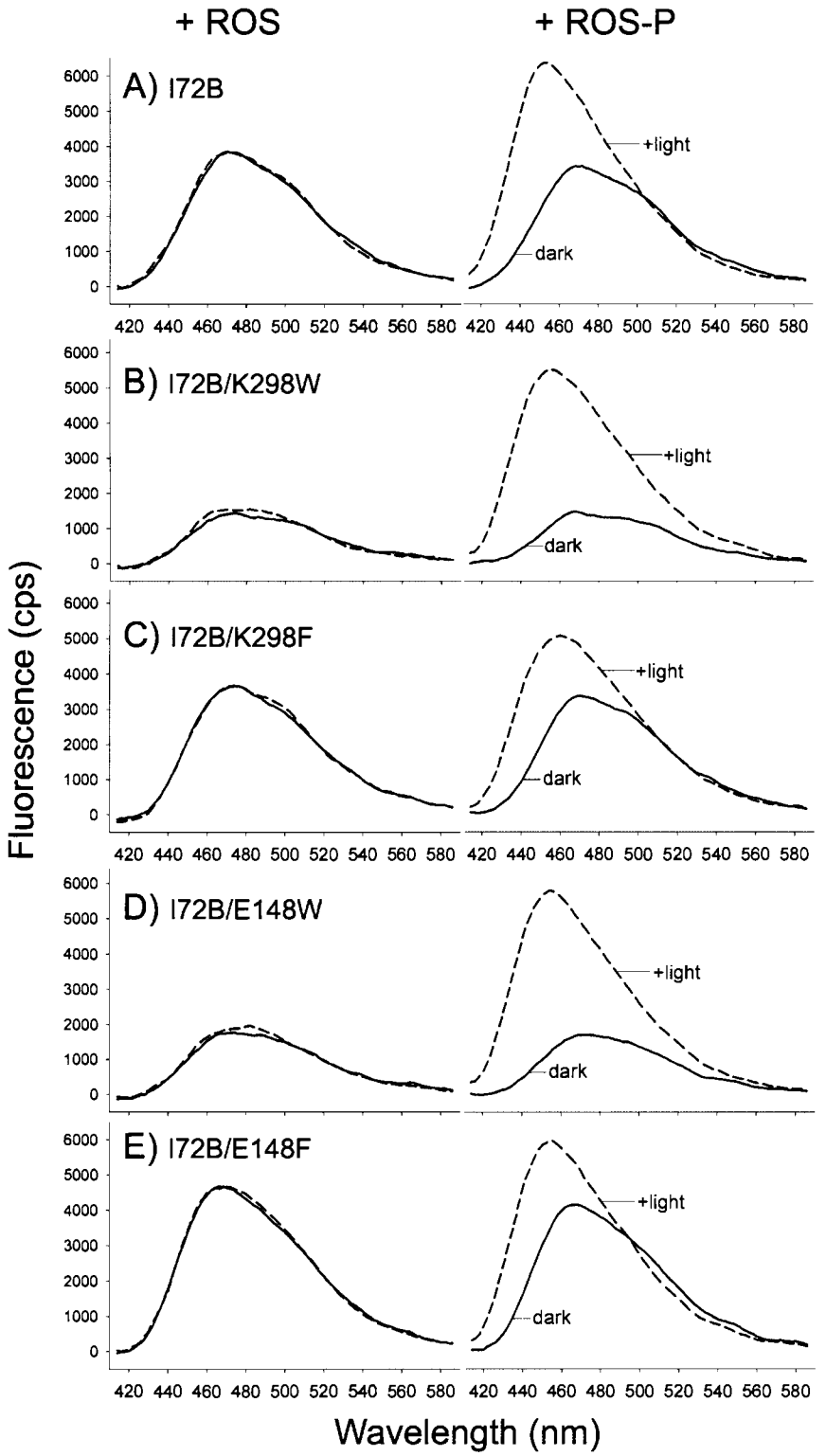
+ ROS
+ ROS-P
A) I72B
B) I72B/K298W
C) I72B/K298F
D) I72B/E148W
E) I72B/E148F
+light
dark
Fluorescence (cps)
Wavelength (nm)
0
1000
2000
3000
4000
5000
6000
420 440 460 480 500 520 540 560 580

Figure A2. 4 Steady-state fluorescence of bimane-labeled arrestin I72C mutants in the presence of phosphopeptide 7PP. The fluorescence of each bimane-labeled arrestin mutant was measured in the absence (*solid spectra*) or presence (*dashed spectra*) of phosphopeptide 7PP, which represents the fully-phosphorylated tail of rhodopsin. **A)** Addition of 7PP causes a ~30% decrease in intensity of arrestin I72B. **B)** In contrast, the fluorescence of I72B/K298W increases in intensity (30%) upon 7PP binding. **C)** Addition of 7PP to the control I72B/K298F results in decrease in intensity (~17%). **D)** 7PP binding causes a fluorescence decrease in I72B/E148W (9%) that is significantly smaller than the drop that occurs with the control I72B/E148F (46%) **(E)**. Note that the fluorescence scale for these spectra is significantly different than that in Figure A2. 3, because wider excitation slits (1 nm) were used in this experiment. Each spectrum represents buffer-subtracted raw data for 1 μM arrestin ± 360 μM 7PP (20 mM HEPES, 150 mM NaCl, pH 7.4, 20 °C, λ_{ex}: 380 nm).

Figure A2. 4

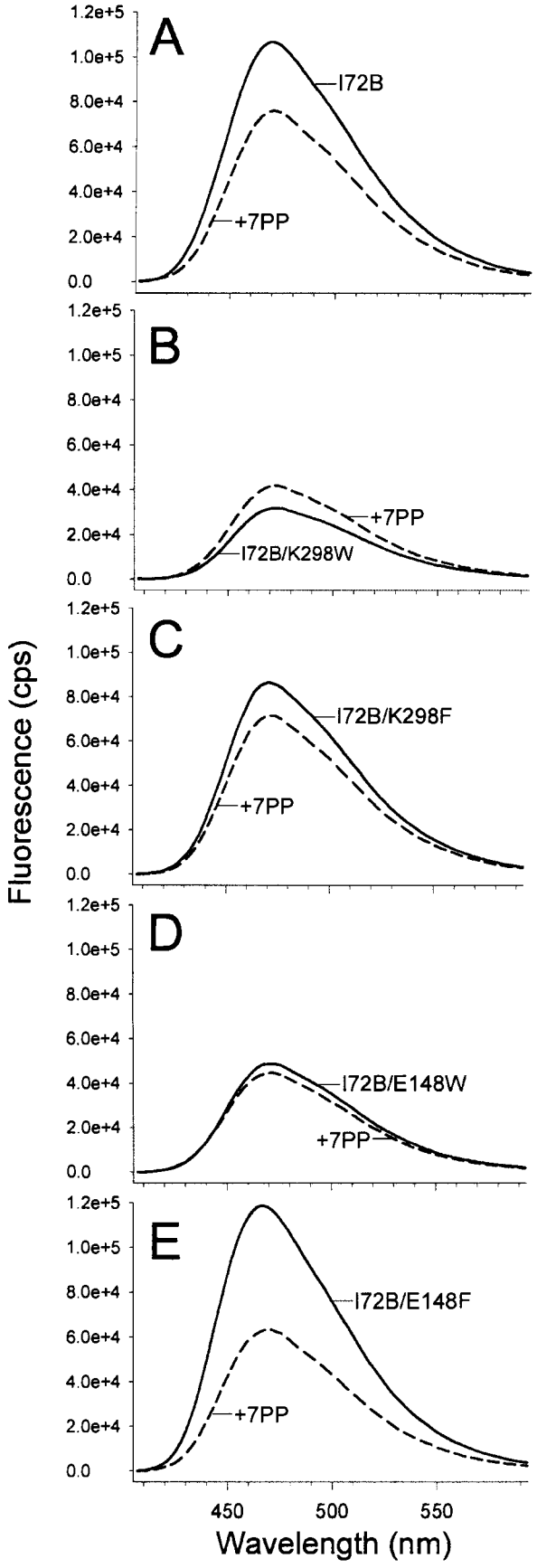
A
I72B
+7PP
B
+7PP
I72B/K298W
C
I72B/K298F
+7PP
D
I72B/E148W
+7PP
E
I72B/E148F
+7PP
1.2e+5
1.0e+5
8.0e+4
6.0e+4
4.0e+4
2.0e+4
0.0
Fluorescence (cps)
450
500
550
Wavelength (nm)